EXPERIMENTAL INVESTIGATIONS ON PERFORMANCE OF DUAL FUEL DIESEL ENGINE USING CNG AND BIODIESEL

A Thesis submitted to the Delhi Technological University, Delhi in partial fulfillment of the requirements for the award of the degree of

DOCTOR OF PHILOSOPHY

in

Mechanical Engineering

by

PARVESH KUMAR

(2K13/PhD/ME/13)

Under the Supervision of

Dr. NAVEEN KUMAR

(Professor)

Mechanical Engineering Department

Delhi Technological University

Shahbad Daulatpur Bawana Road

Delhi – 110042, INDIA

February 2017

DECLARATION

I hereby declare that the thesis entitled **"EXPERIMENTAL INVESTIGATIONS ON PERFORMANCE OF DUAL FUEL DIESEL ENGINE USING CNG AND BIODIESEL"** is an original work carried out by me under the supervision of Dr. Naveen Kumar, Professor, Department of Mechanical Engineering, Delhi Technological University, Delhi. This thesis has been prepared in conformity with the rules and regulations of the Delhi Technological University, Delhi. The research work reported and results presented in the thesis have not been submitted either in part or full to any other university or institute for the award of any other degree or diploma.

Parvesh Kumar

(2K13/PhD/ME/13)
Research Scholar
Mechanical Engineering Department
Delhi Technological University,
Delhi

Date:

Place:

CERTIFICATE

This is to certify that the work embodied in the thesis entitled **"EXPERIMENTAL INVESTIGATIONS ON PERFORMANCE OF DUAL FUEL DIESEL ENGINE USING CNG AND BIODIESEL"** by **Mr. Parvesh Kumar, (Roll No.-2K13/PhD/ME/13)** in partial fulfillment of requirements for the award of Degree of **DOCTOR OF PHILOSOPHY in Mechanical Engineering**, is an authentic record of student's own work carried by him under my supervision.

This is also certified that this work has not been submitted to any other Institute or University for the award of any other diploma or degree.

(Dr. Naveen Kumar)
Professor
Mechanical Engineering Department
Delhi Technological University
Delhi- 110042.

Dedicated

to

My Parents

&

Family

AKNOWLEDGEMENT

The present research work was carried out under the honored supervision of Prof. Naveen Kumar. It is my honor and privilege to express a deep sense of gratitude to him for his panegyric efforts, ever helping attitude, critical and valuable comments and constant inspiration. His mentorship helped me become a good researcher which, I always dreamed. His words of solace and encouragement especially during difficult times shall ever be remembered by me. I also acknowledge the blessing by Smt. Sumeeta Garg who always cared for me during my stay in Delhi. I will be highly indebted to her, for her affection.

I am also grateful to Dr. R. S. Mishra, Professor & Head, Dr. R. C. Singh, Associate Professor, Dr. Rajiv Chaudhari, Associate Professor, Dr. Rangnath M.S., Associate Professor, Mr. Raghvendra Gautam, Assistant Professor, Dr. Mohit Tyagi, Assistant Professor and Mr. Shailesh Mani Pandey, Assistant Professor, Department of Mechanical Engineering, DTU Delhi for their help, encouragement and valuable suggestions.

I owe gratitude to the esteemed colleagues of the Centre for Advanced Studies and Research in Automotive Engineering (**CASRAE**), Delhi Technological University; particularly my research fellow Dr. Alhassan Yahaya and Dr. Harveer Singh Pali, Assistant Professor, Noida Institute of Engineering and Technology, Greater Noida for their excellent support and valuable suggestions.

I am thankful to Mr. Kamal Nain and Mr. Manoj Kumar for providing all laboratory assistance. I am also thankful for Mr. Surendra Singh and Smt. Neetu Mishra, the supporting staff of CASRAE, DTU, Delhi.

There are some friends and colleagues who have helped me along the way for the successful completion of this research work. I take this opportunity to thank Mr. Amarjot Singh, Mr. Siddarth Bansal, Assistant Professor, MAIT, Delhi, Mr. Amardeep, Assistant Professor, IEC, Gr. Noida, Mr. Ashish Kumar Singh, Assistant Professor, SDEC, Ghaziabad, Mr. Abhishek Sharma, Mr. Vasu, Mr. Dhuruv Gupta, Mr. Shailesh Singh and Mr. Santosh, Mr. Ashish Kumar Gupta.

I shall ever cherish the affection and blessings showered on me by my father, Mr. Jai Parkash and my mother Mrs. Nirmala Devi. Whatever, I have achieved in my professional life; it is all because of them. I cannot express in words their efforts put by them to nurture me. I am also indebted to my elder brother Mr. Yogesh Kumar Khatkar and sister in-law Jyoti Khatkar, who always extended help whenever required. I place my sincere respect and a deep sense of gratitude to other family members, my elder sisters, Mrs. Sonu Gulia and Mrs. Ashu Swami, my brother in laws, Mr. Rajkumar Gulia and Mr. Pankaj Swami, my nephew Master Yash Gulia, my niece Princess Riyana Sawami, my father in law Shri Niranjan Shivaji, mother in law Mrs. Vibha Shivaji and my brother in law Kshitij Shivaji.

Finally, I am unable to express my sincere gratitude in words for the affection, encouragement and moral support by my wife during the entire research work. I am ever

beholden to my wife Mrs. Vartika Shivaji Khatkar for not giving due attention and time during the present work.

There are many more persons who have helped me directly or indirectly to complete this research work. I take this opportunity to thank all of them and apologize for their names not being here. Last but not the least; I thank the Almighty for giving me strength and patience to complete this work in all respects and leading to the path of success.

(Parvesh Kumar)

New Delhi

ABSTRACT

The power generation and transportation sectors are heavily dependent on fossil fuels, whose combustion results in high level of air pollution. However, uncertainties about the long-term availability coupled with price perturbation of fossil fuels are a key challenge due to which alternative fuels are getting more attention. Gaseous fuels such as Compressed Natural Gas (CNG) or hydrogen are very promising for use in Spark Ignition (SI) or Compression Ignition (CI) Engines. The research on the use of gaseous fuels in CI engines is still underway unlike SI engines, where it has even been commercialized. The utilization CNG with environmental friendly liquid biofuels is one of the most promising combustion techniques in dual fuel CI engine without a reduction in power. Also, application of exhaust gas recirculation (EGR) will improve the performance of dual fuel engine.

The objective of the present research work is to evaluate dual fuel combustion technique using a different combination of fuels. The effect of the use of CNG as primary fuel and, diesel, Jatropha oil methyl ester (JOME), Orange peel oil methyl ester (OPOME) and their blends as pilot fuel in CI engine, on combustion, performance and emissions characteristics of the engine was studied and compared with baseline data of diesel engine operation.

A Kirloskar diesel engine (Model-CAF 8) was modified in such a way that it can operate in both conventional diesel mode as well as dual fuel mode. The engine was run at the rated speed of 1500 rpm for six loading conditions (i.e. no load, 20%, 40%, 60%, 80% and full load) for both the modes. During dual fuel combustion mode, the mass flow rate of pilot fuel was kept constant and mass flow rate of CNG varied with the load. The engine was connected to a

computer to analyze the in-cylinder pressure data which would further help to calculate the mass-burn fraction, heat release rate, and cumulative heat release. A combustion chamber was also developed to measure the ignition delay of liquid fuels. An exhaust gas recirculation (EGR) set up was also developed for the present work.

Response surface methodology (RSM) was used as an optimization tool for biodiesel production. The evaluation of physicochemical properties (such as density, kinematic viscosity, cetane number, flash point etc.) of all pilot fuels was carried and found suitable for use. The auto-ignition temperature of all pilot fuels was also evaluated. The engine trial was conducted by taking different fuel combinations (i.e. CNG+diesel, CNG+JOME, CNG+J50D50, CNG+OPOME, CNG+OP50D50) with and without application of EGR and the combustion, performance and emissions characteristics of dual fuel engine were studied.

It was found that JOME, OPOME and their blends show better results compared to diesel as pilot fuel in dual fuel engine especially up to higher load. The use of biodiesel shows better BTE and lower CO emissions than diesel as pilot fuel. However, at full load, diesel as pilot fuel has highest BTE compared to all another mode of operations. The highest BTE of the conventional diesel engine was found 28.58%, where the highest BTE for dual fuel mode was found 30.65%, 30.35%, 30.51%, 30.44% and 30.58% for diesel, JOME, J50D50, OPOME and OP50D50 as pilot fuel respectively. It was clearly observed that the blending of biodiesel in diesel improves the BTE of the engine. The utilization of EGR was found to improve the emissions characteristics of dual fuel engine. At low load and with EGR, NO_X emissions reduced by 18.4%. The application of EGR also reduced the CO and UHC emissions by 3.2% and 6.3% respectively. Also, at low load, the application of EGR increases the BTE of the engine by 3%.

It is concluded that dual fuel engines are capable of reducing exhaust emissions without reducing the power and CO and unburned HC can be reduced with the application of EGR in dual fuel engine. Further investigations on advancing injection timing of pilot fuel are recommended in order to meet with emission regulations.

LIST OF CONTENTS

LIST OF FIGURES

LIST OF PLATES

LIST OF TABLES

NOMENCLATURE

@	At the rate
A/F	Air to Fuel
AN	Acid Number
API	American Petroleum Institute
ASTM	American Society for Testing and Materials
ATDC	After Top Dead Center
AVL-437	AVL-437 Smoke Meter
AV	Acid Value
B10	10% Biodiesel/90% Diesel
B20	20% Biodiesel/80% Diesel
B50	50% Biodiesel/50% Diesel
B100	Pure Biodiesel
BHA	Butylated Hydroxyanisole
BHT	Butylated Hydro-toluene
BIS	Bureau of Indian Standard
BMEP	Break Mean Effective Pressure
BSEC	Brake Specific Energy Consumption
BSFC	Brake Specific Fuel Consumption
BTE	Brake Thermal Efficiency
BTDC	Before Top Dead Center
C	Carbon
^{o}C	Degree Celsius
^{o}CA	Degree Crank Angle
cc	Cubic centimeter
CCD	Central Composite Design
CFPP	Cold Filter Plugging Point

CH_3	Methyl
CH_4	Methane
CHN	Carbon, Hydrogen, Nitrogen
CI	Compression Ignition
cm^{-1}	Per Centimeter
CNG	Compressed Natural Gas
CNG + Diesel	CNG Used As Primary Fuel And Diesel As Pilot Fuel
CNG + JOME	CNG Used As Primary Fuel And JOME As Pilot Fuel
CNG + J50D50	CNG Used As Primary Fuel And J50d50 As Pilot Fuel
CNG + OPOME	CNG Used As Primary Fuel And OPOME As Pilot Fuel
CNG + OP50D50	CNG Used As Primary Fuel And OP50D50 As Pilot Fuel
CNG + Diesel With EGR	CNG Used As Primary Fuel And Diesel As Pilot Fuel With Application of EGR
CNG + JOME With EGR	CNG Used As Primary Fuel And JOME As Pilot Fuel With Application of EGR
CNG + J50D50 With EGR	CNG Used As Primary Fuel And J50D50 As Pilot Fuel With Application of EGR
CNG + OPOME With EGR	CNG Used As Primary Fuel And OPOME As Pilot Fuel With Application of EGR
CNG + OP50D50 With EGR	CNG Used As Primary Fuel And OP50D50 As Pilot Fuel With Application of EGR
CO	Carbon Monoxide
CO_2	Carbon Dioxide
CP	Cold Point
cSt	Centi Stoke
CV	Calorific Value
D100	Neat Diesel or Baseline
DI	Direct Injection
DPF	Diesel Particulate Filter
$dQ/d\Theta$	Rate of Heat Transfer in the Engine Cylinder

$dQ_w/d\Theta$	Rate of Heat Transfer from the Wall
DTBHQ	Di-tert Butyl Hydroquinone
EGR	Exhaust Gas Circulation
EN	European Union Standard
EOC	End of Combustion
EOI	End of Injection
^oF	Degree Fahrenheit
F/A	Fuel to Air
FBP	Final Boiling Point
FFA	Free Fatty Acid
FID	Flame Ionisation Detector
FIP	Fuel Injection Pump
FTIR	Fourier Transform Infra red
g	Gram
g/cc	Gram per cubic centimeter
GC	Gas Chromatography
GCMS	Gas Chromatography Mass Spectrometry
GLC	Gas Liquid Chromatographer
h	Hour
HC	Hydrocarbon
HCl	Hydrochloric Acid
HFRR	High Frequency Reciprocating Rig
H_2O	Water
HP	Horse Power
H_2SO_4	Sulphuric Acid
I_2	Iodine
IBP	Initial Boiling Point
IC	Internal Combustion
IDI	Indirect Injection
IR	Infra Red

IS	Indian standard
JOME	Jatropha Oil Methyl Ester
J50D50	50% JOME + 50% Diesel
K	Potassium
KI	Potassium Iodide
KOH	Potassium Hydroxide
KVA	Kilo Volt Ampere
kW	Kilo Watt
kW-h	Kilo Watt Hour
LSD	Low Sulphur Diesel
LPG	Liquefied Petroleum Gas
lph	Liter per Hour
m	Meter
m*	Mass Flow Rate of Fuel
1M	1 Mole
meq/kg	Milli equivalent per Kilogram
Mg	Magnesium
Min.	Minute
ml	Milliliter
mm	Millimeter
Mt	Million Tonnes
Mtoe	Million Tonne of Oil Equivalent
Na	Sodium
NaI	Sodium Iodide
NaOH	Sodium Hydroxide
$Na_2S_2O_3$	Sodium Thiosulphate
$Na_2S_4O_6$	Sodium Dithionate
NaX	Sodium Halide
NMB	National Biodiesel Mission
NO	Nitric Oxide

Nos.	Numbers
NO_2	Nitrogen Di-oxide
NO_x	Oxides of Nitrogen
nPAH	Nitro Poly Aromatic Hydrocarbon
O_2	Oxygen
OPOME	Orange Peel Oil Methyl Ester
OP50D50	50% OPOME + 50% Diesel
P	Instantaneous Cylinder Gas Pressure, (Pa)
PAH	Poly aromatic Hydrocarbon
Pb	Lead
PC	Personal Computer
PDD	Pour Point Depressants
PM	Particulate Matter
PP	Pour Point
ppm	Parts per million
P-Ɵ	Pressure – Crank Angle
PVC	Poly Vinyl Chloride
rpm	Revolutions Per Minute
SAE	Society of Automobile Engineering
SCR	Selective Catalyst Regenerative
sfc	Specific Fuel Consumption
SI	Spark Ignition
SOC	Start of Combustion
SOF	Soluble Organic Fraction
SOI	Start of Injection
ROH	Alkanol
R-OOH	Carboxylic Acid
R/P	Reserve to Production
RSM	Response Surface Metthodology
SO_2	Sulphur Dioxide

SO_x	Oxides of Sulphur
Sp.	Specific
T	Tonnes
TAN	Total Acid Number
TBN	Total Base Number
TBHQ	Tert-Butyl Hydroquinone
TCD	Thermal Conductivity Detector
TDC	Top Dead Center
TG	Tri- Glycerides
THC	Total Hydrocarbon
ULSD	Ultra Low Sulphur Diesel
UBHC	Unburnt Hydrocarbon
V	Instantaneous Cylinder Volume, m^3
vs	Versus
v/v	Volume/ Volume
w	weigh
wt/wt	Weight/Weight
γ	Ratio of Specific heat,
ρ	Density
%	Percent
μ	Dynamic Viscosity
η	Efficiency

CHAPTER 1

INTRODUCTION

1.1 Motivation for the Present Research

The development of any country is dependent on the adequate availability of energy sources and the technologies advancement. Presently, the greater portion of the energy used globally is mainly derived from fossil fuels. The limited resources and increasing energy demand have mandated a rethink on an alternative to fossil fuels. It has been found that industrial sector consumed the highest quantum of energy followed by transportation and agriculture sectors. Diesel engines are highly efficient, due to high compression ratio and are a popular prime mover in transportation, agriculture and industrial sectors. However, they also emit a large amount of particulate matters (PM), SO_X, soot, oxides of nitrogen (NO_X) and smoke emissions, which poses environmental challenges. So, there is a need for emerging cleaner combustion technologies and alternative fuels. Dual fuel combustion system is a promising technology for reducing the emissions of diesel engines without reducing power. The objective of the present work is to explore dual fuel technique using cleaner alternative fuels to reduce the emissions with improved efficiency.

1.2 Energy Scenario

The problem pertaining to depletion of fossil fuels has been felt for a long time. The transportation and power sectors are heavily dependent upon petroleum derived fuels for last many decades. However, concern about long term availability of these fuels coupled with

environmental degradation has triggered extensive research in the area of alternative fuels (Dhingra et al., 2000; Ullah et al., 2015). At present, it is predicted that the world is at its peak of fossil fuels production and consumption, which is causing unprecedented perturbation in the prices (De Almeida and Silva, 2009).

In addition to fuel security, there is another factor that has encouraged an attempt to replace the whole or part of conventional fossil fuels used in motor vehicles. This is because burning fossil fuel produces harmful emissions (including CO_2) for the public and causes adverse effects on the environment and contributes significantly to global warming produced from the fossil fuels (Dhingra et al., 2000).

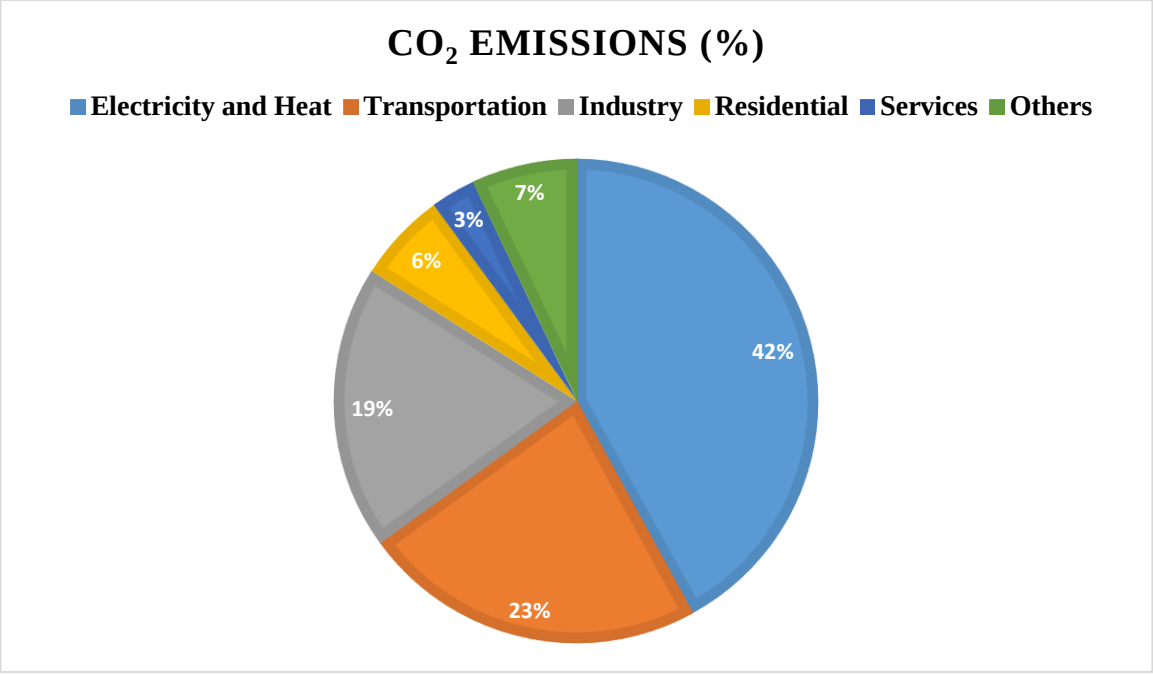

Figure 1.1: World CO_2 emissions by sectors in 2013 (IEA, 2015)

Development of a country is based on the availability of energy sources and technologies used to extract energy from these sources. It is fact that energy is an important drive for development (De Almeida and Silva, 2009). Developing countries like India, China etc. are using more energy than developed countries. Most of the energy produced worldwide is mainly derived from petroleum and wood that's why, Fossil fuel contributes 70-80% of the world's energy needs (Kruyt et al., 2009).

Table 1.1: Self-reliance of India in crude oil

Year	Production (Million Tonnes)	Consumption (Million Tonnes)	Self-Reliance (%)
2006	36	128.3	28.1
2007	36.4	138.1	26.4
2008	37.8	144.7	26.1
2009	38	152.6	24.9
2010	41.3	155.4	26.6
2011	42.9	163	26.3
2012	42.5	173.6	24.5
2013	42.5	175.3	24.2
2014	41.6	180.8	23.1
2015	41.2	195.5	21

India is the fastest growing economy in the world and requires a huge amount of energy. But, it is also well known that the crude oil resources for India are limited, which makes it heavily dependent on import of crude oil (Kumar, 2005). The crude oil consumption of India

during 2015-16 was 195.5 million tons out of which only 41.2 million tons was produced in India (BP energy, 2015). The crude oil consumption of India is increasing every year; however, production has been stagnant (BP Statistical Review, 2015). The self-reliance of India in crude oil for last 10 years shown in Table 1 (Petroleum and Natural Gas Statistics, 2014).

Therefore, sustainable fuels development needs to be improved with the substitution of fossil fuels with renewable and other alternative fuels (both gaseous and liquids).The enhancement in biodiesel production is required, as an alternative and renewable source of energy towards maximizing the self-reliance in energy security (Sahoo and Das, 2009).

1.3 Effect of Exhaust Emissions

The higher compression ratio and higher efficiency of compressed ignition (CI) engines make them popular prime mover for industrial, transportation and agriculture sectors (Seung and Chang, 2011). Moreover, the popularity of CI engine, especially in India, makes petroleum diesel consumption nearly 4 to 5 times that of gasoline (Pali and Kumar, 2016). However, diesel engines are associated with higher harmful emissions like carbon dioxide (CO_2), carbon monoxides (CO), oxides of nitrogen (NO_X), oxides of sulfur (SO_X), particulate matters (PM), soot and smoke etc. These emissions degrade the air quality which results in global warming. Figure 1.2 represents a breakdown of country's percentage of global energy-related CO_2 emissions from fuel combustion in 2013. The USA contributes 17% of global CO while the rest of the world (31.25%), China (28.03%), USA (15.9%), European Union (10.38%), India (5.8%), Russian Federation (4.79%) and Japan (3.84%) (IEA, 2015). The effects of greenhouse and other emissions are alarming. These emissions can result in unhealthy levels of air pollution,

global climate change, acid rain and respiratory problems. Therefore, it is crucial to control the production of air pollution. One way to reduce the emissions is by engine design and control of engine parameters but quite often, this will create other adverse effects. PM emission in the CI engine cannot be reduced to an acceptable level solely by engine design and control. It typically requires an after treatment system to reduce emission levels below regulatory standards. Emission limits are implemented to regulate and control emissions from light-duty, heavy-duty and stationary engines.

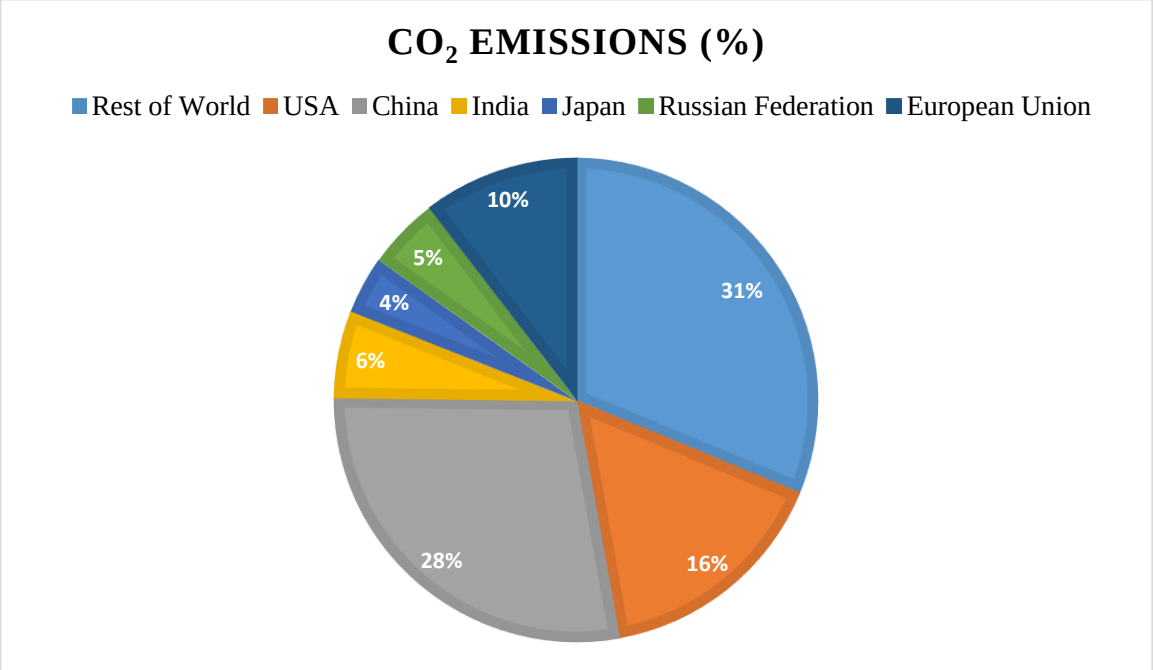

Figure 1.2: Global CO_2 emissions from fuel combustion 2013 (IEA, 2015)

So the new advanced cleaner combustion techniques and cleaner alternative fuels (both liquid and gaseous) are urgently required. A significant amount of research work has been done for reducing exhaust emissions from diesel engines with new combustion techniques (Roy et al., 2010; Bose and Maji, 2009).

1.4 Technologies and Alternative Fuels used to Reduce the Exhaust Emissions:

The use of biofuels (like vegetable oil, alcohols, biodiesel, producer gas, biogas etc.) as fuel and application of exhaust gas recirculation (EGR) and selective catalytic reduction (SCR) reduced diesel engine emissions to some extent. However, biodiesel has found most suitable liquid alternative fuel for diesel engines. The combustion and emissions characteristics of a fuel in an engine can be improved by improving properties of fuel like, ignition delay, density, calorific value, cetane number etc. Ignition delay of a fuel plays a significant role in combustion characteristic.

Biodiesel is one of the alternative fuels that have been gaining interest, since it is produced from renewable sources such as waste cooking oils, animal fats, and vegetable oils (Mohsin et al., 2014; Mo et al., 2013; Pali and Kumar, 2014; Yunus et al., 2014).The utilization has been started a long time ago when the diesel engine was invented by Rudolf Diesel. However, due to the low cost of petroleum derived fuels; utilization of biodiesel for motor vehicles could not be undertaken to a great extent (Demirbas, 2007). Biodiesel has almost similar properties to diesel fuel and it can be used in most diesel engines without any significant engine modifications, while at the same time can substantially reduce engine emissions such as HC and CO (Sun et al., 2010). Apart from having oxygen content, it also contains virtually no sulfur and free aromatics thus emit low PM.

The use of gaseous fuels (like compressed natural gas, hydrogen, liquefied petroleum gas, biogas, producer gas etc.) in diesel engine has a significant impact on performance and emissions characteristics of the engine. When these are used in a diesel engine, they reduce CO_2, NO_X, PM

and smoke emissions. However, high ignition delay and an autoignition temperature of gaseous fuels, they have associated with high HC and CO emissions with low brake thermal efficiency at lower loading conditions. The combustion and emissions characteristics of an engine can be improved by improving properties of fuel like, ignition delay, density, calorific value, cetane number etc. Ignition delay of a fuel plays a significant role in combustion characteristic.

1.5 Effect of Ignition Delay

The ignition delay period is also called the preparatory phase during which some fuel has already been admitted but has not yet ignited (Prakash et al., 1999). There is a definite period of inactivity between the time when the first droplet of fuel hits the hot air in the combustion chamber and the time it starts through the actual burning phase. This period is known as the ignition delay period. This period is counted from the start of injection to the point where the pressure-time curve separates from the motoring curve indicated as the start of combustion.

The delay period in the compression ignition engine exerts a very great influence on both engine design and performance. Ignition delay is an imperative variable in fuel combustion because it has a strong connection to the quantity of fuel that is burned in the combustion phase. Longer ignition delay allows more fuel to be injected and prepared for combustion. It is of extreme importance because of its effect on both combustion rate and knocking and also its influence on engine starting ability and the presence of smoke in the exhaust.

1.6 Dual Fuel Combustion Technique

The basic operation of dual fuel engines is shown in Figure 1.3. In the dual fuel engine, gaseous fuel is mixed with air in the intake manifold by a venturi installed after the air filter. Where a homogeneous mixture of gaseous fuel and air formed before entering the combustion chamber during the intake stroke. The mass flow rate gaseous fuel is controlled by a throttle. The amount of gaseous fuel enters into the combustion chamber is dependent on the engine load and speed. The homogeneous mixture is compressed during the compression stroke and a small quantity of liquid fuel is injected near the end of the compression stroke to the combustion chamber same as CI engines. No modifications are made to the internal workings of the engine or the diesel injection system. The gaseous fuel is the primary source of energy, hence it is known as the primary fuel. While liquid fuel act as an igniting source for primary fuel that why it is known as a pilot fuel. Dual fuel combustion technology decreases the diesel fuel consumption without decreasing the power output of the engine (Mansor et al., 2014).

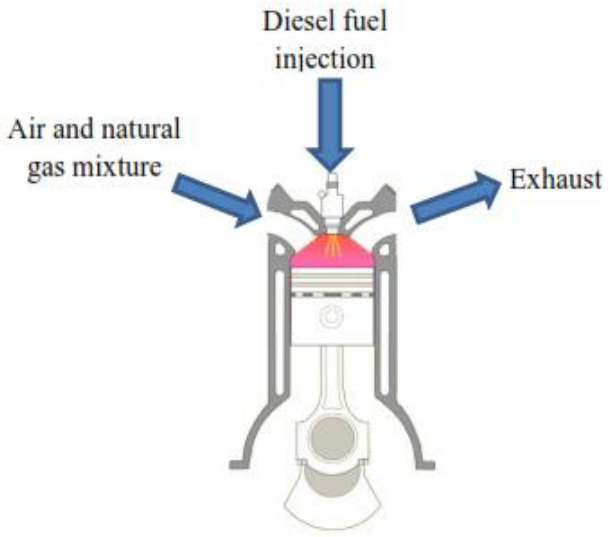

Figure 1.3: Basic dual fuel engine operation

1.6 Exhaust Gas Recirculation

High level of NO_X emissions in CI engines due to high in-cylinder pressure and temperature is the biggest challenge for researchers. In order to overcome these drawbacks, the EGR can be used. Application of EGR is a simplest and effective method for reducing NO_X emissions from a diesel engine. As already discussed, the high in-cylinder pressure, temperature and availability of oxygen inside the combustion chamber are the factors for NO_X emissions. By applying EGR, a portion of the exhaust gas which contains some unburnt hydrocarbons and CO is recirculated, and likely to probably reburnt in the next cycle. The reduction in NO_X is achieved mainly because EGR displaces oxygen concentration in the combustion chamber hence reducing the overall flame temperature. The presence of EGR will alter the combustion process and heat released in three major ways. First, the O_2 concentration is reduced as consequence of the exhaust gas presence in the combustion chamber (dilution effect). This causes the injected fuel spreads further to find oxygen for stoichiometric combustion. Therefore, the flammable region is extended. Apart from stoichiometric mixture the region also includes a portion which contains CO_2, H_2O, and N_2 from the exhaust gas. The reduced oxygen concentration also lowers the oxygen partial pressure affecting the kinetics of NO_X formation reactions (Ghazikhani et al., 2010; Maiboom et al., 2008; Alla, 2002).

The second effect of EGR is a thermal effect. CO_2 and H_2O as the inherent components of EGR have higher specific heat capacity compared to those of substances from the ambient air such as O_2 and N_2. Consequently, the overall heat capacity on the cylinder charge is reduced and hence lowering flame temperature and propensity in NO_X production.

The third effect is a chemical effect. The combustion process occurred in the combustion chamber is altered because of the presence of H_2O and CO_2 flame region. Supported by high temperature these substances undergo dissociation during combustion period modifying both the chemistry of the combustion process and formation of NO_X. Particularly, the flame temperature is reduced by the endothermic dissociation of H_2O (Ghazikhani et al., 2010; Maiboom et al., 2008).

ORGANIZATION OF THESIS

This thesis is made up of five chapters. The organization of the chapters is as follows:

CHAPTER 1: (INTRODUCTION) – This chapter gives an overview of the research topic. It starts by giving an introduction to the importance of energy, GHG emissions, climate change, fluctuating prices and depletion of fossil fuels, new combustion techniques, the significance of biofuels and recommends biodiesel as a solution to the current world energy crisis. This is followed by a background that shows the importance and use of alternative fuels in dual fuel engine, the scope of biodiesel as pilot fuel, the potential of dual fuel engine in reducing emissions for a cleaner environment.

CHAPTER 2: (LITERATURE REVIEW) - This chapter highlights a general description of energy consumption and emissions. It also discusses new combustion techniques for improving the performance of engines, introduction to dual fuel engine, benefits and limitation of new combustion technique, combustion, performance and emissions characteristics of dual fuel engine, the effect of EGR in dual fuel engine. This is followed by biodiesel as one of the emerging energy resources, its advantages and limitations, the available feedstock, technological

challenges in production, biodiesel standards and characterization, properties of biodiesel and blends with diesel.

CHAPTER 3: (SYSTEM DEVELOPMENT AND METHODOLOGY) – It explains the system development for biodiesel production, combustion chamber setup for ignition delay measurement and dual fuel engine setup development which work on both conventional diesel mode and dual fuel mode. The setup development of EGR which can be attached to engine and effect of its application were observed. It also explains research methodology for the optimization of process parameters of production using response surface methodology.

CHAPTER 4: (RESULTS AND DISCUSSION) – This chapter shows all the results that have been obtained from the experimental work and present the findings of the study followed by a detailed discussion and analysis of these findings besides comparing them with the existing results included in the literature.

CHAPTER 5: (CONCLUSION) – It provides a summary of the key findings in the light of the research and puts forward some recommendations for the future studies.

CHAPTER 2

LITERATURE REVIEW

2.1 Introduction

All over the world fossil fuel reserves are diminishing at an alarming rate. As a result, shortage of crude oil leading to increased oil prices is quite natural in foreseeable future. Apart from limited life span, global climate change due to unrestricted combustion of fossil fuels is also a major concern. In addition, there is a serious issue of deteriorating urban air quality and stringent legislations for automotive emissions. The versatility of internal combustion (IC) engines in terms of range and acceleration over battery powered and fuel cell engines makes this main workhorse in the transportation sector. IC engines also enjoy more power to weight ratio than that of its competitors namely battery powered or fuel cell operated vehicles. These factors have influenced scientists and researchers to develop environment-friendly technologies and to introduce cleaner alternative fuels like alcohol, biodiesel, natural gas etc. for ensuring the safe survival of the existing IC engines technology.

2.2 Diesel Engine

The diesel engine was invented by Rudolf Diesel a scientist in 1892. The compressed ignition (CI) engines have higher thermal efficiency than spark ignition (SI) engines. The fresh air from the environment was introduced to the combustion chamber through intake valve in diesel engines when the piston moves downward from top dead center (TDC) to bottom dead center (BDC). The amount of fresh air induced to the cylinder was depended on the speed of the

engine. It increases with increase in engine speed. This fresh air gets compressed when the piston moves upward from BDC to TDC, both intake and exhaust valves were remain closed during this. The fuel was injected at high velocity few degree before the piston reaches TDC through the fuel injector. The high-pressure fuel get atomizes just after injection. The air inside the cylinder mixes with fuel at high temperature and high pressure. The higher in-cylinder temperature makes air-fuel mixture auto ignite as fuel reaches its autoignition temperature (Heywood, 1988). This combustion leads to rapid increase in-cylinder pressure and temperature which moves piston downward with a higher force. During this piston again moves from TDC to BDC, this stroke was known as expansion stroke. Exhaust valve opened when piston reached to BDC. Which cause combust gasses escape from the combustion chamber through exhaust manifold due to the pressure difference. The momentum gets by the crankshaft force during power stroke force the piston to move upward again from BDC to TDC. This stroke is called exhaust stroke and one cycle completed with that stroke.

The complete combustion process consists of four phases; ignition delay, premixed combustion, diffusive combustion and late combustion. The ignition delay period is an important phase for any fuel and engine. Ignition delay period directly affects the other phase of combustion. Longer ignition delay decreases the premixed combustion period, however, the fuel burn in this period remains same which cause rapid combustion of fuel and results in high peak pressure and higher in-cylinder temperature. These effects further increase the NO_X, SO_X, soot, PM and smoke emissions. Hence, the ignition delay of any fuel should be controlled with the help of additives. It can be done only when measurement of ignition delay of fuel used was possible. This phase is affected not only by in-cylinder conditions such as temperature, pressure,

concentration of charge, oxygen availability but also fuel chemical and physical characteristics like viscosity, cetane number etc. (Lata and Misra, 2011).

2.3 Emissions from Diesel Engine

Internal combustion engine was a second largest contributor to air pollution after power generation. The diesel engine is the backbone of transportation due to its high thermal efficiency. However, they are associated with higher harmful emissions like CO_2, NO_X, SO_X, soot, PM and smoke. The concentration of diesel engine emissions depends on factors such as engine design, injection timing, engine speed and load, air-fuel ratio, fuel physical and chemical properties etc.

2.3.1 Carbon dioxide

Carbon dioxide is the primary byproduct of the combustion of carbon-contained fuels. Higher the carbon concentration in the fuel results in higher CO_2 emission. CO_2 is the primary element of greenhouse gasses along with methane, nitrous oxide, sulfur hexafluoride, hydrofluorocarbons and perfluorocarbons (Kaewmai et al., 2012). Although, CO_2 already available in the environment but its concentration is low. But, the amount is increasing at worrying rate from past years. Globally, continuous increasing fossil fuel utilization, deforesting and long life of CO_2 adversely effect on climate changes which make a serious concern to every country.

The projected growth in vehicle ownership drives oil demand growth, with average incomes in India reaching a level at which rapid increases are expected in car ownership. The implications of this for oil demand would be even higher, were it not for the planned introduction

of a national fuel-economy standard of 4.8 liters per 100 kilometers by 2021-2022. Due to the relatively small size of cars in India, average fuel efficiency is relatively high when compared with other countries (IEA, 2015).

The second largest CO_2 contributor, transport sector, some approaches need to be executed to achieve the reduction in CO_2 emissions. The use of engine technologies which increases the fuel conversion efficiency, the use of low carbon content fuels, the use of renewable alternative fuels, use of gaseous fuels and new highly efficient combustion technologies are some of the proposed strategies (Johansson et al., 1996).

2.3.2 Oxides of nitrogen

Oxides of nitrogen (NO_X) is one of the major air pollutants emitted by diesel engines, mainly consist of NO and NO_2 in which NO is predominant component. The tendency of formation of NO_X in combustion chamber generally described by three approaches. The first approach is thermal NO_X, in which NO_X formation depends on the molar concentration of oxygen at higher in-cylinder temperature. The thermal NO_X formation mechanism is described by Zeldovich equations. The Zeldovich equations are expressed below:

$$N_2 + O \longrightarrow NO + O$$

$$N + O_2 \longrightarrow NO + O$$

$$N + OH \longrightarrow NO + H$$

In the second approach, the NO_X was formed from nitrogen present in the fuel. Higher nitrogen contained fuel produced a high amount of NO_X. However, the nitrogen level in current petroleum diesel is not significant. The species of NO_X formed through this approach are CN, HCN, NH, NH_3, etc. (Fernando et al., 2005).

The third approach of NO_X formation is prompt, in which HCN is produced in the combustion chamber by reacting radicals of hydrocarbon with nitrogen. When the richer mixture is supplied to the combustion chamber the equivalence ratio is increased which increase the amount of HC radicals. In other words, higher HC radicals in the combustion process result in higher NO_X formation through this mechanism.

$$CH + N_2 \longrightarrow HCN + N$$

$$CH_2 + N_2 \longrightarrow HCN + NH$$

$$HCN + OH \longrightarrow CN + H_2O$$

$$CN + O_2 \longrightarrow NO + CO$$

Three different approaches which are responsible for total NO_X production during combustion of fuel inside the combustion chamber were discussed. In these three approaches, it was believed that, first approach play most important part in NO_X formation (Ban-Weiss et al., 2007). Apart from this, NO_X formation also depends on the carbon-hydrogen ratio (C/H) of the fuel. It was reported that higher C/H ratio cause higher adiabatic flame temperature which results in higher NO_X formation (Miyamoto et al., 1994). Most of the alternative fuels have lower C/H ratio compared to petroleum diesel which beneficial in lower NO_X emissions.

2.3.3 Particulate matter

Particulate Matter (PM) is the typical emission of diesel engines and significantly higher compared to SI engines. The reason for this is non-homogeneous combustion process in the combustion chamber. Also, PM increases with the higher concentration of fuel inside the combustion temperature. However, the formation of PM decreases with increasing in-cylinder temperature. Hence, its concentration increases with increasing engine load and engine speed. At this engine condition the combustion temperature is high but a significant high fuel concentration the sole results increase in PM emission. Along with that, the concentration of oxygen inside the combustion chamber also play an important role in PM emission. PM emission increases with a decrease in oxygen concentration. Therefore, richer fuel-air ratio results in higher PM emissions.

The aromatic content in fuel also responsible for PM emission (Xinling and Zhen, 2009). Thus, a low aromatic content in fuel results in a reduction in PM concentration. Also, Miyamoto et al., (1996) has recognized that reducing the number of molecular C-C bonds and increasing oxygen content in a fuel significantly reduce PM emission. The sulfur content in the fuel also affects PM emission. Tan et al., (2009) have observed that decrease in PM emissions has been noticed with decreasing sulfur content in the fuel. Moreover, the effect of sulfur content in the fuel on PM emission is more significant at low engine load conditions. Consequently, modifications to in-cylinder conditions through dual fuel combustion mode and changing fuel properties by using oxygenated and free-aromatics fuels were probably controlled the PM emissions.

2.3.4 Carbon monoxides

Carbon monoxide (CO) is a colorless, tasteless and odorless, and non-corrosive gas which is poisonous to human beings. CO is an intermediate product produced due to incomplete combustion of carbon-contained fuels.

The formation process of CO is the first stage of burning of hydrocarbon fuels in the presence of oxygen. First CO produced which further react either with oxygen or hydroxyl (OH) and produce carbon dioxide. Though, the CO oxidized slowly compared to hydrocarbons (Bagal et al., 2009). Thus, the appropriate in-cylinder conditions are required to minimize the CO formation.

The over mixing and under mixing of air and fuel in the diesel engines are two important factors of CO formation (Bagal et al., 2009). The over mixing is associated with leaner fuel-air ratio during ignition delay and low in-cylinder temperature. Therefore, carbon in the fuel is not fully oxidized in this condition ever after the presence of abundant oxygen. On the other hand, under mixing condition is associated with richer premixed combustion. Hence, fuel does not mix with air properly and cannot be fully oxidized and results in high CO formation.

It was concluded that the CO formation in the combustion chamber is affected by in-cylinder temperature, oxygen concentration and charge mixture turbulence. Hence, sufficient availability of oxygen and higher in-cylinder temperature are required to full oxidation of the fuel. Lots of effort have been taken to control the CO emissions to achieve an acceptable level. Such as a change in combustion chamber design, changing fuel injection timing, change in

combustion chamber size and use of oxygenated and alternative fuels (Chen and Iwashina, 2009; Lapuerta et al., 2008a).

2.3.5 Unburnt hydrocarbons

Hydrocarbons are produced from the incomplete combustion of hydrocarbon fuel. The concentration level is related to misfire and poor charge mixture due to insufficient mixing between fuel and air. There are several sources for the formation of the UHC emissions such as oil film layers, wall flame quenching, deposits and crevices in the combustion chamber, liquid fuel, and exhaust valve leakage (Alkidas, 1999). However, the most influential factor for UHC source in fully warmed conditions is combustion chamber crevices (about 38%) whereas under cold start or cold conditions the main UHC sources are wall flame quenching, lubricating oil films and fuel preparation (Alkidas, 1999).

Combustion chamber crevices act as the main place for UHC sources because the very small space available causes flame quenching. The crevices in the cylinder can be a head gasket and valve-seat crevices, and piston-ring-pack (Heywood, 1988).

The occurrence of wall flame quenching is when the propagation of flame reaches the cylinder wall forming a thin layer on the surface without oxidation. This layer then is called quenching distance. In this case, the cylinder wall can act as an interrupt mechanism of the oxidation reaction and the heat sink results in an in-cylinder temperature drop. Therefore, the cylinder wall temperature is very important in terms of determining the UHC emission level.

Moreover, oil used for lubrication between piston rings and cylinder liner also can contribute to the UHC emission. The oil thin film absorbs fuel thus prevents fuel taking part in the combustion process, and escapes the combustion chamber unburned. In addition, fuel used also affects the UHC emission. Fuels which contain aromatics and olefins generally produce a higher concentration of hydrocarbon.

In dual fuel operation, the lower air-fuel ratio due to air replacement results in high UHC emission compared with normal diesel operation. The high heat capacity and lack of oxygen in the combustion chamber leads to a temperature reduction in in-cylinder as a result of misfiring and poor mixing, and hence resulting in slower combustion rate allowing unburned mixture to leave the combustion chamber (Sahoo et al., 2009).

In order to reduce the UHC emission, some techniques are introduced to enhance the mixing time and intensity such as varying the fuel injection timing, increasing fuel injection pressure, and modifying the piston head. The high measured UHC emission concentration can give an indication of high cyclic variability as results of partial burning or misfire cycles (Heywood, 1988).

2.4 Dual Fuel Engine

In dual fuel engine, the combustion of pilot fuel took place in a lean premixed homogeneous mixture of air and gaseous fuel. The combustion of a premixed homogeneous mixture of air and gaseous fuel initiated by diesel flame and further propagated in the cylinder. The pressure and temperature of the homogeneous mixture increase rapidly during the compression stroke, which forms the pre-ignition environment in the combustion chamber

Mustafi and Raine, 2008). The pilot fuel was injected just before piston reach the top dead center so that the combustion of pilot fuel started at the end of compression stroke. The combustion of diesel fuel greatly influenced by swirl, turbulence, and squish within the cylinder.

Rajput (2005) and Sarvanan et al., (2008) observed that convention diesel engine shows higher in-cylinder pressure compared to dual fuel engine, especially at lower and intermediate loading conditions. The reason for this was higher ignition delay, leaner combustion and poor gaseous fuel utilization. The same results were reported by Papagiannakis (2013) and Abdelaal et al., (2012). However, due to larger ignition delay in dual fuel engine, the peak in-cylinder pressure of dual fuel engine occurs slightly later compared to a conventional diesel engine (Abdelaal et al., 2012; Papagiannakis, 2013; Rajput, 2005). Further, with improving gaseous fuel utilization with load, the dual fuel engine shows higher in-cylinder pressure compared to conventional diesel engine at higher loading condition.

Heat release rate (HRR) is an important parameter for determining the performance of an engine (Bueno et al., 2012). The net HRR is calculated by computing the amount of energy released from the fuel to obtain the experimentally observed pressure, while the combustion reaction extent is evaluated through the released fraction of the total fuel chemical energy. Abdelaal et al., (2012) in their study using a naturally aspirated diesel engine, describe that longer ignition delays in the dual fuel engine have a negative impact on the HRR. Generally, the diesel engine exhibits better HRR trends than the dual fuel engine. In the diesel engine, a large amount of diesel is utilized especially at high load resulting in high in- cylinder temperatures. The reduced HRR in dual fuel operation is mainly due to the very lean mixture of air and

gaseous fuels. This affects the combustion in dual fuel; a portion of natural gas usually escapes the combustion process resulting in low combustion efficiency and high HC emissions.

Brake thermal efficiency (BTE) is an important parameter to analyze the performance of any engine. The most of the literature shows a similar trend of BTE for a particular combination of fuel in dual fuel engine. Vijayabalan et al., (2009) identified that dual fuel engine suffering from low BTE compared to a conventional diesel engine, especially at low loading condition. This is due to lean fuel-air mixture at low load which results in poor gaseous fuel utilization. The similar trends were also shown by Papagiannakis et al., (2013); Yadav et al., (2012); Ryu (2013b). Abdelaal et al., (2012) mentioned, due to very lean mixture of air and gaseous fuel, some mixture which comes directly comes in pilot fuel burning zone get combusted; rest was escaped from the combustion chamber. The authors also reported better fuel utilization at high loads in dual fuel engines. This is due to more amount of gaseous fuel is introduced, which leads to better gaseous fuel combustion and higher BTE at high loads. In contrast, at high loads diesel engine combustion sees an increment in heat loss to the cylinder wall, therefore negatively impacting the thermal efficiency. As a consequence, more power may be produced in dual fuel combustion.

Brake specific energy consumption (BSEC) defined the energy consumed by the engine to produce per kilowatt hour work. It is directly proportional to the BSFC. The BSFC is depended upon compression ratio and ϕ (Lounici et al., 2014). Multiple fuels are used in dual fuel engine that's why BSEC was preferred over BSFC (Ryu, 2013b). Ryu, (2013b) observed that dual fuel engine suffers from high BSEC compared to a conventional diesel engine, especially at low load condition. Similar results were observed by Misra et al., (2011); Gross et

al., (2013). This is due to low in-cylinder pressure and temperature and leaner air gaseous fuel mixture at low load condition which results in poor fuel utilization. At higher load, the improved fuel utilization in dual fuel engine improves the BSEC of dual fuel engine. Hence at higher load, the BSEC of dual fuel engine is lower than a conventional diesel engine (Crookes et al., 2009).

The significant numbers of studies have been invested in analyzing the emissions characteristics of dual fuel engines. Uma et al., (2004) in their research article stated that the existence of gaseous fuels reduced the quantity of diffusive combustion in dual fuel engine and replace it with lean premixed combustion, which affects the NO_X emissions. The same declaration is supported by Lounici et al., (2014) in their research in which they used a single cylinder, naturally aspirated Lister Petter-TS1 diesel engine. However, some literature suggested that the NO_X emissions were also lower at high load compared to conventional diesel engines. Whereas, some literature claimed, higher NO_X emissions in dual fuel engines compared to conventional diesel engine at higher load. The author of this study attributes this to the combustion of liquid fuel near TDC creating a high charge temperature which remains at a high temperature longer in dual fuel engine than a conventional diesel engine.

In dual fuel engine, the leaner air-fuel mixture results in high UHC emission compared to a conventional diesel engine. The high heat capacity and lack of oxygen in the combustion chamber leads to a temperature reduction in in-cylinder as a result of misfiring and poor mixing, and hence resulting in slower combustion rate allowing unburned mixture to leave the combustion chamber (Sahoo et al., 2009; Singh et al., 2004). Namasivayam et al., (2009) have reported that trend of UHC emissions for dual fuel engine was higher in all operating conditions compared to a conventional diesel engine. Similar trends were given by Alla et al., (2001).

2.5 Primary Fuels

There have been many published studies on the use of gaseous fuels in CI engines such as biogas, producer gas, hydrogen, natural gas, compressed natural gas (CNG) and liquefied petroleum gas (LPG). These fuels vary in chemical composition, which has a significant impact on engine emissions and performance. As already discussed earlier, the gaseous fuel act as main fuel in dual fuel engine so known as the primary fuel. Therefore, the choice of primary fuel is important in dual fuel engine.

2.5.1 Biogas

Biogas is the combustible fuel which is produced by the organic breakdown of organic matter in the absence of oxygen (Chen et al., 2016). The organic matters are a by-product of alcohol or biodiesel production and residue of agriculture they also include animal dung, food processing, municipal and industrial waste (Yoon et al., 2011). As discussed earlier, the production of biogas is possible in the lack of oxygen environments. The process involves three stages; hydrolysis, acid formation, and methane fermentation (Rahmouni et al., 2002). The main content of biogas are; methane (CH_4), hydrogen (H_2) and carbon monoxide (CO). However, the composition of biogas depends on the feedstocks and the process conditions such as temperature, pH, water content etc. (Huang and Crookes, 1998). The energy content in the biogas goes up to 28.8 MJ/kg in some favorable conditions (Deublein and Steinhauser, 2008).

Presently, the biogas is mostly used for electricity production and cooking of foods. In other option, biogas can be used as fuel in internal combustion engines. However, the use of biogas is still under consideration due to several factors; poor quality of biogas, commercial

availability, limited fuelling and distribution stations and relatively higher cost of dual-fuel vehicles compared to those which are running from other alternative fuels (Lantz et al., 2007).

The use of biogas as the primary fuel in dual fuel engine decrease the CO_2 emissions because of its mainly composed of methane which has low carbon-hydrogen ratio and easily forms a homogeneous mixture with air (Corbo et al., 1995). Also, methane has high octane number which reduces the knock tendency of biogas. However, the presence of CO_2 in biogas possibly decreases the flammability range which results in deterioration in combustion process such as increasing ignition delay, lowering the flame temperature and prolonging cyclic combustion variation (Sahoo et al., 2009; Bora and Saha, 2016). Also, the presence of CO_2 reduced the calorific value of biogas and decrease fuel conversion efficiency by reducing combustion enthalpy and flame speed. The higher autoignition temperature of biogas is also a big problem to use it in vehicles. However, with improved engine design and optimizing operating conditions help in enhancing the combustion and thermal efficiency of the (Roubaud et al., 2005).

Bora and Saha (2016) found that the application of biogas as the primary fuel with diesel in dual fuel engine decreases the BTE of the engine due to the low calorific value of biogas. Also, increased exhaust gas temperature in dual fuel engine than conventional diesel engine at higher load was noticed by Cacua et al., (2016). Other exhaust emissions such as NO_X, CO, UHC etc. were found lower when biogas was used as primary fuel in dual fuel engine.

2.5.2 Hydrogen

The use of alternative fuels for internal combustion engines is an effective approach for reducing pollutant emissions occurs due to combustion of fossil fuel and improve national energy security by reducing dependency on imported crude oil (Gatts et al., 2012). Due to better performance drives and clean burning characteristics, hydrogen becomes most promising alternative fuel for transportation and powertrains systems (Saravanan et al., 2008; Gopal et al., 1982). Apart from emissions benefits of hydrogen some other properties like; higher calorific value, flame propagation speed and flammable limit of hydrogen makes it favorable fuel for automobiles (Verhelst and Sierens, 2001; Mathur et al., 1993; Tomita et al., 2001).

Hydrogen has high octane number, which makes it a good substitute for petroleum gasoline fuel. High octane number resist knocking under SI engine operation (Korakianitis et al., 2010). Further, as hydrogen doesn't have carbon so it produces low pollutions compared to other carbon containing fuels. Hydrogen can be burn at lean mixture so vehicle using hydrogen as a fuel can operate at low equivalence ratio. In this condition, the possibility of NO_X formation is low. However, at higher loading condition, the NO_X formation was found higher compared to other fuels (Das, 2002; Edwin-Geo et al., 2008). The reason for this is low ignition energy of hydrogen which makes it ignite in the presence of hot spots and gasses. This cause early start of combustion which then increases the heat release rate and further higher in-cylinder pressure and temperature. Some other issues like premature ignition and backfire cause knocking in the engine (White et al., 2006; Karim and Zhigang, 1992).

The mass specific heating value of hydrogen is higher than other gaseous and liquid fuels. However, the energy density of hydrogen is much lower than other fuels due to low density. Stoichiometric combustion of hydrogen required an air-hydrogen ratio of 34:1 which is much higher compared to other fuels. However, hydrogen displaces more of the combustion chamber compared with other fuels. This leads to less air in the combustion chamber but at the same time improve energy content of the stoichiometric mixture of air and hydrogen.

The utilization of hydrogen is expanded to compression ignition engines to capitalize the benefit of hydrogen combustion characteristics. In his research, Boretti (2011) modified the combustion chamber for pre-chamber injection of hydrogen with a glow plug unit. It is found that the brake thermal efficiency of the engine is improved for the same BMEP output compared to conventional diesel fuel operation.

The hydrogen is also used as primary fuel in dual fuel engine. Different researchers use hydrogen in dual fuel engine as primary fuel either injected through intake manifold or directly into the combustion chamber. The direct hydrogen injection into combustion chamber technique improves the volumetric efficiency and power density of the engine compared to port injection technique (White et al., 2006). Mohammadi et al., (2007) investigated, the reduction in exhaust emissions with improved engine performance was observed with increasing load when hydrogen concentration kept constant. All research done on hydrogen are carried out on stationary engines. The application of hydrogen in a car is still a technical challenge.

2.5.3 Liquefied petroleum gas

Liquefied petroleum gas (LPG) is a hydrocarbon-based gas which is produced during the refining of crude oil (Ashok et al., 2015). LPG is primarily consists of butane, propane, propylene and other lighter hydrocarbons (Raslavicius et al., 2014; Goldsworthy, 2012). However, the actual composition of LPG which is commercially available in different countries depends on refining process, quality of crude oil used, season and cost (Masi, 2012). In warm countries, the proportion of butane is more while in cold countries propane has higher proportion help to maintain enough vapor pressure in winter (Price et al., 2004). LPG can be easily liquefied at atmospheric temperature and low pressure (0.7–0.8 Mpa). So, storage and transportation of LPG are much easier than other gaseous fuels, it can be easily stored in steel cylinders.

The emissions of LPG-driven vehicles are low and LPG is commercially available in most countries (Johnson, 2003). It has been proven that LPG-operated vehicles have benefit in reducing emissions compared to that of petroleum liquid fuels. A decrease in main emissions such as HC, CO, NO_X, PM, CO_2, soot and smoke is obtained mainly due to high hydrogen-carbon ratio and no aromatic hydrocarbons of LPG. This is supposed to encourage the utilization for transportation. However, its utilization both for the heating system and the motor vehicle is still limited.

LPG has high octane number, the high calorific value compared to some other gaseous fuel but it has low cetane number. The high octane number of LPG makes it a good fuel for SI engines (Ashok et al., 2015). However, it has been required to utilize LPG in CI engines to gain better engine thermal efficiency as well as improved emissions characteristics. High octane

number permits LPG to be used at high compression ratio with less chance of detonation. However, the use of LPG in CI engines is a big challenge and rarely used. But, LPG is used in the CI engine in the dual fuel mode only and in this operating mode it has been widely studied.

LPG has low molecular weight due to high vapor pressure and its simple chemical compound than conventional diesel. Therefore, in dual fuel engines, homogeneous air-fuel mixture followed by premixed combustion can be easily attained. Thus, significantly lower soot and CO_2 emissions are noticed while using LPG as the primary fuel in dual fuel engines (Alam et al., 2001; Campbell et al., 2004). In addition, the premixed combustion rapidly increases while the quantity of LPG increases in dual fuel engine, because LPG is a reactive gaseous fuel (Stewart et al., 2007). However, the low cetane number of LPG increases the ignition delay of the mixture with increasing LPG concentration. The change in injection timing may restore the start of ignition for keeping the combustion benefits.

The application of LPG in dual fuel engines shows some adverse effect such as poor brake thermal efficiency and high UHC emissions, especially at low load conditions (Krishnan et al., 2016). The UHC emissions can be reduced by increasing pilot fuel quantity, but soot and PM emissions increases (Li et al., 2016). However, with increasing load, the brake thermal efficiency of the engine improves due to improved LPG combustion (Krishnan et al., 2016).

2.5.4 Compressed natural gas

Compressed natural gas (CNG) is a colorless, odorless and tasteless combustible gas. The emissions out after combustion of CNG are very less compared to other fuels, that's why CNG is considered as ideal fossil fuel. Another advantage of CNG is that it is safer to transport and store

compared to other gaseous fuels. The major constituent of CNG is methane (CH_4). The other constituents of CNG are ethane (C_2H_6), propane (C_3H_8), butane (C_4H_{10}), pentane (C_5H_{12}), hexane (C_6H_{14}) etc.

CNG is basically natural gas which is compressed to 250 bar. In 1000 B.C, Natural Gas was discovered during a lightning strike, which caused it to seep out through the earth's surface. This appears as a spring of fire commonly known as a "burning spring". One of the most popular burning springs was found in Greece on Mount Parnassus, now known as Oracle of Delphi. These types of springs were observed in Greece, India and Persia (Natural Gas.org, 2013). In 500 B.C the Chinese were the first to capture and use Natural Gas as a fuel for cooking by transporting them through bamboo pipelines. While the British were the first to commercialize its use in 1785, the commercial use of Natural Gas began in the U.S in 1816, as a source of energy to light streetlights in Baltimore, Maryland (Natural Gas.org, 2013).

During most of the 19^{th} century, Natural gas was used almost exclusively as a source of light, but the invention of the Bunsen burner by Robert Bunsen in 1885 opened new opportunities to use Natural gas. Since then, Natural gas applications have expanded to home appliances such as stoves, clothes dryers, and furnaces and industrial applications such as engines for electrical power generation, pumping, and compression and boilers for process heating.

Technology for environmental pleasant vehicles is continuously being developed. To reduce air pollution various strict emission regulation laws are enforced by governments of many countries. Therefore, to fulfill the new emission regulations many automobile companies have

explored new environmentally friendly vehicle (Ismael et al., 2015; Weaver and Turner, 1994). Furthermore, the technology used in currently used SI and CI engines are continuously improved to enhance the performance and emissions characteristics of the engines. The CNG has become a lower priority than gasoline fuel, even though it is considered an environmentally friendly fuel because gasoline is cheaper and easier to transport than CNG. However, continuous increasing crude oil prices and increasing production of gaseous fuels, increase the supply of CNG which results in a decrease in CNG price. Therefore, the use of CNG as a fuel in internal combustion engines is rising.

CNG has high octane number (120) and higher calorific value (49-53 MJ/kg), which make it an ideal fuel for SI engines. The autoignition temperature of CNG is higher than gasoline. Therefore, it required powerful ignition source than required for gasoline. The application of CNG in SI engine give better brake thermal efficiency with low exhaust emissions, that's why CNG is used in SI engines worldwide. Another reason for increasing demand of CNG as a fuel for internal combustion engines is commercially available of CNG worldwide. In India, the application of CNG as a fuel for internal combustion engines is increasing rapidly. The reason for that is high thermal efficiency, cheaper than diesel and gasoline and commercially available of CNG at filling stations. However, the use of CNG in CI engines is a big challenge and rarely used. But, CNG is used in the CI engine in the dual fuel mode only and in this operating mode it has been widely studied.

Dual-fuel combustion, burning CNG and diesel, is an attractive alternative to diesel because CNG is clean-burning, abundant, and has been shown to decrease particulate matter (PM) emissions (Carlucci et al., 2008; Namasivayam et al, 2010). CNG is inexpensive, has low

greenhouse gas emissions, and yields lower NOx and CO emissions (McTaggart-Cowan et al., 2006; Olsen et al., 2007). CNG consumption has risen since 1995 due to tax incentives, increased CNG supply, and falling prices (Nithyanandan et al., 2016). Performance and emissions of diesel/CNG dual-fuel combustion have been extensively studied. It has been shown that dual-fuel combustion can achieve efficiencies similar to that of diesel (Nithyanandan et al., 2016). Unburned hydrocarbons (UHC) and carbon monoxide (CO) emissions are typically higher compared to pure diesel, however, significantly decreased soot emissions have been reported (Korakianitis et al., 2011; Yoon and Lee, 2011; Karavalakis et al., 2012).

PM has been a serious concern for human health due to its direct and broad impact on the respiratory organs, as well as contributing to the global warming issue. Diesel exhaust gas is a major contributor to combustion-derived PM air pollution. As such, PM emission standards are continually evolving and becoming more stringent globally.

2.6 Biodiesel as Pilot Fuel

As discussed earlier the gaseous fuel used as primary fuel in dual fuel engine, which generally has higher autoignition temperature. That's why the air-fuel mixture doesn't auto ignite after compression stroke. The pilot fuel act as an ignition source for primary fuel, which has low self-ignition temperature and cetane number near to diesel fuel (Paul et al., 2014; Gautam et al., 2013; Kumar and Kumar, 2016c). Most of the biodiesel has lower autoignition temperature (180-230 °C) and higher cetane number (45-65) compared to petroleum diesel. These properties indicate that biodiesel can be used as pilot fuel.

2.6.1 Biodiesel production

Biodiesel is long chain mono-alkyl fatty acids produced from renewable sources such as vegetable oils, waste cooking oil or animal fats and alcohol with or without the presence of a catalyst (Sinha et al., 2008; Gautam et al., 2016). It is one of fastest growing interest alternative fuel. The utilization has been started a long time ago when the diesel engine was invented by Rudolf Diesel. However, due to the low cost of diesel and gasoline, the utilization of biodiesel for motor vehicles decreases. As the global crude oil price increases due to its gradually declining sources and the concern for the environmental problem, the attention for its utilization arises again. In addition, the main raw materials for biodiesel production are abundant, biodegradable and relatively easy to find and hence can reduce the dependency on petroleum (Demirbas, 2007; Vibhanshu et al., 2014).

Biodiesel, as an alternative fuel, has relatively similar properties to diesel fuel and it can be used in most diesel engines (neat or as an additive) without any significant engine modifications while at the same time can substantially reduce engine-out emissions such as HC and CO (Sun et al., 2010). Apart from its oxygen content it also contains virtually no sulfur and free aromatics thus emit low PM (Kitamura et al., 2002). As an additive, the more biodiesel content in the fuel blend the more emission advantages. It is also a nontoxic and biodegradable fuel and hence minimizing the risk to environment and ground water (Shahid and Jamal, 2008; Ahmed et al., 2014). Because of all the advantages biodiesel has been used widely as a vehicular fuel.

However, biodiesel has some limitations which need to be addressed. Some major properties that can affect the engine performance and emissions are higher viscosity, less favorable cold flow properties, and lower heating value and volatility. In addition, its high bulk modulus of compressibility can lead to the advanced fuel injection timing which can increase NO_X emissions. The lower heating value results in an increase in fuel consumption while its cold flow property results in difficulty to start the engine in cold weather. However, its high viscosity improves engine lubricity thus can lengthen the engine life (Shahid and Jamal, 2008; Boehman et al., 2005). In addition, it is suggested that the combination of biodiesel and gaseous fuels with their specific characteristics in dual fuel engine may become a solution for dual fuelling system to overcome the emission issues (Selim et al., 2008).

Biodiesel can be produced through transesterification which aims to reduce the viscosity, improve cold flow properties and cetane number of the raw oil. In this regards transesterification is found one of the best methods due to high yields, simplicity and its low cost advantages over other methods (Agarwal, 2007; Nigam and Singh, 2010). Transesterification is also known as alcoholysis. Transesterification is defined as the chemical reaction of vegetable oils with alcohol in the presence of a catalyst, sometimes catalysts may not be used. One mole of oil is reacted with three moles of alcohol in the presence of a catalyst and produce one mole of glycerine with three moles of alkyl esters (Van Gerpen, 2005). These alkyl esters are known as biodiesel. The triglycerides are converted stepwise into diglycerides, monoglyceride and finally glycerol which are easily separated through gravity separation into biodiesel and glycerol. Glycerol is an important by-product of the cosmetic industry. Methanol and ethanol are the two main alcohols which are generally used in transesterification process as they are relatively low cost.

Generally, transesterification process includes two main processes; catalytic and non-catalytic methods. The catalyst enhances the solubility of alcohol and thus increases the reaction rate. The most frequently used process is the catalytic transesterification process. The alkaline catalytic method is the fast and economical. An alkaline catalyst proceeds at around 4000 times faster than with the same amount of acid catalyst (Silitonga et al., 2011; Atabani et al., 2013). Moreover, this method can achieve high yield and purity of biodiesel product in a short time (30-60min). The widely reported alkaline catalysts include NaOH, KOH, $NaOCH_3$ and $KOCH_3$. Researchers have reported that both sodium and potassium hydroxide perform equally well. Sodium and potassium methoxides favored high yields than other base catalysts but they are costly.

However, in using alkaline catalysts, free fatty acid (FFA) level should be below the desired limit (ranging from less than 0.5% to less than 3%). Beyond this limit the reaction proceeds with difficulty and challenges such as soap formation and reduced esters yields (Lin and Fan, 2011). In addition to this, the reaction has several drawbacks; it is energy intensive; recovery of glycerol is difficult; the catalyst has to be removed from the product; alkaline wastewater requires treatment and the level of free fatty acids and water greatly interfere with the reaction (Sharma et al., 2008; Shahid and Jamal, 2011).

Acid catalysts include sulphuric acid, hydrochloric acid, ferric sulfate acid, phosphoric acid, para-toluene sulfonic acid (PTSA) and Lewis acids ($AlCl_3$ or $ZnCl_2$). Researchers have shown that acid catalysts are more tolerant than alkaline catalysts for vegetable oils having high FFA and water. Therefore, the acid catalyst is used to reduce the free fatty acids contents to a level enough for alkaline transesterification which is preferred over the acid catalyst after the

acid value is reduced to the desired limit. It has been reported that acid-catalyzed reaction gives very high yield in esters. However, the reaction is slow (3-48h). It has been reported that the homogeneous transesterification consumes a large amount of water for wet washing to remove the excess salt from the neutralization process, and the residual acid or base catalyst (Teo et al., 2014). Nevertheless, this technology has relatively low energy use, high conversion efficiency and cost effective reactants and catalyst (Sharma et al., 2008; Shahid and Jamal, 2011).

The catalytic transesterification has some challenges such as; long reaction time, poor catalysts solubility and poor separation of the products. Furthermore, the wastewater generated during biodiesel purification is not environment-friendly. To overcome these challenges, other faster methods such as supercritical fluids method have been developed. For example, during supercritical esterification, reaction completes in a very short time (2-4 min) compared to catalytic transesterification.

Further, since no catalyst is used, the purification of biodiesel and the recovery of glycerol are much easier, trouble-free and environment-friendly (Manuale et al., 2011; Demirbas, 2009). However, the method has a high cost in reactor and operation (due to high pressures and high temperatures) and high methanol consumption (e.g. high methanol/crude-oil molar ratio of 40/1) (Gupta et al., 2014; Deshpande et al., 2010; Rathore and Madras, 2007).

Transesterification reaction is affected by various parameters depending upon the reaction conditions. The reaction is either incomplete or the yield is reduced to a significant extent if the parameters are not optimized. The most important parameters that affect the

transesterification process reported include molar ratio, reaction temperature, reaction time, catalyst concentration and stirring speed (Balat and Balat, 2010).

2.6.2 Optimization of biodiesel production

Gandure et al., (2014) emphasized the need for process optimization for biodiesel production, the author reported the importance of process optimization which includes large scaling of production, development of reaction kinetics, reduced production cost, reactor design, and predicting yields. The statements also supported by Tan et al., (2011). The optimization of biodiesel was done by various researchers on different feedstocks. Uzun et. al., (2012) take castor oil and investigated the optimization of biodiesel production using full factorial design. Effects of methanol/oil molar ratio, catalyst concentration and temperature were optimized according to the 24 full factorial central composite designs (CCD). The yield of biodiesel was obtained according to second order model as a function of these variables.

After going through a number of literature it was noticed that average yield of more than 90% was obtained in most of the cases. Lee et. al., (2011) employed CaO–MgO mixed oxide catalyst in the transesterification of non-edible Jatropha curcas oil into biodiesel. Response surface methodology (RSM) using central composite design (CCD) was employed to statistically evaluate and optimize the biodiesel production process. It was found that the production of biodiesel achieved an optimum level of 93.55% yield at the following reaction conditions: 1) Methanol/oil molar ratio: 38.67; 2) Reaction time: 3.44 h; 3) Catalyst amount: 3.70 wt.%; and 4) Reaction temperature: 115.87 °C.

Economically, transesterification of Jatropha curcas oil using heterogeneous catalyst CaO–MgO mixed oxide required less energy which contributed to high production cost in biodiesel production. Wu and Leung (2011) carried out an optimization study on the production of biodiesel from Camelina seed oil using alkaline transesterification. The optimization was based on sixteen well-planned orthogonal experiments. Parameters including methanol ratio, reaction time, temperature and catalyst concentration were investigated. It was found that the order of significant factors for biodiesel production was reaction temperature > catalyst concentration > methanol to oil ratio > reaction time. Based on the results of the range analysis and analysis of variance (ANOVA), the maximum biodiesel yield was found at a molar ratio of methanol to oil of 8:1, a reaction time of 70 min, a reaction temperature of 50°C, and a catalyst concentration of 1 wt.%. The product and FAME yields of biodiesel under this optimal conditions reached 95.8% and 98.4%, respectively.

Enzymes as catalysts have also been very effective catalysts in biodiesel production. Yucel (2012) immobilized microbial lipase from T. lanuginous supported on poly-glutaraldehyde activated olive Pomace powder. The support was used to produce biodiesel with Pomace oil and methanol. RSM using CCD was used to optimize the biodiesel production parameters. The predicted Pomace oil methyl ester yield was 92.87% under the optimal conditions. Verification experiment yield was 91.81%, confirmed the validity by suggested model. Biodiesel yield reached 93.73% by adding water (1% w/w) in the reaction medium under the optimal conditions.

Also, Uzun et al., (2012) carried out alkali-catalysed transesterification of waste frying oils (WFO) in various conditions to investigate the effects of catalyst concentration, reaction time, methanol/oil molar ratio, reaction temperature, catalyst type (hydroxides, methoxides and

ethoxides), and purification type (such as washing with hot water, purification with silica gel and dowex) on the biodiesel yields. The optimum conditions were 0.5% wt. of NaOH, 30 min reaction time, 50°C reaction temperature, 7.5 methanol to oil ratio and purification with hot distilled water. A 96% biodiesel yield was obtained, and the activation energy was found to be as 11741 J mol-1. The determined specifications of obtained biodiesel according to ASTM D 6751 and EN 14214 standards were in accordance with the required limits.

2.6.3 Engine combustion, performance and emissions characteristics of biodiesel

The biodiesel proved itself effective alternative fuel for CI engines in term of improving exhaust emissions like CO, UHC, SO_X, PM, soot etc. without any hardware modification. It also improves the engine combustion and emissions characteristics of CI engines. But the use of biodiesel as pilot fuel in dual fuel engine is still under consideration. Ryu (2013a) reported that the application of biodiesel as pilot fuel in dual fuel engine improves the brake thermal efficiency of the engine, especially at low loading condition. However, a slight decrease in engine performance was noticed at higher load compared to diesel as pilot fuel. Similar results were reported by Olsen et al., (2007), Kannan et al., (2012), Papagiannakis et al., (2004) and Labeckas et al., (2006). However, the feedstocks used by the authors were different in these cases. Tarabet et al., (2014) used eucalyptus oil biodiesel as pilot fuel, the author reported that dual fuel engine has low brake specific fuel consumption compared to conventional diesel engine at higher load. However, use of biodiesel as pilot fuel for natural gas has higher BSFC than diesel as pilot fuel. The author also reported that both the pilot fuels show a nearly similar trend of exhaust gas emissions. However, the application of biodiesel reduces the UHC and CO emissions at higher load compared to diesel as pilot fuel.

Most of the biodiesel has higher cetane number compared to petroleum diesel fuel which results in lower autoignition temperature and lower ignition delay. All these properties of biodiesel make it better pilot fuel than petroleum diesel at low and intermediate loading condition where the in-cylinder pressure and temperature was found lower due to leaner air gaseous fuel mixture. The shorter ignition delay of pilot fuel in dual fuel engine improves the combustion characteristics of the engine and also decrease the exhaust emissions. Ryu (2013a) reported that the ignition delay in the dual fuel engine mode is about 1.2–2.6 °CA longer than that of a conventional diesel engine, but the ignition delay decreases with the increasing pilot injection pressure. The author also reported that Smoke is decreased and NO_X is increased as the pilot injection pressure increases in the biodiesel–CNG DFC mode.

2.7 Strategies for Improving Combustion, Performance and Emissions Characteristics of Dual Fuel Engine.

Performance and emissions in the dual fuel can be reduced by engine design and controlling operating parameters. The following parameters were studied by previous researchers in order to improve engine performance and efficiency, along with the reduction of HC, CO, and NO_X emissions at high load.

2.7.1 Pilot fuel injection timing

Injection timing of pilot fuel is a major factor which affects the combustion, performance and emissions characteristics of dual fuel engine. Generally, two type of injection timing (advanced injection timing and retard injection timing) are applied in CI engines. As dual fuel engine is a modified version of CI engines, so both these injection timing are also applicable for

dual fuel engines. However, the effect of changing injection timing of pilot fuel in dual fuel engine is not adequately studied.

2.7.1.1 Advanced injection timing

Advanced injection timing results in longer ignition delay. In CI engines, the longer ignition increases the time of air-fuel mixing which results in better combustible mixture quality. Hence, increased in-cylinder pressure and temperature has been noticed. The higher in—cylinder temperature and pressure speed up the chemical reaction of the mixture in the cylinder, which results in a decrease in combustion products like UHC and CO emissions. For dual fuel engine, the retardation in combustion has been noticed due to longer ignition delay. Hence, advancing the pilot fuel injection minimize the combustion alteration because of the gaseous fuel in the combustion chamber.

Alla et al., (2002) studied the effects of changing injection timing of pilot fuel in dual fuel engine and reported that the poor emissions and low efficiency at low and intermediate loads are significantly improved by advancing the pilot injection timing. Papagiannakis et al., (2007) also investigated the influence of pilot injection timing on combustion and emissions characteristics of a dual-fuel engine at low loads and they confirmed that higher efficiency and lower emissions can be achieved by advancing the pilot injection timing. Ryu (2013a) also studied the effects of pilot injection timing on the combustion and emissions characteristics in a dual-fuel engine and reported that the performance of dual fuel engine at low loads could be optimized by advancing the pilot injection timing. Yang et al., (2016) investigated that, at low load, the emissions and combustion noise of dual fuel engine is notably affected by pilot fuel injection timing. By

suitable advancing the pilot fuel injection timing, higher brake thermal efficiency, lower UHC and CO emissions are attained.

2.7.1.2 Retarded injection timing

The retarded injection timing is mainly used to reduce the NO_X emissions. Lateral injection timing results in shorter ignition delay. In CI engines, the shorter ignition decreases the time of air-fuel mixing which results in poor combustible mixture quality. Hence, decrease in-cylinder pressure and temperature have been noticed. This also affects the combustion process rate becoming slower which in turn minimizes the capability of combustion product oxidation. Which results in increasing UHC and CO emissions of CI engines. The end of combustion is also extended as the process of combustion is shifted to the expansion stroke. The combustion behavior describes that majority of combustion is located after TDC and hence reducing the effective work cycle. In dual fuel engines, the higher ignition delay of pilot fuel due to the presence of air and gaseous fuel mixture is a big concern to the researcher, further retarded injection timing of pilot fuel will result in further increase in ignition timing of pilot fuel which is not desirable.

2.7.2 Pilot fuel quantity

Sombatwong et al., (2013) investigated using a naturally aspirated diesel engine that, the definite pilot fuel quantity is a vital parameter to control the combustion, performance and emissions characteristics of the dual fuel. The author used methane as a primary fuel and diesel as pilot fuel in this study and found that increasing the amount of pilot fuel results in higher in-cylinder pressure and temperature as diesel fuel contributed to the larger amount of energy. Also,

a larger amount of pilot fuel create larger reaction zone and results in more ignition center for the combustion of gaseous fuel. Hence, the flame reaches the air and gaseous fuel mixture in a shorter time. Figure 2.1 shows the impact of pilot fuel quantity on HC emissions.

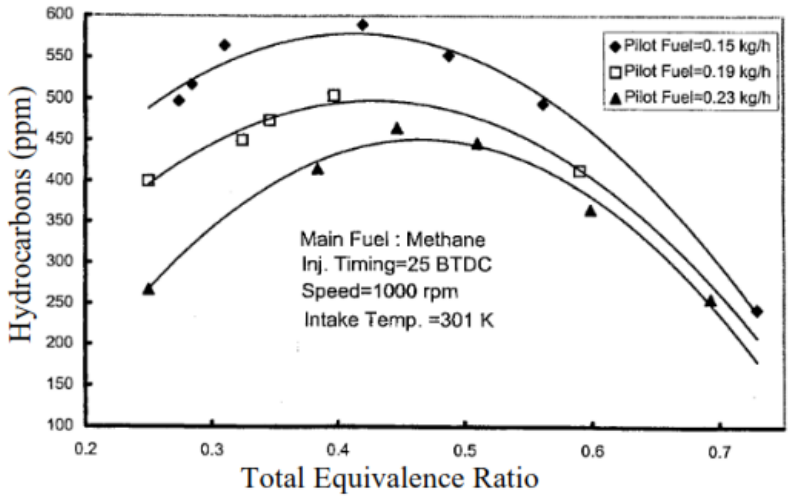

Figure 2.1: Unburned HC as a function of pilot fuel quantity and equivalence ratio (Sombatwong et al., 2013)

The improvement in combustion characteristics of dual fuel engine results in a decrease in CO emissions as fuel moves towards complete combustion. However, CO and UHC emissions decrease with increasing pilot fuel quantity but emissions of NO_X, PM, soot and smoke likely to be increased. Hence, selection for an optimum quantity of pilot fuel is a big challenge in dual fuel operation.

2.7.3 Intake manifold temperature

Krishnan et al., (2004) investigated that, the change in intake manifold temperature also affects the combustion, performance and emissions characteristics of dual fuel engine. It was found that, when the temperature of the intake manifold is increased to over 100°C, the mass

burning rate of air and gaseous fuel mixture is also increased which leads to a complete combustion (Soloiu et al., 2013). Hence, improvements in BTE, BSFC are noticed with a reduction in UHC and CO emissions. However, the exhaust gas temperature and NO_X emissions are increased.

2.7.4 Hydrogen production from fuel reforming

One of the mechanisms to obtain hydrogen is through reforming of the hydrocarbon fuel. The fuel reforming process for hydrogen production can be performed by either non-catalytic or catalytic processes. However, the hydrogen production catalytically is promising as the process requires less residence time and relatively low operating temperature (Chaniotis and Poulikakos, 2005).

Exhaust gas fuel reforming is an onboard technique for providing the engine with hydrogen-rich gaseous fuel. Hydrogen production is carried out by the catalytic interaction of hydrocarbon fuel directly assisted by exhaust gas in a reforming reactor. The reformed gas then is recirculated into the engine. Therefore, the method is also known as reformed EGR (REGR) (Tsolakis et al., 2005). The production of hydrogen via reforming of hydrocarbon fuels involves all basic reforming processes. Those techniques are explained briefly as follows. Steam reforming is a process using high-temperature steam to yield hydrogen and carbon monoxide. The process is highly endothermic requiring a high level of heat input (Tsolakis and Megaritis, 2004). To eliminate the CO produced in the reaction, a further water-gas shift reaction may be involved. With this reaction, more hydrogen can be produced.

Partial oxidation is another process to produce hydrogen. In this process hydrocarbon, fuel is burned using lower stoichiometric oxygen. The advantages of this process are: is able to be started quickly, is appropriate in a small system and is an exothermic reaction. With this process syngas produced contains less calorific value than that of steam reforming (less hydrogen content in the syngas) (Tsolakis et al., 2003). Complete oxidation may take place depending on the condition of the reactor. This is undesirable as there is no hydrogen produced. If the reaction occurred at relatively high temperature (> 800 °C) where the availability of steam is limited, the endothermic dry reforming can take place. Auto-thermal reforming is a process which combines steam reforming and partial oxidation in a reactor. The process requires no external heat (unlike steam reforming) and the reaction temperature is lower compared to that of partial oxidation. In this process, partial oxidation reaction generates heat which is used to drive the steam reforming reaction. Therefore, the production of hydrogen with this process is possible using simple and small reactor with relatively high efficiency. Moreover, the hydrogen yield is higher than that produced by partial oxidation (Park et al., 2010). Hydrogen-rich gas production assisted by exhaust gas has an advantage as the source of oxygen (from water and air) is already available abundantly from diesel exhaust thus requires no additional equipment. Furthermore, the liquid fuel in the reactor is evaporated by heat from the exhaust while water is already provided in the form of steam.

2.7.5 Exhaust gas recirculation

Exhaust gas recirculation (EGR) is the most well-known and established technique for reducing NO_X due to its simplicity and low cost implementation (Rolf, 2000; Pradeep and Sharma, 2007). This effective NO_X emission control method is commonly used in much modern

high speed direct injection (HSDI) diesel engines. The application of EGR is simple and straightforward, especially in a naturally aspirated diesel engine. The exhaust gas flows to the intake manifold through the throttling valve as exhaust pressure is higher compared with the intake (Zheng et al., 2004).

Selim (2003) found that at low load conditions dual fuel engines suffer low efficiency and higher emissions. By applying exhaust gas recirculation (EGR), the combustion improves and the efficiency increases. By re-circulating exhaust gas into the combustion chamber, active radicals in the exhaust gas enhance the pre-flame activities and the exhaust gasses are re-burnt. Hussain et al., (2012) investigated that, NO_X emission is reduced substantially due to reduced oxygen concentration (some oxygen is displaced by EGR) and decreased the flame temperature in the chamber. However, increasing the rate of EGR too high can deteriorate engine performance and result in increases in HC and CO emissions, even though doing so can further reduce NO_X formation (Pirouzpanah and Khoshbakhti, 2007a; Pirouzpanah et al., 2007b). Poonia et al., (1999) reported that the addition of EGR along with increasing intake manifold temperature and pilot fuel quantity can improve brake thermal efficiency considerably, but these measures also increase ignition delay. At high load, no significant improvements in thermal efficiency or ignition delay are observed at any EGR ratio. It was also noticed that the application of EGR at higher load shows adverse effects on performance and emissions characteristics of dual fuel engine.

2.8 Outcomes of Literature Review

The number of literature has been studied about the dual fuel engine and techniques related to it during the research. It was found that dual fuel combustion technique is one of the best combustion technique used for reducing the emissions of compressed ignition engines without decreasing the power and thermal efficiency. As an outcome of exhaustive review of literature, the following major findings can be drawn;

1. Most of the literature suggested that dual fuel operating strategy has economic benefits because various alternative fuels can be used, which typically has a lower cost than that of conventional fossil fuel and requires no major hardware modifications. It also can be operated on any combinations of gaseous and liquid fuel.
2. Literature agreed that incomplete combustion of gaseous fuel causes lower in-cylinder pressure in dual fuel engine compared to diesel fuel engine, especially at low load condition. However, with increasing load, the gaseous fuel combustion was improved and results in a higher in-cylinder pressure of dual fuel engine.
3. The incomplete combustion of gaseous fuel at low and intermediate loading conditions was reported in most of the literature which causes higher carbon monoxides (CO) and unburnt hydrocarbons (UHC) emissions for dual fuel engine compared to petroleum diesel engine. The higher CO and UHC emissions results in poor brake thermal efficiency (BTE) and brake specific energy consumption. Hence, up to intermediate load, the performance characteristics of dual fuel engine was lower than conventional diesel engine [38-45].

4. The improved gaseous fuel utilization at higher load results in lower CO and HC emissions which result in enhancement of performance characteristics of dual fuel engine. Hence, at higher load, the dual fuel engine shows better BTE and BSEC compared to a conventional diesel engine.
5. The improved gaseous fuel utilization also results in higher in-cylinder temperature. Hence, at higher load, dual fuel engine exhibits high NO_X emissions compared to conventional diesel engine as reported in most of the literature.
6. Some of the literature suggested that use of biodiesel as pilot fuel improves the performance and emissions characteristics due to higher cetane number, the low autoignition temperature of dual fuel engine at all loading conditions.
7. Most of the literature agreed that use of exhaust gas recirculation (EGR) shows a better result in reducing of NO_X emissions. However, use of EGR at higher load shows some adverse effect on performance characteristics of dual fuel engine.
8. The improved performance and emissions characteristics of dual fuel engine at lower and intermediate loading conditions by using EGR was also reported in some of the literature.
9. The improvement in combustion, performance and emissions characteristics of dual fuel engine was notice by advancing the pilot fuel injection timing.
10. Literature suggested that the emission of unburnt hydrocarbons and CO were reduced by increasing the pilot fuel quantity. However, the emissions like NO_X, PM, soot and smoke were increases.
11. Improved combustion characteristics of dual fuel engine were observed with increasing intake manifold temperature by several authors in their research.

2.9 Research Gap

On the basis of exhaustive literature review, the following research gaps were identified.

1. The trend of NO_X emissions in dual fuel engine was not clear and requires further exploration. Moreover, some literature suggested that at full load condition, NO_X emissions for dual fuel engine were higher as compared to a conventional diesel engine. In view of above, there is a need to explore the use of EGR for NO_X reduction in dual fuel engine.
2. A little quantum of work was done for improving performance and emissions characteristics of dual fuel engine at low and intermediate loading conditions.
3. Combustion characteristics based on mass fraction burn model and rate of heat release model yet to be explored for dual fuel engine.
4. Diesel was used as pilot fuel in most of the cases, the use of biodiesel as pilot fuel in dual fuel engine needed further exploration.
5. The use of Jatropha oil methyl ester (JOME) and Orange peel oil methyl ester (OPOME) as pilot fuel for CNG in dual fuel engine need to be explored.
6. Ignition delay is an important characteristic for a pilot fuel and not studied adequately.

2.10 Problem Statement

After the exhaustive literature review and identification of the research gap, it was concluded that dual fuel combustion is a promising technique for improving the combustion and emission characteristics of a conventional diesel engine. Dual fuel operating strategy has economic benefits because various alternative fuels can be used. The pilot fuels are very important in dual fuel engine. The unutilized feedstocks of biodiesel are identified and selected for the use as pilot fuel. The optimization tools are used to prepare the biodiesel. The JOME and OPOME as pilot fuel in the dual fuel engine have not been studied adequately. Therefore, exhaustive trials on dual fuel engine using JOME, OPOME and their blends with diesel in various proportions as pilot fuel for CNG were carried. Also, the effect of EGR on performance and emissions characteristics for all fuel combination was also done. Furthermore, the ignition delay of all pilot fuel was also measure which further helps in improving the performance of dual fuel engine.

2.11 Research Objectives

The following objectives were envisaged for the present research work.

1. Comprehensive literature survey to identify unutilized methyl ester as a pilot fuel for CNG.
2. Biodiesel production and optimization for maximizing the yield using response surface methodology (RSM).
3. Evaluation of physicochemical properties like Density, kinematic viscosity, flash point, cetane index, calorific value and autoignition temperature of Diesel, JOME, OPOME and different blends as per the appropriate standards.
4. To study the effect of various operating parameters on ignition delay of all pilot fuels.
5. To study the effect of introducing CNG at different operating condition on combustion, performance and emissions characteristics of a diesel engine.
6. To understand the effect of different pilot fuels (Diesel, JOME, OPOME, J50D50 and OP50D50) having different properties and their combination with CNG on combustion, performance and emissions characteristics.
7. To analyze the effect of the application of EGR on combustion, performance and emissions characteristics of dual fuel combustion at different operating conditions.

CHAPTER 3

SYSTEM DEVELOPMENT AND METHODOLOGY

3.1 Introduction

This chapter explains how the whole research was conducted with the systematic execution of steps followed and as mentioned in the problem statement section. The step by step orientation of the objectives given bellow:

- Selection of primary fuel.
- Selection of pilot fuel
- Biodiesel production and optimization
- Preparation of pilot fuels
- Determination of physicochemical properties of all pilot fuels
- System development to determine the ignition delay of all pilot fuels.
- System development of engine testing
- System development of exhaust gas recirculation
- Analyze the combustion, performance and emissions characteristics of dual fuel engine

The number of literature has been reviewed to find out the combination of primary and pilot fuels for the present research. The arrangement and production of the fuel have been done after that. The physicochemical properties like density, kinematic viscosity, calorific value, cetane number and auto-ignition temperature etc. of all pilot fuel were measured. A small setup

for measuring the ignition delay of all pilot fuel was also developed. After measuring all the properties; the combustion, performance and emissions characteristics of dual fuel engine was measured. To do so the setup for engine test rigid was developed which work on both conventional diesel engine mode and dual fuel engine mode. The exhaust gas recirculation unit was also developed which can be attached to the engine and effect of the application of EGR on dual fuel engine performance was analyzed. All these parameters, components, properties and system development were explained in detail in this chapter.

3.2 Selection of Primary Fuel

The selection of primary fuel was a major challenge in the present research. The selection should be done on the basis of its properties (like; calorific value, auto ignition temperature, density, kinematic viscosity etc.), availability, safety, storage etc. After going through the literature of current research and points mentioned above, it was found that CNG was one of the best option among all gaseous fuel. The main reason for selecting CNG as primary fuel was its commercial used as fuel in India which makes it easily available. A number of filling stations for CNG are available in India which is continuously increasing.

The other reason of selecting CNG as the primary fuel for the present research was advantages over gasoline and petroleum diesel fuels. These include reduced fuel cost, cleaner exhaust gas emissions and higher octane number. Therefore, the numbers of engine vehicles powered by CNG were growing rapidly. The extraordinary octane number of CNG is another advantage, which makes it suitable for spark ignition engines. CNG engine can also be operated on high compression ratio. Hence the use of CNG in compressed ignition engine improves it

combustion, performance and emission characteristics. However, the higher autoignition temperature of CNG makes it difficult to auto ignite after compression in CI engines. So a small quantity of pilot fuel was required to start the ignition of CNG. Hence, the pilot fuel plays an important role in CNG combustion. So the selection of pilot fuel for CNG becomes very crucial and important.

3.3 Selection of Pilot Fuel

As discussed earlier that the most of the energy in dual fuel engine comes from primary fuel, but its combustion was totally dependent upon pilot fuel. So, the selection of pilot fuel in such condition becomes more complicated, crucial and important. Most of the literature suggested that use of diesel as pilot fuel gave good results at higher loading condition, but at lower load, the performance of dual fuel engine decreases. The use of biodiesel as pilot fuel improves the combustion, performance and emissions characteristics of dual fuel engine. In such condition, the finding of unutilized feedstock for biodiesel production becomes very crucial. After going through number of literature, it was observed that highly used Jatropha biodiesel in CI engine was still not used as pilot fuel in dual fuel engine with CNG. This help to select one pilot fuel for the present research. To analyze the effect of biodiesel as pilot fuel on the performance of dual fuel engine, at least one more feedstock for pilot fuel was required. After comparing the properties of different feedstock, it was observed that Orange peel oil has the better properties compared to some other feedstock, but still unutilized as pilot fuel in dual fuel engine.

Biodiesel from Jatropha seed is important because most of the states of India are tribal where it is found abundantly. Jatropha seed contains 30-40 percent fatty oil called Jatropha oil. The Jatropha tree starts bearing seeds from the seventh year of planting. Jatropha seed oil is a common ingredient of hydrogenated fat in India. It is obtained from the seed kernels and is a pale yellow, semi-solid fat at room temperature. It is also used in the manufacture of various products such as soap and glycerin. Crude Jatropha oil generally contains high % Free Fatty Acid and conversion of FFA to biodiesel is very important Properties of biodiesel depend on the nature of the vegetable oil used for the preparation of biodiesel by esterification and/or transesterification. From the chemical composition, it is found that Jatropha oil is almost similar to that of other non-edible oils.

The Orange fruits are largely produced in countries such as Brazil, USA, India, China etc. India is a third largest country in producing Oranges with annual production 6 million tons. Here the fruit flesh (carpel) is used and the peel is disposed of as waste. Researchers have proved that the Orange peel can be in used in the production of methane as well as a quality fertilizer. It has also proved to be a very good anti-oxidant. The Orange peel powder diesel solution was proved to be used as an alternative fuel for C.I engine. Also, the Orange peel oil has good calorific value 38.6 MJ/kg with low density and kinematic viscosity of 821 kg/m^3 and of 1.8 mm^2/s respectively. Which make it a good alternative fuel for CI engine. However, the direct use of Orange peel oil in engines cause short term problems like cold weather starting, plugging, gumming of filter lines and engine knocking. Also, use of vegetable oil in direct injection diesel engines creates poor fuel atomization, incomplete combustion, carbon deposition on the injector and fuel build up in the lubricant oil resulting in serious engine fouling (Kumar and Sharma,

2005). So it was required to convert straight vegetable oil into esters. After finalizing the feedstock the biodiesels and their blends were prepared.

3.4 Biodiesel Production

The biodiesel of vegetable oil, waste cooking oil and animal fat was prepared with transesterification process. To go for transesterification process, the free fatty acid (FFA) content in the oil was measured. The process of measuring the acid number and FFA of oil was given in next section. If the FFA of oil was found less than 2%, the oil was converted into biodiesel through transesterification process. Otherwise, the FFA of the oil was reduced to less than 2% through esterification.

3.4.1 Acid value and free fatty acid content

The Acid value of oil is defined as the milligrams of potassium or sodium hydroxide consumed during neutralizing the FFA present in one gram of oil. It is a relative of rancidity as FFA are normally formed during the decay of oil glycerides. Also, acid number defines the acidic components in a fuel. The value is also defined as the percent of FFA measured as oleic acid. To determine the acid number, one gram of oil was taken into the burette in which 10 ml of methanol was mixed. Two drops of phenolphthalein were also mixed in the solution as indicator. The solution was then titrated by adding potassium hydroxide solution (0.1N) from the burette drop by drop to the mixture until the solution to a faint pink color and which remains for 30 seconds and more. Read the burette accurately up to two decimal places. After the process, the acid number and FFA content of oil were measured as.

$$\text{Acid Value} = \frac{56.1\,VN}{W}$$

Where,

V= Volume of potassium or sodium hydroxide (in ml) consumed

N = Normality of potassium or sodium hydroxide solution, and

W= Weight of oil sample (in gm)

The FFA of oil was calculated after calculation of acid value. The formula used for calculating the FFA is given as;

$$\text{FFA} = \frac{28.2\,VN}{W}$$

$$\text{FFA} = \text{Acid Value}/\ 1.99$$

The FFA content determined by using phenolphthalein as indicator needs to be corrected. The formula for calculating the real FFA content is given below;

$$\text{Real FFA} = \text{Observed FFA} - (\%\ \text{oryzanol in the oil}) \times 0.425$$

3.4.2 Esterification

After measuring, if the FFA of the oil is found higher than two, then it becomes necessary to reduce the FFA of the oil to less than two, otherwise, soap can be formed during transesterification process. The process used to reduce the FFA of oil is known as esterification. For the present research, a one liter three necks round bottom flask was selected to perform the esterification process. One neck was reserved for connecting the water cooled condenser on the top of the reactor which helps in reducing evaporative loss of methanol. The thermometer was installed on another neck to measure the temperature inside the flask. The third neck was

reserved for chemical addition and sample collection which was covered with removable air tight rubber. The reactor was put on the hotplate having magnetic stirrer. Before putting the sample into the round bottom flask, the oil was first heated around 120 °C for 30-45 minutes in one liter cylindrical beaker, so that the moisture present in the oil get evaporated. After removal of all moisture, the oil was put to cool down to 60°C in the same beaker. The oil was then put into the one liter three neck round bottom flask. A magnetic bit was put into the flash for continuous agitation at desired speed which was controlled by controlling the speed of stirrer.

The mixture of methanol and para toluene sulphonic acid (PTSA) was prepared in a small beaker. The molar ratio of methanol to oil was taken in the range of 3:1 to 9:1 and catalyst concentration was taken in the range of 0.5%w/w to 1.5%w/w. The reaction temperature was selected in the range of 45°C to 65°C. The highest range of reaction temperature was chosen in such a way that it does not exceed the boiling point of methanol. First of all the oil was heated to the desired temperature before the addition of methanol and PTSA mixture. The agitator speed was kept constant at 350 rpm to ensure the efficient mixing as methanol was immiscible in oil. 1-ml sample was withdrawn at the interval of 5, 10, 20, 30, 45, 60, 90 and 120 minutes from the flask for the titration. The reaction takes place during esterification process is shown below;

$$R_1\text{-}COOH + ROH \xleftrightarrow{H^+} R - O - CO - R_1 + H_2O$$

(FFA) (Alcohol) (Fatty acid ester) (water)

As shown in the equation the water was formed during esterification. So it was required to remove the water before transesterification. For doing that the mixture was put into a separating funnel for gravity separation. After removing water the mixture was heated to 120°C

for 30 minutes to ensure no further water and methanol contain remains in the mixture. After that, the sample was ready for transesterification process.

3.4.3 Transesterification

Transesterification is the most used method which converts vegetable oil, waste cooking oil and animal fats into fatty acid methyl ester by reacting with alcohol in the presence of catalysts. This fatty acid methyl ester was commonly known as biodiesel. The purpose of converting vegetable oil into biodiesel was to decrease the viscosity of the oil. Both basic and acidic catalyst can be used for transesterification process. The acidic catalysts produce high yields of fatty acid methyl ester, but the reactions are slow and required reaction temperature above 100 °C. The time required for the reaction is also higher i.e. more than 3 hours. The base-catalyzed transesterification was faster compared to acid-catalyzed reactions. Also, the base catalysts are less corrosive compared to acidic catalysts. The base catalyzed transesterification process was selected to prepare the biodiesel for the present research.

The alcohol used for the present reaction was methanol and potassium hydroxide (KOH) was selected as a base catalyst. The chemicals used in the present research (i.e. methanol, KOH, NaOH, PTSA) were 99% pure. The mixture of methanol and KOH was prepared in a small beaker. The reaction followed by base catalyzed transesterification process is given as:

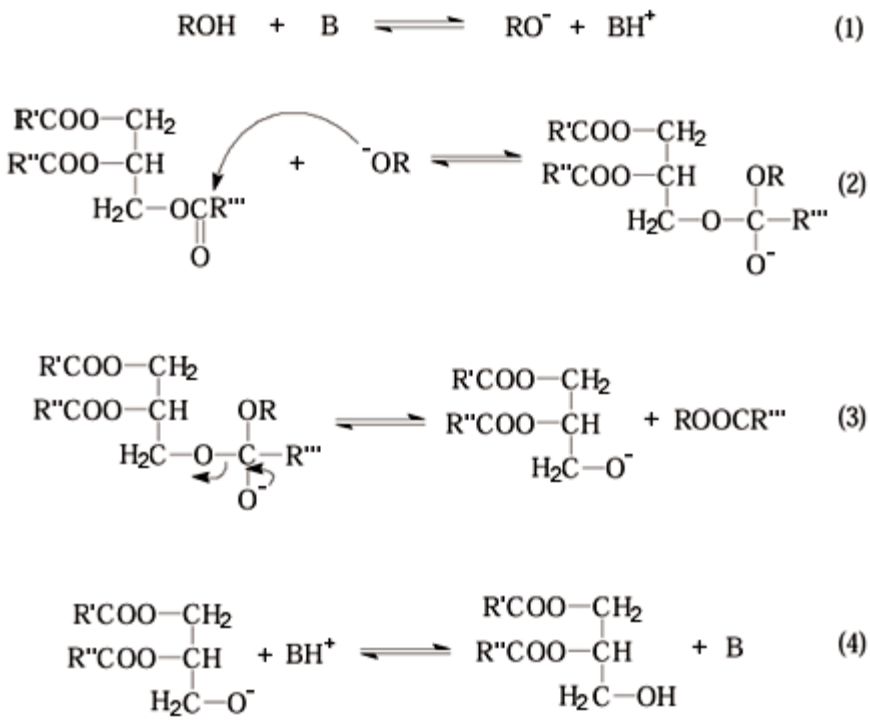

The molar ratio of methanol to oil was taken in the range of 3:1 to 9:1 and catalyst concentration was taken in the range of 0.5%w/w to 1.5%w/w. The reaction temperature was selected in the range of 45°C to 65°C. The highest range of reaction temperature was chosen in such a way that it does not exceed the boiling point of methanol. First of all the oil was heated to the desired temperature before the addition of methanol and KOH mixture. The agitator speed was kept constant at 350 rpm, same that of esterification process, to ensure the efficient mixing as methanol was immiscible in oil. The reaction time was lies between 30-90 min depending on the characteristics of the oil. After completion of transesterification process, the mixture was put into a separating funnel for gravity separation. This process took the 18-24 house. After gravity separation two layers were formed, lower layer was dark in color, which contains glycerol. The upper layer was lighter in color and contain a mixture of biodiesel, methanol and a small quantity of glycerol. The glycerol was removed from the biodiesel. The biodiesel was thereafter water-

washed with warm water to remove the catalyst, glycerol and excess alcohol. The process was repeated till the all the glycerol was washed out from the biodiesel and clear water layer was formed on the lower side of separating funnel. The biodiesel was then heated to 110 °C so that extra alcohol and moisture present in the biodiesel removed. After heating pure biodiesel left behind.

3.5 Optimization of Biodiesel Production

Transesterification process is one of the most used processes for biodiesel production. As discussed earlier in this process vegetable oil, animal fat and waste cooking oil reacted with alcohol in the presence of a catalyst to produce biodiesel and glycerol. The transesterification process was affected by the type of catalysts used. Other factors like the free fatty acid content of oil, methanol-oil molar ratio, catalyst concentration, reaction temperature, reaction time, stirring speed etc. also affects the yield of the biodiesel. The energy consumed to prepare the biodiesel, play a significant role in biodiesel price. So the cost of biodiesel production can be reduced only after analyzing the effect of above discussed factors on the yield of biodiesel. A number of experiments have to conduct to analyses these effects. The number of experiments performed can be reduced with the help of some optimizing tool. The optimizing tool also gives the clear cut picture of factors affecting the yield.

RSM in experimental design has increasingly attracted the attention of many researchers. The most widely used model was Central Composite Design (CCD) of Response Surface Methodology (RSM) as found from the literature review. CCD was employed to determine the optimal reaction conditions. It is a second order experimental model which composed of factorial

design, set of central points, and axial points equidistant to the center point. The factorial design component of CCD is of the class 2^k factorial, where k represents the number of appropriate factors or variables. Each of the variables is chosen at two levels meaning that each variable has a low (coded numeric value of -1) and high numeric value (coded numeric value of +1).

3.5.1 Optimization of esterification process

Esterification is a process of reducing FFA of oil having more than 2% FFA contents. As discussed earlier two vegetable oil were selected as feedstocks name as Jatropha oil and Orange peel oil. Jatropha oil has higher FFA contents where Orange peel oil has low FFA contents. That's why the biodiesel of Jatropha oil was produced in two-stage transesterification process. In the first stage the FFA of oil was reduced below 2% and the process was known as esterification process and in the second stage the low FFA Jatropha oil was converted into biodiesel, the process was named as transesterification process.

The optimization of esterification process for Jatropha oil was done in this section. Optimization of the esterification process was conducted via 4-factor experiment to examine the effects of Catalyst concentration (A), Reaction temperature (B), Time (C) and Methanol/oil molar ratio (D) of methyl esters using central composite design (CCD). A total of 30 experimental-sets including factorial points, axial points and central points were developed. Number of experimental sets was calculated from the standard design of experiments formula given in equation below;

$$N = 2^k + 2k + N_o$$

Where,

k is the number of independent variables = 4;

N_o is the number of repetition of experiments at the central point for the design to be rotatable = 6.

Process parameters with their ranges for esterification of Jatropha oil are shown in Table 3.1 and based on that range the experiment matrix suggested by response surface methodology software named as design expert V10 is shown in Table 3.2. Total 30 number of experiment suggested by the software. These experiments were performed by changing one parameter while other parameters kept constant.

Table 3.1: Process parameters with their ranges for esterification of Jatropha oil

Name	**Factor**	**Units**	**Low Level**	**High Level**
Catalyst concentration	A	% (w/w)	0.5	1.5
Reaction temperature	B	℃	45	65
Time	C	Min	30	90
Molar Ratio	D	Methanol:oil	4	12

Table 3.2: Design matrix for esterification of Jatropha oil

Run	**A: Catalyst concentration (w/w%)**	**B: Temperature (^{0}C)**	**C: Time (min)**	**D: Molar Ratio**
1	1.5	45	90	4
2	2	55	60	8
3	1.5	65	90	4
4	1	55	60	8
5	1	55	60	8
6	0.5	65	90	4

7	1.5	45	30	4
8	1	55	0	8
9	1	55	120	8
10	1	55	60	8
11	0.5	45	90	12
12	1.5	65	30	4
13	0.5	45	30	4
14	0.5	65	90	12
15	0.5	65	30	12
16	1	75	60	8
17	1.5	65	30	12
18	1	55	60	8
19	1	55	60	0
20	0.5	45	90	4
21	0.5	65	30	4
22	1	55	60	16
23	1	55	60	8
24	1	55	60	8
25	0.5	45	30	12
26	1.5	65	90	12
27	1.5	45	90	12
28	1.5	45	30	12
29	0	55	60	8
30	1	35	60	8

The experiment for FFA reduction was done according to the matrix suggested by the software. The detail result of FFA reduction was given in the result and discussion section.

3.5.2 Optimization of transesterification process

Two different feedstock were selected for biodiesel production in the present research. The characteristics of both the feedstock were different. So it was required to take a different range of parameters for transesterification process. However, after esterification process, the FFA of Jatropha oil reduced to 1.4% from 7.1%. This cause some similarity in the range of some parameters. Process parameters with their ranges for transesterification of Jatropha oil are shown in Table 3.3 and based on that range the experiment matrix suggested by the software is shown in Table 3.4. Similar to esterification process total 30 number of experiments were suggested by the software to analyze the effect of different parameters on the yield of biodiesel.

Table 3.3: Process parameters with their ranges for esterification of Jatropha oil

Name	Factor	Units	Low Level	High Level
Catalyst concentration	A	% (w/w)	0.25	1
Reaction temperature	B	℃	45	65
Time	C	Min	20	60
Molar Ratio	D	Methanol: Oil	3	9

Table 3.4: Design matrix for transesterification of Jatropha oil

Run	A: Catalyst concentration (w/w%)	B: Temperature (^{0}C)	C: Time (min)	D: Molar Ratio
1	0.25	45	20	3
2	1	45	20	3
3	0.25	65	20	3
4	1	65	20	3
5	0.25	45	60	3
6	1	45	60	3

7	0.25	65	60	3
8	1	65	60	3
9	0.25	45	20	9
10	1	45	20	9
11	0.25	65	20	9
12	1	65	20	9
13	0.25	45	60	9
14	1	45	60	9
15	0.25	65	60	9
16	1	65	60	9
17	-0.125	55	40	6
18	1.375	55	40	6
19	0.625	35	40	6
20	0.625	75	40	6
21	0.625	55	0	6
22	0.625	55	80	6
23	0.625	55	40	0
24	0.625	55	40	12
25	0.625	55	40	6
26	0.625	55	40	6
27	0.625	55	40	6
28	0.625	55	40	6
29	0.625	55	40	6
30	0.625	55	40	6

Process parameters with their ranges for transesterification of Orange peel oil are shown in Table 3.5 and based on that range the experiment matrix suggested by the software is shown in Table 3.6.

Table 3.5: Process parameters with their ranges for esterification of Orange peel oil

Name	Factor	Units	Low Level	High Level
Catalyst concentration	A	% (w/w)	0.25	1
Reaction temperature	B	℃	45	65
Time	C	Min	30	90
Molar Ratio	D	Methanol: Oil	3	9

Table 3.6: Design matrix for transesterification of Orange peel oil

Run	A: Catalyst concentration (w/w%)	B: Temperature (^{0}C)	C: Time (min)	D: Molar Ratio
1	0.625	55	60	6
2	0.625	55	120	6
3	-0.125	55	60	6
4	0.625	75	60	6
5	1	65	30	3
6	0.625	55	60	6
7	0.25	65	90	9
8	1	65	90	9
9	0.625	55	60	6
10	0.25	65	90	3
11	1	65	30	9
12	1.375	55	60	6
13	0.625	55	60	6

14	1	45	90	3
15	1	45	30	9
16	0.25	45	90	3
17	0.625	55	0	6
18	1	65	90	3
19	0.25	45	30	9
20	0.25	65	30	9
21	0.25	45	90	9
22	0.625	55	60	12
23	1	45	90	9
24	0.625	55	60	0
25	0.625	55	60	6
26	0.625	55	60	6
27	1	45	30	3
28	0.625	35	60	6
29	0.25	65	30	3
30	0.25	45	30	3

3.6 Preparation of Pilot Fuels

Pilot fuel plays an important role in dual fuel engine. After significant literature reviews, it was found that biodiesel of Jatropha oil and Orange peel oil was not significantly used as pilot fuel in dual fuel engine. Hence, biodiesel of Jatropha oil and Orange peel oil was prepared. It was also found from the literature survey, that the blends of biodiesel and diesel were not used as

pilot fuel. Hence the blends diesel with biodiesel were prepared to analyze the effect on combustion, performance and emissions characteristics of dual fuel engine.

The quantity of pilot fuel used in dual fuel engine was much smaller than primary fuel. That's why, it effect on combustion, performance and emissions characteristics of the engine was small. So the blending of biodiesel in diesel in small ratio does not show marginal changes on engine performance. So, the blending of diesel and biodiesel in same proportion was done for the present research. The pilot fuel samples were prepared by volume wise substitution of Jatropha and Orange peel oil biodiesel in the diesel. Blending was done using rigorous agitation at a high rpm by hand blender. Therefore, the pilot fuels of CNG in dual fuel engine trial comprised of diesel, JOME, J50D50, OPOME and OP50D50. The nomenclature and composition of various test fuels are shown in Table 3.7.

Table 3.7: Nomenclature and composition of various pilot fuels

S. No.	Test Fuel's composition	Nomenclature
1.	Neat petroleum diesel	Diesel and D100
2.	100% Jatropha oil methyl ester	JOME
3.	100% Orange peel oil methyl ester	OPOME
4.	50% Jatropha oil methyl ester and 50% Diesel	J50D50
5.	50% Orange peel oil methyl ester and 50% Diesel	OP50D50

3.7 Physicochemical Properties of All Pilot Fuels

In this section, the physicochemical properties of all pilot fuels were measured according to ASTM standards. The density was measured using a digital density meter as per ASTM D4052, while the viscosity was measured as per ASTM D445 standard using capillary column viscometer. The flash points of all pilot fuels were measured using automatic flash point tester based on ASTM D93. For the determination of calorific value, an oxygen bomb calorimeter was used according to ASTM D240. Finally, the cetane number was evaluated by using formula method according to ASTM D613. All physicochemical properties of fuel and their performance were measured in Centre for Advanced Studies and Research in Automotive Engineering (CASRAE), Delhi Technological University (DTU), Delhi. The equipment used to analyze these properties, their manufacturers, their standards and operating range are shown in Table 3.8.

Table 3.8: List of equipment used for measuring physicochemical properties.

Properties	**Name of Equipment**	**Make**	**ASTM Standard**	**Operating Range**
Density	DMA 4500	Anton Paar	D4052	0 g/cm^3 to 1.5 g/cm^3
Kinematic Viscosity	Capillary Viscosity - High Temperature	Petrotest	D445	+ 5°C to +150°C
Calorific Value	Bomb Calorimeter	Parr	D240	52 to 12000 calorie
Flash Point	Automatic Flashpoint Tester	Pensky-Martens	D93	up to 405 °C

All these properties were discussed further in coming section in detail. Apart from these properties the fatty acid composition of JOME and OPOME were also measured by gas chromatography–mass spectrometry (GC-MS) as per ASTM D-6584.

3.7.1 Density

The instrument used to determine the density of all pilot fuel for the present research was density meter DMA 4500 Anto Paar model. The working principle of this equipment is oscillating U-tube. The oscillating U-tube is a technique to determine the density of liquids and gasses based on an electronic measurement of the frequency of oscillation, from which the density value is calculated. This measuring principle is based on the Mass-Spring Model. The density meter used in the present research is shown in plate 3.1.

Plate 3.1: Density meter

Before injecting the sample, the test fuel pipeline was rinsed by injecting 10 ml of toluene through the sample injection port. The 10 ml sample was then injected to the instrument through injecting port. The process was repeated for five times for one pilot fuel and the average of this

measurement was taken in the end as the final value. Taking the measurement decreases the error of the reading if any.

3.7.2 Kinematic viscosity

Viscosity is an important property of fuel and it can be defined as a measure of the resistance of a fluid which is being deformed by either shear stress or tensile stress. Viscosity describes a fluid's internal resistance to flow and may be thought of as a measure of fluid friction. In general, too viscous fuel tends to form scum and deposits on cylinder walls, piston head etc., and cause atomization problems. So it is desirable that viscosity of fuel should be low. The different blend samples are prepared are investigated for viscosity at 40 °C using a kinematic viscometer as per the specification is given in ASTM D445. It consists of a capillary tube in which sample to be tested is filled. The capillary tube has two marks engraved on it. The time for flow of fuel sample from upper mark to lower mark is measured and kinematic viscosity is calculated using the time taken for each sample. The plate of the kinematic viscometer apparatus is shown in plate 3.2.

The kinematic viscosity of different fuel blends can be calculated as:

$$\upsilon = k \times t$$

Where,

υ= kinematic viscosity of sample;

k = constant for viscometer = 0.005675 mm^2/sec^2;

t = time taken by the fluid to flow through the capillary tube.

Plate 3.2: Kinematic viscometer

3.7.3 Calorific value

The calorific value is defined in terms of the number of heat units liberated when a unit mass of fuel is completely burnt in a calorimeter under specified conditions. The Higher calorific value of fuel is the total heat liberated in kJ per kg or m^3. All fuels containing hydrogen in the available form will combine with oxygen and form steam during the process of combustion. If the products of combustion are cooled to its initial temperature, the steam formed as a result will condense. Thus maximum heat is abstracted. This heating value is called the higher calorific value.

The calorific value of the fuel was determined with the Isothermal Bomb Calorimeter as per the specification is given in ASTM D240. The combustion of fuel takes place at constant

volume in a totally enclosed vessel in the presence of oxygen. The sample of fuel was ignited electrically. Then the fuel samples were burnt in a bomb calorimeter and the calorific value of all samples was calculated. Parr Model 6100EF was used in the laboratory for measuring calorific value of biodiesel. The Bomb Calorimeter used for determination of Calorific value is shown in plate 3.3.

Plate 3.3: Isothermal bomb calorimeter

3.7.4 Flash point

Flash point is the minimum temperature at which the oil vapor, which when mixed with air forms an ignitable mixture and gives a momentary flash on the application of a small pilot flame (Sinha et. al, 2007). The flash and fire point of the test fuels were measured as per the standard of ASTM D93 by Pensky-Martens Automatic Flash Point apparatus as shown in Plate 3.4. The sample was heated in a test cup before the small pilot flame was directed into the cup

through the opening provided at the top cover at the regular intervals. The IS-15607, EN-14214 and ASTM D-6751 specify the minimum value of flash point as 120°C and 130°C respectively.

Plate 3.4: Pensky Marten's automatic flash point apparatus

3.7.5 Saponification value

The saponification value or saponification number is a measure of the average molecular weight of the triglyceride in a sample, such that fatty acids by treatment with alkali is shown in the equation below.

Triglyceride + 3 KOH = Glycerol + 3 Fatty acid Salts of potassium

Saponification value is a measure of the free fatty acid and saponifiable ester groups. It is expressed as the number of milligrams of potassium hydroxide required to neutralize the free acids and saponify the esters contained in one gram of the material. It is calculated as the difference between the saponification value and the acid value.

The lipid is dissolved in an ethanol solution which contains a known excess of KOH. This solution is then heated so that the reaction goes to completion. The un-reacted KOH is then determined by adding an indicator and titrating the sample with HCl. The saponification number is then calculated from the amount of KOH which reacted.

3.7.6 Iodine value

The iodine value is the measure of the unsaturation (or amount of double bonds) of fats and oils, expressed in terms of a number of grams of iodine absorbed per 100g of a sample of oil. Firstly, sample fat is dissolved in carbon tetrachloride, and Hanus reagent is added and left in a dark room for reaction. Then, potassium iodide is added for titration with 0.1mol/L sodium thiosulfate. The iodine value of the fatty sample is calculated from titration volume of sodium thiosulfate.

3.7.7 Cetane number

Cetane number is a measure of the ignition quality of a diesel fuel. One of the ways of solving the problem of cetane number determination is to develop models to predict the cetane number when saponification value and iodine value are known of the biodiesel. The predicted cetane number of biodiesel is comparable to that of the actual cetane number of the biodiesel,

and it has been concluded that the cetane number of biodiesel can be predicted based on thermal properties using the empirical equation for predicting the cetane number of biodiesel.

$$Cetane\ Number = 46.3 + \frac{5458}{Saponification\ value} - (0.225 * Iodine\ value)$$

3.8 Fatty Acid Composition

A gas chromatograph-mass spectroscopy is a chemical analysis instrument for separating chemicals in a complex sample. A gas chromatograph uses a flow-through narrow tube known as the column, through which different chemical constituents of a sample pass in a gas stream (carrier gas, mobile phase) at different rates depending on their various chemical and physical properties and their interaction with a specific column filling, called the stationary phase. As the chemicals exit the end of the column, they are detected and identified electronically. The function of the stationary phase in the column is to separate different components, causing each one to exit the column at a different time (retention time). Other parameters that can be used to alter the order or time of retention are the carrier gas flow rate, column length and the temperature. In a gas-liquid chromatography, an inert carrier gas (Helium or Nitrogen) acts as the mobile phase. This carries the components of analyte (a substance whose chemical constituents are being identified and measured) mixture and elutes through the column. The column usually contains an immobilized stationary phase. In a mass spectrometer, gas is converted into ions in the mass spectrometer. Gas chromatography–mass spectrometry (GC-MS) equipment was used in the present study as shown in Plate 3.5.

Plate 3.5: Gas chromatography–mass spectrometry (GC-MS) equipment

3.9 Experimental Set-Up to Measure the Ignition Delay

To improve the combustion and emission characteristics of any fuel or its blend, ignition delay becomes very fateful property. So to measure the ignition delay a small experimental setup was prefabricated in the laboratory. It consists of a stainless steel cylinder having a capacity of 2l. The thickness of the cylinder chosen was 10mm so that it can sustain at higher pressure and temperature. The ends of the cylinder were closed by 25mm thick stainless steel plates. The welding between plates and cylinder was done in such a way that it sustained at higher pressure and make sure that the welding should leak proof. Two needle valves were fitted on one side of the cylinder which acts as intake valve and exhaust valve. The air at varying pressure was supplied by an air compressor (NIMPRA ESKON SERIES) to the combustion chamber. A pressure gauge was installed to measure the in-cylinder pressure. The air inside the cylinder was heated with the help of two electric heaters of capacity 1.5 kW and 400 W. The higher capacity heater was wrapped outside the cylinder while, the small capacity heater was inset inside the

combustion chamber. A K-type thermocouple was also installed to measure the in-cylinder temperature which was connected with a digital temperature controller. The arrangement is done in such a way that, it automatically cut the power supply of the heaters when the in-cylinder temperature reaches the desired point. Fuel injection system, consist of Bosch fuel injector, Bosch fuel injection pump, fuel tank and fuel injection mechanism, was installed to supply the fuel. A piezoelectric sensor was installed on the fuel supply pipe, which was connected with oscilloscope (FLUKE 190-202 oscilloscope with a multimeter). A glass window was provided on one side of the combustion chamber to detect the combustion. To detect the ignition a photo sensor was put in front of glass window which was attached with an oscilloscope. The schematic diagram of experimental setup is shown in Figure 3.1.

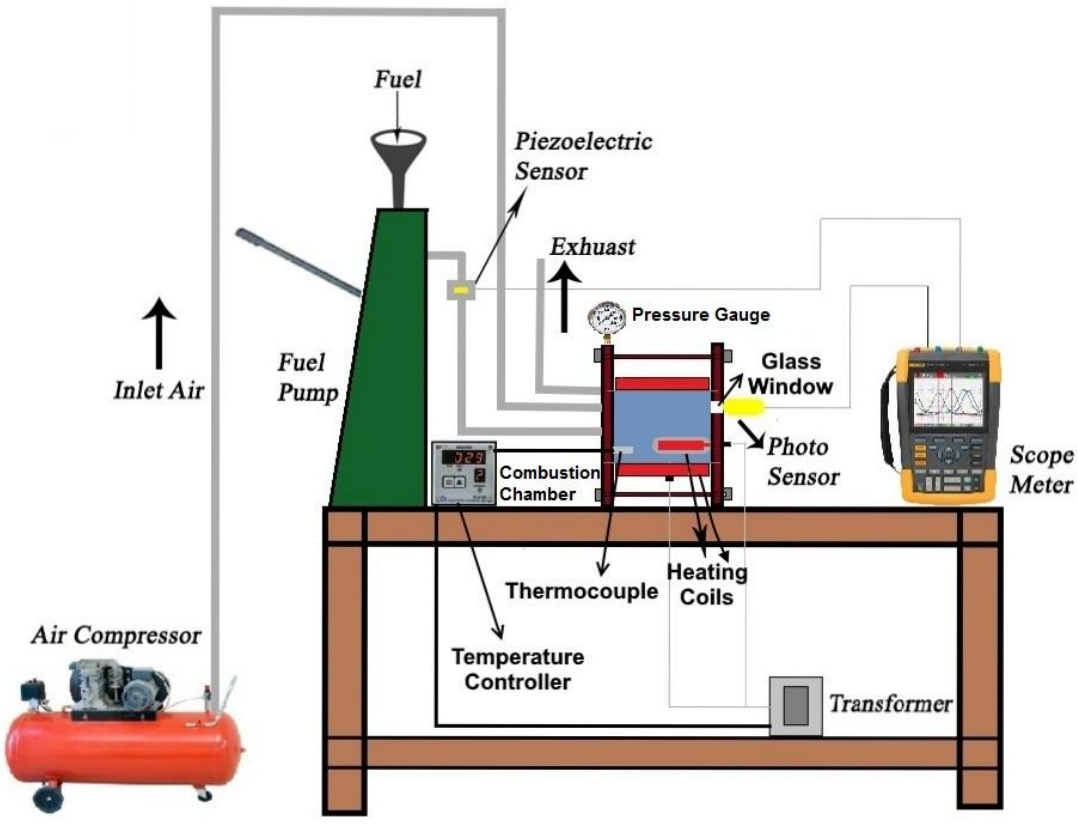

Figure 3.1: Ignition delay measurement setup

3.10 Various Component of Experimental Setup

The experimental set-up for measuring the ignition delay consist of following components:

- Combustion Chamber
- Inlet Valve and Exhaust Valve
- Air Compressor
- Pressure Gauge
- Heating Coils
- Temperature Indicator and Controller
- Fuel Injection Pump
- Piezoelectric Sensor
- Digital Scope Meter with Multimeter
- Fuel Injector
- Optical Window
- Photo Sensor

3.10.1 Combustion chamber

A stainless steel cylinder of dimension 100x100 mm and thickness 10mm was taken to fabricate the combustion chamber shown in plate 3.6. The cylinder was covered with two stainless steel plate of 28mm thickness. The grooves of cylinder size were provided on the plate so that better quality of welding taken place. A small groove was provided inside one plate on

which pressure gauge was installed. Two needle valves were installed on one side of the combustion chamber with one k type thermocouple and fuel injector. On the other side of the combustion chamber, a glass window was provided. A small heating coil was also inserted into the combustion chamber from that side. A high capacity heating coil was wrapped over the combustion chamber. The air at 50 bars was stored into the combustion chamber for one hour to check that all the welding and the attachments were leak proof. The specification of combustion chamber is shown in Table 3.9.

Table 3.9: Specification of combustion chamber

S.No.	Equipment	Specification
1	Combustion chamber	Length= 100mm, Diameter= 100mm and Thickness= 10mm
2	Material	Stainless steel
3	Intake and Exhaust Valves	Needle type
4	Temperature indicator and controller	
5	Start of Injection	Piezoelectric sensor
6	Start of Combustion	Photo sensor
7	Maximum Temperature	900° C
8	Maximum Pressure	70 bar

Plate 3.6: Combustion chamber

3.10.2 Inlet and exhaust valves

These both were fitted on the same side of the combustion chamber. The pressure inside the combustion chamber was higher that's why the needle valves were selected. One valve was used as an inlet valve, the compressed air from the compressor supplied to the combustion chamber through this valve. The second valve was used as an exhaust valve. The combust particles from the combustion chamber release to the environment through this valve.

3.10.3 Air compressor

The air compressor was the important unit for this setup. It was used to supply the compressed air to the combustion chamber. The compressor used in the present research was two stage high pressure reciprocating air compressor shown in plate 3.7. The detail air compressor was given in Table 3.10.

Plate 3.7: Air compressor

Table 3.10: Specification of air compressor

Make	**Nimpra Equipment Pvt. Ltd**
SI No of compressor	10-AC-6665
Model	NPHPC-100
Power	7.5/10 kW/HP
Piston displacement	22 CFM
Compressor RPM	920
Maximum pressure	50 PSI

3.10.4 Pressure gauge

The pressure inside the combustion chamber was measured by pressure gauge which was installed on the top of one plate. The pressure inside the combustion chamber before combustion

and after combustion was measured. The pressure gauge used in the present research is shown in plate 3.8.

Plate 3.8: Pressure gauge

3.10.5 Heating coils

Two heating coils were used to heat the temperature of the air inside the combustion chamber. The small heating coil of capacity 400 W was fitted inside the combustion chamber. While higher capacity heating coil of 1500 W was wrapped over the combustion chamber. Both heating coils were connected to the transformer through temperature controller. The maximum temperature of heating coil for present research was 1500 °C.

3.10.6 Thermocouple

A K-type thermocouple was used for present research to measure the inside temperature of the combustion chamber. The K type is the most common type of thermocouple. It is economical, precise, reliable, and used for wide range of temperature. The type K is commonly found in nuclear applications because of its relative radiation hardness. Maximum operating temperature is around 1,100°C.

3.10.7 Temperature indicator and controller

The thermocouple was attached to temperature indicator and controller which indicate the inside temperature of the combustion chamber. The power was supplied to the heating coils through temperature controller. It maintains the temperature inside the combustion chamber by cutting down the power supply to the heater when the temperature inside the combustion temperature goes beyond the set limit.

3.10.8 Fuel injection pump

For the production of pressure to deliver fuel to pintle nozzle, fuel injection pump is used. The amount of fuel delivered per stroke is controlled by rotating the plunger by means of a control rod. As the plunger is rotated by moving the control rod, a different portion of the helix come in front of the inlet part thus varying the effective stroke of the plunger, the actual plunger travel remaining constant. Fuel pump used in this experiment is a Bosch fuel injection pump and its specifications are given in Table 3.11.

Table 3.11: Specifications of fuel injection pump

Make	Bosch
Type	Single Barrel
Length of stroke	8 mm
Bore	7 mm
Injection Pressure	500 bar
Maximum fuel delivery per stroke	0.2 ml

3.10.9 Piezoelectric sensor

The piezoelectric sensor is a device that uses the piezoelectric effect to measure pressure, acceleration, strain or force by converting them to an electrical charge. In the present research, the piezoelectric sensor was used to determine the moment of fuel injection or start of fuel injection. The piezoelectric sensor was attached to fuel supply pipeline. When fuel was injected the strain was produced in the fuel supply pipeline. This strain was sensed by the piezoelectric sensor which was read by scope meter.

3.10.10 Digital scope meter

Scope Meters are commonly used to observe the exact wave shape of an electrical signal. Scope Meters are usually calibrated so that voltage and time can be read as well as possible to observe by the eye. This allows the measurement of the peak-to-peak voltage of a waveform, the frequency of periodic signals, the time between pulses, the time taken for a signal to rise to full amplitude (rise time), and relative timing of several related signals. The Scope Meter used in this experimental is a digital storage two channel Scope Meter. One channel shows the start of injection and the other channel shows the start of combustion. The combustion characteristics can easily be measured on the screen of Scope Meter by noting of injection and start of combustion on adjusting the time scale. The digital scope meter used in the present research is shown in plate 3.9 and its specification was given in Table 3.12.

Plate 3.9: Digital oscilloscope with multimeter

Table 3.12: Specification of digital scope meter

Make	Fluke
Type	190-062 digital storage scope meter, 2 channel
Model	60 MHz

3.10.11 Fuel injector

The fuel injector is a device which is used to inject the specific amount of fuel into the combustion chamber at fix pressure. The single point fuel injector was used for present research.

3.10.12 Optical window

The optical window was provided on one side of the combustion chamber to determine the start of injection. The borosil glass was used for an optical window in the present research. The fitting was done in such a way that can be removed and put back after cleaning. A photo sensor was put in front of the optical window to sense the combustion inside the cylinder.

3.10.13 Photo sensor

Photoelectric sensor, or photo eye, is a device used to detect the distance, absence, or presence of an object by using a light transmitter, often infrared, and a photoelectric receiver. They may use extensively in industrial manufacturing. There are three different functional types: opposed (through beam), retro-reflective and proximity-sensing (diffused). For this project, a photodetector with 5 μsec rise time is installed in front of the optical window.

3.11 Selection of Engine

The engine used for present research was a Kirloskar four stroke, single cylinder, direct injection stationary constant speed diesel engine. This was a light duty diesel engine commonly used for irrigation in a rural area of India. It is the air cooled engine which makes it popular in stationary light duty engines. The cylinder was made of cast iron and fitted with a hardened high-phosphorus cast iron liner. The lubrication system used in this engine was wet sump type and oil was delivered to the crankshaft. An overhead camshaft was used to operate the Intel and exhaust valves which were driven from the crankshaft. The engine specifications are shown in Table 3.13.

Table 3.13: Test engine specification

Engine Specification	
Make	Kirloskar oil Engine Ltd., India
Model	CAF 8
Rated Brake Power (bhp/kW)	8/5.9
Bore X Stroke (mm)	95 X 110
Compression Ratio	17.5: 1
Cooling System	Air Cooled (Radial Cooled)
Lubrication System	Forced Feed
Cubic Capacity	0.78 L
Starting	Hand Start with cranking handle
Dynamometer Specification	
Manufacturer	Kirloskar Electric Co. Ltd., India
Dynamometer Type	Single phase, 50 Hz, AC alternator
Rated Output	5 KVA @ 1500 rpm
Rated Voltage	230 V
Rated Current	32.6 A

To run a diesel engine on dual fuel mode the modification was done in the intake manifold. The engine intake system is modified via the installation of a specially designed venturi-type gas mixer that allows the introduction of CNG and mixes it with the fresh air. The mixture is allowed to induce to the cylinder as a result of engine suction. The natural gas is supplied through high-pressure (200 bars) commercial CNG cylinder; typical to those used in vehicular applications. A multi-stage pressure regulator is used to reduce CNG pressure to sub-atmospheric level for suction of engine.

An electrical dynamometer coupled to the engine was used as a loading device. A high precision strain gauge type load cell was attached to the dynamometer to accurately transmit the engine loading. A magnetic pickup type rpm sensor was attached at the end of the dynamometer to measure rpm. Two fuel tanks for diesel and the other tank are meant for the biodiesel/diesel blends were provided. The cyclic variation of combustion pressure and the corresponding crank angle was recorded using a "Kubeler" piezoelectric transducer, with low noise cable, mounted on the engine head. The pressure transmitter contained piezoelectric sensor and charge amplifier. The maximum resolution of the pressure sensor was 1°CA. For exhaust gas temperature measurement, Chrome-Alumel K-Type thermocouples were employed close to the engine exhaust manifold. Air flow rate was measured using a mass airflow sensor. The mass flow rate of CNG changes according to load, while the rate of consumption of pilot fuel remains constant throughout loading condition. A rotameter was installed between reducer and lambda controller to measure the mass flow rate of primary fuel while pilot fuel consumption rate was measured by 20cc burette and stopwatch with level sensors. Fuel flow rate, air flow rate, load, rpm, pressure crank angle history and temperature data were fed to a centralized data acquisition system NI USB-6210, 16-bit. A personal computer with a software package "Enginesoft" was connected to the data acquisition system for online and subsequent offline analysis. The control panel is shown in plate 3.10.

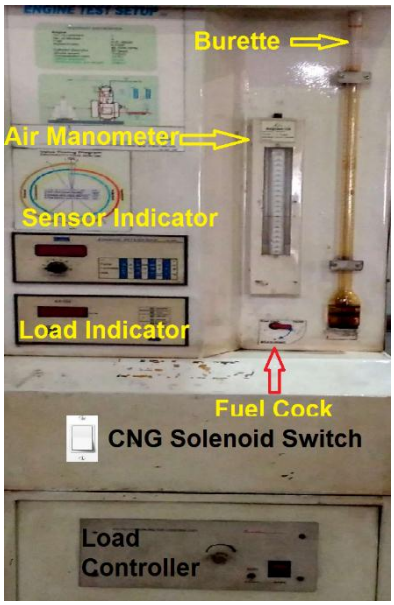

Plate 3.10: Control panel

The control panel of the engine test rig comprised of the data acquisition system, burette for fuel measurement, "U" tube manometer for air measurement, sensor indicator for manual data access, load variation switch etc. The control panel was used for loading and unloading the engine. Besides, the air and fuel consumption data of the sensor was verified from the manual measurements. The data acquisition system inside the control panel received the signals and transmitted them to the computer. The major pollutants in the exhaust of a diesel engine are the oxides of nitrogen, smoke opacity, unburnt hydrocarbons, carbon monoxide, carbon dioxide, etc. For measuring the smoke opacity, AVL 437 smoke meter was utilized. A light beam projected across a flowing stream of exhaust gasses, a certain portion of the light is absorbed or scattered by the suspended soot particles in the exhaust. The remaining portion of the light falls on a photocell, generating a photoelectric current, which is a measure of smoke density. AVL 4000 Light Di-Gas Analyzer was used for measurement of exhaust emissions like total hydrocarbon,

carbon monoxide, carbon dioxide and oxides of nitrogen. The gas analyzer was connected to the engine exhaust by means of probes and the smoke meter was extension pipe. The final experimental test setup consisted of the CI engine, engine cooling water system, the fuel supply and measurement system, air supply and measurement system, load variation and measurement system, rpm measurement system, in-cylinder pressure measurement system, emission measurement system, digital data acquisition system and computer. The schematic diagram of the engine setup is shown in Figure 3.2.

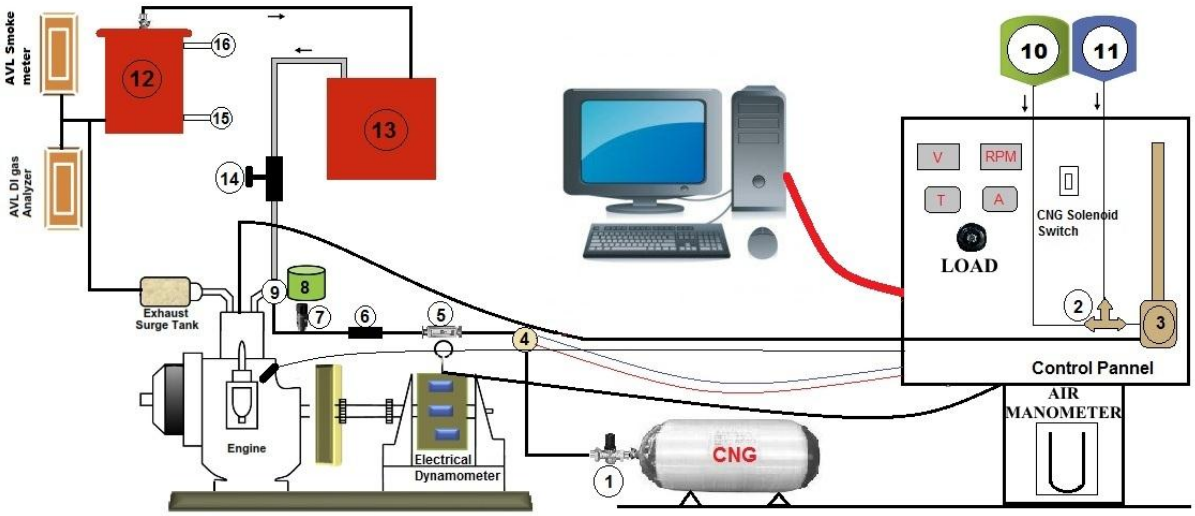

Figure 3.2: Schematic diagram of the test engine.

To recirculate the exhaust gas an EGR system (consist of pipelines, cold water tank, exhaust gas collector, EGR control valve, cold water inlet and hot water outlet) was installed. The hot exhaust gas was passed through the cold water tank and get cold. The water inside the cold water tank was recirculated continuously to remain the inside tank water cold. The cold exhaust gas was then introduced into the combustion chamber through exhaust gas collector. An EGR control valve installed before venturi to control the mass flow rate of exhaust gas. The EGR

design in such a way that both type i.e. cold and hot EGR can be operated with same EGR system. The EGR system is shown in plate 3.11.

Plate 3.11: EGR setup

3.12 Engine Test Parameters

The selections of appropriate parameters were essential for engine calculations, and parameters were selected very judiciously. The engine test was done as specified by IS: 10000. The main parameters desired from the engine are listed below.

Observed parameters are enlisted below.

1. Engine speed.
2. Engine load.
3. Primary fuel consumption rate.
4. Pilot fuel consumption rate
5. Air flow rate.

6. In-cylinder pressure.
7. Exhaust temperature.
8. Emissions of UHC, CO, NO_X, CO_2.
9. Smoke opacity.

Calculated parameters are given below.

1. Brake mean effective pressure (BMEP).
2. Brake thermal efficiency (BTE).
3. Brake specific energy consumption (BSEC).
4. Heat release rate (HRR).
5. Mass fraction burnt rate (MFB).

Once the parameters were selected, the essential instruments required for sensing these parameters were installed at the appropriate points in the experimental set-up.

3.13 Measured Parameters

The measured parameters were listed above. These parameters were measured with the help of instruments. The procedure for measuring and corresponding instruments used to measure these parameters was discussed in detail in this section.

3.13.1 Measurement of engine speed

A magnetic pickup type rpm sensor was attached to the end of the dynamometer shaft which was toothed. This type of sensor consists of a permanent magnet, yoke, and coil. This sensor was mounted close to a toothed gear. As each tooth moved by the sensor, an AC voltage pulse was induced in the coil. Each tooth produced a pulse. As the gear rotated faster more

pulses were produced. These impulse signals were fed digitally to the data acquisition system. The engine control module of the data acquisition system calculated the engine rpm which was subsequently displayed both in the control panel and the enginesoft database in the computer.

$$\text{Engine speed (RPM)} = \frac{Number\ of\ pulses\ per\ minute}{Number\ of\ teeth\ on\ the\ shaft}$$

3.13.2 Engine load

The engine used for the present research has rated the power of 6 kW. But it was found that engine was running smoothly up to 7.5kW load at 1500 rpm. With the dynamometer arm length of 0.185 meters, it was calculated that 27.6 kg corresponded to 100% of the engine load and 0.3kg was equivalent to the zero load. Therefore, various loads applied to the engine were 0.3 kg, 5.76kg, 11.22kg, 16.68kg, 22.14kg and 27.6kg corresponding to the loads of 0%, 20%, 40%, 60%, 80% and 100% of the calibrated load. All performance, emission, and combustion data were recorded at each load for various test fuels. On the basis of the above calculation, the brake power at 0%, 20%, 40%, 60%, 80% and 100% loads were 0.087kW, 1.56kW, 3,052kW, 4.535kW, 6.017kW and 7.5kW respectively.

3.13.3 Measurement of fuel flow

Two fuels were used in dual fuel engine i.e. primary fuel and pilot fuel. The fuel consumption of an engine is measured by determining the time required for consumption of a given volume of fuel. The mass of fuel consumed can be determined by multiplication of the volumetric fuel consumption to its density. The CNG throttling valve position was recorded for all dual fuel engine test data. Upstream CNG pressure was held constant throughout testing. A

rotameter was installed for measuring the mass flow rate of CNG. While, volumetric fuel consumption of pilot fuel was measured using a fuel flow sensor inserted inside the control panel. The sensor signal was fed to the data acquisition system. The sensor data in many cases was validated by manually taking the time for 20cc fuel consumptions in the burette by blocking the fuel cock. However, it was observed that the fuel sensor data was more precise.

3.13.4 Measurement of air flow

The air flow was measured using air sensor (turbine type flow meter) installed inside the control panel. Plate 3.9 shows the sensor in the previous sections. In principle, the turbine flow meters use the mechanical energy of the fluid to rotate a "pinwheel" (rotor) in the flow stream. Blades on the rotor are angled to transform energy from the flow stream into rotational energy. The rotor shaft spins on bearings. When the fluid moves faster, the rotor spins proportionally faster. Blade movement is often detected magnetically, with each blade or embedded piece of metal generating a pulse. The transmitter processes the pulse signal to the data acquisition system that determines the flow of the fluid. The air flow data was available in the sensor indicator of the control panel and the enginesoft database. Moreover, there was another method available to validate the sensor data. It was based on the orifice and the air box method. The differential pressure across the orifice inserted in the air flow channel provides the air flow rate using the formula in the equation.

$$\text{Mass of air (m)} = C_d \times A \times \sqrt{(2gh_w\rho_w\rho_a)} \qquad (3.1)$$

Where C_d = Coefficient of discharge of orifice (0.6 in the present case); A = Orifice area; g = Acceleration due to gravity; h_w = Height of water column; ρ_w/ρ_a = Density of water/air

3.13.5 In-cylinder pressure measurement

As discussed in the earlier sections, the "Kubeler" piezoelectric transducer was used for in-cylinder pressure measurement. Plate 3.12 shows the pressure transducer. The signals from the charge amplifier were fed to the data acquisition system where the engine control module converted the signals into digital data. The in-cylinder pressure data in terms of pressure – crank angle history was only obtained in the enginesoft database. In the present study, the average of 91 cycles was considered for analysis of in-cylinder pressure crank angle data.

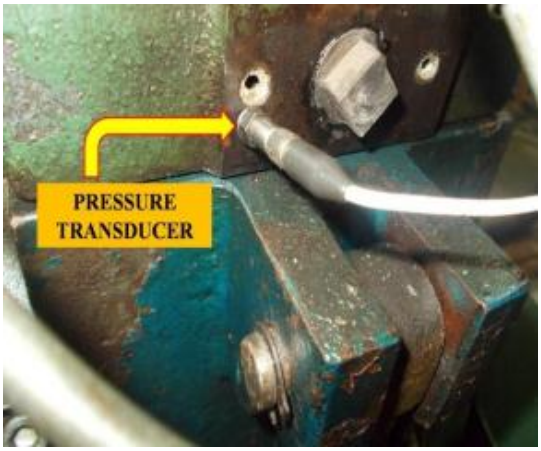

Plate 3.12: Pressure transducer

3.13.6 Measurement of exhaust temperature

Chromel-Alumel K-type thermocouples plate 3.13 were connected to a six-channel digital panel meter to measure temperatures of exhaust gas. The meter was calibrated by a millivolt source up to 800o C. The sensor was placed close to the exhaust manifold of the engine. The temperature data was observed both at the sensor indicator in the control panel as well as the engine-soft database.

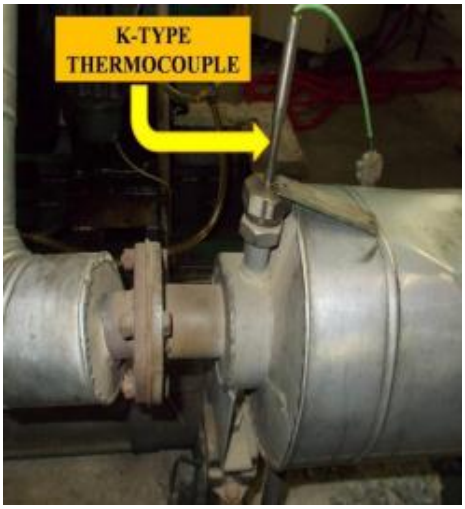

Plate 3.13: K-type thermocouple

3.13.7 Measurement of exhaust emissions

The exhaust emissions (NO_X, HC, CO and smoke opacity) were important parameters for the environment. The AVL 4000 di-gas analyzer and AVL 437-smoke meter were used to measure the exhaust emissions. The gas and smoke meter were made stable and ready to work first and then use for measurement of exhaust emissions. The emission measurement of NO_X, UHC and CO was done first and after that smoke opacity was measured. The specifications of AVL di-gas analyzer and AVL smoke meter are given in Table 3.14.

Table 3.14: Specifications of the di-gas analyzer and smoke meter.

S. No.	Instrument Name	Measurement Parameters	Measurement Range	Resolution	Measurement Technique
1.	AVL DI-GAS ANALYZER	CO	0-10% Volume	0.01% Volume	Non dispersive infra-red sensor
		HC	0-20000 ppm Volume	1ppm	Non dispersive infra-red sensor
		NOx	0-10000 ppm Volume	1ppm	Chemi-luminescence principle, electro-chemical sensor
2.	AVL- Smoke Meter	Smoke Opacity	0-100 %	0,1 %	Photochemical

3.14 Calculated Parameters

The calculated parameters were listed in section 3.12. These parameters show the effectiveness and combustion characteristics of the engine. Once the measured parameters were observed, the calculation of these parameters starts manually or with the help of a computer. The equations and relationship used to calculate these parameters are shown in this section.

3.14.1 Calculation of brake mean effective pressure

To calculate the brake mean effective pressure (BMEP) of the engine, brake power (BP) need to be calculated first. The formula used for calculating the brake power at the engine shaft is shown in equation 3.2.

$$\text{BP (kW)} = \frac{2\pi \times rpm \times Load\ (kg) \times 9.81 \times Dynamometer\ arm\ length\ (m)}{60 \times 1000} \quad (3.2)$$

The equation 3.3 used to calculate BMEP after calculating BP of the engine shaft is shown as.

$$\text{BMEP (bar)} = \frac{120 \times BP\ (kW)}{L \times A \times N \times 101.325} \quad (3.3)$$

Where L = Stroke length in meter; A = Piston area in m^2; N = Engine rpm.

3.14.2 Brake thermal efficiency

Brake thermal efficiency (BTE) is the ratio of brake power to the energy used to produce that brake power. This energy comes from the combustion of fuel. In dual fuel engine, the total

heating value is the sum of the heating value of gaseous fuel and pilot fuel. The formula used to calculate the BTE of the engine was given in equation.

$$\text{BTE (\%)} = \frac{\text{BP (kW)}}{(m^* \times \text{Qcv})g + (m^* \times \text{Qcv})p} \quad (3.4)$$

Where, m* = Mass flow rate of fuel in (kg/s); Qcv = Calorific value of fuel (kJ/kg); (m*× Qcv)g = heating value of gaseous fuel and (m*× Qcv)p = heating value of pilot fuel

3.14.3 Brake specific energy consumption

The brake specific energy consumption (BSEC) and BTE are mutually inversely proportional. The BSEC is the ratio of the sum of the heating value of gaseous fuel and pilot fuel to the BP produced from that energy. The formula used to calculate the BSEC of the engine was given in equation.

$$\text{BSEC (MJ/kWh)} = \frac{[(m^* \times \text{Qcv})g + (m^* \times \text{Qcv})p] \times 3600}{\text{BP(kW)}} \quad (3.5)$$

3.14.4 Calculation of heat release rate

Evaluation of cyclic heat release is very much significant for combustion study. Various heat release models have been proposed by researchers for determining critical combustion parameters like heat release rate, pressure rise rate etc. In the present investigation, the heat release calculations described by Rakopoulos et al., (2011) was referred. Although combustion in a CI, DI (compression-ignition, direct injection) engine is quite heterogeneous, the contents of the combustion chamber are assumed to be homogeneous in the method suggested by Sorenson

(Ying et al., 2009). This type of heat release model is generally termed as a zero-dimensional model in the literature. In the light of the above fact, the zero-dimensional model proposed by Sorenson was considered for combustion characterization.

The Sorenson's model is a thermodynamic model based on energy conservation principle (Pali et al., 2014; Heywood, 1988). Neglecting the heat loss through piston rings (Lu et al., 2006) the energy balance inside the engine may be written as:

$$\frac{dQ}{d\theta}-\frac{dQw}{d\theta} = \frac{d(\mathrm{mu})}{d\theta} + P\frac{dV}{d\theta} = mC_v\frac{dT}{d\theta} + P\frac{dV}{d\theta} \qquad (3.6)$$

Where: $dQ/d\theta$ = Rate of net heat release inside the engine cylinder (J/°CA); $dQ_w/d\theta$ = Rate of heat transfer from the wall (J/°CA); m = Mass flow of the gas (kg); u = Internal energy of the gas (J/kg); P = Cylinder pressure (bar); V = Gas volume (m^3); θ = Crank angle (°CA); T = Gas temperature (K); C_v = Specific heat at constant volume (J/kg K)

Now the ideal gas equation is given as

$$PV = mRT \qquad (3.7)$$

Where R = Universal gas constant

The derivative of universal gas equation with respect to crank angle is given by

$$P\frac{dV}{d\theta} + V\frac{dP}{d\theta} = mR\frac{dT}{d\theta} \qquad (3.8)$$

Putting equation (3.8) in equation (3.6), the heat release rate is derived as follows.

$$\frac{dQ}{d\theta} = P\frac{Cp}{R}\frac{dV}{d\theta}+V.\frac{Cv}{R}\frac{dP}{d\theta}+mT\frac{dCv}{d\theta} + \frac{dQw}{d\theta} \qquad (3.9)$$

Where C_p = Specific heat at constant pressure (J/kg°K)

The above equation is further simplified for actual heat release calculation and is given below.

$$\frac{dQ}{d\theta} = \frac{1}{\gamma-1}\left(V\frac{dP}{d\theta} + \gamma P\frac{dV}{d\theta}\right) - \frac{dQw}{d\theta} \qquad (3.10)$$

Where γ = ratio of specific heats

In a four-stroke engine, crank angles are typically given with zero values at the TDC, (top dead center) between the intake and exhaust strokes. However, the important heat release events occur between SOI (start of injection, typically about 337°) and EVO (exhaust valve opening, typically about 500°).

The trigonometric functions require their arguments in radians that are essential for gas volume calculations. The formula for calculating the arguments for the trigonometric functions, equation 3.11 was used.

$$\theta_{rad} = \frac{\pi(\theta - 360 + \text{Phase})}{180} \qquad (3.11)$$

Where: θ_{rad} = argument of trigonometric functions (radians); Phase = phase shift angle (°CA)

The piston displacement was needed in calculating the gas volume. It is provided in equation 3.12.

$$\frac{S}{R} = [1 - \cos(\theta_{rad})] + \frac{L}{R}\left\{1 - \left[\sqrt{1 - \frac{\sin(\theta rad)}{L/R}}\right]^2\right\} \qquad (3.12)$$

Where: S = piston displacement from TDC (m); R = radius to crank pin (m); L = connecting rod length (m)

Then the gas volume was calculated as in the equation 3.13

$$V = V_{cl} + S\,A_p \qquad (3.13)$$

Where: A_p = top area of piston (m^2) = $\pi(\text{bore})^2/4$; bore = cylinder bore (m); V_{cl} = clearance volume (m^3); r = compression ratio; Stroke = piston stroke (m)

The combustion chamber wall area, needed for heat transfer calculations, was given in the equation.

$$A_{wall} = 2A_p + \pi \text{ (bore) } S \qquad (3.14)$$

Equation 3.14 ignores the area associated with the piston cup, but the approximation has little effect on the heat release results.

The heat release equation 3.10 was required for the calculation of dP/dθ. It can be shown that the slope at the j^{th} point of the curve defined by n sequential points is as shown in equation 3.15.

$$\frac{dPj}{d\theta} = \frac{n\Sigma(Pi\theta i) - \Sigma Pi\ \Sigma\theta i}{n\Sigma(\theta i)^2 - (\Sigma\theta i)^2} \qquad (3.15)$$

Where n is an odd number and each summation is from [j – (n – 1)/2] to [j + (n – 1)/2].

When a shaft encoder is used to trigger pressure measurements, the points are equally spaced along the θ axis at spacing Δθ. The choice of n is a compromise; a larger n helps to combat noise in the pressure data, but may also obscure real changes in the heat release curve. In the present case with Δθ = 1°, choice of n = 7 was found to fit the equation 3.15 over 4° of the pressure trace and was a suitable compromise. The equation 3.16 shows the pressure smoothing technique applied to the noise in pressure data.

$$P_{j+1} = P_j + \frac{dPj}{d\theta}\Delta\theta \qquad (3.16)$$

Calculation of dV/dθ was accomplished as per the equation 3.17.

$$\frac{dVj}{d\theta} = V_j - V_{j-1} \qquad (3.17)$$

In-cylinder gas temperature varies rapidly throughout the cycle. Consequently, the value of γ varies with temperature. The ideal gas law was used to calculate the spatially averaged temperature in the combustion chamber as mentioned in the equation 3.18.

$$T_j = \frac{PjVj}{MR_g} \qquad (3.18)$$

Where: T_j = bulk gas temperature at point j (K); R_g = idea gas constant = 8.314/29 = 0.287; M = mass of charge, g = (1 + AF) mf; AF = air/fuel ratio of engine; m_f = mass of fuel injected into each engine cycle (g)

2.14.5 Calculation of mass fraction burn

Mass fraction burned (MFB) in each individual engine cycle is a normalized quantity with a scale of 0 to 1, describing the process of chemical energy release as a function of crank angle. The determination of MBF is commonly based on burn rate analysis – a procedure developed by Rassweiler and Withrow. It is still widely used because of its relative simplicity and computational efficiency, despite the approximate nature of this method (Mendera et al., 2002).

The Rassweiler and Withrow procedure are based on the assumption that, during engine combustion, the pressure rise Δp_j (at crank angle increment) consists of two parts: pressure rise due combustion (Δpc_j) and pressure change due to volume change (Δpv_j).

$$\text{Therefore, } \Delta p_j = \Delta pc_j + \Delta pv_j \qquad (3.19)$$

Assuming that the pressure rise Δpc_j is proportional to the heat added to the in-cylinder medium during the crank angle interval, the mass fraction burned at the end of the considered j^{th} interval may be calculated as (Mendera et al., 2002).

$$\text{MFB} = \frac{mb\ (i)}{mb\ (total)} = \frac{\Sigma_0^i \Delta Pc}{\Sigma_0^N \Delta Pc} \qquad (3.20)$$

Where N is the total number of crank angles in the in-cylinder pressure ~ crank angle data

The cumulative heat release was calculated by summing up the heat release per crank angle data throughout the cycle. The pressure rise rate for various test fuels was calculated from the spreadsheet database using equation (3.16) and (3.17). The mass fraction burnt was calculated from equation (3.20). Ignition delay for the test fuels was calculated as the difference between the fuel injection angle and the crank angle corresponding to the MFB of 0.05. Similarly, the total combustion duration for the test fuels was calculated as the difference between the crank angles corresponding to MFB of 0.10 to MFB of 0.95.

3.15 Experimental Procedure

The engine was started at no load with decompression lever by pressing the exhaust valve and released suddenly when the engine was hand cranked at sufficient speed. After feed control was adjusted so that engine attained rated speed and was allowed to run (about 30 minutes) till the steady state condition was reached and the exhaust gas temperature corresponding to that load stabilized. The enginesoft software was connected to the data acquisition system and allowed to run. Automatic data entry system was activated and the resolutions of various sensors were set. All the sensors were allowed to perform at their minimum resolutions. For pressure crank angle history the average of 91 cycles was chosen for each load whereas for performance

and emission studies the average of 10 consecutive data was chosen to minimize error. The reading of all parameters was measured for the engine using diesel as a fuel and take it as baseline data. The engine was then switched to dual fuel mode by supplying the CNG from the CNG cylinder. The quantity of liquid fuel was reduced to 15% by adjusting the governor. The mass flow rate of CNG changes with load while the mass flow rate of pilot fuel remains constant. As discussed earlier the mass flow rate of CNG was measured with the help of rotameter and mass flow rate of pilot fuel was measured with a burette.

To validate the sensors, and the electronic gadgets, the time for 20 cc pilot fuel consumption and the manometric readings of air consumption were taken repeatedly and averaged several times. The manual data so obtained was compared with the "enginesoft" data and found very close to each other. Similarly, data in the printed copies of emission analyzers were often compared with the emission data of the enginesoft database and found all most identical.

All the combustion, performance and emissions parameters were evaluated at each load thoroughly. Many times the trial was repeated to avoid any discrepancy in results. As mentioned earlier, for baseline data, diesel tank was used and thereafter for blends the biodiesel tank was used by swapping the fuel line by the rotary valve. Every time the engine was started with diesel and stopped after running at least 20 minutes on diesel.

It may be observed that all of the measurements exhibited higher accuracy. The repeatability of all measurements was checked throughout the experimental trial and found

sufficiently close. The accuracies and uncertainties associated with various measurements are shown in Table 3.15.

Table.3.15: Accuracies and uncertainties of measurements

S.N.	Measurements	Measurement Principle	Range	Accuracy
1	Engine load	Strain gauge type load cell	0-25 kg	±0.1kg
2	Speed	Magnetic pickup type	0-2000 rpm	±20 rpm
3	Time	Stop watch	--	±0.5%
4	Exhaust Temperature	K-type thermocouple	0-1000°C	$\pm 1^0$C
5	Carbon monoxide	Non-dispersive infrared	0-10% vol.	±0.2%
6	Carbon dioxide	Non-dispersive infrared	0-20% vol.	±0.2%
7	Total hydrocarbons	Non-dispersive infrared	0-20,000 ppm	±2 ppm
8	Oxides of nitrogen	Electrochemical	0-4000 ppm	±15ppm
9	Smoke	Photochemical	0-100%	± 2%
10	Crank angle encoder	Optical	0-720 °CA	$\pm 0.2^0$CA
11	Pressure	Piezoelectric	0-200 bar	± 1 bar
	Calculated results			**Uncertainty**
12	Engine power	--	0-8 kW	±1.0%
13	Fuel consumption	Level sensor	--	±2.0%
14	Air consumption	Turbine flow type	--	±1.0%
15	BTE	--	--	±1.0%
16	BSEC	--	--	±1.5%
17	Heat release	Sorenson model	--	±5.0%
18	In-cylinder temp.	Ideal gas equation	Up to 3000 K	±5.0%

CHAPTER 4

RESULTS AND DISCUSSIONS

4.1 Introduction

In this chapter, all results of the present research are presented with their discussion. These results start from the selection of fuel, their production, process optimization of production and measuring of physicochemical properties of tested fuel. The ignition delay of all pilot fuels is also measured. After production, all fuels are tested on a dual fuel engine. The combustion, performance and emissions characteristics of dual fuel engine are measured for all test fuels and results are compared with conventional diesel engine data, which is taken as baseline data. The effect of the application of EGR in dual fuel engine is also analyzed whose results are also shown in this chapter.

In the initial phase of the present research work, the effect of both hot and cold EGR on the performance of dual fuel engine is analyzed. However, it is found that the application of hot EGR improves the performance of dual fuel engine at lower and intermediate load but decrease the performance of the engine at higher load. Also, hot EGR increases the NO_X emissions of the dual fuel engine. On the other hand, the application of cold EGR also improves the performance of the dual fuel engine but it is lower than hot EGR. However, at higher load, cold EGR shows better results compared to hot EGR in term of engine performance. Also, with improving the performance of dual fuel engine, NO_X emissions of the engine is also reduced by applying cold EGR. Keeping these factors into consideration, cold EGR is selected for the present research

work. The quantity of EGR also affects the performance of the engine. Therefore, the optimum value of cold EGR (i.e. 10% EGR) is evaluated after a number of trials.

4.2 Biodiesel Production and Optimization

As discussed in the preceding chapter, the biodiesel can be produced through a single stage and double stage transesterification process depending on the free fatty acid (FFA) content of oil. The FFA content is found to be 7.1% and 1.2% for Jatropha oil (JO) and Orange peel oil (OPO) respectively. The FFA content of OPO is theoretically favorable for direct transesterification or single stage transesterification since it is less than 2%. While the FFA of Jatropha oil is above the limit, so esterification is required to reduce the FFA to the acceptable limit of 2% before conversion into esters. Afterward, biodiesel is prepared by converting low FFA oil into esters through transesterification process. The process of biodiesel production has already been discussed in the preceding chapter.

The variables affecting the esterification and transesterification are; catalyst concentration, methanol: oil molar ratio, temperature, reaction time and stirring speed. So, it is required to find out the optimum values of these variables. However, stirring speed does not affect much after a specific value compared to other variables, so the stirring speed is kept constant at 350 rpm in the present work. The effects of other variables on FFA reduction and biodiesel production are analyzed with the help of response surface methodology (RSM) optimizing tool. Three level-four factors Central Composite Design (CCD) is designed to analyze the effects of each variable (catalyst concentration, methanol: oil molar ratio, temperature and reaction time) and also the combination of two variables interactions. The

independent variable is selected from the primary study conducted, which recognized the most significant variable which affects the esterification and transesterification reaction. The catalyst concentration, methanol: oil molar ratio, temperature and reaction time as well as the stirring speed has different grades of effect on the reaction. Total 30 experiments are suggested by the Design Expert 10.0.3.0 software (academic version) in which 24 experiments are augmented and 6 replications as the center point to evaluate the pure error (Yuan et al., 2008). The minimum value of the FFA and maximum values of the yield are taken as the responses of the experimental design.

4.2.1 Optimization of esterification process

The optimization of reaction condition is important in determining parameters such as reactor design, energy recovery of the final products and its quality. The optimization of two-stage transesterification reaction is conducted. Reducing the FFA content of vegetable oils is desirable in ensuring the feasibility of transesterification reaction. It has been reported that esterification reaction is capable of reducing the FFA content of oil (Kumar and Kumar, 2016a; Jain and Sharma, 2011). From the results, the initial FFA content of Jatropha seed oil is found as 7.1 (mg KOH/g), as such, the esterification reaction is required to reduce the FFA content of the oil to less than 2. The optimization indicated that the required catalyst concentration needed for the FFA reduction is 1.39%. High catalyst concentration promotes saponification reaction, thereby producing soap in preference to the needed esterification reaction. The reaction temperature is probably the most influencing parameter in the esterification reaction, the optimum reaction temperature is found to be 55.03 °C. The ramp function graph for optimum FFA reduction with values of all variables is shown in Figure 4.1.

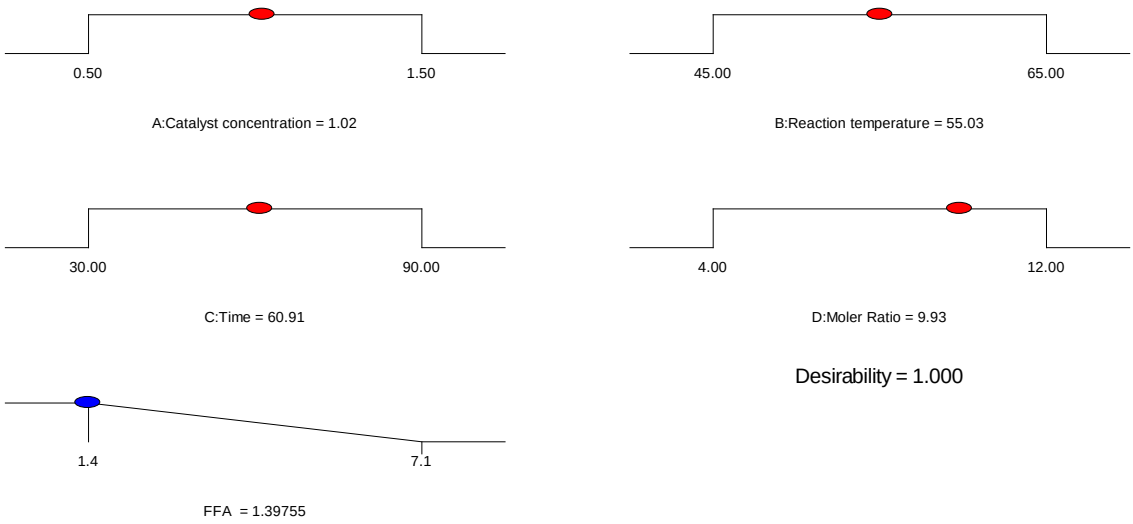

Figure 4.1: Ramp function graph for optimum FFA.

The low reaction temperature is desirable to ensure lower energy consumption. The temperature reported in this work is within the range of other similar research work ranging from 50 °C to 65 °C. From the results, reaction time is found as 60.91 min, which is relatively low as compared to other highly acidic oils. It is reported that high acid oils require longer reaction time in addition to high temperature and catalyst concentration. Under these conditions, the optimum FFA reduction obtained is 1.39 (mg KOH/g).

The graphical interpretation in form of contour lines indicated the significance of each parameter on the FFA reduction. The main process parameters affect the FFA reduction with different degree of significance. From the results, the contours enable the visualization of the correlations between the experimental runs and the response (FFA reduction). Figure 4.2 presents the contour showing the regression between combinations of variables. Each line presented in the contour presents the mutual interaction between two or more variables.

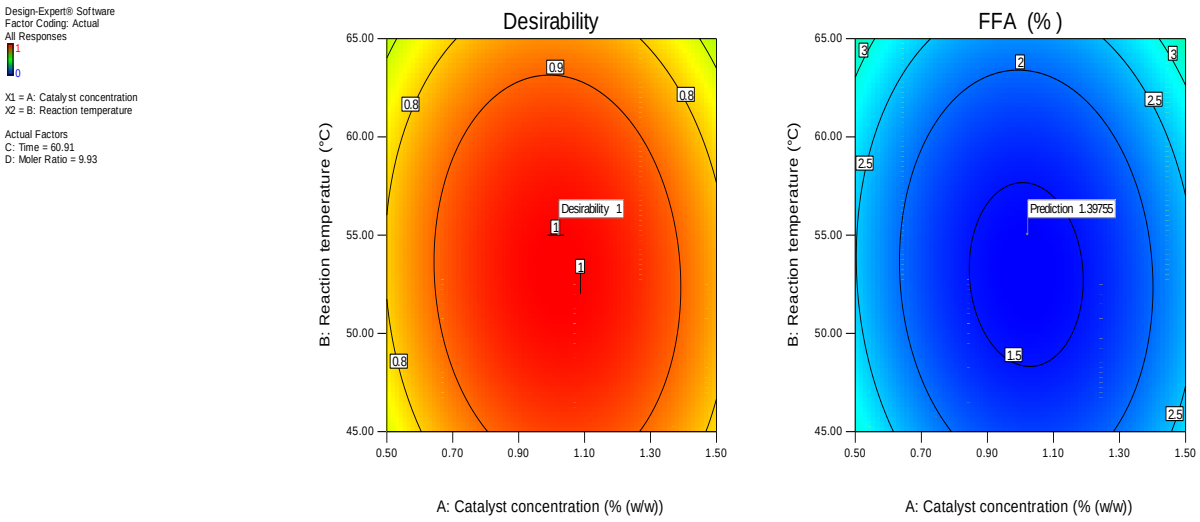

Figure 4.2: Regression between combinations of variables.

For example, the effect of catalyst concentration and temperature on FFA reduction is showing at the pointwise interval. The uniform contour lines distribution indicate a mutual interaction between the catalyst concentration and reaction temperature on the FFA reduction. Distorted contour lines indicate a moderate interaction between the main factors as regards to the FFA reduction. This is further confirmed by the second order polynomials in the ANOVA Table, showing a high level of significance in the interactions. Similarly, it could be observed from the contours plotted for the different combination of factors. Figure 4.2 presents the contour lines for the effect of the combination of reaction temperature and catalysts which had predicted the FFA reduction value down to 1.39 (mg KOH/g).

The predicted model is only suitable if there exist a reasonable agreement between the predicted values and the actual or experimental values. The plot describing this relationship is presented in Figure 4.3. It is obvious from the plot that, there is a high degree of agreement

between the two. The indication of this is shown in R^2 value approaching unity. From the plot, R^2 value (0.99) showed high variability, meaning that the model is well fitted and more than 99% of the data is captured by the predicted model. Table 4.1 shows the analysis of variance for esterification. Considering the value of P> F indicated the model significance with less than 0.01, an indication that the predicted desirable set for the model is perfectly fitted. It is reported that, the value of P < 0.0001 is noise expected from experiment error, but the chance of the model fit is not higher than 0.01% as indicated by the F-value. The predicted vs. actual herein reported is an indication of this observation.

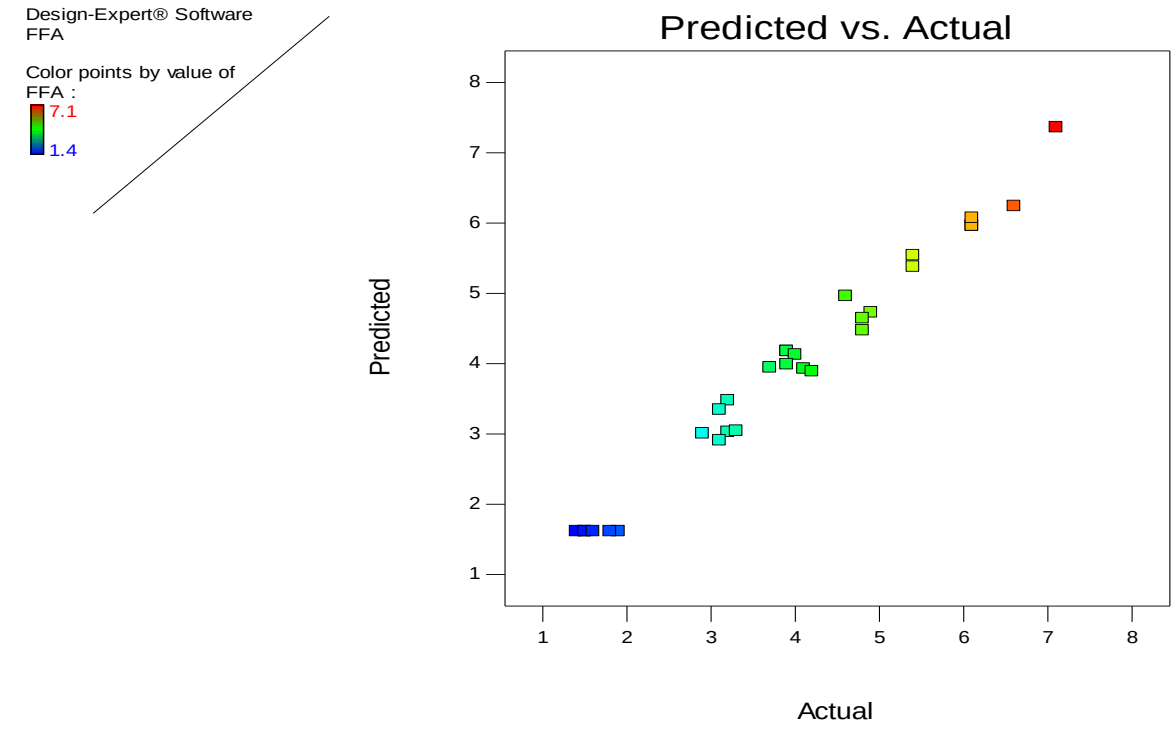

Figure 4.3: Predicted vs. Actual plot for FFA

Table. 4.1: Variance for esterification of Jatropha oil

Source	Sum of Squares	df	Mean Square	F Value	p-value Prob > F	
Model	73.50883	14	5.250631	57.03763	$2.04x10^{-10}$	significant
A-Catalyst concentration	0.735	1	0.735	7.984309	0.01278	
B-Reaction temperature	0.015	1	0.015	0.162945	0.692155	
C-Time	3.226667	1	3.226667	35.0513	0.000028	
D-Moler Ratio	15.04167	1	15.04167	163.3977	$1.81x10^{-09}$	
AB	0.16	1	0.16	1.738081	0.207159	
AC	0.5625	1	0.5625	6.110441	0.0259	
AD	0.9025	1	0.9025	9.803862	0.006866	
BC	0.04	1	0.04	0.43452	0.519771	
BD	4.41	1	4.41	47.90585	$4.88x10^{-06}$	
CD	2.4025	1	2.4025	26.09837	0.000128	
A^2	31.32964	1	31.32964	340.3341	$1.01x10^{-11}$	
B^2	9.266786	1	9.266786	100.6651	$4.78x10^{-08}$	
C^2	7.741071	1	7.741071	84.0913	$1.54x10^{-07}$	
D^2	14.16964	1	14.16964	153.9249	$2.74x10^{-09}$	
Residual	1.380833	15	0.092056			
Lack of Fit	1.1925	10	0.11925	3.165929	0.107642	not significant
Pure Error	0.188333	5	0.037667			
Cor Total	74.88967	29				
R-Squared = 0.981562						

The graphical presentation of the regression equation (Equation 4.1) is best presented by the response surface plots for the different combination of factors. Figure 4.4 presents the response surface plot for the combination of catalyst concentration and reaction temperature on the FFA reduction. Also, Figure 4.5, Figure 4.6, Figure 4.7, Figure 4.8 and Figure 4.9 presents the response surface plot for the combination of time vs. reaction temperature, catalyst concentration vs. time, molar ratio vs. reaction temperature, catalyst concentration vs. molar ratio and molar ratio vs. time respectively on the FFA reduction.

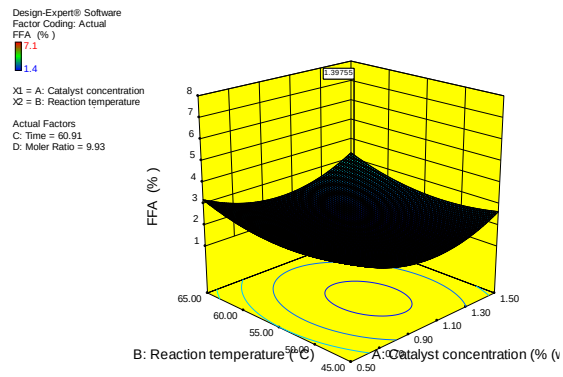

Figure 4.4: Interaction effect of catalyst concentration and reaction temperature

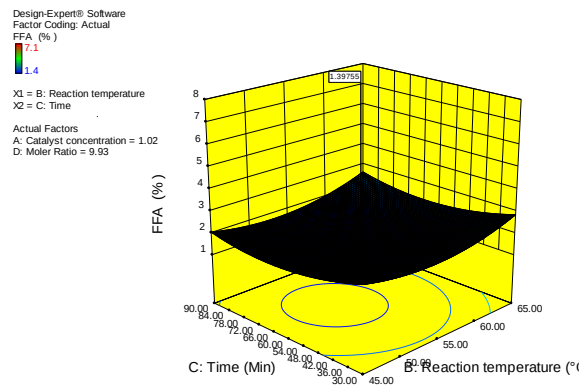

Figure 4.5: Interaction effect of time and reaction temperature

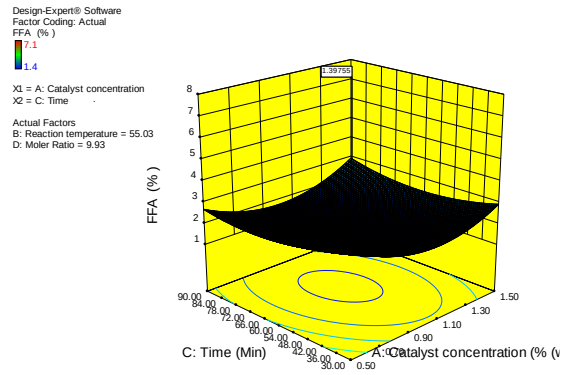

Figure 4.6: Interaction effect of catalyst concentration and time

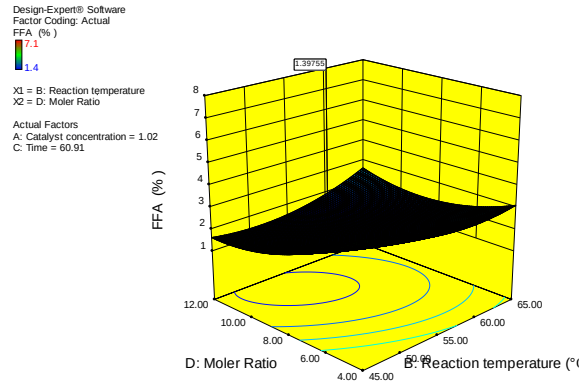

Figure 4.7: Interaction effect of molar ratio and reaction temperature

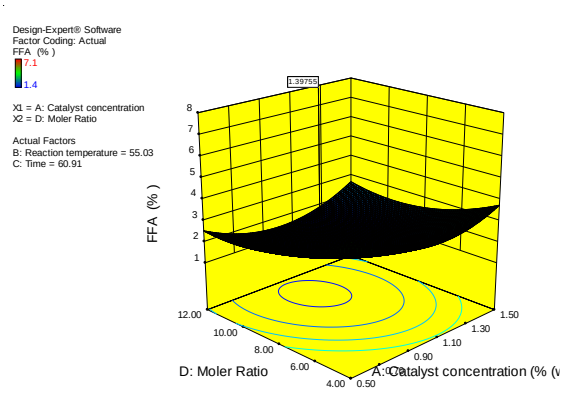

Figure 4.8: Interaction effect of catalyst concentration and molar ratio

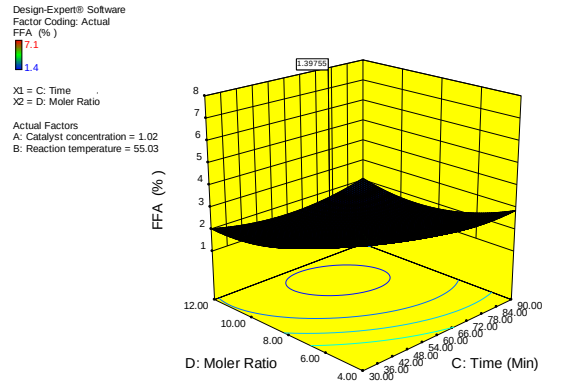

Figure 4.9: Interaction effect of molar ratio and time

As earlier predicted by the ANOVA Table, the FFA reduction is largely affected by the individual effects of reaction temperature and catalysts concentration. In addition, the combined effects of these factors also contributed significantly to the FFA reduction.

$$FFA = 1.616667 - 0.175*A - 0.025*B - 0.36667*C - 0.79167*D + 0.1*A*B + 0.1875*A*C + 0.2375*A*D + 0.05*B*C + 0.525*B*D + 0.3875*C*D + 1.06875*A^2 + 0.58125*B^2 + 0.53125*C^2 + 0.71875*D^2 \quad (4.1)$$

4.2.2 Optimization of transesterification process

The FFA of Jatropha oil is reduced to 1.4% from 7.1% through esterification as discussed in the previous section. As mentioned earlier, Jatropha oil and Orange peel oil are selected for biodiesel production for the present research. The FFA content of OPO is 1.2% so biodiesel of the oil is made through transesterification process. Since Jatropha oil has higher FFA, the biodiesel production is carried out in two stage process. The FFA content of Jatropha oil is 1.4% after esterification. Transesterification process is carried out by monitoring; catalyst concentration (A), reaction temperature (B), reaction time (C) and methanol to oil molar ratio (D) at the constant stirring speed at 350 rpm to determine corresponding optimum conditions using RSM. These results are similar to the results reported for iste rapeseed oil, cotton seed oil and used frying oil (Yuan et al., 2008; Atapouret al., 2013; Alhassan et al., 2014). Characterization of JOME and OPOME samples produced in the transesterification is an integral part of biodiesel quality control.

Similar to the esterification process discussed in the last section, the same methodology is also implemented in the transesterification process. The predicted model is only suitable if there

exist a reasonable agreement between the predicted values and the actual or experimental values. The plot describing this relationship is presented in Figure 4.10 and Figure 4.11 for JOME and OPOME respectively. It is obvious from the plot that, there is a high degree of agreement between the two. The indication of this is shown in R^2 value approaching unity. From the plot, R^2 value showed high variability, meaning that the model is well fitted and greater than 99% of the data is captured by the predicted model. Table 4.2 and Table 4.3 shows the analysis of variance for transesterification for JOME and OPOME respectively. Considering the value of P> F indicated the model significance with less than 0.01, an indication that the predicted desirable set for the model is perfectly fitted. It is reported that, the value of P < 0.0001 is noise expected from experiment error, but the chance of the model fit is not higher than 0.01% as indicated by the F-value. The predicted vs. actual herein reported is an indication of this observation.

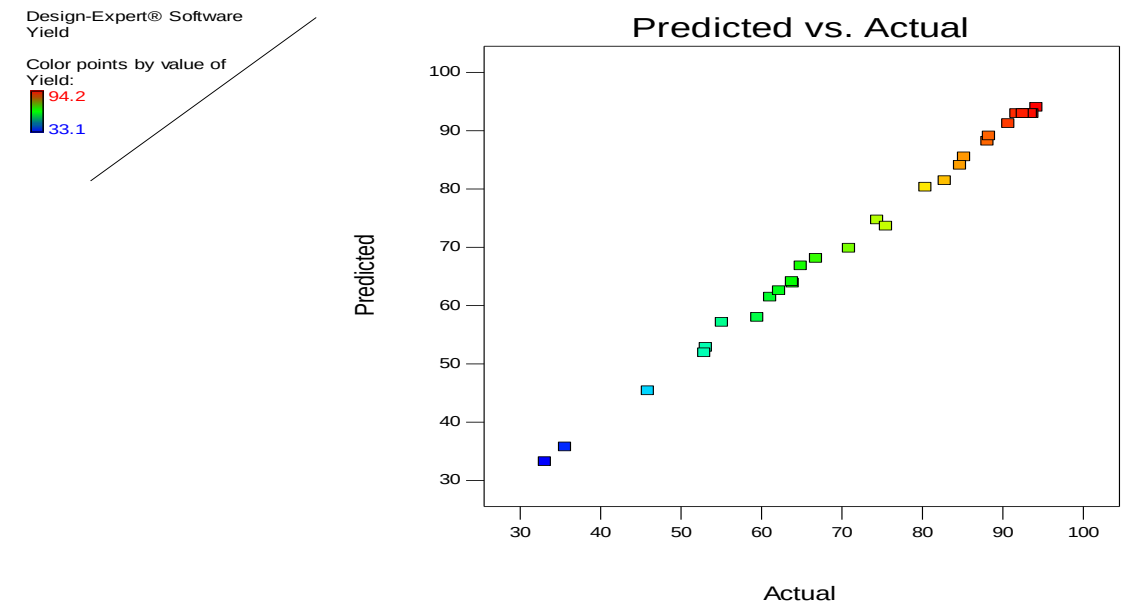

Figure 4.10: Predicted vs. Actual for JOME

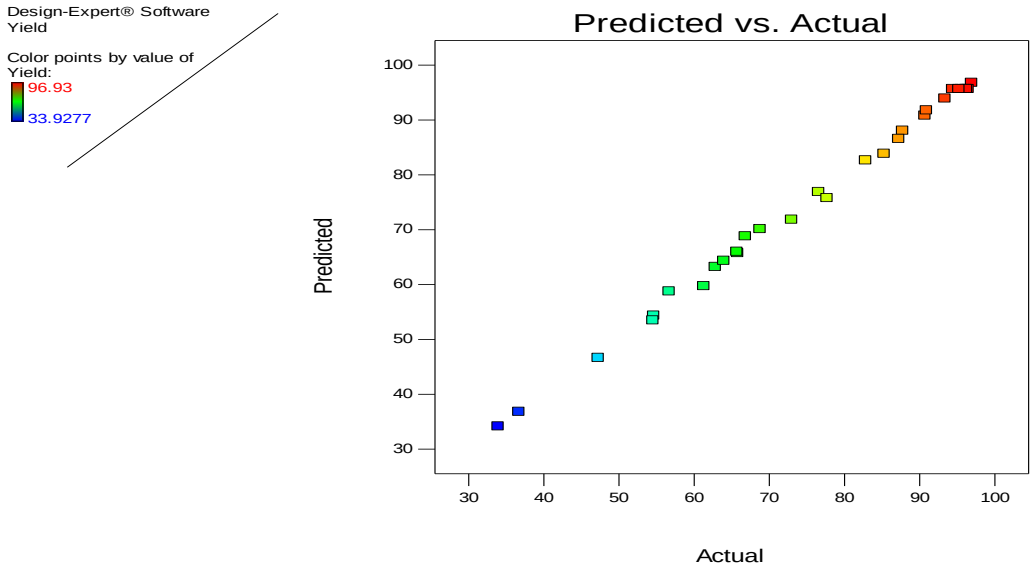

Figure 4.11: Predicted vs. Actual for OPOME

Table 4.2: Variance for transesterification of Jatropha oil

Source	Sum of Squares	df	Mean Square	F Value	p-value Prob > F	
Model	9594.055	14	685.2896	421.299	$7.68x10^{-17}$	significant
A-Catalyst concentration	3.681667	1	3.681667	2.263397	0.153226	
B-Reaction temperature	382.4017	1	382.4017	235.091	$1.42x10^{-10}$	
C-Reaction Time	885.735	1	885.735	544.5278	$3.34x10^{-13}$	
D-Molar Ratio	4614.827	1	4614.827	2837.081	$1.64x10^{-18}$	
AB	299.29	1	299.29	183.996	$7.96x10^{-10}$	
AC	0.04	1	0.04	0.024591	0.877482	
AD	69.7225	1	69.7225	42.86366	$9.24x10^{-6}$	
BC	97.0225	1	97.0225	59.64702	$1.33\ x10^{-6}$	
BD	40.96	1	40.96	25.18119	0.000153	
CD	9	1	9	5.532976	0.032736	
A^2	1501.989	1	1501.989	923.3852	$6.88x10^{-15}$	
B^2	486.7243	1	486.7243	299.226	2.55x10-11	
C^2	958.8386	1	958.8386	589.4701	$1.87x10^{-13}$	
D^2	1486.804	1	1486.804	914.0502	$7.42x10^{-15}$	
Residual	1.380833	15	0.092056			
Lack of Fit	1.1925	10	0.11925	3.165929	0.107642	not significant
Pure Error	0.188333	5	0.037667			
Cor Total	74.88967	29				
R-Squared = 0.981562						

Table 4.3: Variance for transesterification of Orange peel oil

Source	Sum of Squares	df	Mean Square	F Value	p-value Prob > F	
Model	9594.055	14	685.2896	421.299	$7.68x10^{-17}$	significant
A-Catalyst concentration	3.681667	1	3.681667	2.263397	0.153226	
B-Reaction temperature	382.4017	1	382.4017	235.091	$1.42x10^{-10}$	
C-Reaction Time	885.735	1	885.735	544.5278	$3.34x10^{-13}$	
D-Molar Ratio	4614.827	1	4614.827	2837.081	$1.64x10^{-18}$	
AB	299.29	1	299.29	183.996	$7.96x10^{-10}$	
AC	0.04	1	0.04	0.024591	0.877482	
AD	69.7225	1	69.7225	42.86366	$9.24x10^{-6}$	
BC	97.0225	1	97.0225	59.64702	$1.33x10^{-6}$	
BD	40.96	1	40.96	25.18119	0.000153	
CD	9	1	9	5.532976	0.032736	
A^2	1501.989	1	1501.989	923.3852	$6.88x10^{-15}$	
B^2	486.7243	1	486.7243	299.226	$2.55x10^{-11}$	
C^2	958.8386	1	958.8386	589.4701	$1.87x10^{-13}$	
D^2	1486.804	1	1486.804	914.0502	$7.42x10^{-15}$	
Residual	1.380833	15	0.092056			
Lack of Fit	1.1925	10	0.11925	3.165929	0.107642	not significant
Pure Error	0.188333	5	0.037667			
Cor Total	74.88967	29				
R-Squared = 0.981562						

The equation of regression for a yield of JOME and OPOME are shown in equation 4.2 and equation 4.3 respectively. The graphical presentation of the regression equation is best presented by the response surface plots for the different combination of variables. Figure 4.12 to Figure 4.17 presents the response surface plot for the combination of two variables on the yield of JOME and Figure 4.18 to Figure 4.23 for the yield of OPOME. As earlier predicted by the ANOVA Table, the yield is largely affected by the individual effects of reaction temperature and catalysts concentration.

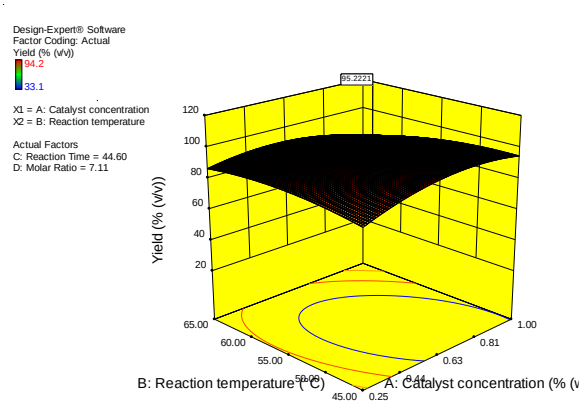

Figure 4.12: Interaction effect of catalyst concentration and reaction temperature

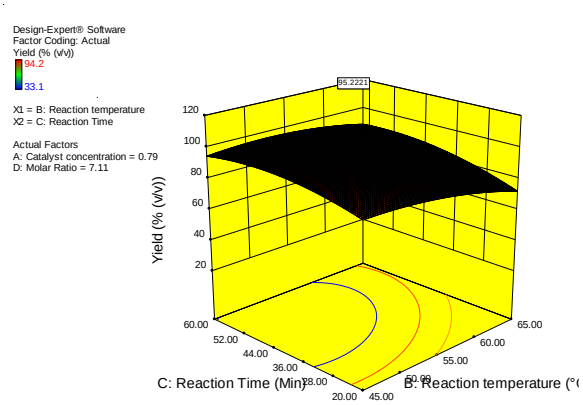

Figure 4.13: Interaction effect of reaction time and reaction temperature

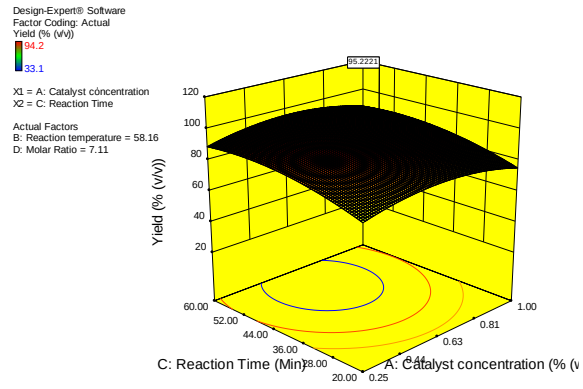

Figure 4.14: Interaction effect of catalyst concentration and reaction time

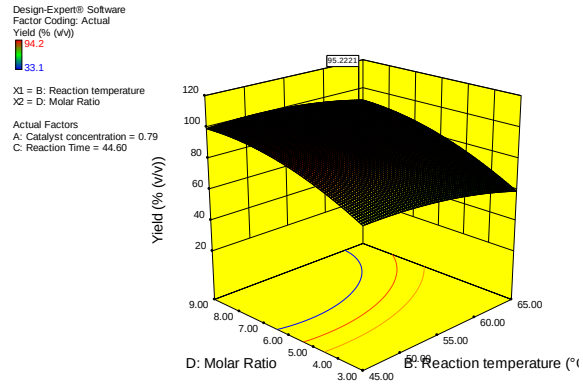

Figure 4.15: Interaction effect of molar ratio and reaction temperature

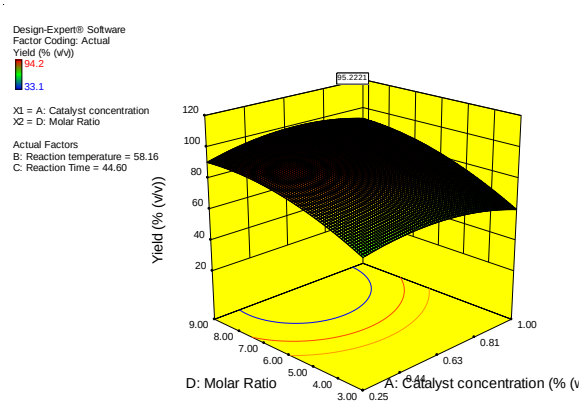

Figure 4.16: Interaction effect of catalyst concentration and molar ratio

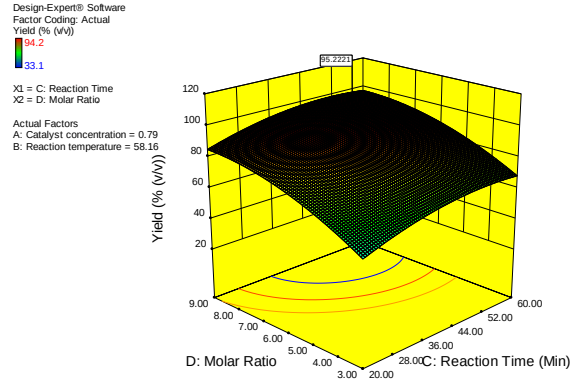

Figure 4.17: Interaction effect of molar ratio and reaction time

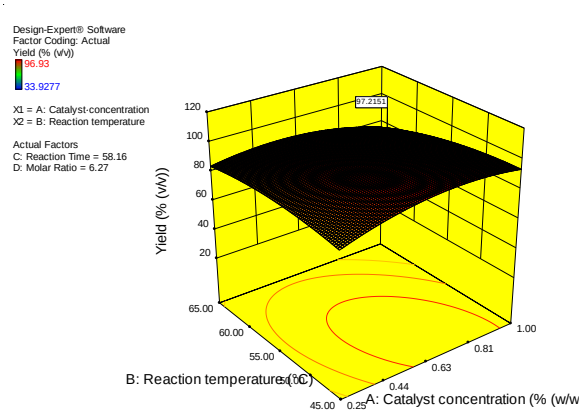

Figure 4.18: Interaction effect of catalyst concentration and reaction temperature

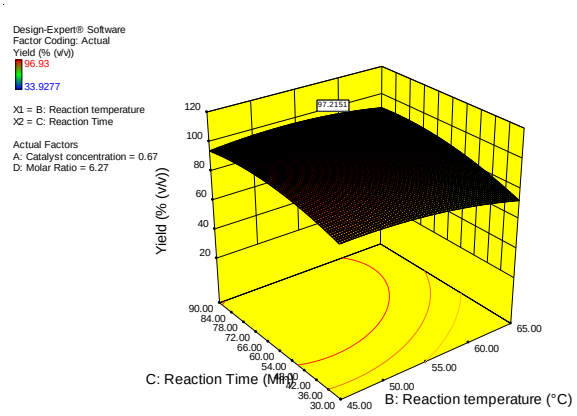

Figure 4.19: Interaction effect of reaction time and reaction temperature

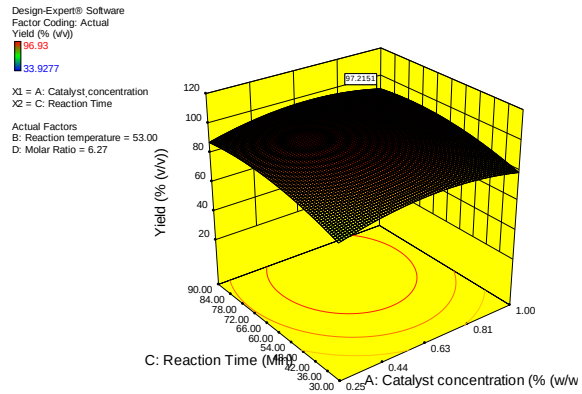

Figure 4.20: Interaction effect of catalyst concentration and reaction time

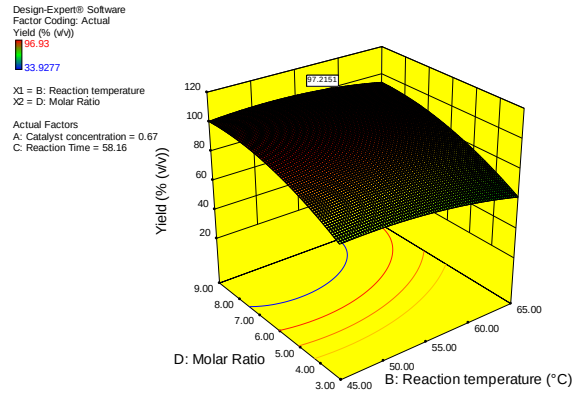

Figure 4.21: Interaction effect of molar ratio and reaction temperature

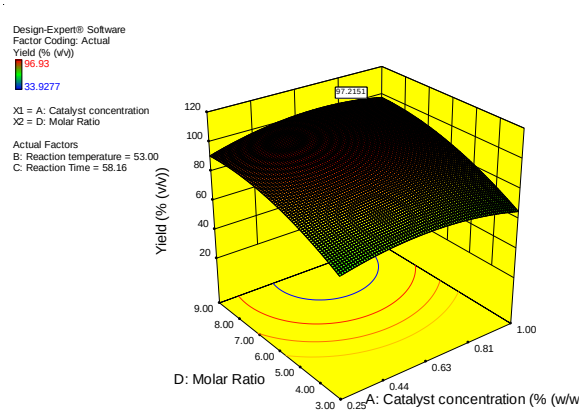

Figure 4.22: Interaction effect of catalyst concentration and molar ratio

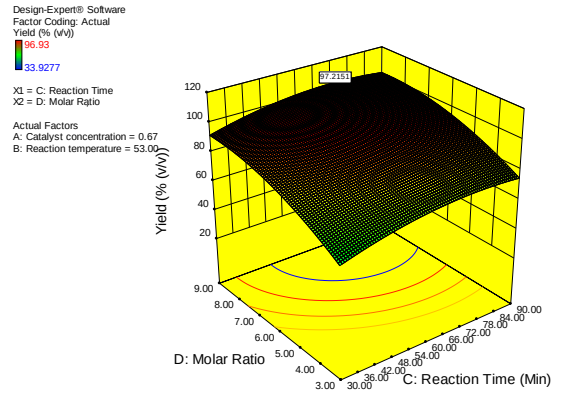

Figure 4.23: Interaction effect of molar ratio and reaction time

Yield = +92.93333 + 0.391667*A - 3.99167*B + 6.075*C + 13.86667*D - 4.325 *A*B + 0.05*A*C + 2.0875*A*D + 2.4625*B*C + 1.6*B*D - 0.75*C*D – $7.4*A^2$ - $4.2125*B^2$ – $5.9125*C^2$ – $7.3625*D^2$ (4.2)

Yield = +95.66726 + 0.414273*A – 4.11284*B + 6.273893*C + 14.27748*D – 4.46518 *A*B + 0.057657*A*C + 2.146107*A*D + 2.55611*B*C + 1.646416*B*D - 0.77516*C*D – $7.62455*A^2$ - $4.33172*B^2$ – $6.08704*C^2$ - $7.5733*D^2$ (4.3)

4.3 Physico-chemical Properties of Pilot Fuels

The physico-chemical properties (kinematic viscosity, density, calorific value, flash point, autoignition temperature and cetane number etc.) of diesel, JOME, OPOME, J50D50 and OP50D50 are evaluated according to ASTM standards. The fatty acid profile of JOME and OPOME are also evaluated.

4.3.1 Kinematic viscosity

Kinematic viscosity is a key property for any fuels. Kinematic viscosity is the internal resistance of a fluid to flow. The effects of kinematic viscosity can be seen in the quality of fuel injected and atomization (Tate et al., 2006). The kinematic viscosity of fuel is the function of temperature. It decreases with increasing temperature. The fluidity of any fuel is a concern especially at a lower temperature because they have high viscosity at a lower temperature. The kinematic viscosity of biodiesel is the main concern so it must satisfy the standards. The high kinematic viscosities of biodiesel fuels are reportedly responsible for premature injector fouling leading to poorer atomization which further causes high soot (Graboski and McCormick, 1998).

The kinematic viscosity of Jatropha oil is 51.8 mm^2/s, which is much higher compared to petroleum diesel. The reason for the high kinematic viscosity of Jatropha oil is large molecular mass, which makes it good lubricating fuel. The high kinematic viscosity can cause choking in the fuel supply manifold. So, the kinematic viscosity of Jatropha oil is reduced by converting it to methyl ester. However, Orange peel oil has a lower kinematic viscosity of 1.8 mm^2/s compared to diesel fuel (2.65 mm^2/s).

The kinematic viscosity of JOME and OPOME is 4.2 mm^2/s and 1.04 mm^2/s respectively, which is less than their parent vegetable oils. The trend of kinematic viscosity of JOME, OPOME and their blend with diesel fuel are shown in Figure 4.24 and kinematic viscosity of all pilot fuels (diesel, JOME, OPOME, J50D50 and OP50D50) are shown in Figure 4.25.

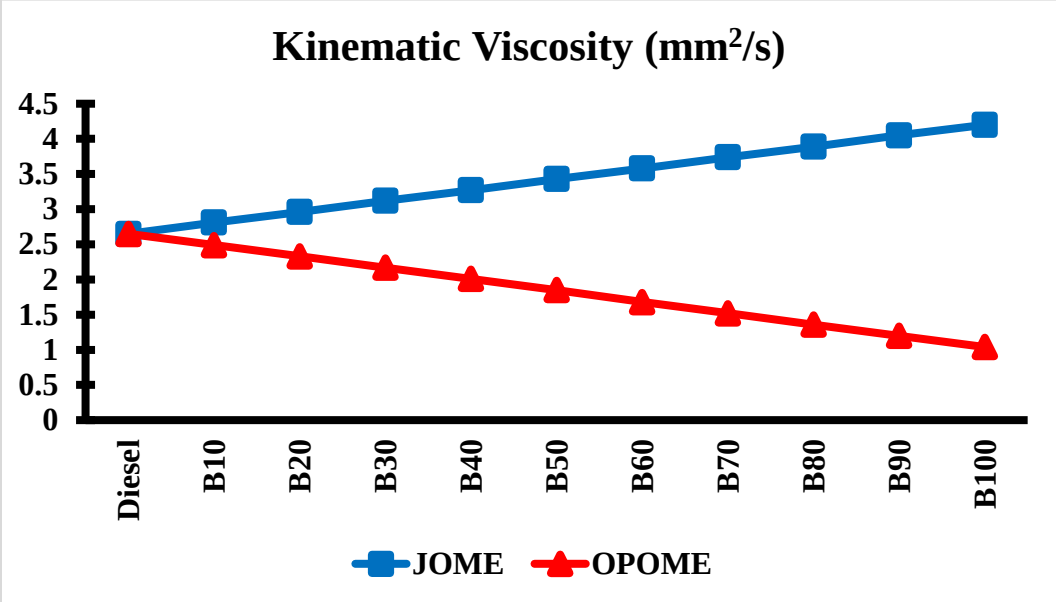

Figure 4.24: Kinematic viscosity of JOME, OPOME and their blends

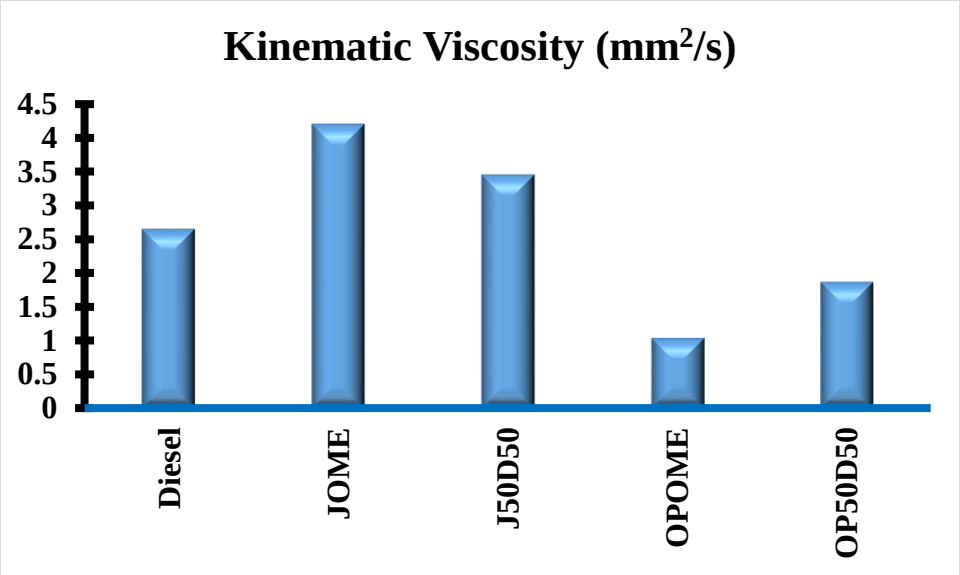

Figure 4.25: Kinematic viscosity of all pilot fuels

4.3.2 Density

The density of the liquid is defined as mass per unit volume. The density of the fuel is not itself an important parameter for the diesel engine, but it is generally related to the fuel's energy content. As fuel is sold volumetrically, it can be said that the higher the density, the greater the potential energy on a volume basis (Van Gerpen et al., 2004). It is known that biodiesel has lower energy content than the diesel fuel. But if it is thought of by volumetric basis, as the density of biodiesel is higher than diesel, energy difference becomes less than before.

As discussed earlier the density of all pilot fuels is measured by U-tube density meter. The density of JOME and OPOME is found less compared to their parent vegetable oils. The density of diesel, JOME, OPOME, J50D50 and OP50D50 are measured and found 823 kg/m^3, 872 kg/m^3, 812 kg/m^3, 846 kg/m^3 and 817.5 kg/m^3 respectively. It is observed that OPOME has lowest density and JOME has highest one. The variation of density for all pilot fuels is shown in Figure 4.26 and effect of blending on density for JOME and OPOME is shown in Figure 4.27.

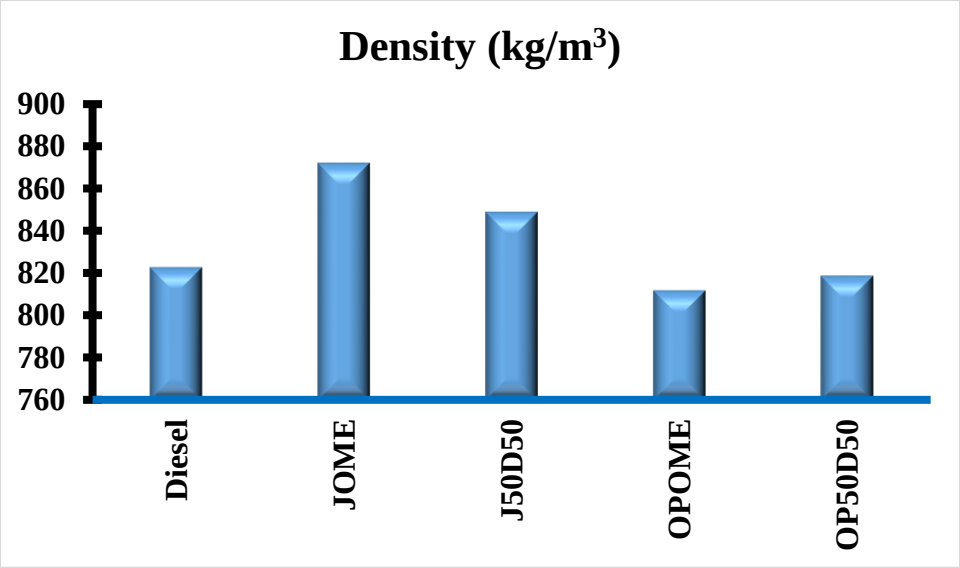

Figure 4.26: Density of all pilot fuels

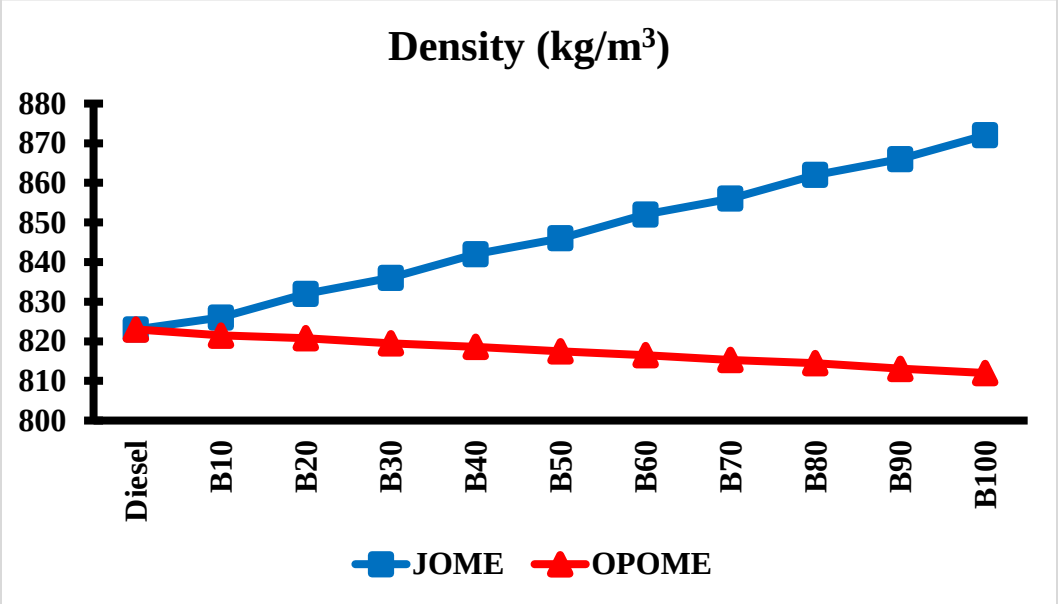

Figure 4.27: Density of JOME, OPOME and their blends.

4.3.3 Flash point

Flash point is an important parameter for any fuel. The flash point is defined as the lowest temperature at which application of an ignition source causes the vapors of a specimen to ignite under specified conditions of the test. Generally, biodiesel has higher flash point values compared to petroleum diesel fuel if the residual alcohol is completely removed. So biodiesel is safer in handling, transportation and storage than diesel fuel. The flash point of Jatropha oil and Orange peel oil is 246°C and 228°C respectively.

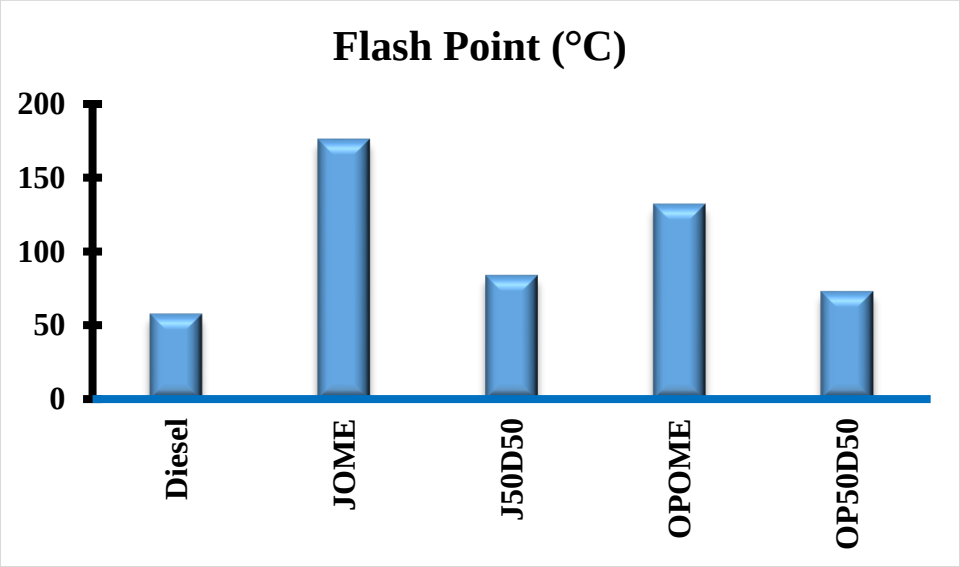

Figure 4.28: Flash point of all pilot fuels

Conversion of straight vegetable oil into methyl ester reduced the flash point. The flash point of pilot fuels is measured in the lab. The flash point of diesel is found 58°C which is much lower compared to other pilot fuels. Flash point of JOME, OPOME, J50D50 and OP50D50 is 176°C, 132°C, 84°C and 73°C respectively. According to ASTM standard, the flash point of biodiesel should not less than 120°C. Hence, the biodiesel prepared in present research satisfy the ASTM standard. The comparative result on flash point of all pilot fuels is shown in Figure 4.28 and the effect of blending on flash point is shown in Figure 4.29.

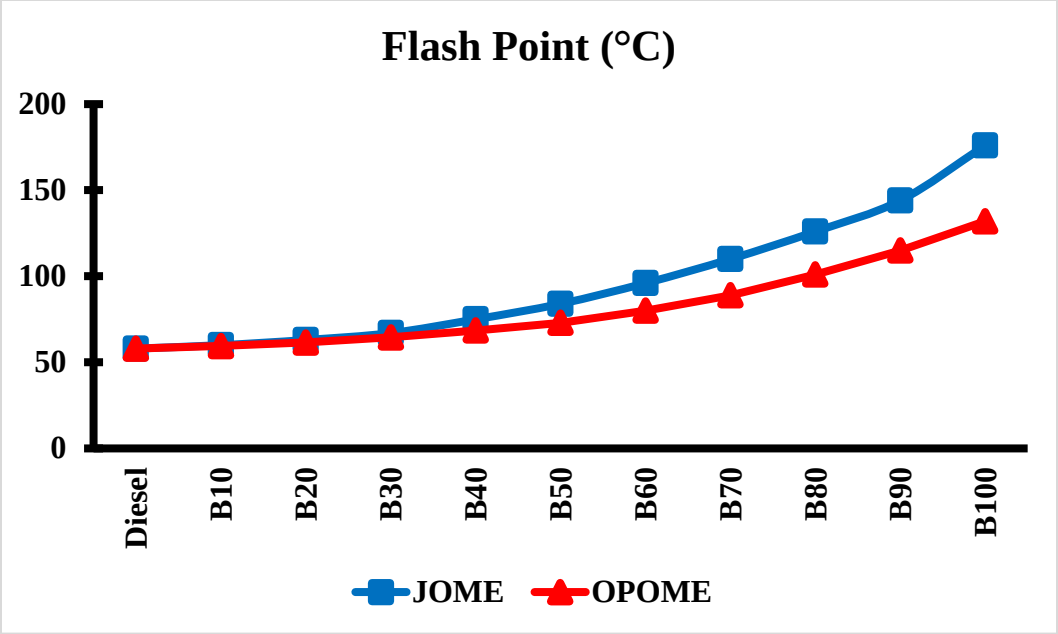

Figure 4.29: Flash point of blends

4.3.4 Calorific value

The calorific value is the most important parameter for any fuel. Most commonly lower heating value of fuels is used in internal combustion engines. The calorific value of all pilot fuels is measured with the help of bomb calorie meter, whose working principle is already explained in an earlier section. It is found that straight vegetable oils have lower calorific value compared to their methyl ester. However, most of the biodiesel has low calorific value than petroleum diesel.

Diesel fuel has the calorific value of 43.3 MJ/kg which is highest among all pilot fuels. The calorific value of JOME, OPOME, J50D50 and OP50D50 is 39.8 MJ/kg, 40.6 MJ/kg, 41.5 MJ/kg and 41.9MJ/kg respectively. It is observed that OPOME has higher calorific value than JOME. The variation in the calorific value of all pilot fuel is shown in Figure 4.30 and the effect of blending on calorific value is shown in Figure 4.31.

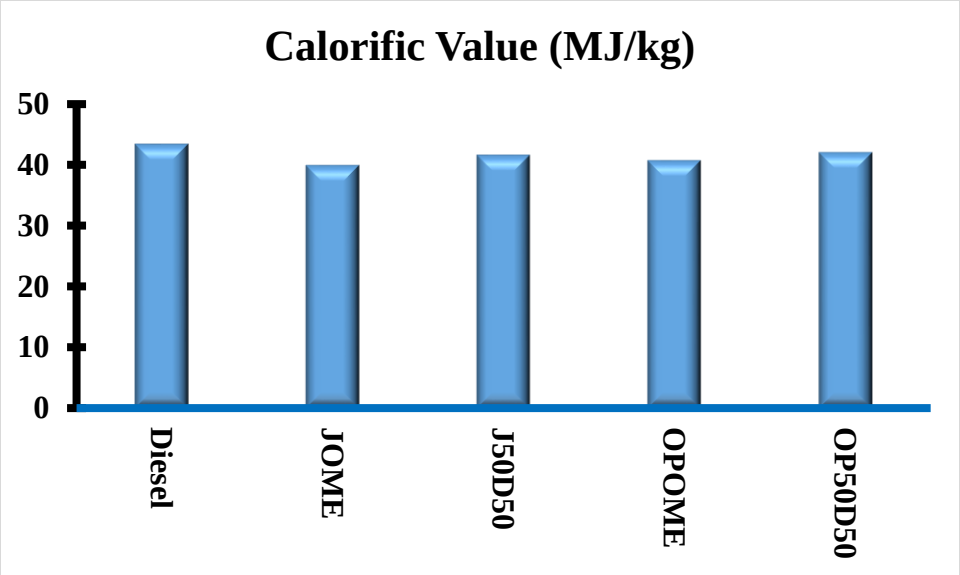

Figure 4.30: Calorific value of all pilot fuels

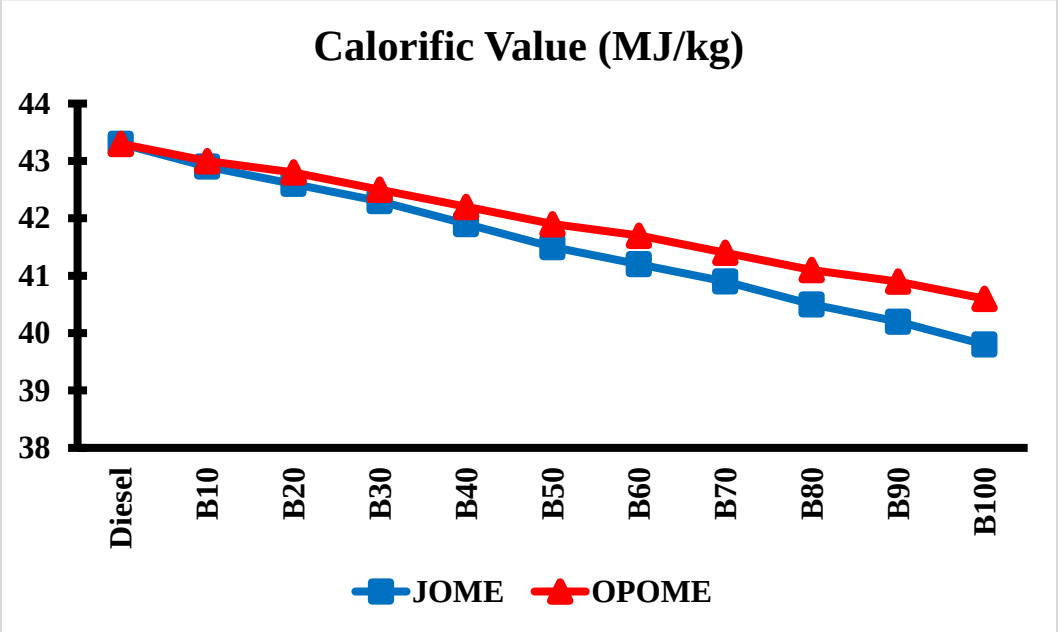

Figure 4.31: Calorific value of all blends

4.3.5 Cetane number

Cetane number measured the ignition quality and ignition delay of a liquid fuel which auto ignite after injection into a compression ignition engine. CN is based on two compounds,

namely hexadecane with a cetane of 100 and heptamethylnonane with a cetane of 15. The more saturated molecules and longer fatty acid carbon chains in fuel results in higher cetane number. The cetane number of biodiesel depends on the distribution of fatty acids in parent oil. The longer the fatty acid carbon chains and the more saturated the molecules, the higher the cetane number. The cetane number is determined with real engine test. However, cetane index is a calculated from the density and volatility obtained from boiling characteristics of the fuel. CI usually gives a reasonably close approximation to real cetane number (Song, 2000).

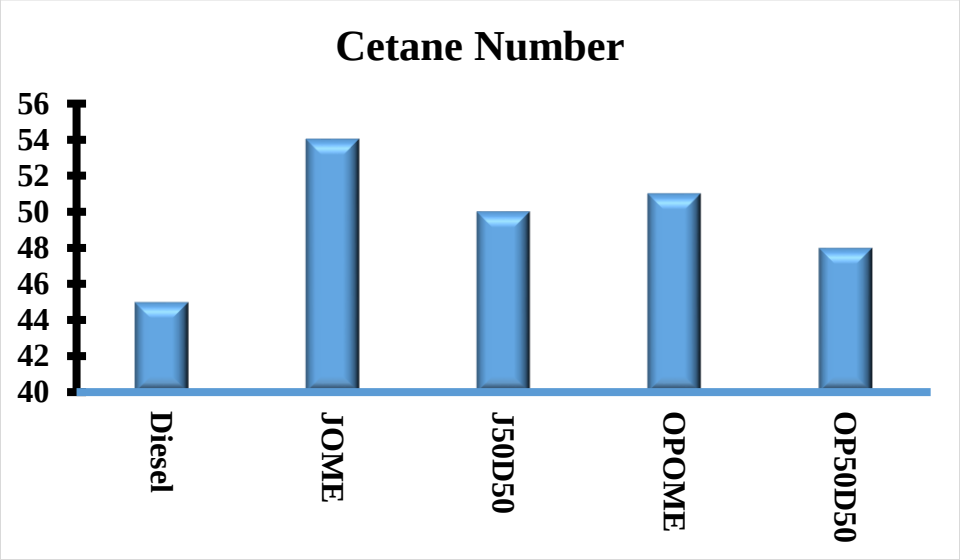

Figure 4.32: Cetane number of all pilot fuels

Generally, biodiesel has higher cetane number compared to petroleum diesel. It is found that JOME has the highest cetane number of 54 followed by OPOME and diesel whose cetane number are 51 and 45 respectively. The reason for higher cetane number of JOME is longer fatty acid carbon change and more saturated bonds. The cetane number of all pilot fuel is shown in Figure 4.32 and effect of blending on cetane number is shown in Figure 4.33.

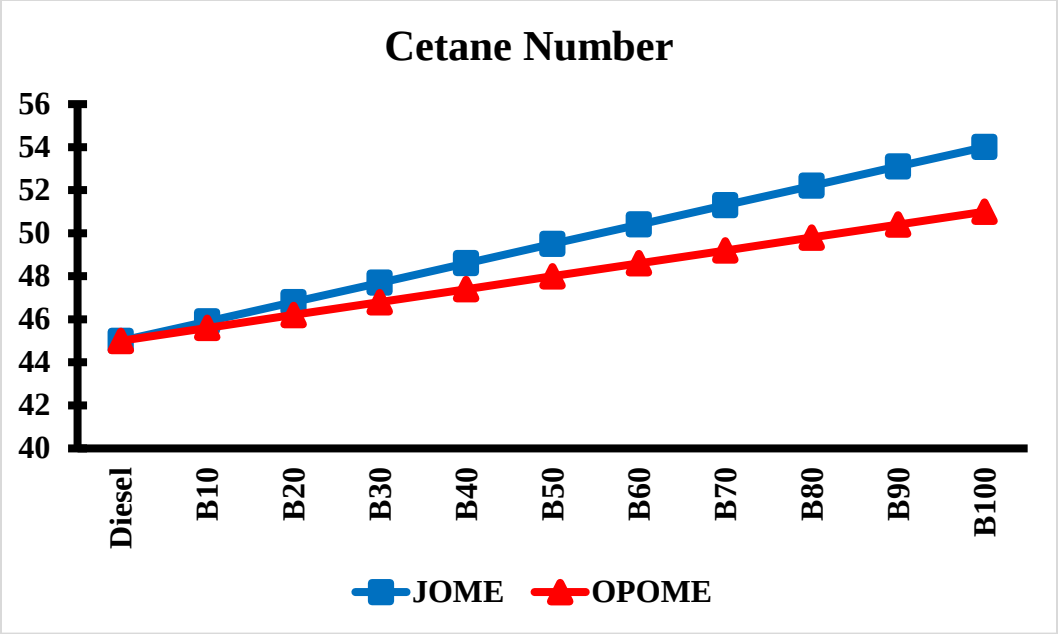

Figure 4.33: Cetane number of all blends

4.3.6 Other physicochemical properties

Physico-chemical properties like specific gravity, auto ignition temperature, oxygen availability and H/C ratio are also measured for present research. The specific density is defined as the ratio of the density of fuel to the density of reference fluid. Generally, water is taken as the reference fluid. The density of JOME is higher among all pilot fuel hence, the specific gravity of JOME is also higher compared to other pilot fuels used in present research. It is found that OPOME has lowest autoignition temperature among all pilot fuels. On the other hand, JOME has highest oxygen availability followed by OPOME and diesel. The oxygen availability in diesel is negligible. However, diesel has highest H/C ratio among all pilot fuels. The physicochemical properties of all pilot fuels and CNG are given in Table 4.4.

Table 4.4: Physicochemical properties of all tested fuels

Properties	CNG	Diesel	JOME	OPOME	J50D50	OP50D50
Density at 40 °C (kg/m^3)	0.742*	823	872	812	849	819
Viscosity at 25 °C (mm^2/s)	-	2.65	4.2	1.04	3.45	1.87
Flash Point (°C)	-	58	176	132	84	73
Cetane Number	-	45	54	51	50	48
Octane Number	120*	-	-	-	-	-
Higher Calorific Value (MJ/kg)	49.6*	43.3	39.8	40.6	41.5	41.9
Auto Ignition Temp. (°C)	510*	230	208	194	216	202
Oxygen availability (%)	-	-	10.2	9.1	5.3	4.5
H/C ratio	3.82*	2.16	1.3	1.4	1.76	1.8

* Values are taken from filling station

4.3.7 Fatty acid profile

The gas chromatography and mass spectroscopy (GC-MS) is used to study the chemical composition of the biodiesel. Few major peaks are observed in the GC spectrum with a number of minor peaks. Each peak corresponds to a fatty acid methyl ester that is identified from the library match software with their retention time. The identity of FAMEs is verified by mass spectrometric analysis and retention time data. The mass spectrum is obtained by an electron impact (EI) ion source.

4.3.7.1 Fatty acid composition of JOME

The fatty acid composition of JOME is measured using GCMS. Three major peaks are noticed in the GC spectrum as shown in Figure 4.34. The first major peak shows the hexadecanoic acid, methyl ester contributes to 19.15% of the area while second and third major peaks are of 9-octadecenoic acid methyl ester (68.26%) and methyl stearate (10.16%). The composition of all fatty acid present in JOME is shown in Table 4.5.

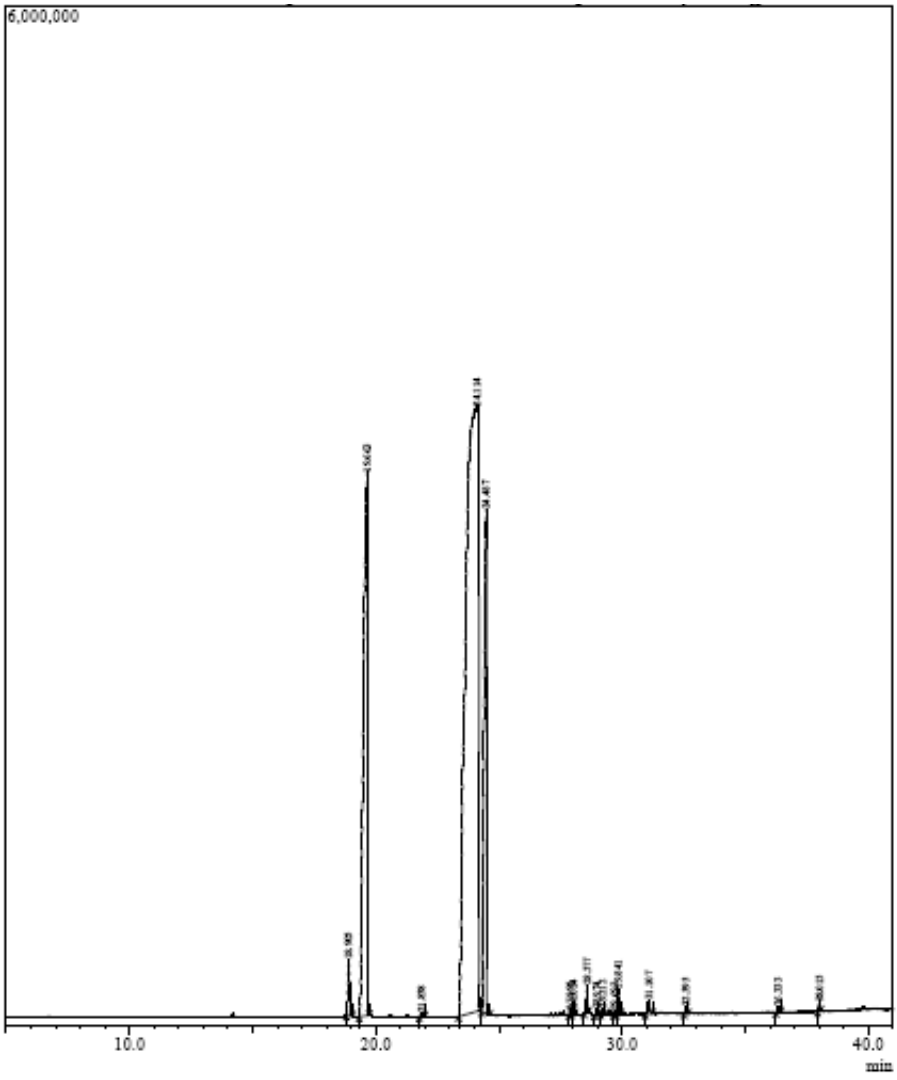

Figure 4.34: Fatty acid profile of JOME

Table 4.5: Fatty acid composition of JOME

Peak	R.Time	Area	Area%	Name
1	18.905	1854687	0.99	9-Hexadecenoic Acid, Methyl Ester, (Z)-
2	19.663	35732124	19.15	Hexadecanoic Acid, Methyl Ester
3	21.858	138088	0.07	Tetradecanoic Acid, 12-Methyl-, Methyl Est
4	24.114	127381781	68.26	9-Octadecenoic Acid, Methyl Ester
5	24.487	18961140	10.16	Methyl Stearate
6	27.895	90014	0.05	9-Octadecenoic Acid (Z)-, Methyl Ester
7	28.024	115513	0.06	Cyclopropaneoctanoic Acid, 2-Hexyl-, Meth
8	28.577	478594	0.26	Eicosanoic Acid, Methyl Ester
9	28.974	115854	0.06	Oxacyclohexadecan-2-One, 16-Methyl-13-Ni
10	29.212	129633	0.07	(2s,5r)-2-Isopropyl--5methylhept-6-En-1-Ol
11	29.693	74293	0.04	Naphthalene, Decahydro-2,2-Dimethyl-
12	29.841	572830	0.31	Prost-13-En-1-Oic Acid, 9,11,15-Trihydroxy-6-Oxo-, Methyl Es
13	31.107	524374	0.28	2,5-Methano-1h-Inden-7(4H)-One, Hexahydro-
14	32.595	141072	0.08	Eicosanoic Acid, Methyl Ester
15	36.333	131419	0.07	Eicosanoic Acid, Methyl Ester
16	38.015	163066	0.09	Squalene
		186604482	100.00	

4.3.7.2 Fatty acid composition of OPOME

The fatty acid profile of OPOME is shown in Figure 4.35. Only one major peak is noticed in GC spectrum. The main component in OPOME is limonene which acquires 96.28% of the area. The other component and their composition in OPOME is shown in Table 4.6.

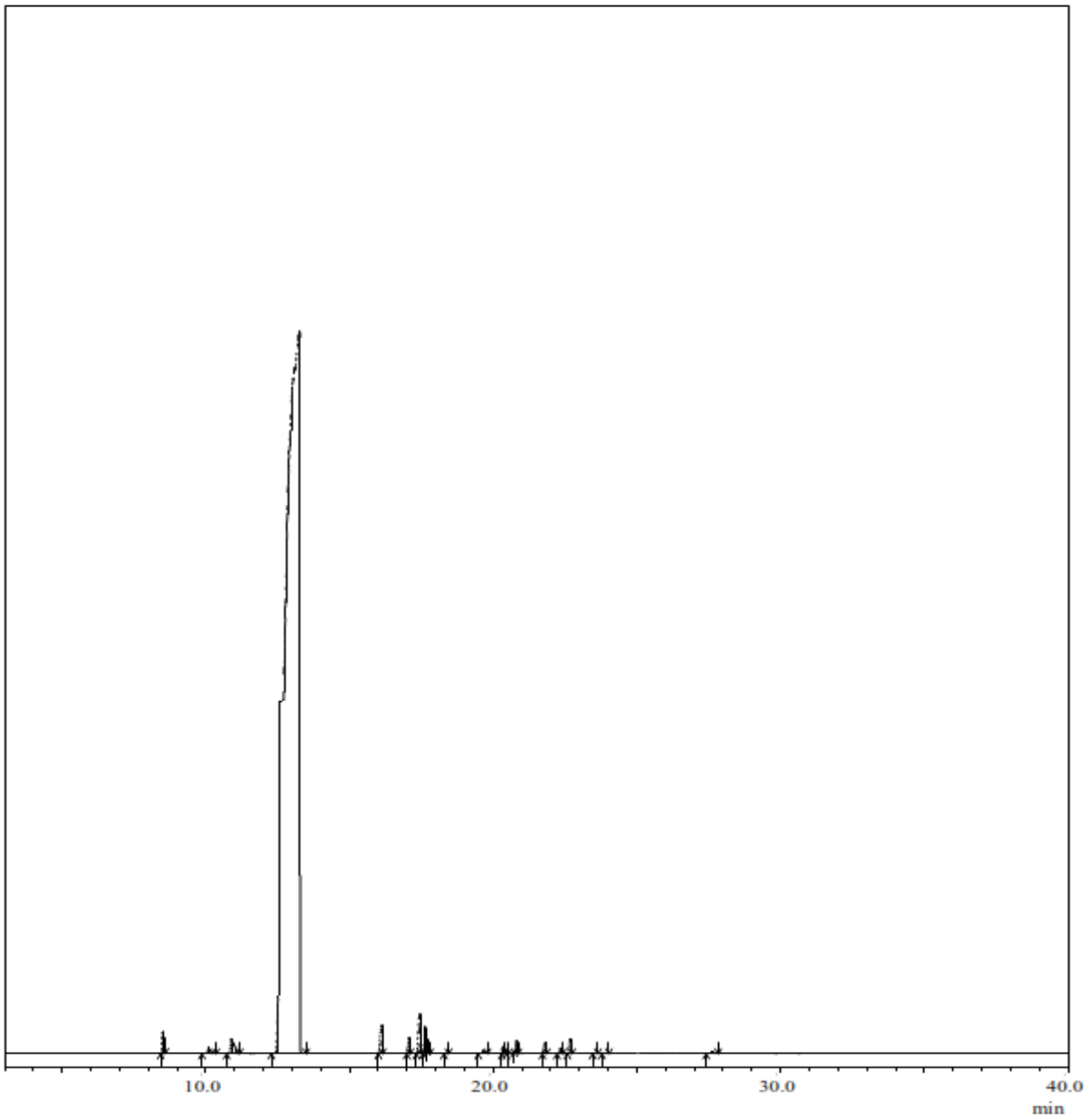

Figure 4.35: Fatty acid profile of OPOME

Table 4.6: Fatty acid composition of OPOME

Peak	R.Time	Area	Area%	Name
1	8.497	334605	0.36	Bicyclo[3.1.1]Hept-2-Ene, 2,6,6-Trimethyl-
2	10.105	139657	0.15	Cyclohexene, 3-Methylene-6-(1-Methylethy
3	10.890	525455	0.56	1,6-Octadiene, 7-Methyl-3-Methylene-
4	13.275	90125980	96.28	Limonene
5	16.107	431660	0.46	Cyclohexene, 1-Methyl-4-(1-Methylethylide
6	17.072	214732	0.23	Mentha-2,8-Dien-1-Ol <Trans-, Para->
7	17.426	527334	0.56	4-Isopropenyl-1-Methyl-7-Oxabicyclo[4.1.0]H
8	17.644	293073	0.31	Trans-Limonene Oxide
9	17.738	131490	0.14	P-Mentha-2,8-Dien-1-Ol, Trans-(.+-.)-
10	18.346	5494	0.01	2-Propenoic Acid, 2-Methyl-, 2-Propenyl Este
11	19.648	36741	0.04	3-Penten-2-One
12	20.347	86978	0.09	(4r,8r)-8,9-Epoxy-P--Menth-1-Ene
13	20.501	37022	0.04	1,3-Cyclononadiene, 2-Methyl-
14	20.812	167972	0.18	Decanal <N-> Db5-893
15	21.797	184700	0.20	Carveol <Trans-> Db5-923
16	22.342	72064	0.08	2-Cyclohexen-1-Ol, 2-Methyl-5-(1-Methyleth
17	22.675	210354	0.22	2-Cyclohexen-1-One, 2-Methyl-5-(1-Methylet
18	23.553	7276	0.01	.Alpha.-D-Glucofuranose, 6-Deoxy-1,2-O-(1-Me
19	23.855	25180	0.03	3-Butenenitrile, 3-Methyl-2-Oxo-
20	27.640	47973	0.05	3-Oxo-1-Butenyl 2-Methylpropanoate
		93605740	100.00	

4.4 Ignition Delay

Before each trial, it is making sure that not a single combustion product remains inside the combustion chamber. For doing this outlet valve is opened after each combustion and the sufficient fresh air is supplied to the combustion chamber which makes combust particles force exit. After that ignition delay of all pilot fuels is measured at different parameters i.e. injection pressure, in-cylinder pressure and in-cylinder temperature. The injection pressure is set to 100 bar to 300 bar by taking an interval of 50 bar with the help of spring mechanism. The injection pressure is read by injection pressure gauge.

The air from the air compressor is supplied to the combustion chamber through the intake valve. The valve is closed when a fixed pressure inside the cylinder is achieved. After closing intake and exhaust valve and achieving fixed in-cylinder pressure and temperature, the fuel is injected into the combustion chamber through injection system. The instant of fuel injection is sensed by the piezoelectric sensor and gave the signal to scope meter. If there is no burning activity inside the combustion chamber the luminosity of the flame will be zero and therefore the optical sensor will not give any signal. The signal curve will be parallel to the horizontal axis on the screen of the oscilloscope. Thus three distinct events are read by the oscilloscope i.e start of injection, end of injection and start of ignition. The interval between the event of the start of injection and event of the start of ignition gives the ignition delay of the tested fuel. For each operating condition, the ignition delay is measured for three times and the average of these three measurements is taken as the ignition delay period for that operating condition.

In this section, the ignition delay of all pilot fuels i.e. diesel, JOME, OPOME, J50D50 and OP50D50 is measured. The range for injection pressure, in-cylinder pressure and temperature is taken 100 bar to 300 bar, 10 bar to 40 bar and 300°C to 400°C respectively. As discussed earlier the interval of 50 bar is taken for injection pressure while the interval for in-cylinder pressure and the temperature is chosen 10 bar and 50°C respectively.

The variation of ignition delay with respect to injection pressure at various inside combustion chamber condition for all pilot fuel are shown in Figure 4.36 to Figure 4.47. It is clear from the Figure that increasing injection pressure decreases the ignition delay. The reason for this is a reduction in physical delay of the fuel. When the fuel injection pressure increases, the fuel droplet diameter decreases and longer penetration of fuel occurs which helps in better mixing and results in complete combustion.

It is known that the compression ratio has a strong influence on this ignition delay. As expected, increasing the cylinder air pressure increases the compression ratio which in turn reduces the ignition delay of all fuels. Because a higher compression ratio increases the temperature and pressure of the air at the beginning of injection. Self-ignition temperature is another reason for the reduction of ignition delay with the increase in compression ratio. The self-ignition temperature reduces with the increase in compression ratio. This is apparently due to the increased density of the compressed air, resulting in closer contact of the molecules which thereby reduces the time of reaction when the fuel is injected. In practice, the higher the compression ratio, the higher will be the engine friction, the leakage, and the torque required for starting. Thus, the diesel engine designers use the lowest compression ratio. It also makes the cold starting of the engine easier. The design practice is just the opposite of that adopted in SI

engine design, where the highest possible compression ratio is used which is limited only by knocking.

The autoignition temperature of a fuel is a very important parameter in term of ignition quality. If the autoignition temperature of a fuel is low, the delay period is reduced. The autoignition temperature of the fuel mainly depends on cetane number, higher the cetane number lower the autoignition temperature.

As measured and discoursed earlier the cetane number of biodiesel is generally higher than conventional diesel fuel which results in lower autoignition temperature. It is notable that the ignition delay of the fuels may be affected by volatility, latent heat, viscosity and surface tension. Volatility and latent heat affect the time taken to form an envelope of the vapor while the viscosity and Surface tension influence the fineness of atomization of the fuel.

It is found that OPOME has the shortest ignition delay among all tested fuel while petroleum diesel has longest for all operating conditions. This is due to the lower autoignition temperature of OPOME among all tested pilot fuels. Another reason for this is high cetane number and low viscosity of OPOME. However, this difference reduces with increasing pressure and temperature of the combustion chamber.

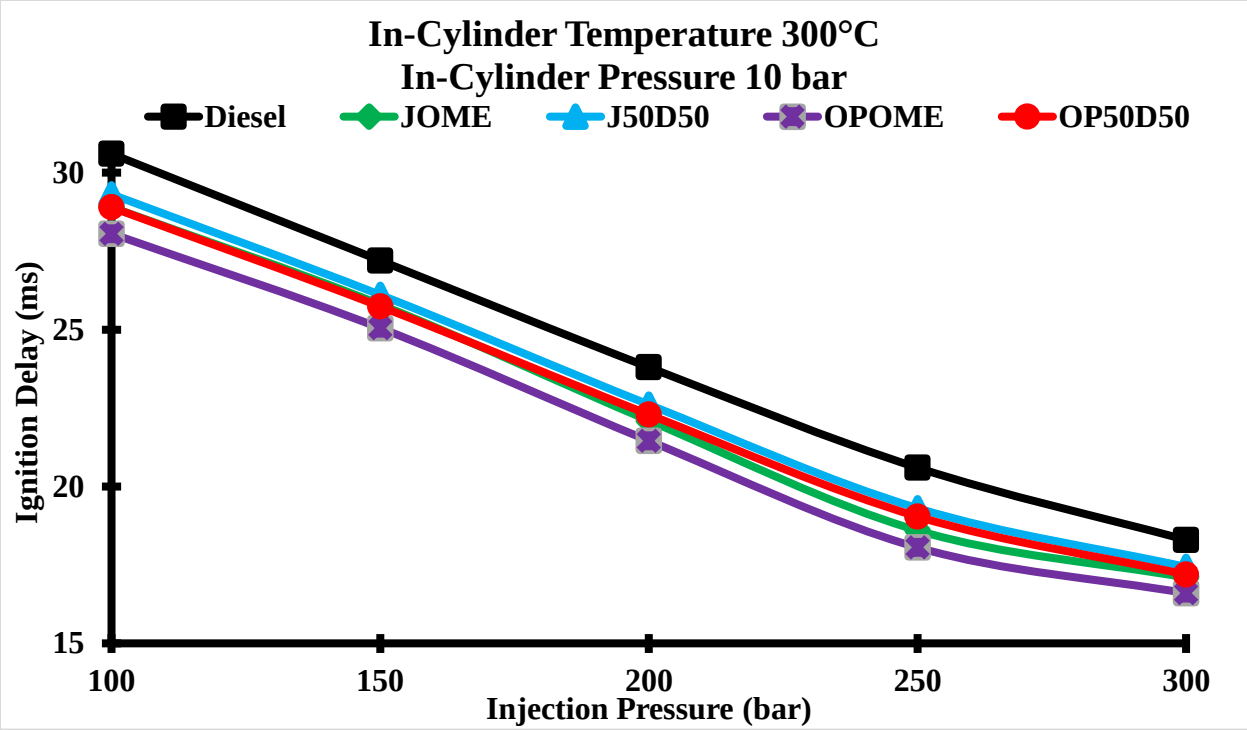

Figure 4.36: Variation of ignition delay of all pilot fuels with injection pressure

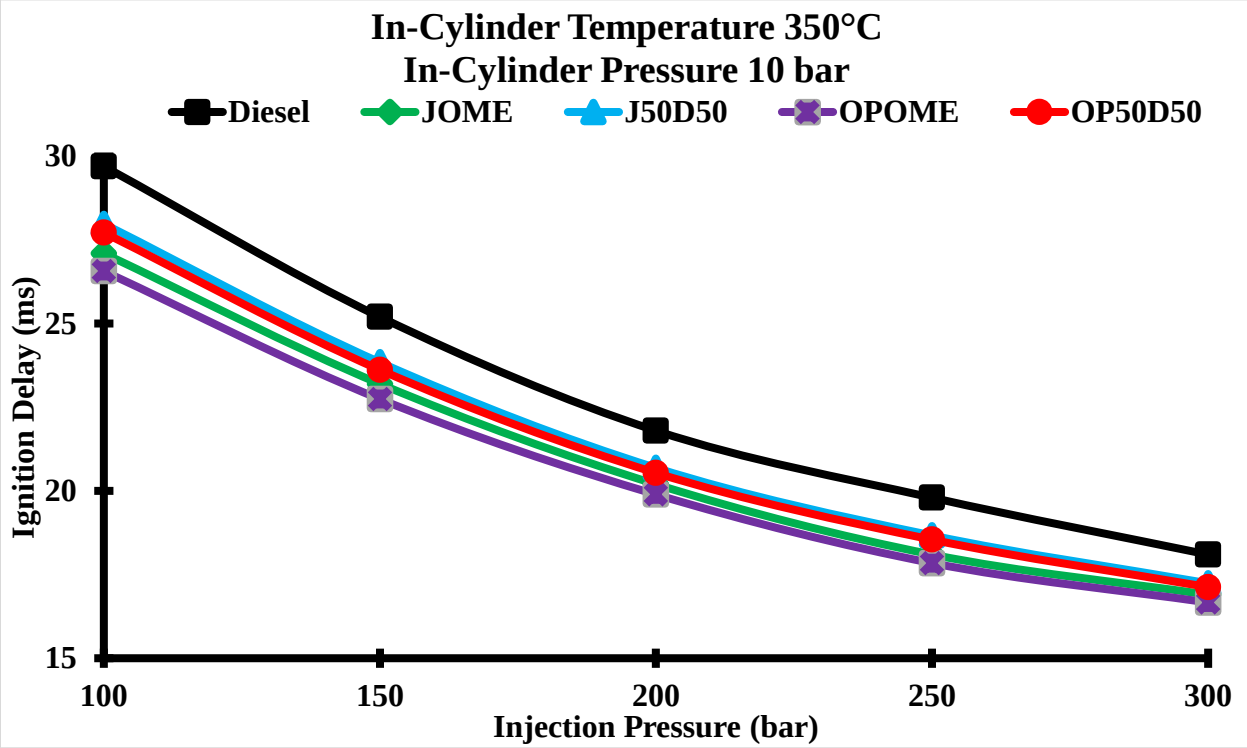

Figure 4.37: Variation of ignition delay of all pilot fuels with injection pressure

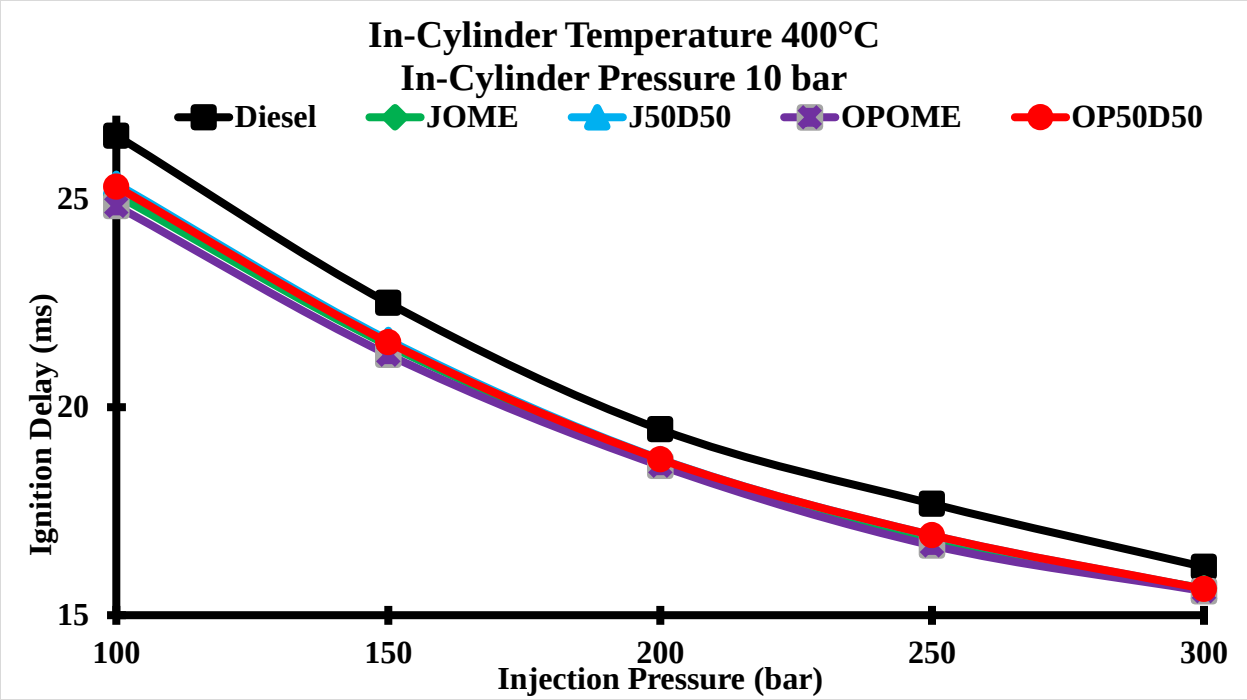

Figure 4.38: Variation of ignition delay of all pilot fuels with injection pressure

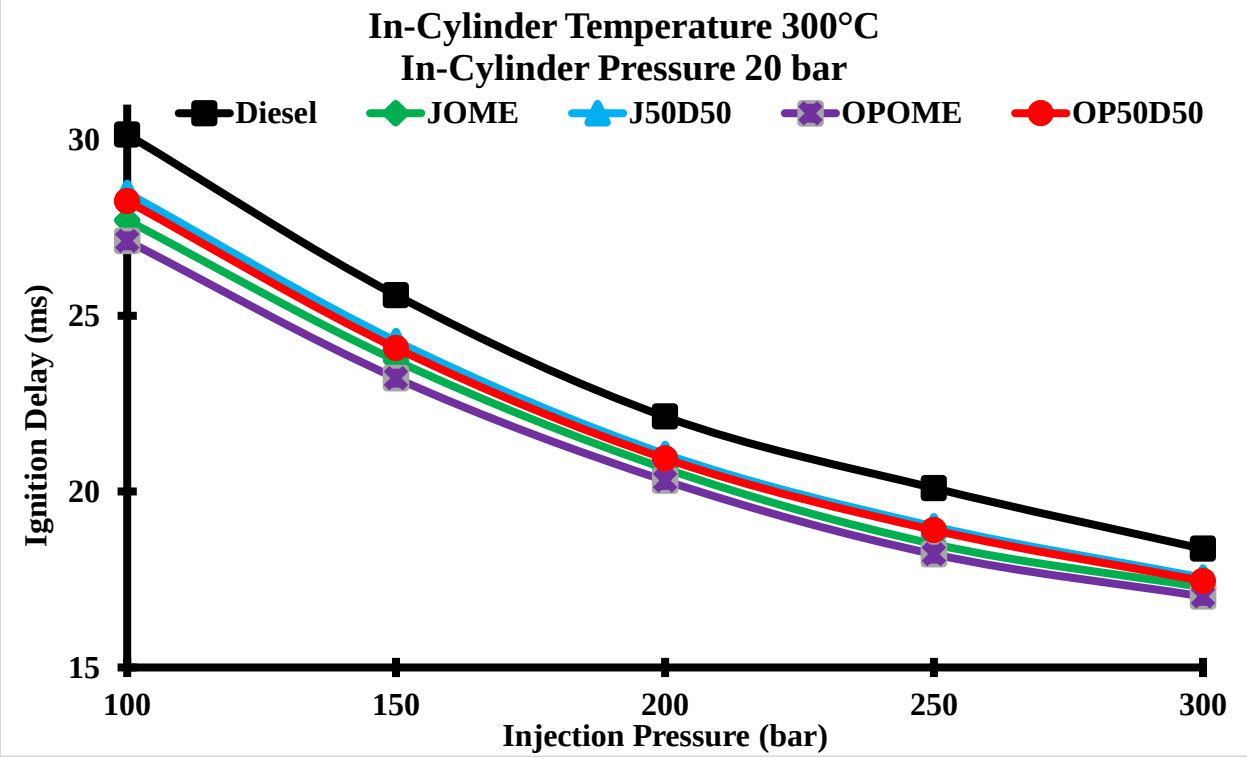

Figure 4.39: Variation of ignition delay of all pilot fuels with injection pressure

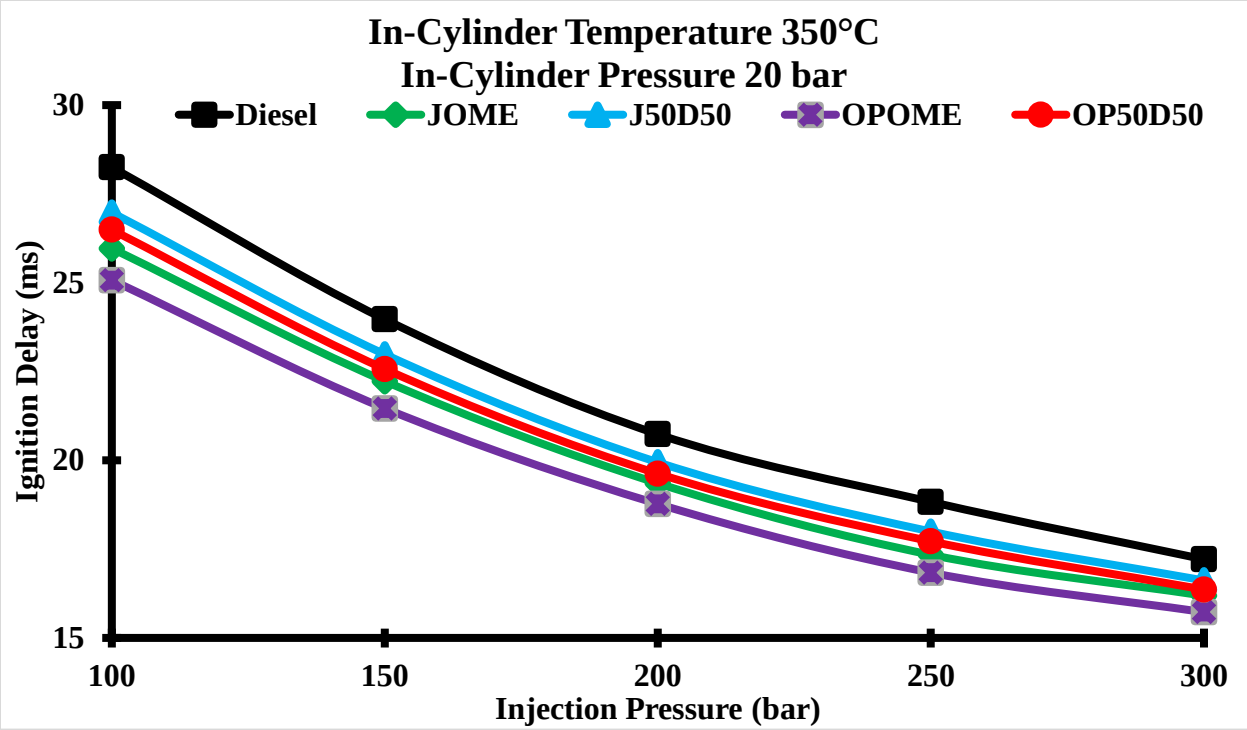

Figure 4.40: Variation of ignition delay of all pilot fuels with injection pressure

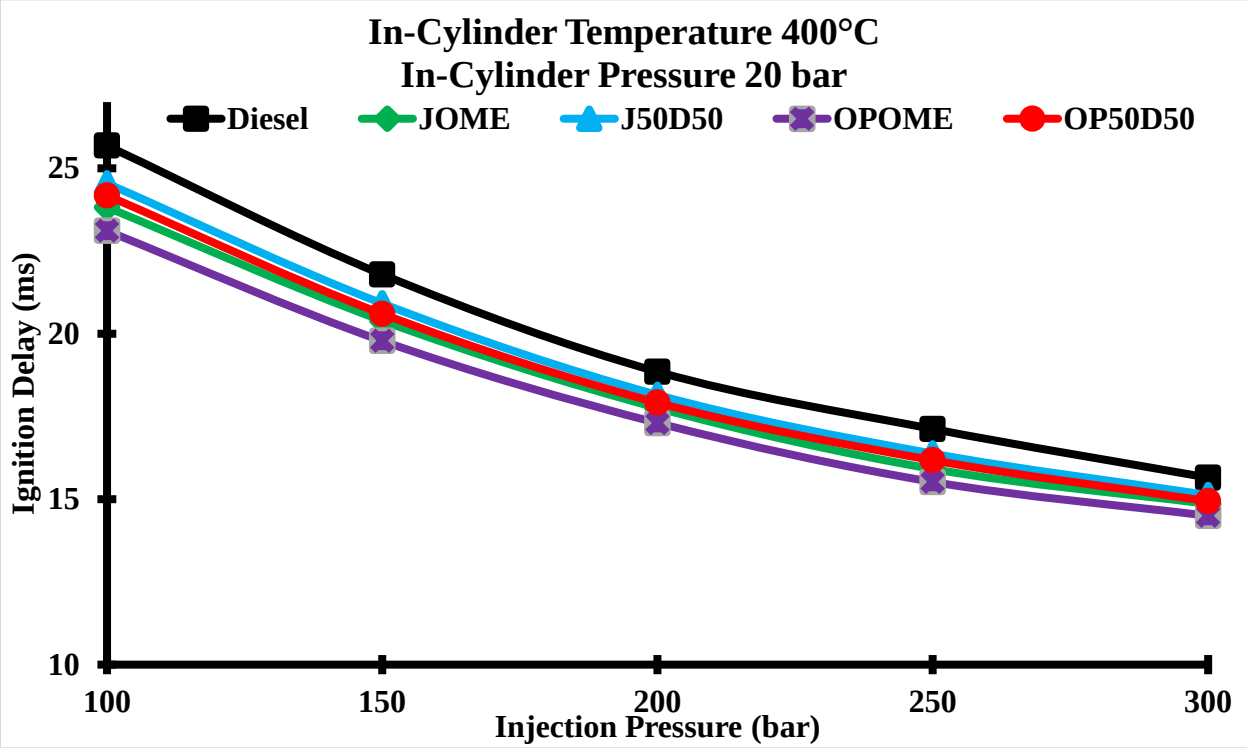

Figure 4.41: Variation of ignition delay of all pilot fuels with injection pressure

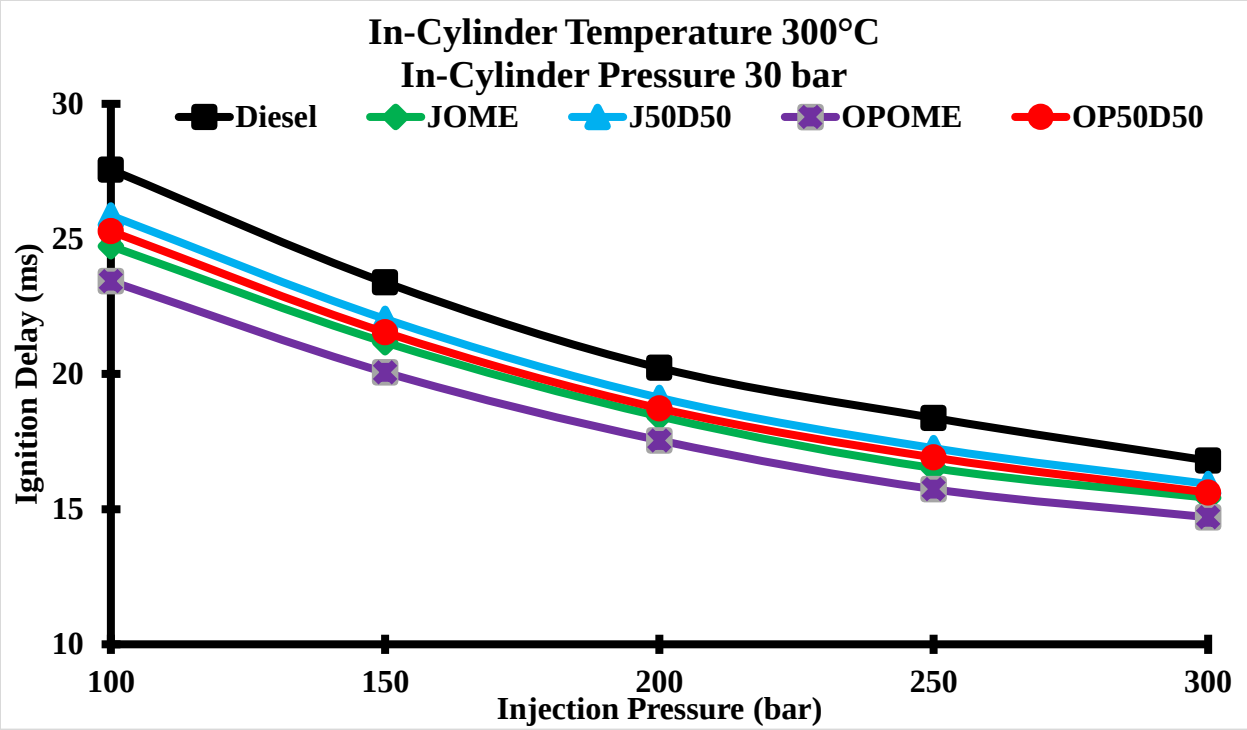

Figure 4.42: Variation of ignition delay of all pilot fuels with injection pressure

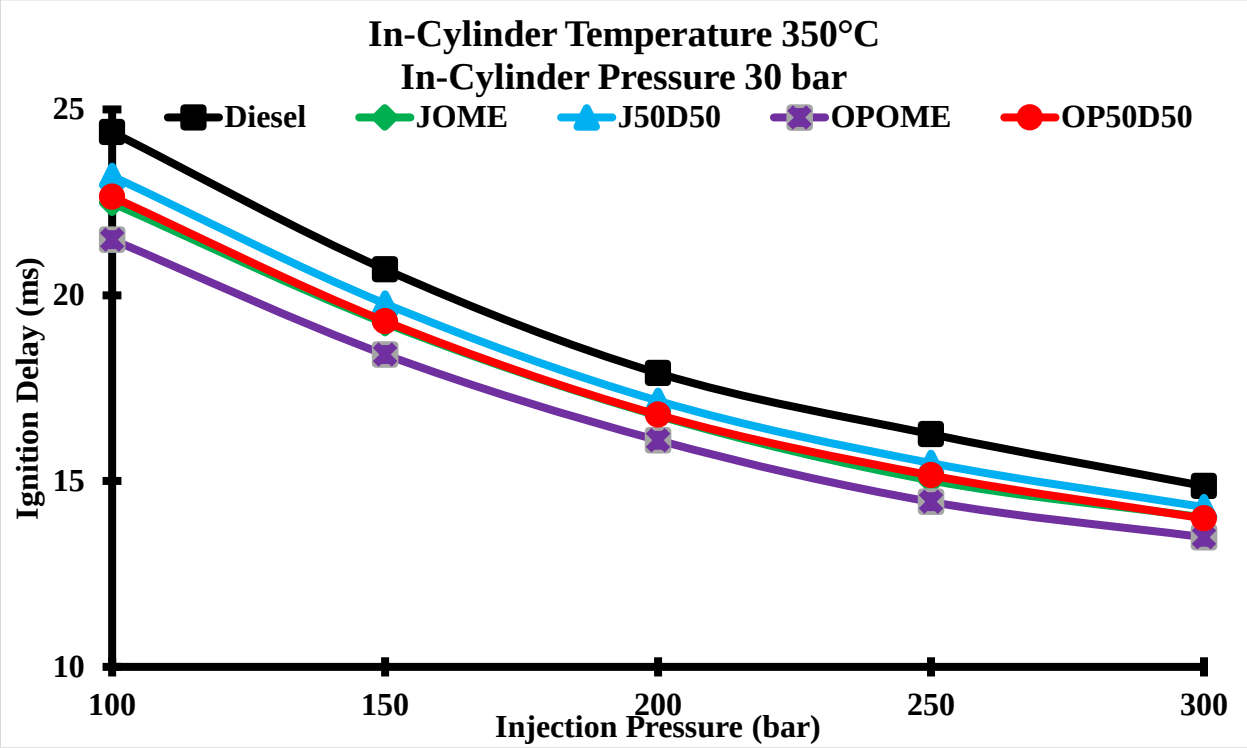

Figure 4.43: Variation of ignition delay of all pilot fuels with injection pressure

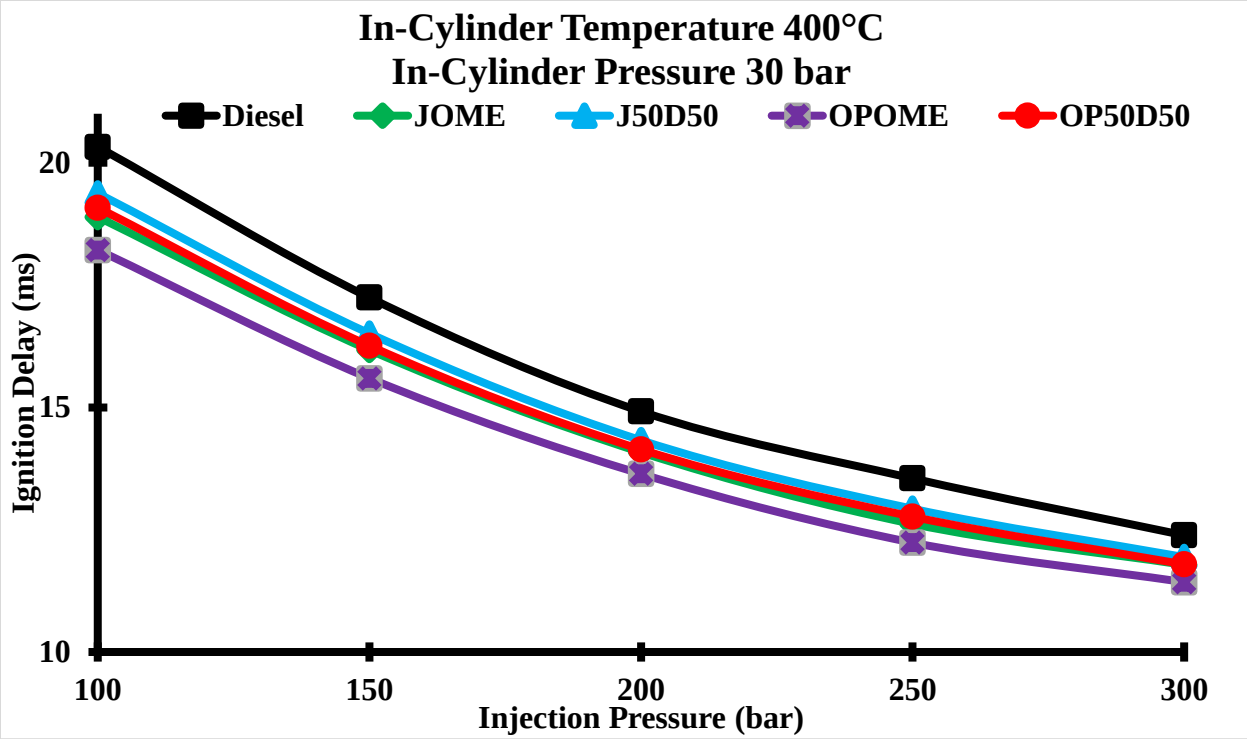

Figure 4.44: Variation of ignition delay of all pilot fuels with injection pressure

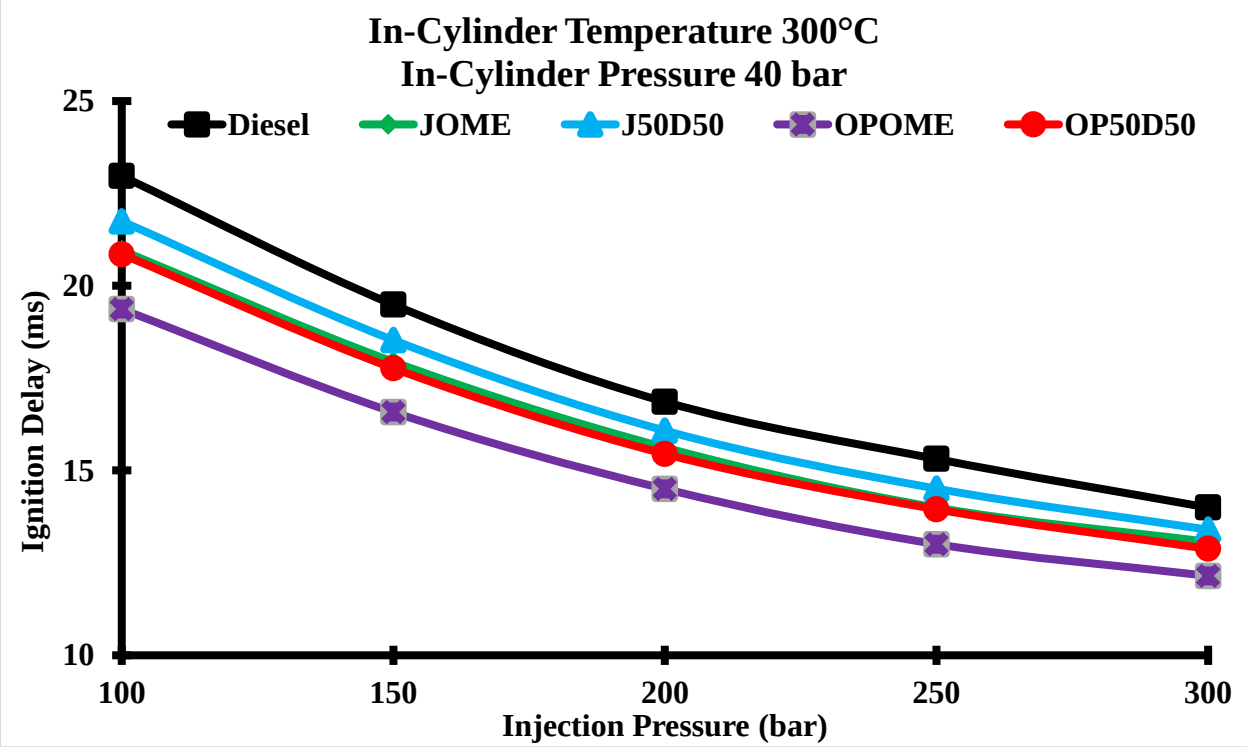

Figure 4.45: Variation of ignition delay of all pilot fuels with injection pressure

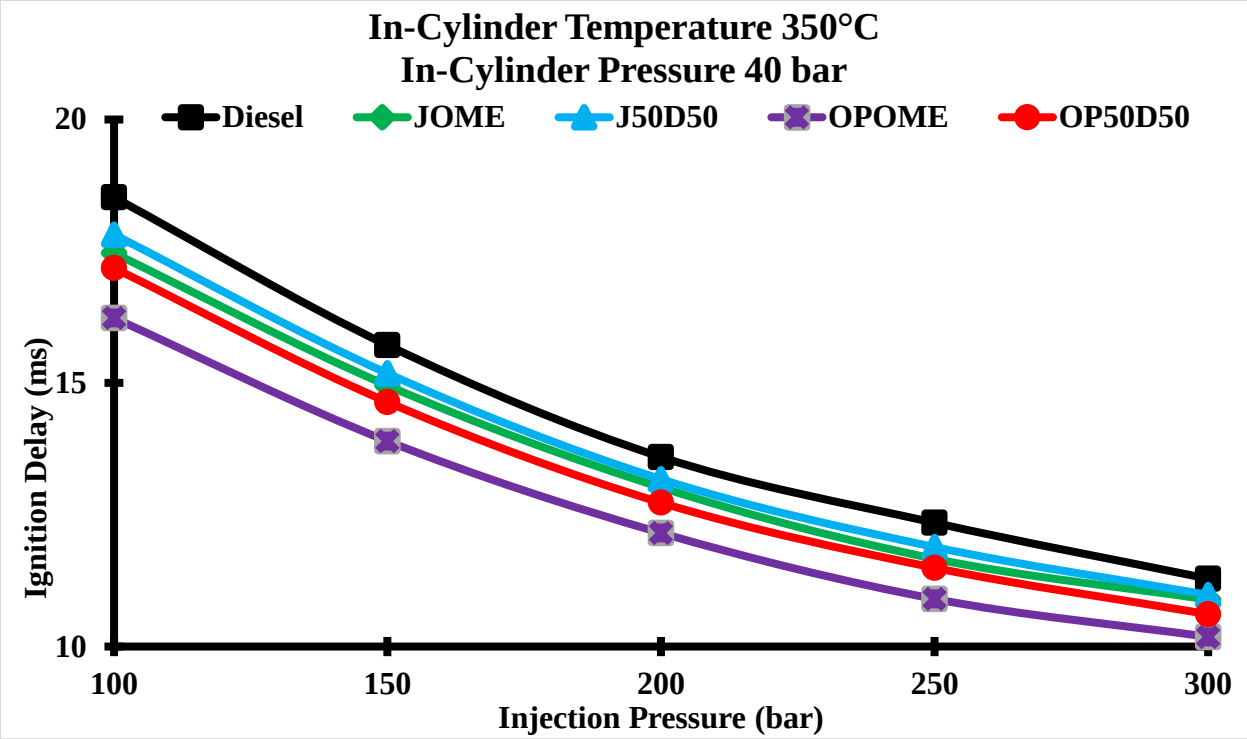

Figure 4.46: Variation of ignition delay of all pilot fuels with injection pressure

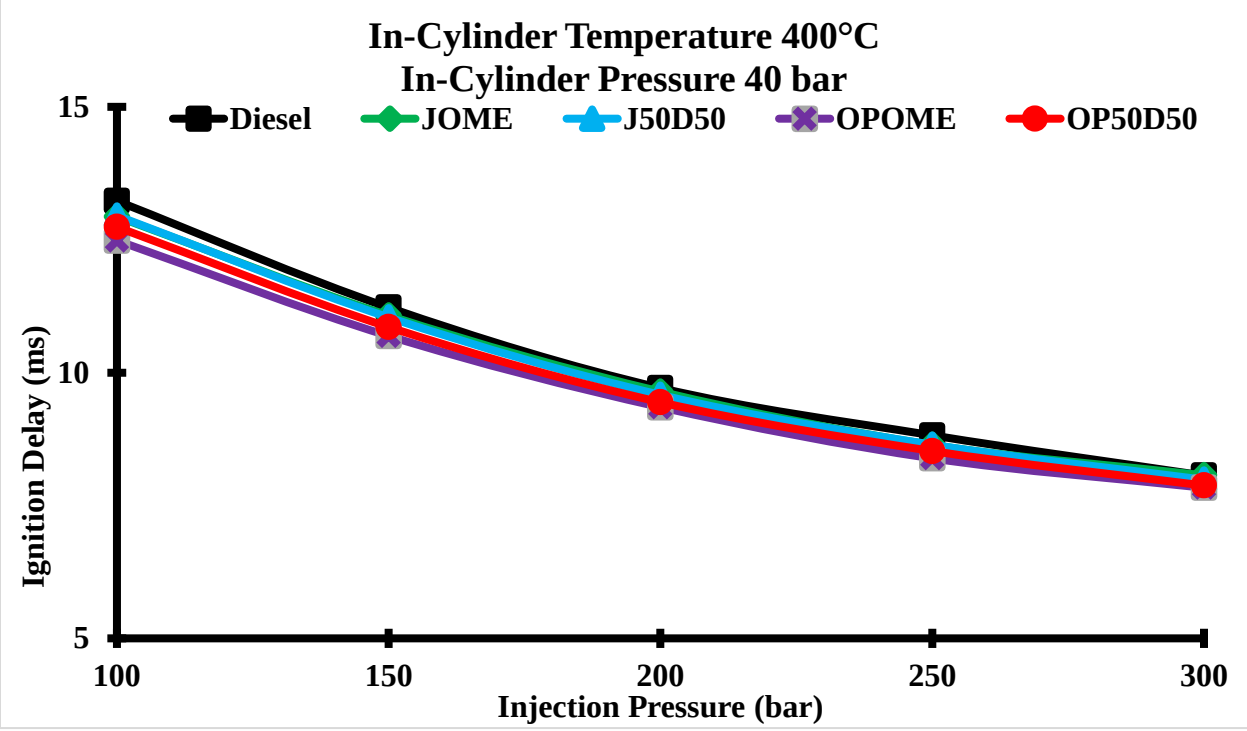

Figure 4.47: Variation of ignition delay of all pilot fuels with injection pressure

4.5 Engine Combustion Characteristics

Combustion process of dual fuel engine is more complex compared to spark ignition engine and compressed ignition engine. It needs to be studied very effectively to understand the performance and emissions characteristics of the engine. In this section, the important parameters (like; in-cylinder pressure, heat release rate, cumulative heat release and mass fraction burn) which define the combustion characteristics are measured. In-cylinder pressure is measured directly from the engine with the help of a computer. While, other parameters are calculated with the help of in-cylinder pressure as discussed in preceding chapter.

The engine combustion characteristics of dual fuel engine using diesel, JOME, OPOME, J50D50 and OP50D50 as pilot fuel for CNG are measured and compared with baseline data mode taking as the baseline data. The effect on combustion characteristics of dual fuel engine using EGR on is also analyzed in this section. Most of the parameters are measured at higher loading condition accept in-cylinder pressure. As discussed in the earlier section that dual fuel engine suffers from poor gaseous fuel utilization at lower load. So its effect on in-cylinder pressure is analyzed which further help to explain the performance and emissions characteristics of dual fuel engine at lower loading conditions.

4.5.1 In-cylinder pressure at lower loading condition

In-cylinder pressure is a valuable parameter to analyze the combustion characteristics of dual fuel engine. In-cylinder pressure provides the brief information of the start of ignition, ignition delay, peak in-cylinder pressure etc. Usually, for optimal combustion and engine

performance, ignition should be such that the resulting peak pressure location needs to be around 10–15° after the TDC position.

In the present section, the variation of in-cylinder pressure of dual fuel engine at low load condition is analyzed and compared with the baseline data mode. It is observed that dual fuel engine has longer ignition delay that baseline data. The reason for that is the dilution of air with CNG which increase the ignition delay of pilot fuel (Kumar and Kumar, 2016a). Two ignition delay has been noticed which are also seen in P-θ diagram, first one for pilot fuel and the second one for primary fuel. The ignition delay of primary fuel is much less than that of pilot fuel. The variation of in-cylinder pressure with respect to crank angle rotation for dual fuel engine without application of EGR and conventional diesel mode at low load condition is shown in Figure 4.48. It is found that, at low loading condition, dual fuel engine suffers from low peak in-cylinder pressure than the baseline data. In dual fuel engine, diesel as pilot fuel has lowest peak in-cylinder pressure of 65.8 bar compared to other pilot fuels. The reasons for this are higher autoignition temperature, longer ignition delay and incomplete combustion of diesel at low load. Peak in-cylinder pressure for CNG-JOME, CNG-J50D50, CNG-OPOME, CNG-OP50D50 and baseline data mode is 67.93 bar, 66.99 bar, 68.6 bar, 68.83 bar and 70.07 bar respectively.

The application of EGR decreases the oxygen concentration inside the cylinder which improves the combustion characteristics of dual fuel engine, especially at lower loads (Kumar and Kumar, 2016b). Hence, use of EGR at low load condition increases the peak in-cylinder pressure of dual fuel engine, but it still less than that of a baseline data. The application of EGR further increases the ignition delay of pilot fuel in dual fuel engine hence resulted in further retardation in the start of combustion and lower in-cylinder temperature.

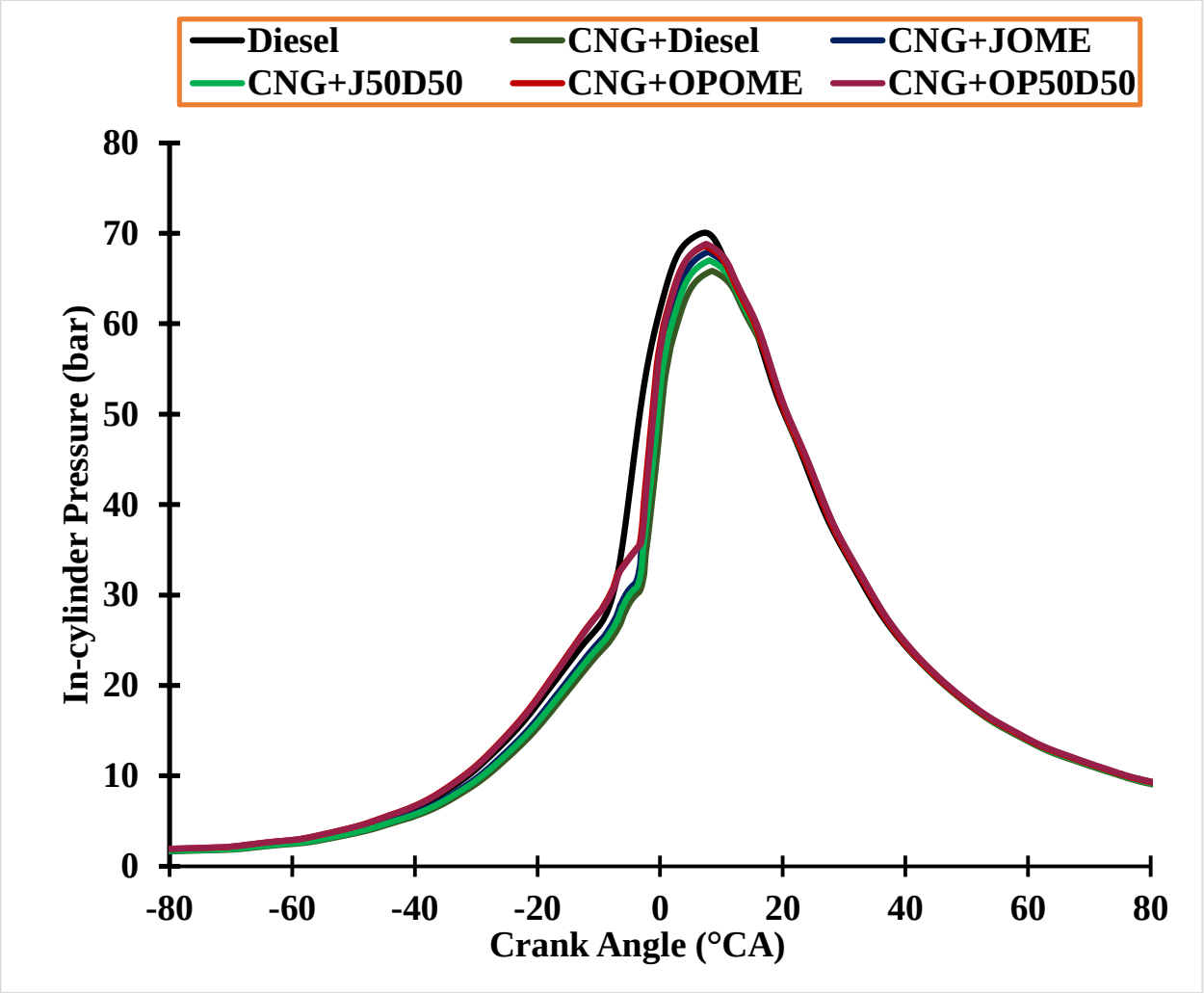

Figure 4.48: Variation of in-cylinder pressure for dual fuel engine, at low load, without application of EGR

The Variation of in-cylinder pressure for dual fuel engine with the application of EGR is shown in Figure 4.49. In dual fuel engine, CNG-OP50D50 with EGR shows highest peak in-cylinder of 69.45 bar at low loading condition.

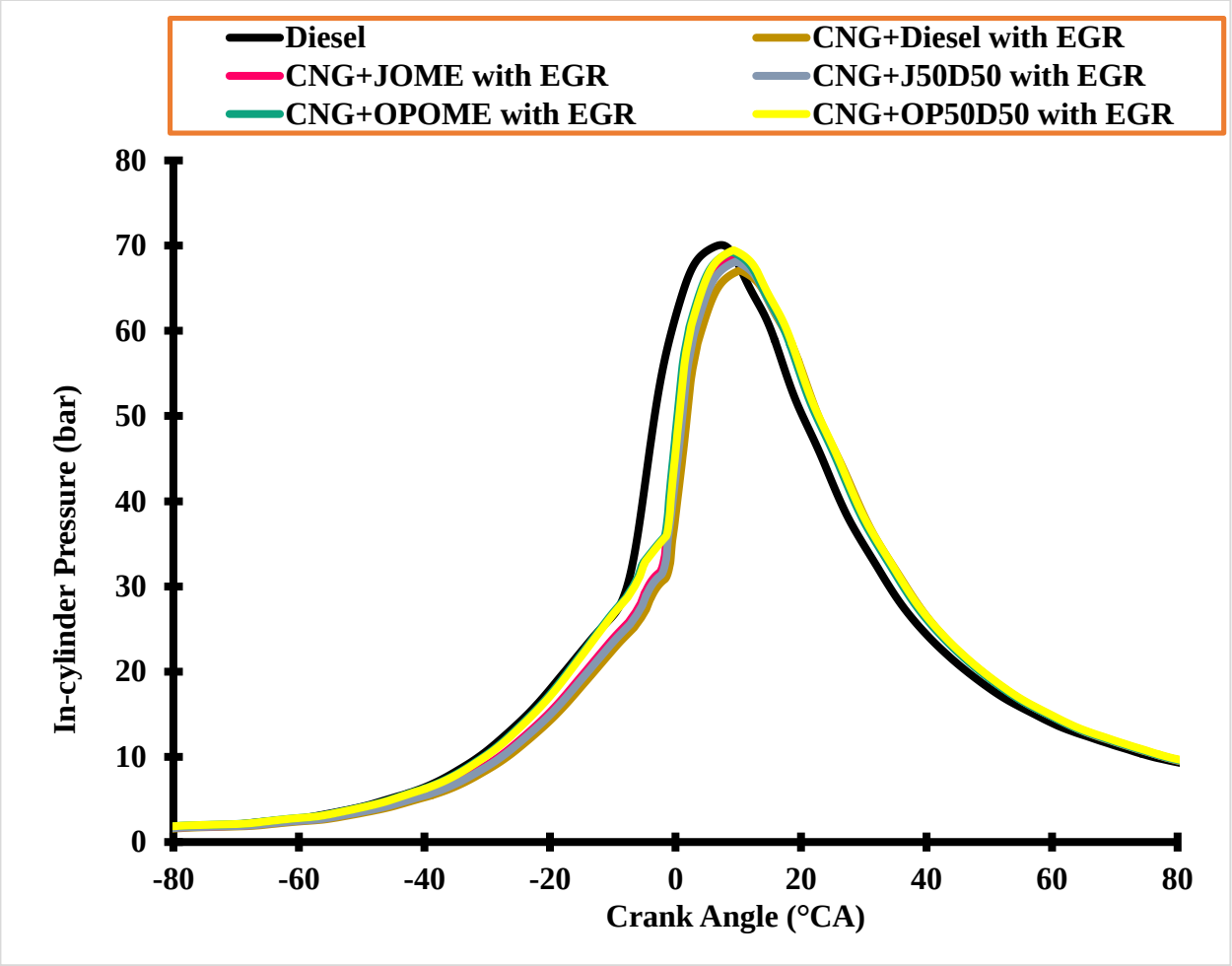

Figure 4.49: Variation of in-cylinder pressure for dual fuel engine with application of EGR at low load

The peak pressure for all operating modes, at low loading condition, is shown in Figure 4.50. Variation of peak in-cylinder pressure of dual fuel engine for all combination of fuel with respect to baseline data mode at low load is shown in Figure 4.51. It is observed that dual fuel engine, diesel as pilot fuel has lowest in-cylinder pressure compared to other operating modes. The application of EGR improves the peak in-cylinder pressure of dual fuel engine for all fuel combination.

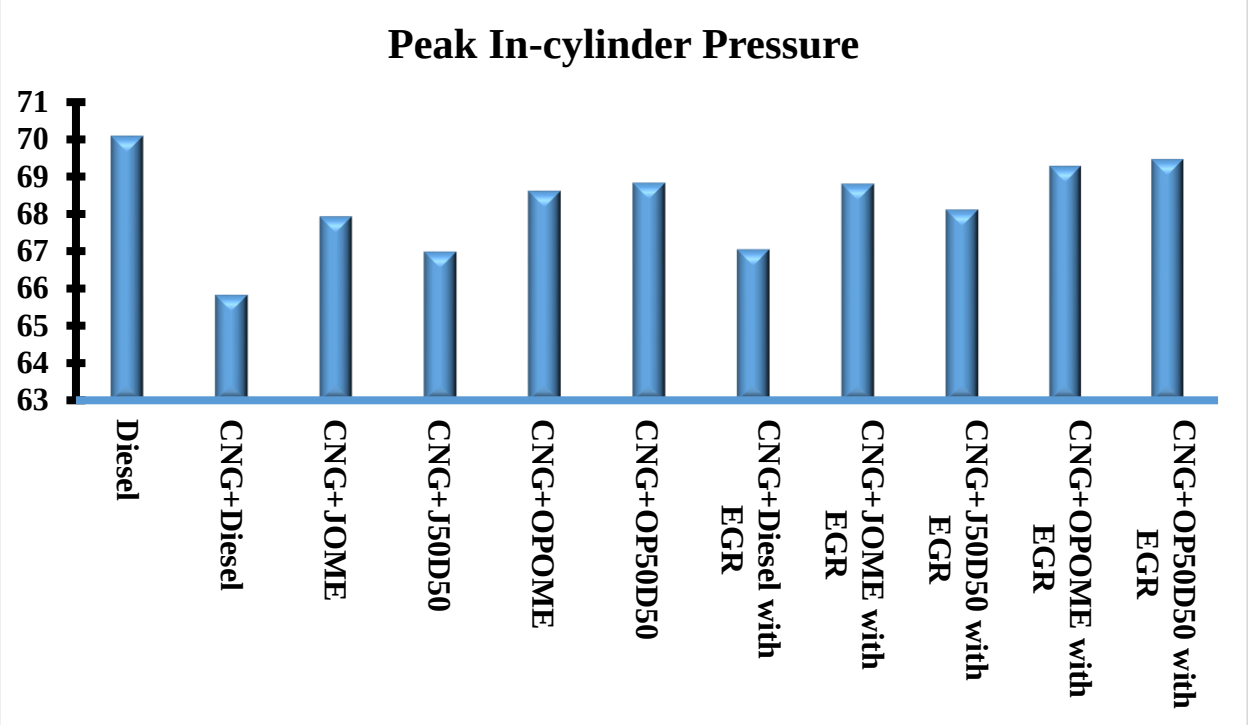

Figure 4.50: Peak in-cylinder pressure of all operating modes.

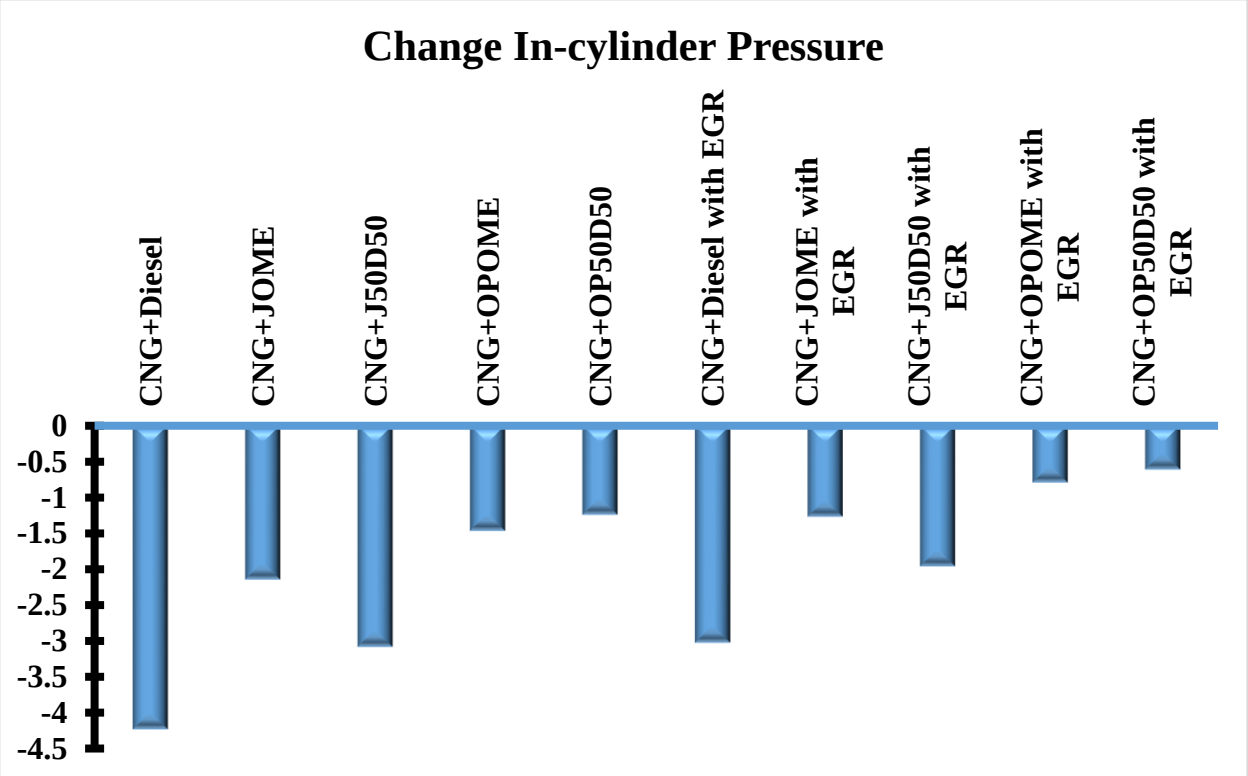

Figure 4.51: Change in-cylinder pressure of dual engine w.r.t. baseline data

4.5.2 In-cylinder pressure at higher loading condition

In this section, the variation of in-cylinder pressure, at higher load, of dual fuel engine with a various combination of fuels is analyzed and compared the results with the baseline data. The combustion of primary fuel improves with increasing engine loads. Hence, at higher loading condition, improved gaseous fuel combustion enhances the in-cylinder pressure rate. It is observed that at higher load, dual fuel engine shows higher peak pressure compared to baseline data for all combination of fuel. The increased in-cylinder pressure and temperature also results in complete combustion of diesel in dual fuel engine, which further increase the peak in-cylinder pressure (Kumar and Kumar, 2016a). Also, higher in-cylinder pressure and temperature reduce the autoignition delay of pilot fuel. However, ignition delay of primary fuel seems unchanged, but improvement in the rate of burning is noticed. Hence, at higher load, dual fuel engine using diesel as pilot fuel shows highest peak in-cylinder pressure among all mode of operations. The improved in-cylinder pressure and temperature of dual fuel engine also improve the efficiency of the engine. The rate of change of in-cylinder pressure with respect to the crank angle rotation of dual fuel engine without application of EGR is shown in Figure 4.52.

The richer fuel-air mixture is introduced into the combustion chamber at higher load (Mustafi and Raine, 2013). The application of EGR further reduces the oxygen concentration inside the cylinder which results in an increase in ignition delay and poor combustion of primary fuel. Hence, at higher load, the application of EGR adversely effect on combustion characteristics of dual fuel engine and results in low in-cylinder pressure compared to normal dual fuel engine mode. But, the peak pressure of dual fuel engine is still higher than baseline data after application of EGR. The effect of the application of EGR on the rate of change of in-

cylinder pressure with respect to crank angle rotation for dual fuel engine is shown in Figure 4.53.

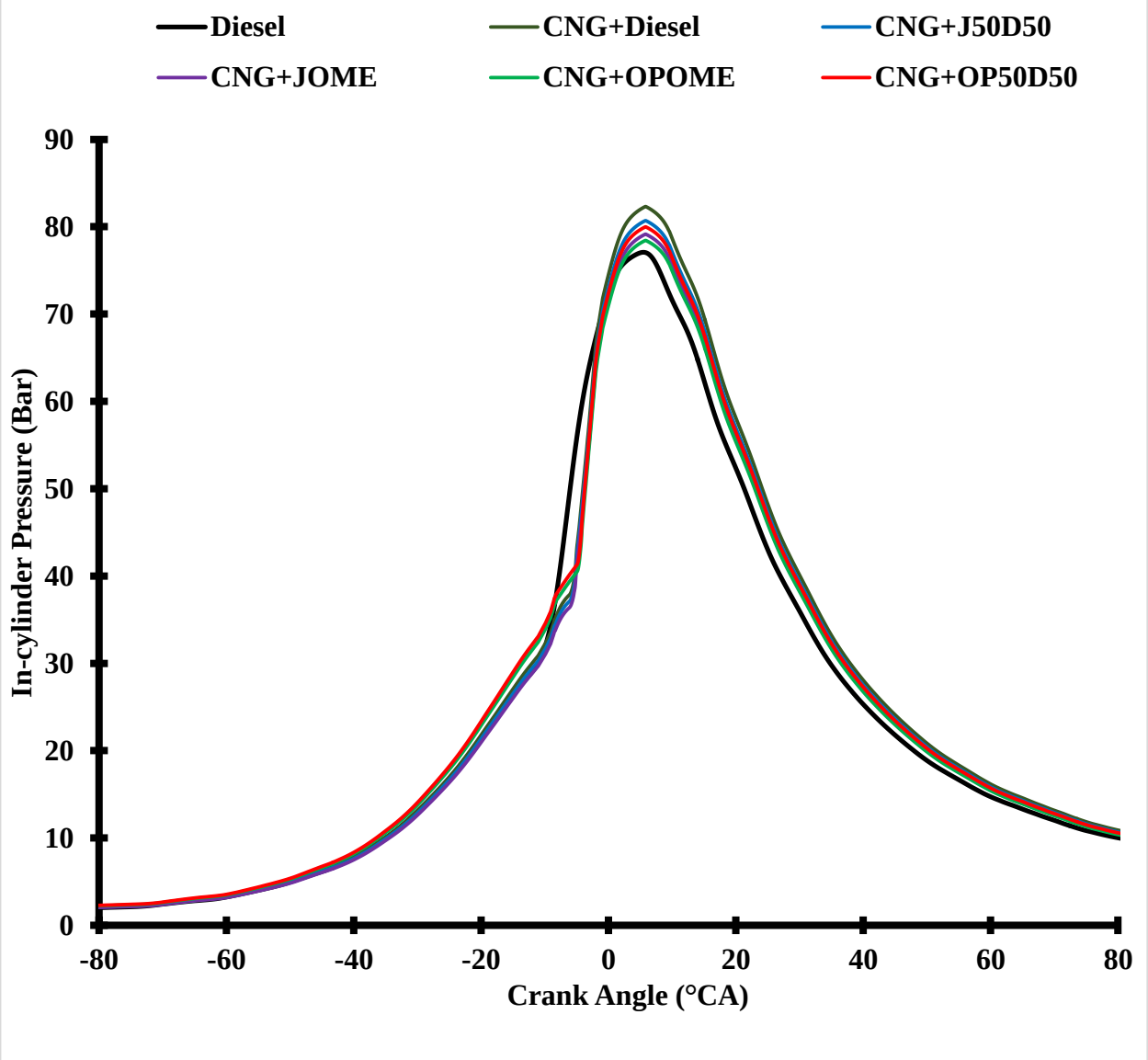

Figure 4.52: Variation of in-cylinder pressure for dual fuel engine, at higher loading condition, without application of EGR

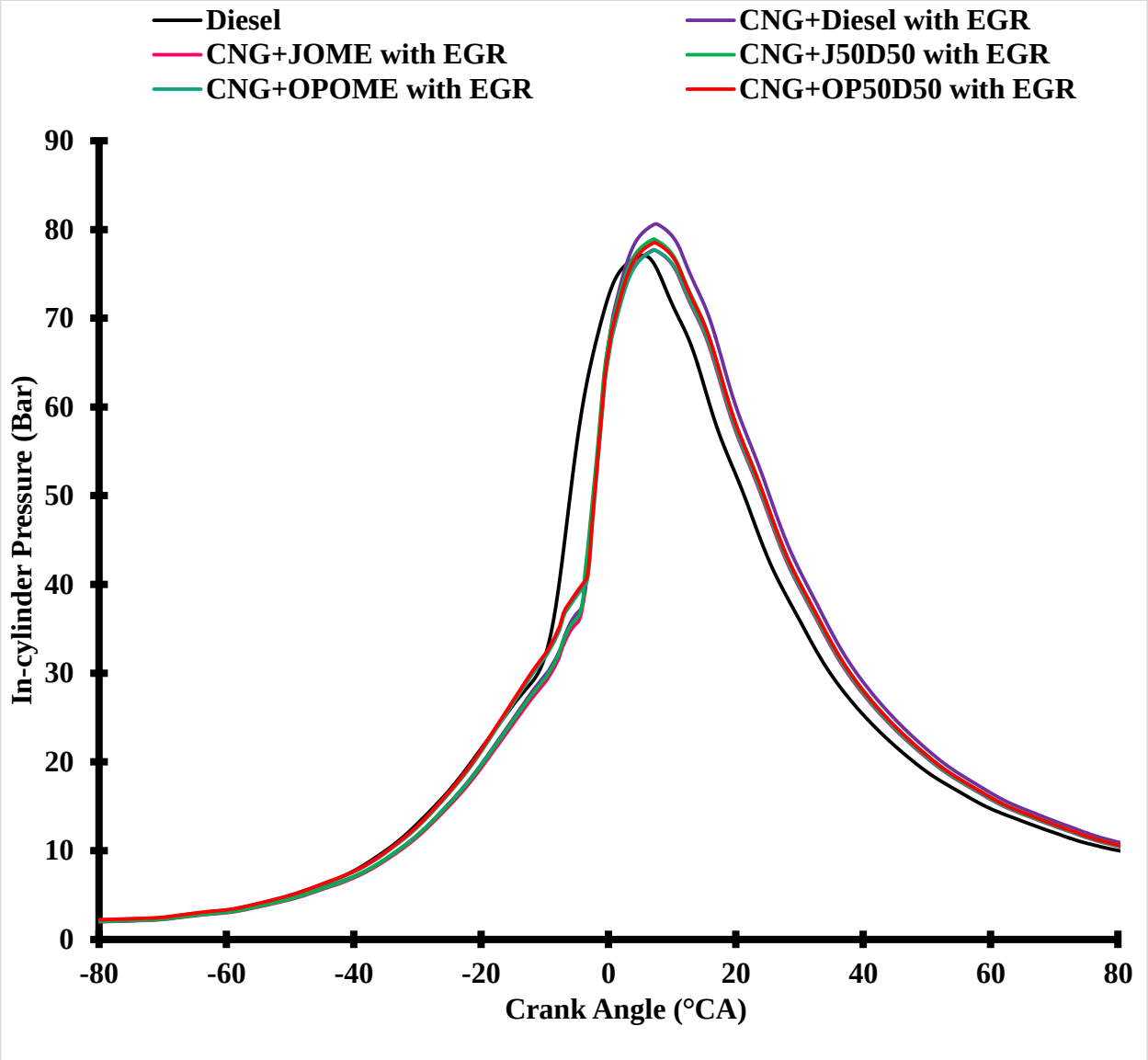

Figure 4.53: Variation of in-cylinder pressure for dual fuel engine, at higher load, with application of EGR

The peak pressure for all operating modes, at low loading condition, is shown in Figure 4.54. Variation of peak in-cylinder pressure of dual fuel engine for all combination of fuel with respect to baseline data at low load is shown in Figure 4.55.

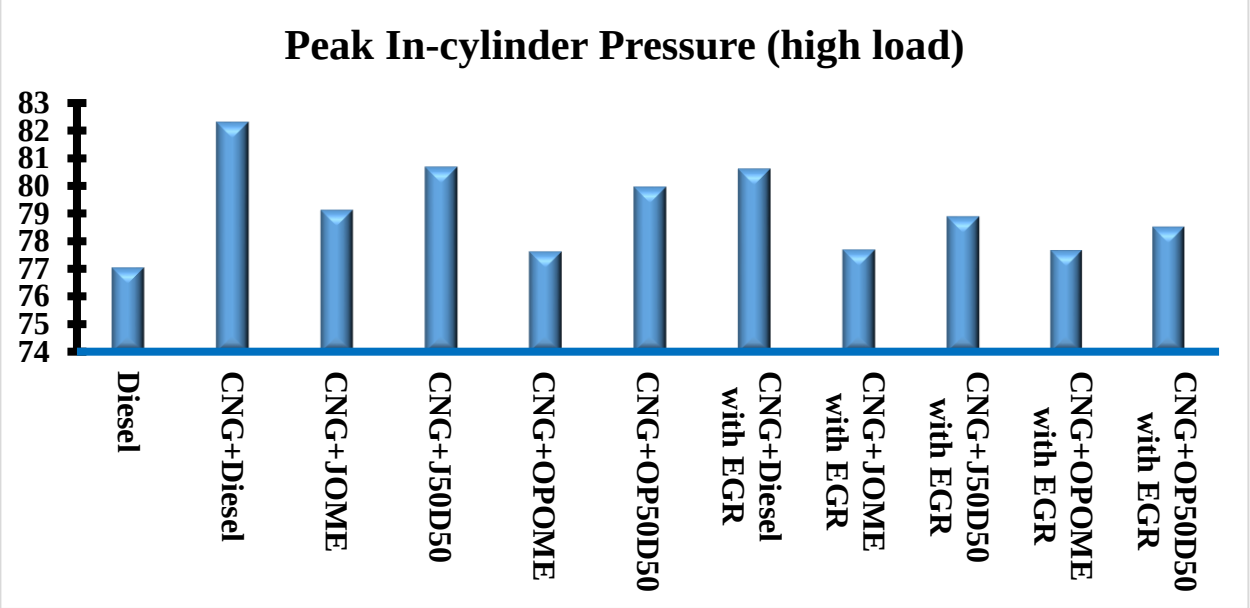

Figure 4.54: Peak in-cylinder pressure of all operating modes

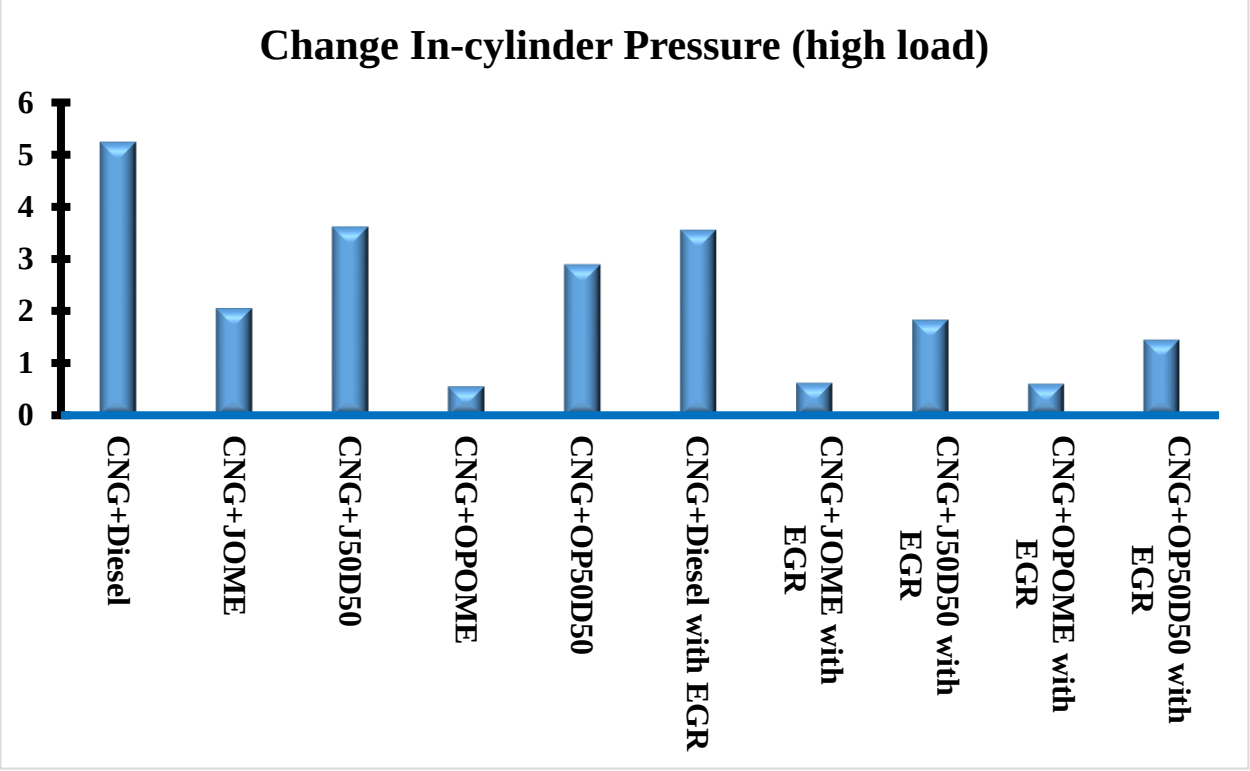

Figure 4.55: Change in-cylinder pressure of dual engine w.r.t. baseline data

4.5.3 Heat release rate

The heat release rate gives the clear picture of fuel burn in the combustion chamber during the power stroke. However, for present research work, the heat release rate is calculated with the help on pressure rise rate. The heat release rate is calculated by Sorenson's heat release model discoursed earlier. The heat release rate of fuel in combustion chamber mainly depends upon; ignition delay, oxygen concentration, in-cylinder pressure and temperature etc. (Pali et al., 2014). The trend of heat release rate of dual fuel engine is slightly different than a baseline data. In dual fuel engine, two peaks of heat release are noticed i.e. one for pilot fuel and other for primary fuel. For baseline data, the maximum heat release rate at the premixed combustion phase is lower than that of dual fuel engine and occurred earlier.

The negative heat release rate is observed for some period of time. This occurred because some quantity of heat is absorbed by the injected fuel during its ignition delay period (Pali et al., 2014). Heat release rate starts increasing with start of ignition. In the premixed phase of combustion, due to longer ignition delay of pilot fuel, heat release rate start later in dual fuel engine compared to baseline data. The heat release rate in premixed combustion phase is higher for all operating modes because of combustion of fuel after ignition delay. Two premixed phase are noticed in dual fuel engine. The multipoint burning of primary fuel occurred in dual fuel engine which results in higher heat release rate compared to baseline data. After this phase, the combustion continues slowly until most of the fuel is burned. This phase of combustion is called mixing-controlled combustion. The heat release rate of dual fuel engine with a various combination of fuel without application of EGR is shown in Figure 4.56.

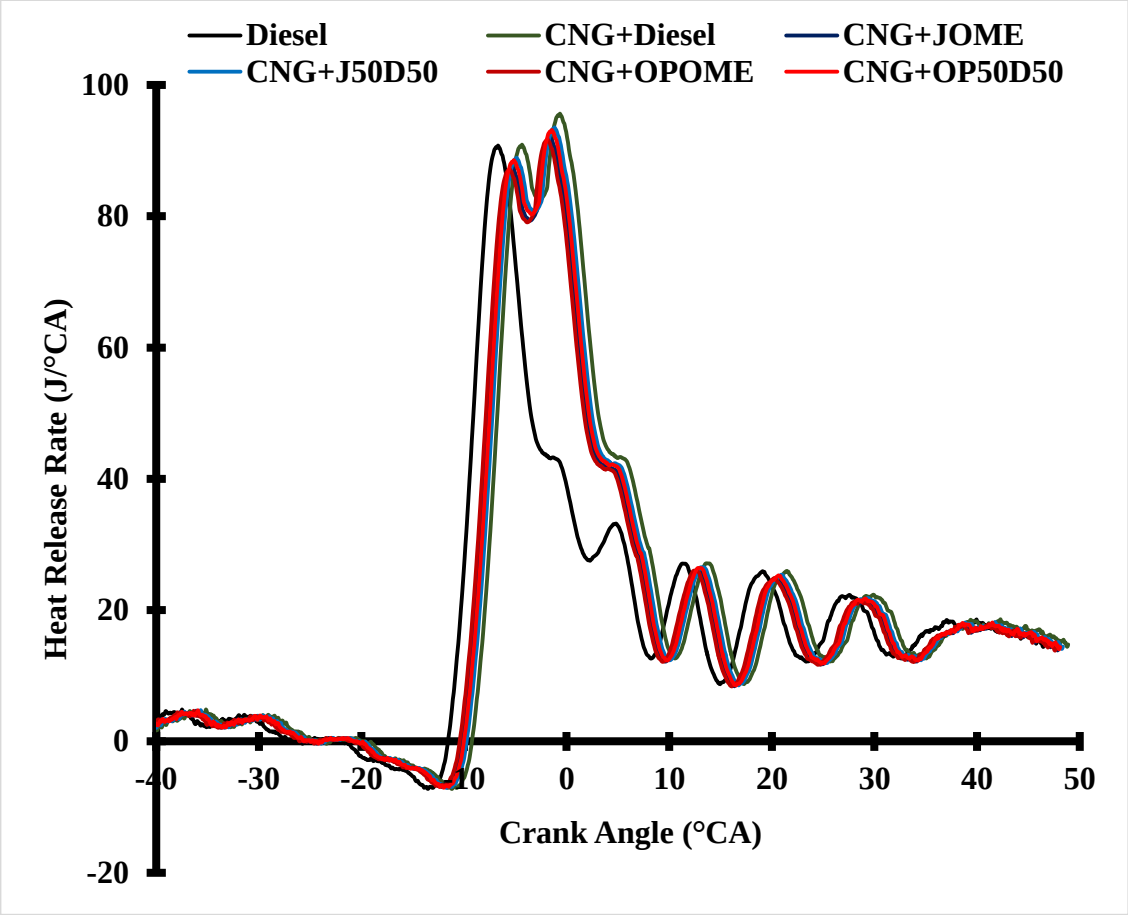

Figure 4.56: Heat release rate of dual fuel engine without application of EGR

In dual fuel engine, heat release rate of CNG+OPOME is faster and lower than other fuel combination, because of shorter ignition delay of OPOME. However, CNG+JOME mode has nearly similar heat release rate that of CNG+OPOME. The diesel and biodiesel blend as pilot fuel increase the heat release rate in premixed combustion phase than biodiesel as pilot fuel. The reason for that is low cetane number of blends compared to parent biodiesel. CNG+diesel mode shows highest heat release rate among all operating modes. Due to multipoint ignition of CNG, the heat release rate in diffusion combustion phase of dual fuel engine is much higher than baseline data.

The application of EGR in dual fuel engine reduces the oxygen concentration inside the combustion chamber which further increases the ignition delay of pilot fuel and results in lower heat release rate in premixed combustion phase. However, the heat release rate is seemed unaffected in diffusion combustion phase. The heat release rate of dual fuel engine with a various combination of fuel using EGR is shown in Figure 4.57.

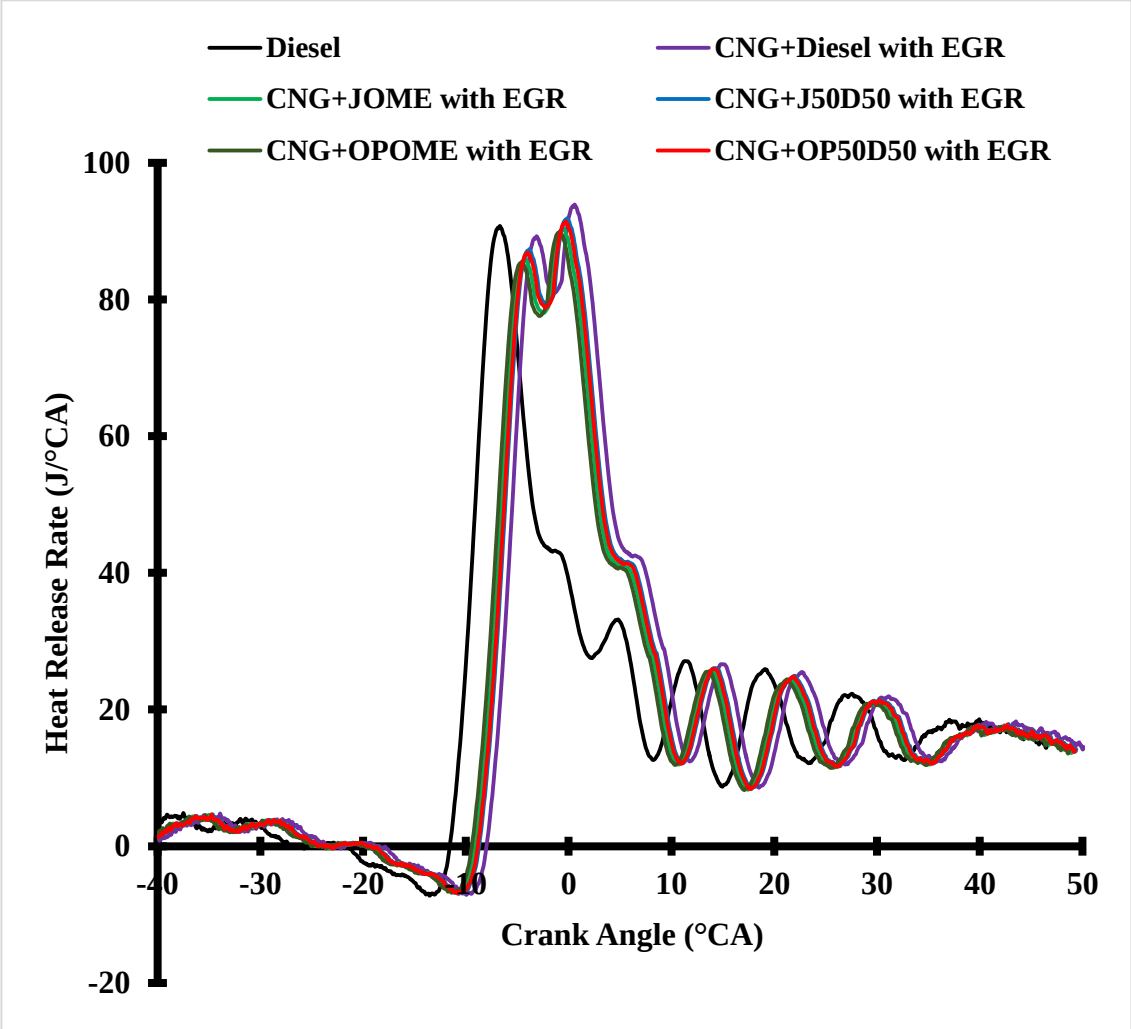

Figure 4.57: Heat release rate of dual fuel engine using EGR

4.5.4 Cumulative heat release

The cumulative heat release gives the total heat release during the combustion process up to particular crank angle rotation. The cumulative heat release for baseline data is found higher compared to dual fuel engine due to the early start of combustion. As discoursed earlier the decreased oxygen concentration in dual fuel engine increases the ignition delay period of pilot fuel which results in the late start of combustion. The cumulative of heat release of dual fuel engine without and with the application of EGR is shown in Figure 4.58 and Figure 4.59 respectively.

The dual fuel engine shows higher cumulative heat release after premixed combustion phase than the baseline data. However, in premixed combustion phase, the cumulative heat release of the baseline data is higher. In diffusive combustion phase, the burning of CNG occurs at a higher rate and also CNG has a higher calorific value which results in higher cumulative heat release.

In dual fuel engine, the variation in cumulative heat release is noticed during premixed combustion phase due to different combustion characteristics of various pilot fuels. Further, it affects the CNG combustion and results in different trends of cumulative heat release for various combinations of fuels. The cumulative heat release for CNG+OPOME is higher in premixed combustion phase in dual fuel mode also CNG+JOME has nearly same cumulative heat release. However, I diffusive combustion phase, CNG+diesel shows highest cumulative heat release of 1772.9 J while conventional diesel with 1526.2 J has the lowest. The other fuel combinations for

dual fuel engine i.e. CNG+JOME, CNG+J50D50, CNG+OPOME and CNG+OP50D50 have cumulative heat release of 1705.6J, 1733.2J, 1700.2J and 1726.9J respectively.

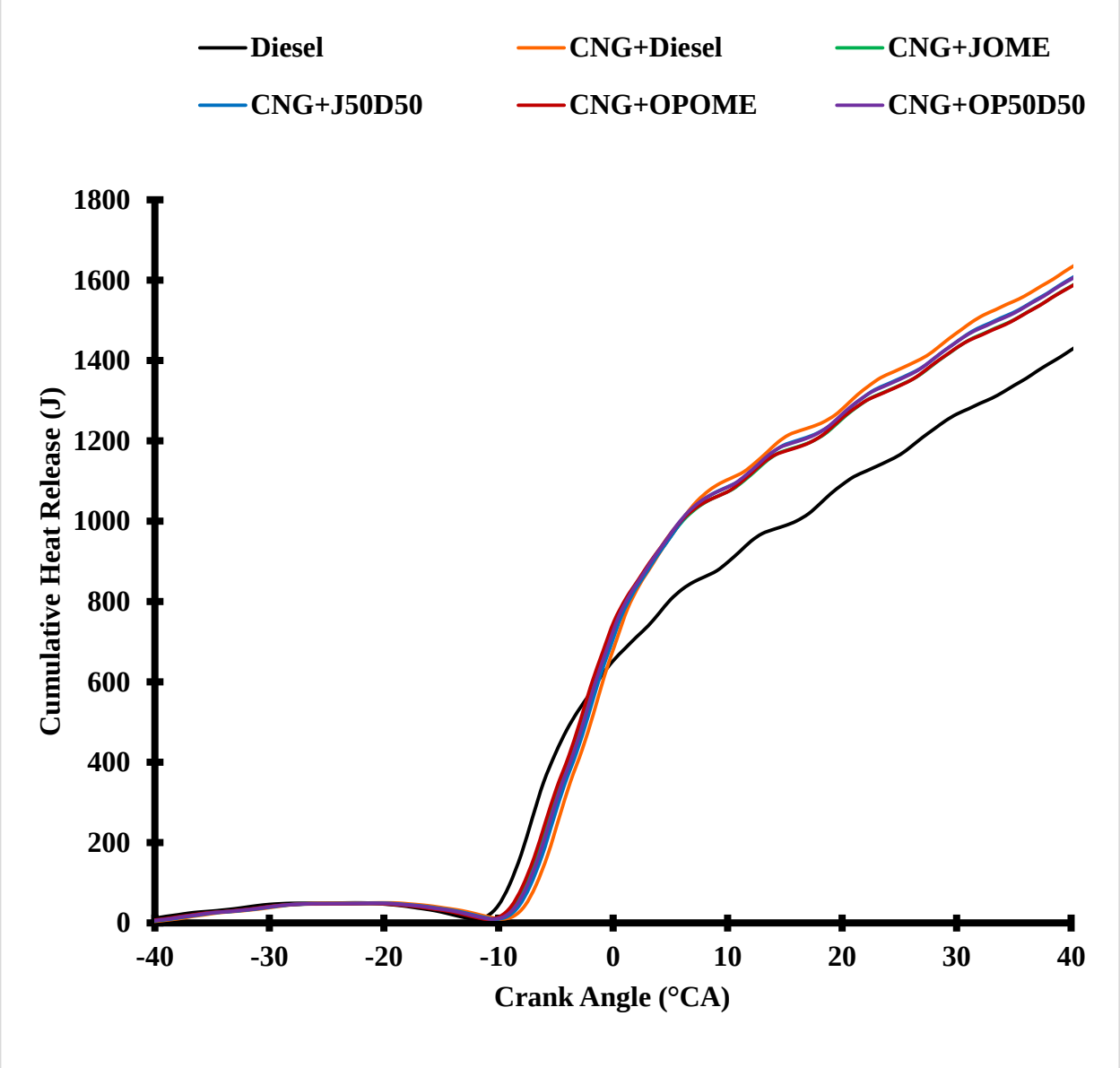

Figure 4.58: Cumulative heat release of dual fuel engine without application of EGR

The application of EGR in dual fuel engine decreases the heat release rate as discoursed earlier section that results, a slight decrease in cumulative heat release of the engine. However, it is still higher enough than the baseline data.

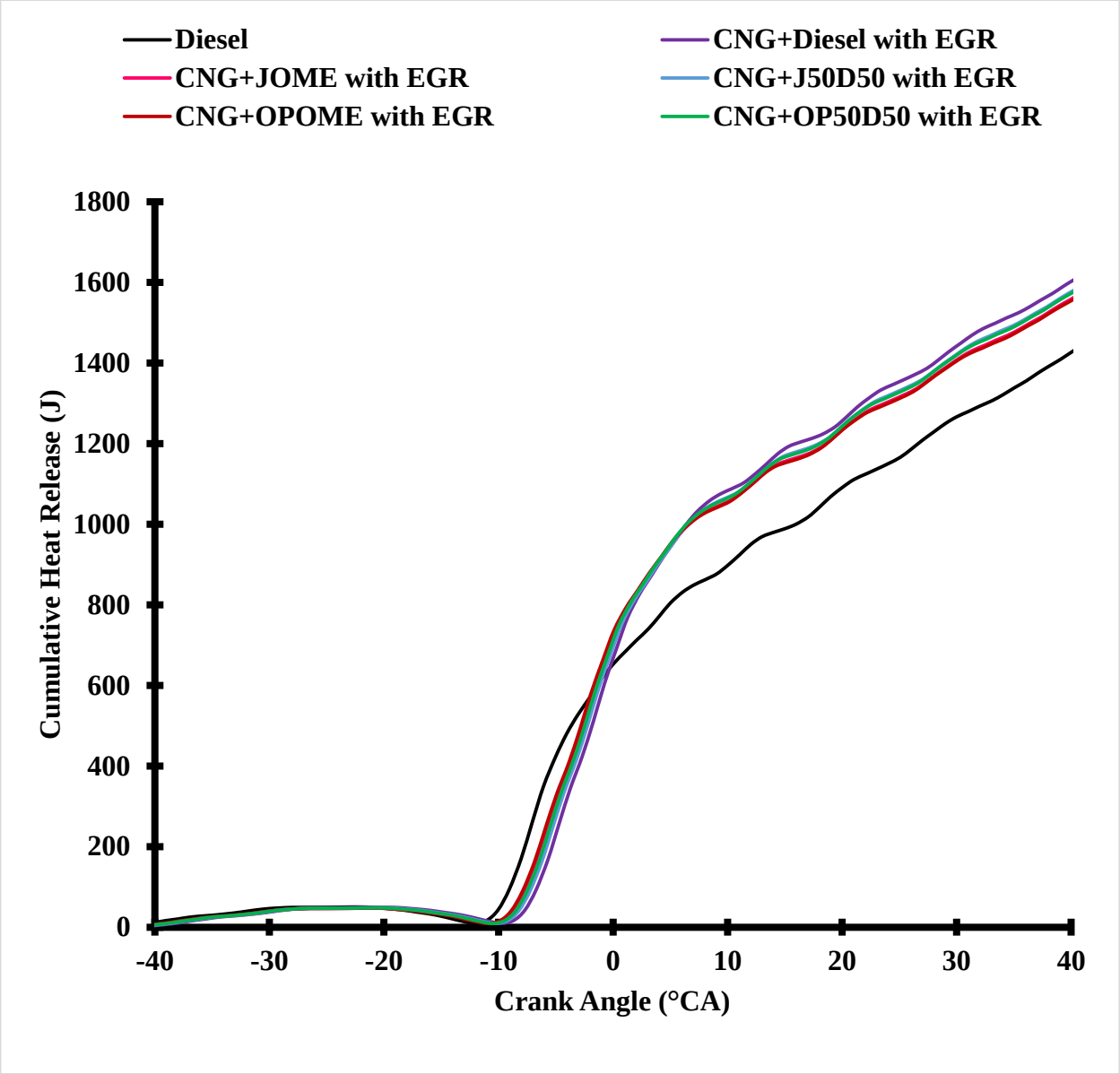

Figure 4.59: Cumulative heat release of dual fuel engine using EGR

4.5.5 Mass fraction burnt

The mass fraction burnt represents the quantity of fuel burnt during the combustion process. The mass fraction burnt is calculated by an analysis commonly based on burnt rate which is developed by Rassweiler and Withrow as discoursed in an earlier section. This procedure highly used these days, due to its simplicity and accuracy (Mendera et al., 2002). The mass fraction burnt is generally varied between 0 and 1 for any engine. The mass fraction burnt of dual fuel is measured at full load condition. The mass fraction burnt of dual fuel engine without application of EGR is shown in Figure 4.60. It is noticed that the mass fraction burnt for dual fuel engine is lower than baseline data at full load condition. The reason for that is high autoignition temperature of CNG which result in its incomplete combustion and hence low mass fraction burnt. It is also observed that in starting of combustion the mass fraction burnt of the baseline data is much higher than dual fuel engine. However, the difference reduced as crank moves toward the bottom dead center.

In dual fuel engine, the use of biodiesel as pilot fuel not much affect the mass fraction burnt. However, in starting phase of combustion using JOME and OPOME increases the mass fraction burnt but in the end of combustion, it becomes less than diesel as pilot fuel. The mass fraction burnt diagram also helps to calculate the ignition delay and the total combustion period. The ignition delay is measured as crank angle rotation between the start of ignition and mass fraction burnt of 0.05. Also, the total combustion period is calculated by measuring the crank angle rotation between mass fraction burn of 0.05 and mass fraction burnt of 0.95 for most of the engines. The total mass fraction burnt till the end of combustion for baseline data is found 0.972698 where, for CNG+diesel, CNG+JOME, CNG+J50D50, CNG+OPOME and

CNG+OP50D50 dual fuel mode is measured of 0.964721, 0.966084, 0.965403, 0.96511 and 0.964916 respectively.

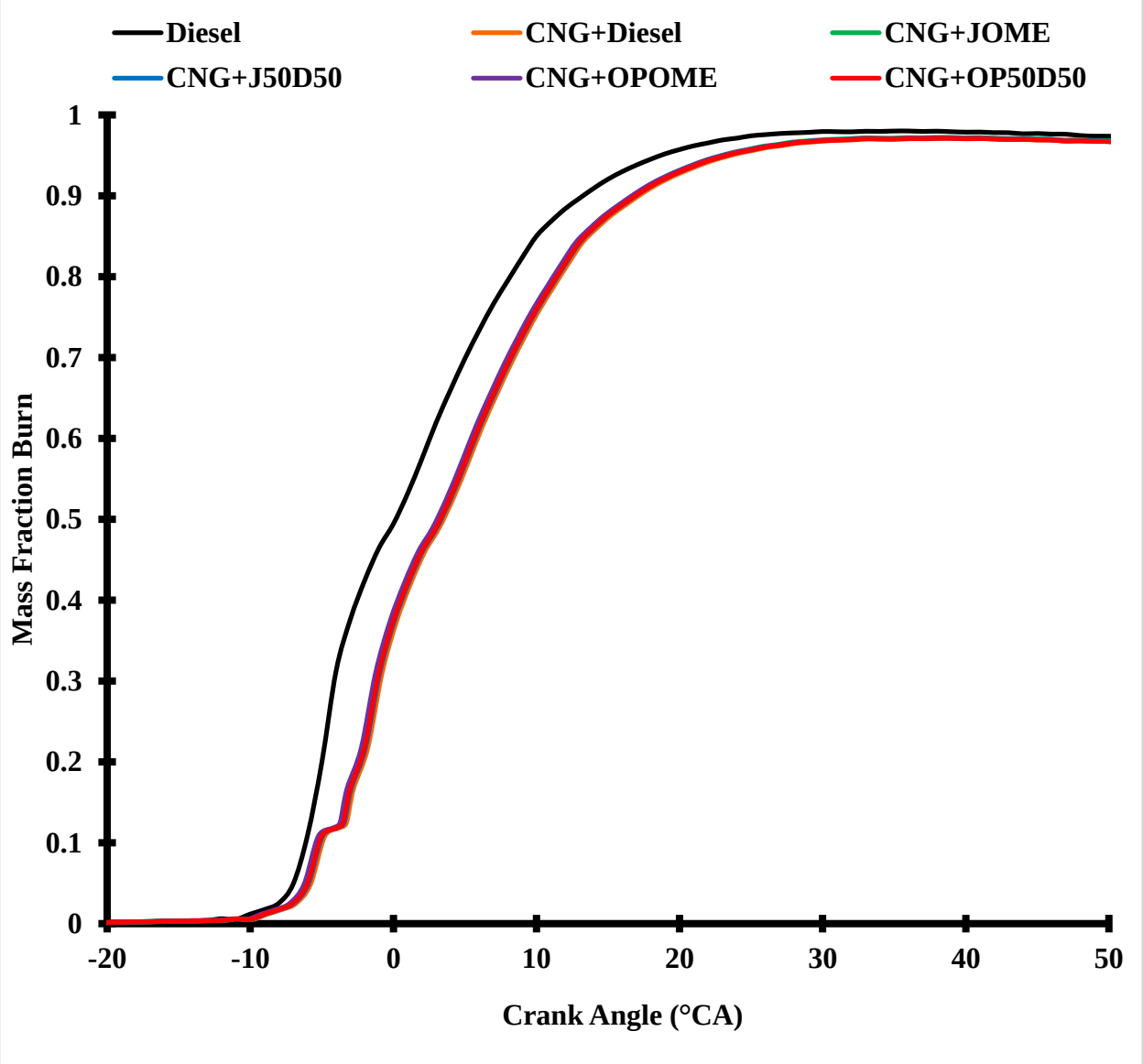

Figure 4.60: Mass fraction burnt for dual fuel engine without application of EGR

The application of EGR in dual fuel engine increases the duration of ignition delay and combustion. The mass fraction burnt of dual fuel engine without application of EGR is shown in Figure 4.61. Furthermore, application of EGR has an adverse effect on combustion

characteristics of dual fuel engine at full load; hence low mass fraction burnt has been noticed. Nearly 1% reduction in mass fraction burnt is notice while EGR is applied. This causes reduction in performance and emissions characteristics of the engine. The low mass fraction burnt indicates incomplete combustion of fuel which leads to high unburnt hydrocarbons and carbon monoxides emissions.

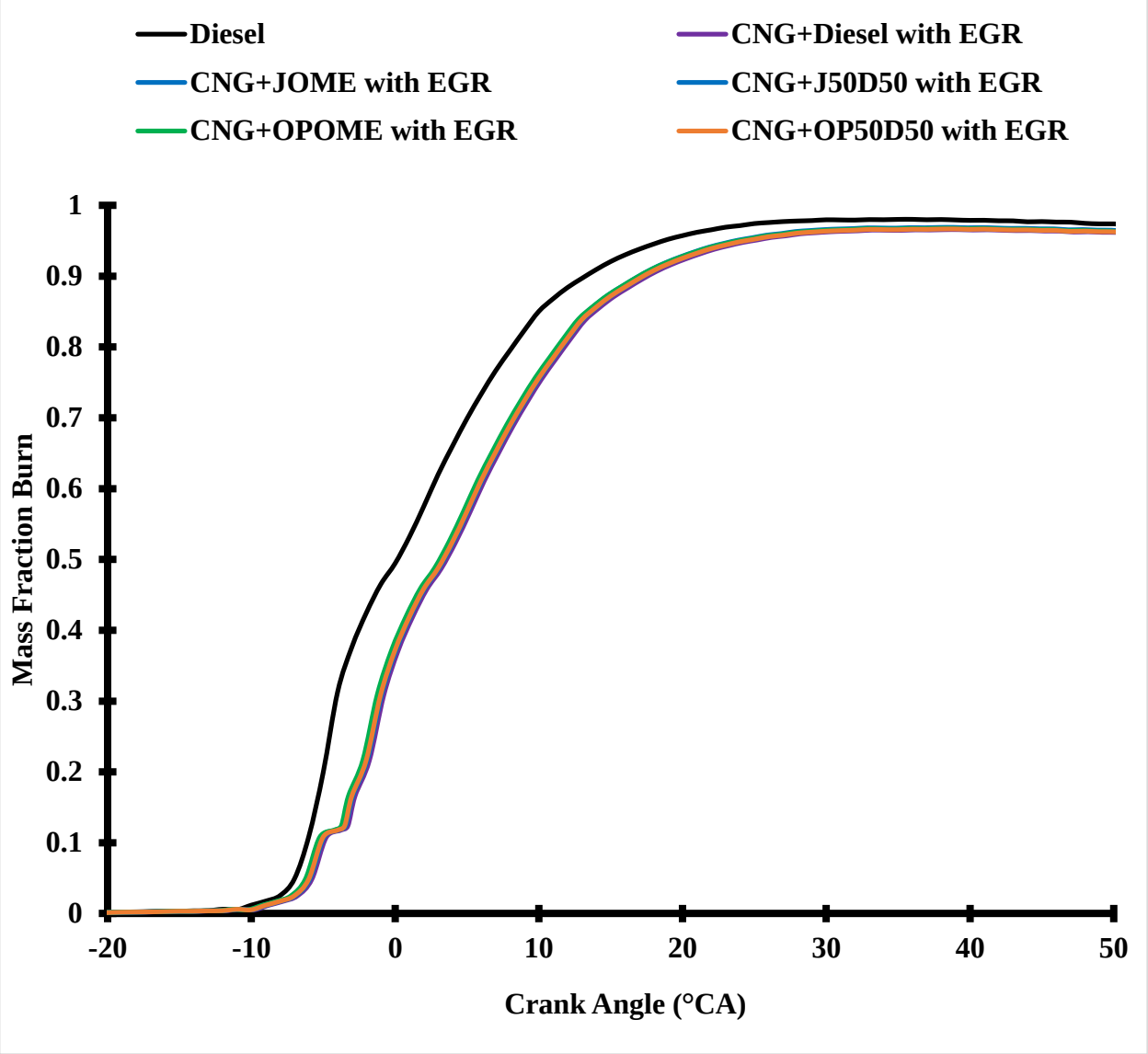

Figure 4.61: Mass fraction burnt for dual fuel engine using EGR

4.6 Performance Characteristics of Dual Fuel Engine

In this section performance characteristics of dual fuel engine (like brake thermal efficiency, brake specific energy consumption and exhaust gas temperature) are measured and compared with the baseline data. The all fuel combination of dual fuel engine used in the present work (i.e. CNG+diesel, CNG+JOME, CNG+J50D50, CNG+OPOME and CNG+OP50D50) without and with the application of EGR is explored in detail. The effect of the application of EGR to improve the performance characteristics of dual fuel engine at low and intermediate loading is also analyzed. The effects of using EGR on performance characteristics of dual fuel engine at higher loading conditions are also investigated in this section.

4.6.1 Brake thermal efficiency

The chemical energy of the fuel is converted into heat energy in the combustion chamber of the engine. This heat energy is further converted into the mechanical energy by the moving parts of the engine. The brake thermal efficiency (BTE) of the engine is an important parameter which tells how efficiently an engine converts heat energy into mechanical energy. The BTE is the ratio of mechanical work on the output shaft to the energy consumed to produce that work. BTE of an engine is increased with increasing load for most of the engine. However, some engine shows a reduction in the BTE at full loading condition (Agarwal et al., 2006). The BTE of dual fuel engine is found highest at full loading condition.

The BTE of the baseline data mode and dual fuel engine mode with various fuels combination is measured at 20%, 40%, 60%, 80% and 100% loads in the present section. The BTE and brake specific energy consumption are not taken into account for no loading condition (0%) as they

tended to infinity. The variation of BTE with a load for dual fuel engine without and with the application of EGR is shown in Figure 4.62 and Figure 4.63 respectively.

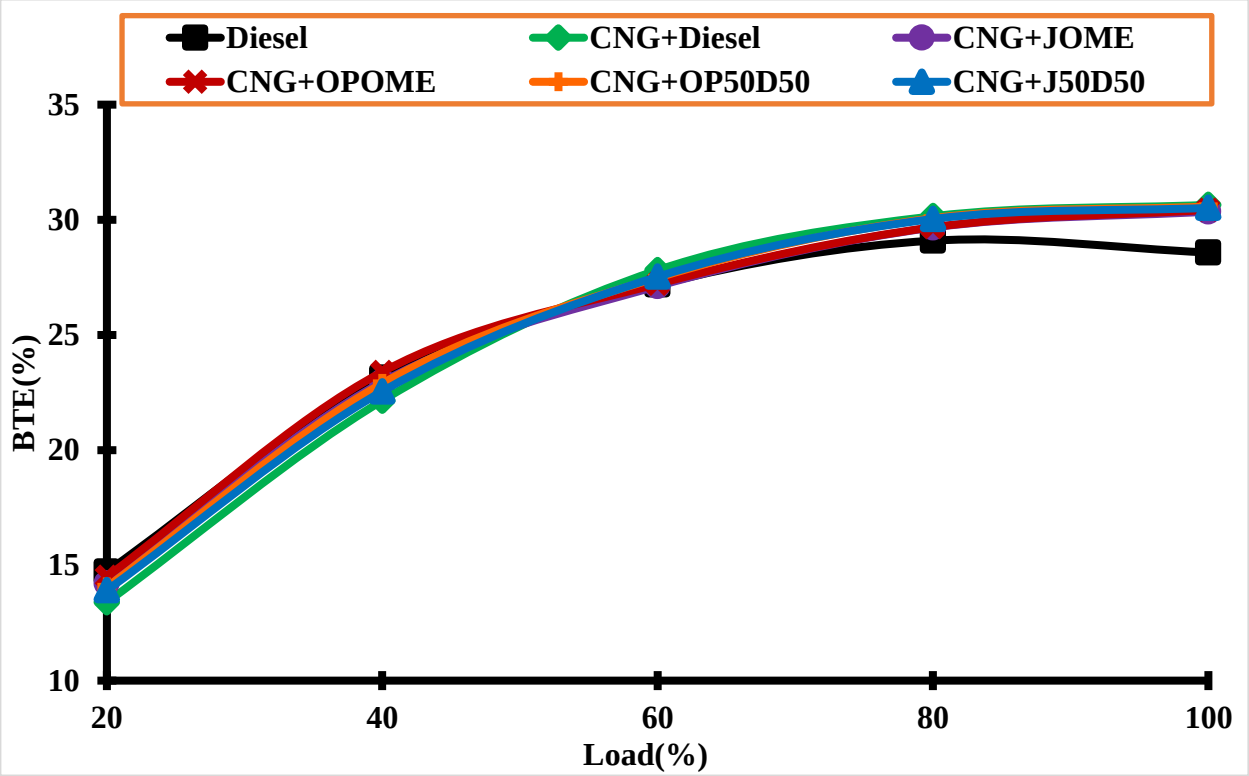

Figure 4.62: Variation in BTE of dual fuel engine without the application of EGR.

It is observed that dual fuel engine has lower BTE than the baseline data, especially at lower loading condition. This is due to slower combustion rate and poor utilization of the primary fuel inside the combustion chamber (Liu et al., 2013; Kumar and Kumar, 2016a). Also, the specific heat of CNG is higher than pure air and diesel vapor which play the main role in reducing combustion temperature and consequently slowing the combustion process (Tira, 2013). The trends are improved at intermediate and high loading condition. It is observed that ignition delay is decreased at high loads in dual fuel engine mode, which endorses faster combustion. Hence, at higher load, the BTE of dual fuel engine is higher than the baseline data

for all combination of fuels. The maximum BTE of 30.65% is obtained by CNG + diesel dual fuel engine mode, which is 2.07% higher than the baseline data having maximum BTE of 28.58%, at full load.

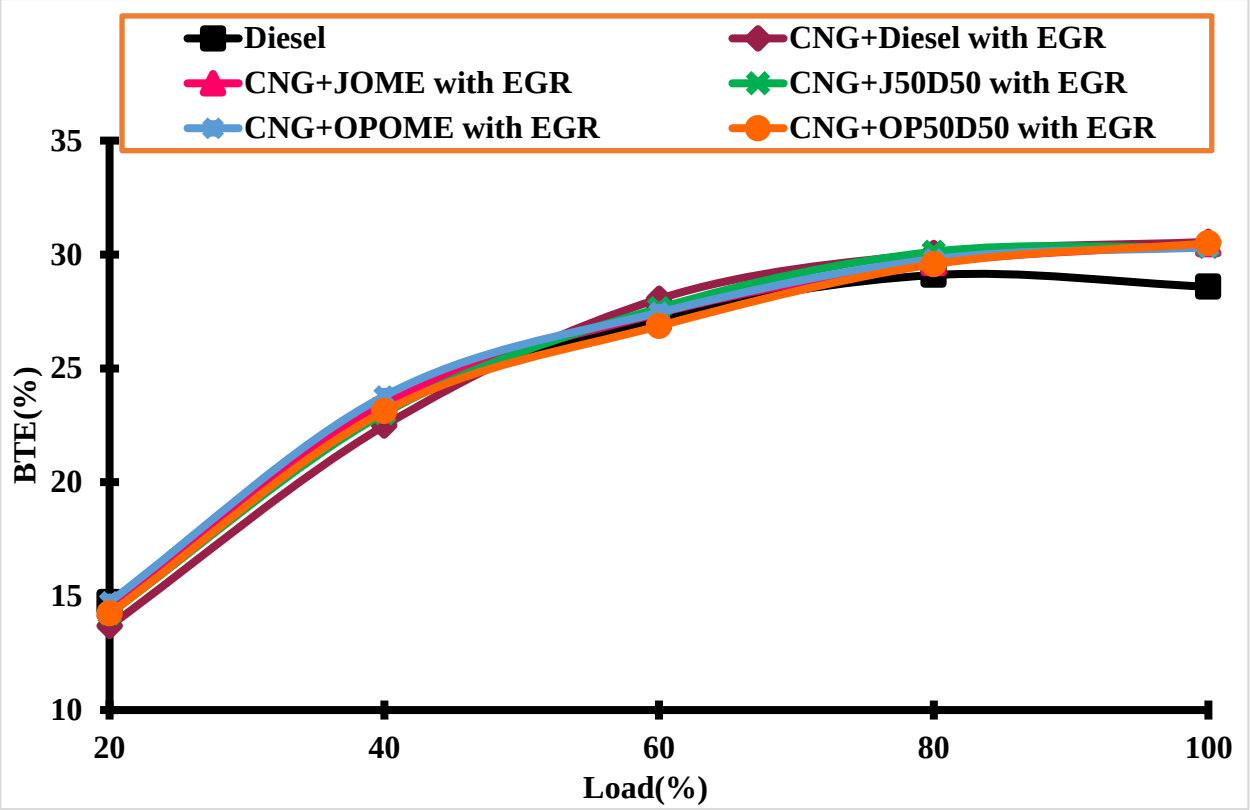

Figure 4.63: Variation in BTE of dual fuel engine with the application of EGR.

It is well known that most of the biodiesel has higher cetane number than petroleum diesel fuel, which causes shorter ignition delay and lower autoignition temperature (Padhi, 2010; Chauhan et al., 2010). The ignition delay and autoignition temperature play an important role at lower loading conditions where the in-cylinder pressure and temperature are slightly lower. Hence, using biodiesel as pilot fuel in dual fuel engine improves the BTE at lower loading condition compared to diesel as pilot fuel. However, it is still less than that of the baseline data. As load increases, the in-cylinder pressure and temperature increases, which results in shorter

ignition delay of pilot fuel and move the primary fuel towards complete combustion. Hence, at higher load, the calorific value of both fuels predominates over cetane number and autoignition temperature. In the present research, the CNG is selected as the primary fuel for different pilot fuels out of which diesel has the highest calorific value. This results in highest BTE of CNG+diesel dual fuel mode. However, the amount of pilot fuel used varied between 10% and 15%, that why the difference between BTE of all other dual fuel combination modes are not significant. The highest BTE achieved by CNG+diesel, CNG+JOME, CNG+J50D50, CNG+OPOME and CNG+OP50D50 dual fuel modes are 30.65%, 30.35%, 30.51%, 30.43% and 30.58% respectively. It is clearly seen from the results that, the blending of biodiesel with diesel improves the BTE of dual fuel engine, however, the changes are not significant.

The effect of the application of exhaust gas recirculation (EGR) on the BTE of dual fuel engine is also analyzed. The application of EGR improves the combustion characteristics of the engine and results in improved efficiency. By re-circulating exhaust gas into the combustion chamber, active radicals in the exhaust gas enhance the pre-flame activities and the exhaust gasses are re-burnt (Kumar and Kumar, 2016b). The leaner fuel-air mixture is available in the combustion chamber up to intermediate load, hence the application of EGR is predominating up to this loading condition. It is observed that the application of EGR enhances the BTE of dual fuel engine up to intermediate loading condition. As mixture moves toward the richer side, the application of EGR shows an adverse effect on engine performance. It is noticed that use of EGR at higher load decrease the BTE of the engine. However, decreasing rate is higher for diesel, J50D50 and OP50D50 compared to JOME and OPOME as a pilot fuel. The highest BTE achieved by CNG+diesel, CNG+JOME, CNG+J50D50, CNG+OPOME and CNG+OP50D50 dual fuel modes using EGR are 30.45%, 30.3%, 30.35%, 30.37% and 30.44% respectively.

The variation of BTE with load for dual fuel engine using JOME as pilot fuel without and with the application of EGR is shown in Figure 4.64 and the variation of BTE with load for dual fuel engine using OPOME as pilot fuel without and with the application of EGR is shown in Figure 4.65. Figure 4.66 shows the percentage change in BTE of all duel fuel operating modes with respect to the baseline data. Figure 4.67 shows the highest BTE of all operating modes.

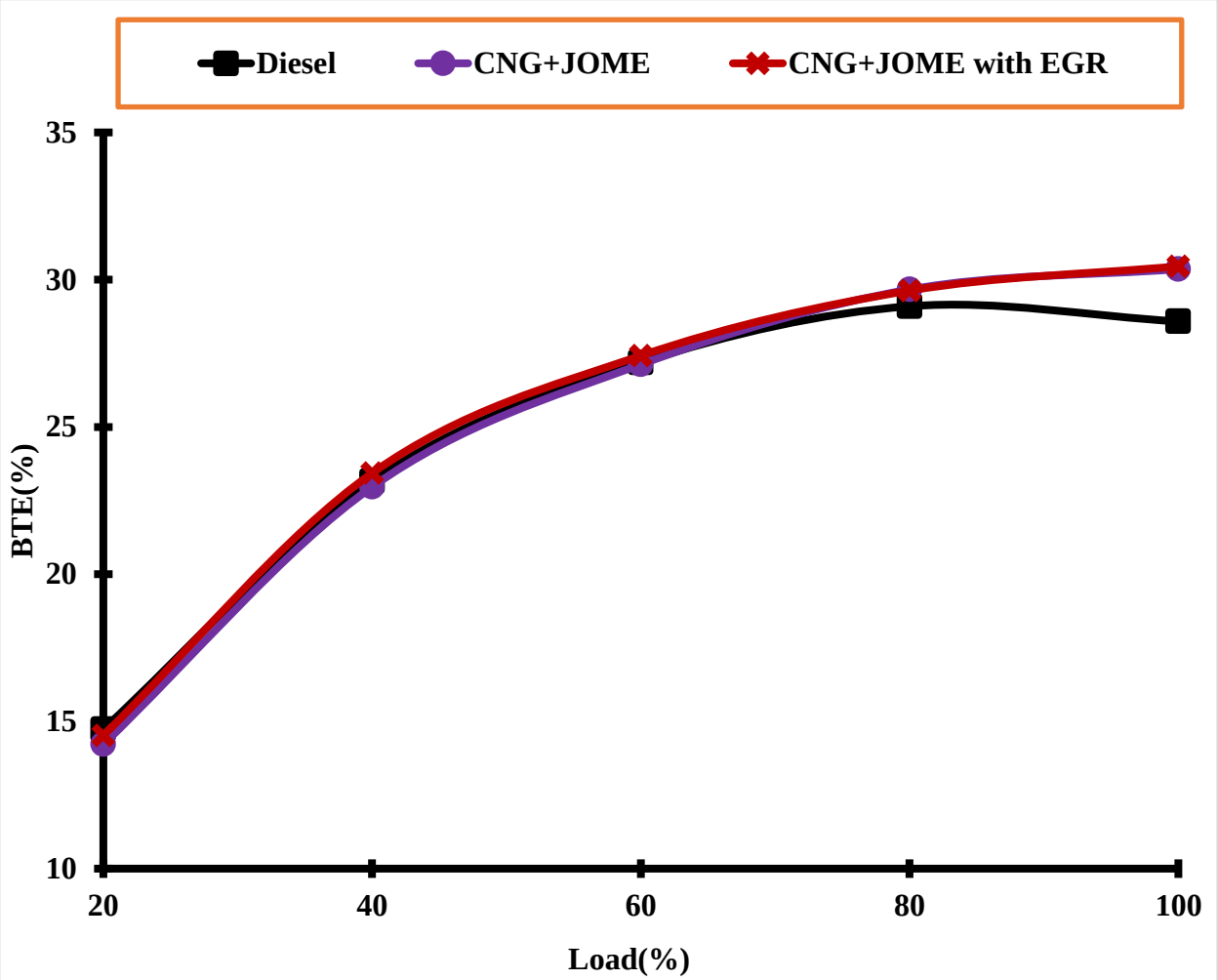

Figure 4.64: Variation in BTE for JOME as pilot fuel without and with the application of EGR.

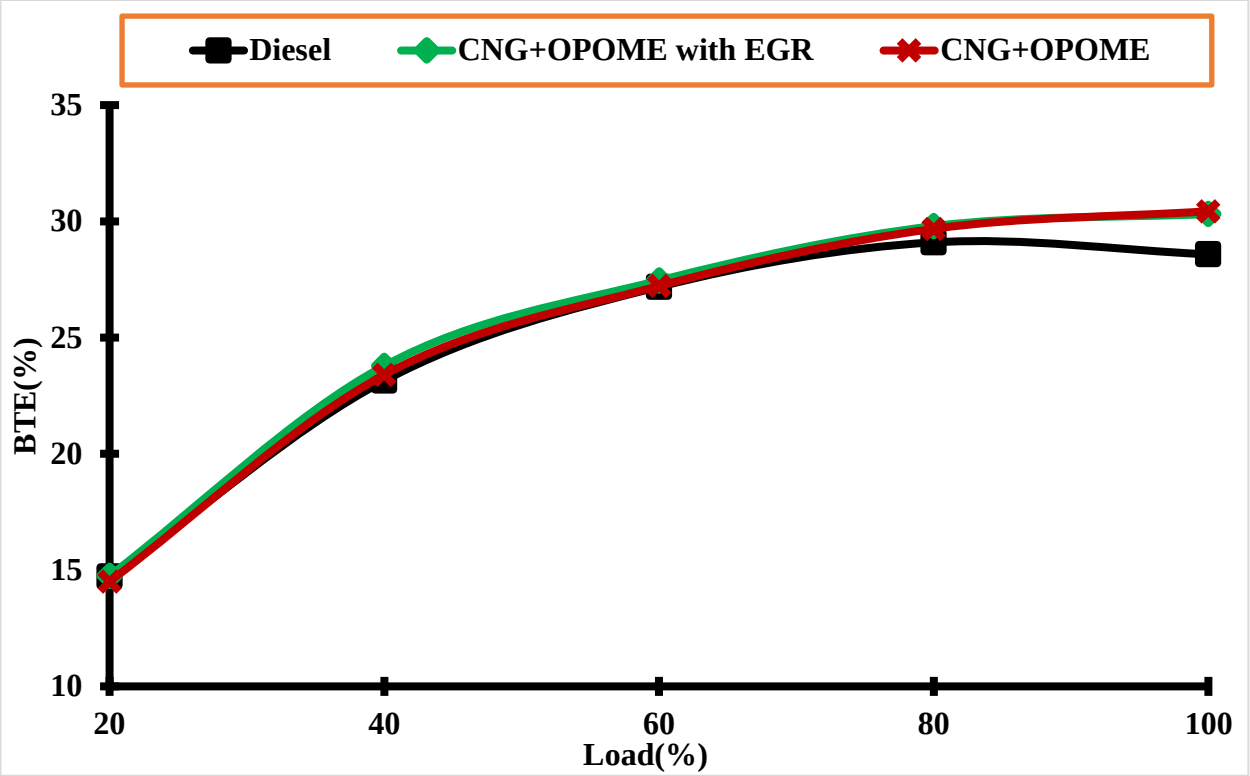

Figure 4.65: Variation in BTE for OPOME as pilot fuel without and with the application of EGR.

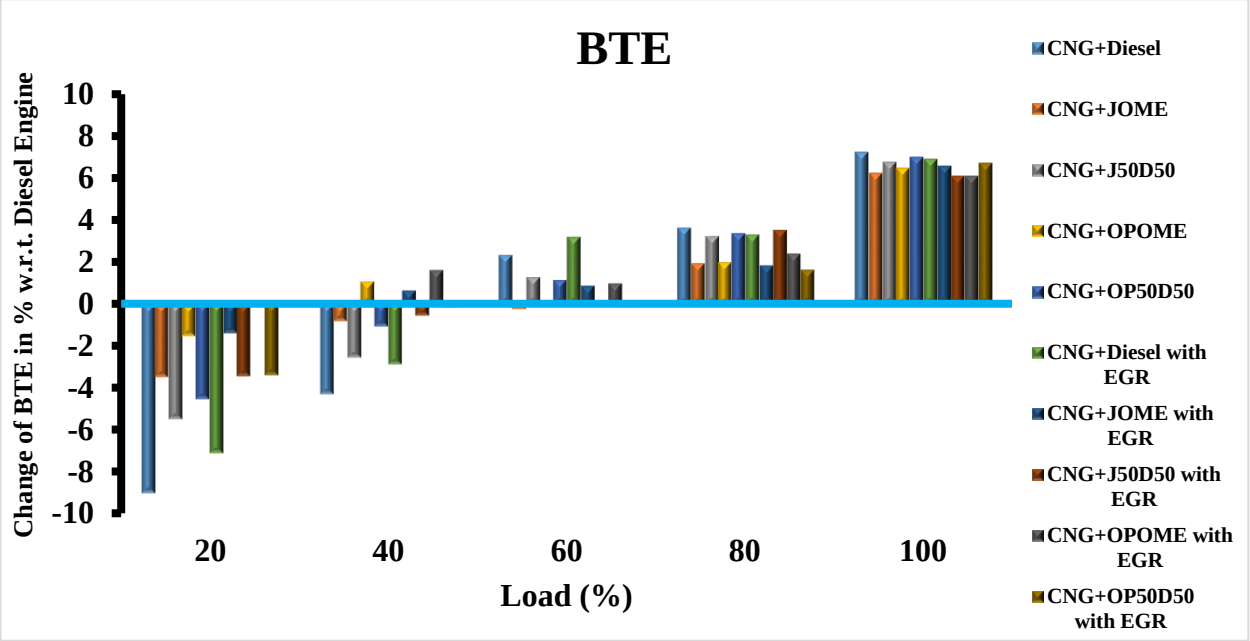

Figure 4.66: Percentage change in BTE of dual fuel engine from baseline data at various loads

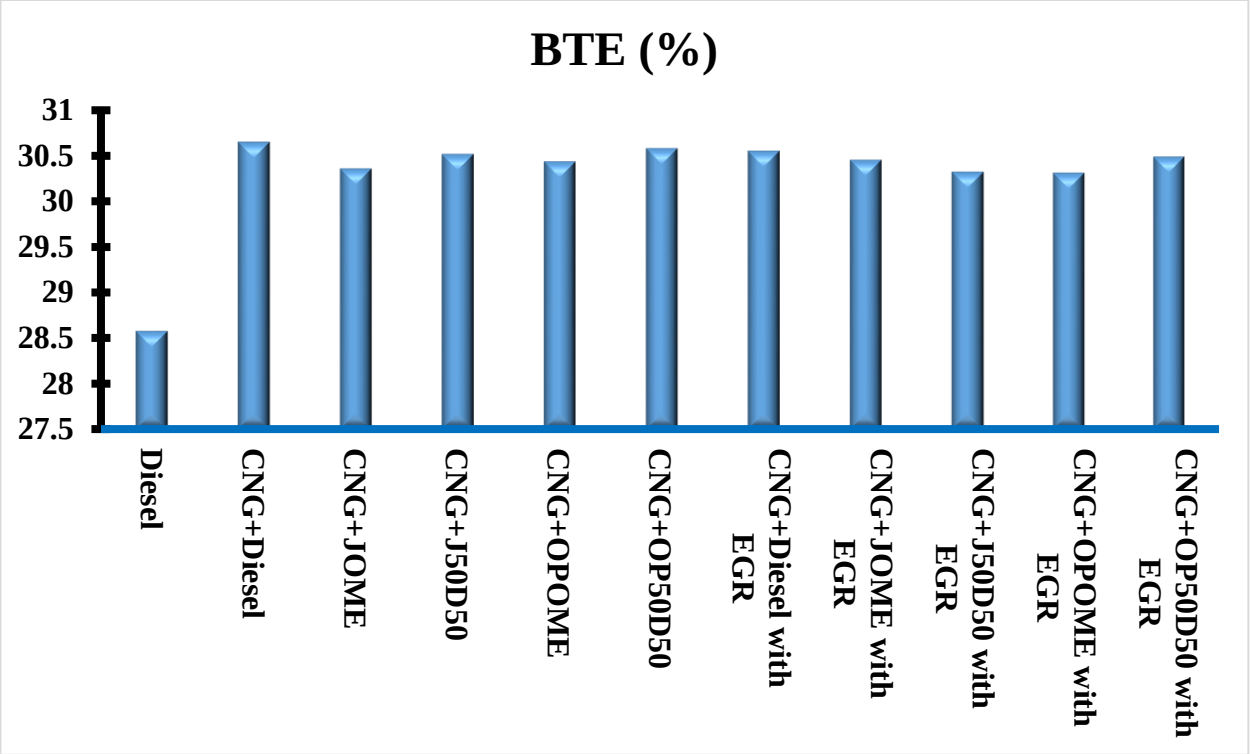

Figure 4.67: Highest BTE of all operating modes

4.6.2 Brake specific energy consumption

The brake specific energy consumption (BSEC) and BTE are mutually inversely proportional to each other. The BSEC of the engine is not directly measured but it is calculated with the help of brake specific fuel consumption (Kumar and Kumar, 2016a; Balasubramanian et al., 1995). The different fuel has different calorific value and different density so need to be compared on the same platform. The importance of BSEC over BSFC is increased in dual fuel engine as it used gaseous and liquid fuel simultaneously. The procedure of measurement of BSEC is explained in detail in the preceding chapter. The BSEC is the ratio between total energy consumed by the engine to the mechanical work output on the shaft. The BSEC is the main parameter to understand the performance parameter of the engine. The variation of BSEC with

load for dual fuel engine without and with the application of EGR is shown in Figure 4.68 and Figure 4.69 respectively.

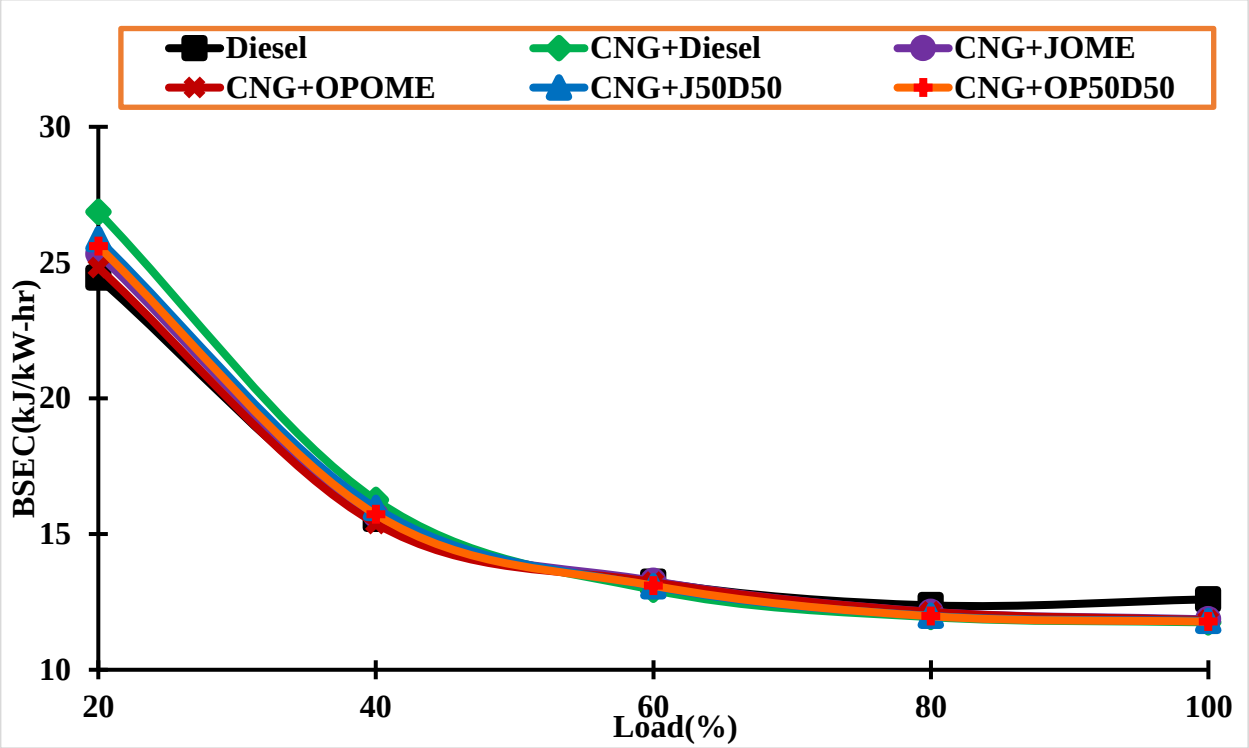

Figure 4.68: Variation in BSEC of dual fuel engine without the application of EGR.

It is observed that dual fuel engine has higher BSEC compared to the baseline data at low loading condition. This is due to low in-cylinder pressure and temperature which results in poor gaseous fuel combustion. As discoursed earlier, the main energy in dual fuel engine comes from gaseous fuel. The poor utilization of gaseous fuel at lower loading condition increase the BSEC of the dual fuel engine. However, with increasing load, the mixture turn to be richer which results in increase in-cylinder pressure and temperature. Hence, the gaseous fuel combustion improved which improves the BSEC of the dual fuel engine. Hence at higher loading condition, the BSEC of dual fuel engine is noticed lower compared to a baseline data. At full load, the

BSEC of the conventional diesel engine is 12.595 kJ/kW-hr, which is highest among all operating modes.

In dual fuel engine, the properties of pilot fuel play an important role for BSEC especially at lower loading condition where pilot fuel is predominating. It is noticed that CNG+diesel has shown highest BSEC among all dual fuel operating modes at lower loading condition. The OPOME has better physicochemical properties among all pilot fuel which make it a better pilot fuel. That's why, at low load, the CNG+OPOME dual fuel mode has the lowest BSEC among all dual fuel operating modes. As discoursed earlier, the increasing load improves the gaseous fuel combustion which makes gaseous fuel dominated over pilot fuel (Hountalas and Papagiannakis, 2000). Hence, at higher load, CNG+diesel dual fuel mode shows the lowest BSEC. This is due to high calorific value and low viscosity of petroleum diesel. The lowest BSEC measured for CNG+diesel, CNG+JOME, CNG+J50D50, CNG+OPOME and CNG+OP50D50 dual fuel modes are 11.75 kJ/kW-hr, 11.85 kJ/kW-hr, 11.79 kJ/kW-hr, 11.82 kJ/kW-hr and 11.77 kJ/kW-hr respectively. The use of biodiesel and diesel blend as pilot fuel improves the BSEC of dual fuel engine at higher load. However, the difference in BSEC of different dual fuel mode is insignificant.

The application of EGR in dual fuel engine improves the BSEC of the engine at lower loading condition. As discoursed earlier the application of EGR decreases the oxygen concentration inside the cylinder which improves the combustion of gaseous fuel (Alla et al., 2001; Ladommatos et al., 2000). The CNG+OPOME dual fuel mode shows the lowest BSEC here as well and CNG+diesel has the highest. As load increases the oxygen concentration decreases inside the combustion chamber and the use of EGR further decrease the oxygen

concentration which results in incomplete combustion of both primary as well as pilot fuels. Hence, at higher load, the application of EGR increases the BSEC of the dual fuel engine but it is still lower than that of a baseline data.

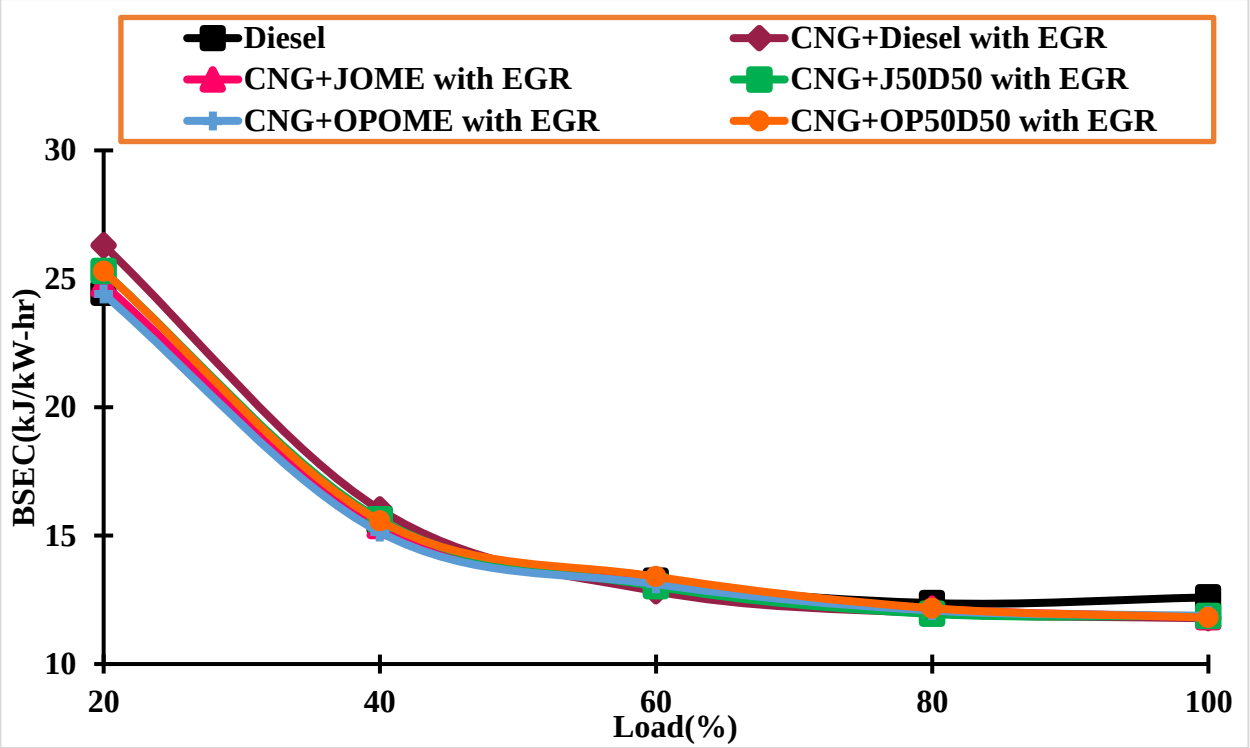

Figure 4.69: Variation in BSEC of dual fuel engine with the application of EGR.

The lowest BSEC of 11.78 kJ/kW-hr, 11.88 kJ/kW-hr, 11.87 kJ/kW-hr, 11.87 kJ/kW-hr and 11.83 kJ/kW-hr is observed for CNG+diesel, CNG+JOME, CNG+J50D50, CNG+OPOME and CNG+OP50D50 dual fuel modes respectively with the application of EGR at full load. The variation of BSEC with load for dual fuel engine using JOME as pilot fuel without and with the application of EGR is shown in Figure 4.70 and the variation of BSEC with load for dual fuel engine using OPOME as pilot fuel without and with the application of EGR is shown in Figure 4.71. Figure 4.72 shows the percentage change in BSEC of all duel fuel operating modes with respect to a baseline data. Figure 4.73 shows the highest BSEC of all operating modes.

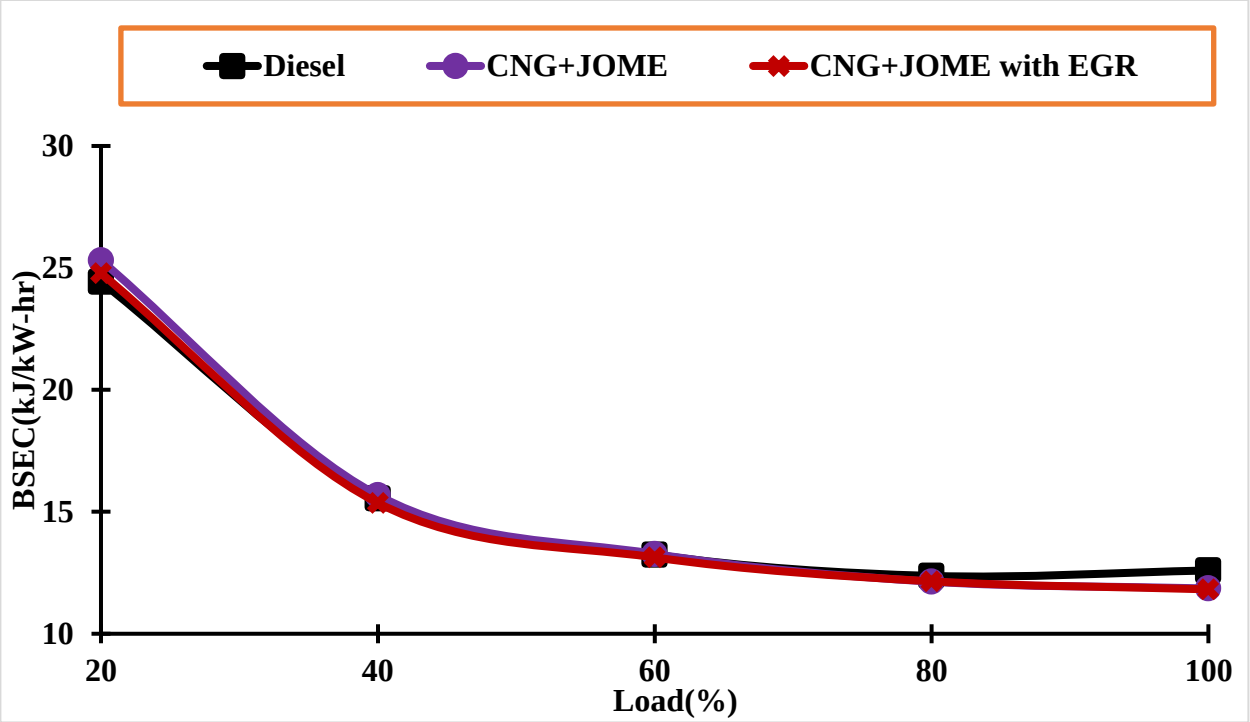

Figure 4.70: Variation in BSEC for JOME as pilot fuel without and with the application of EGR.

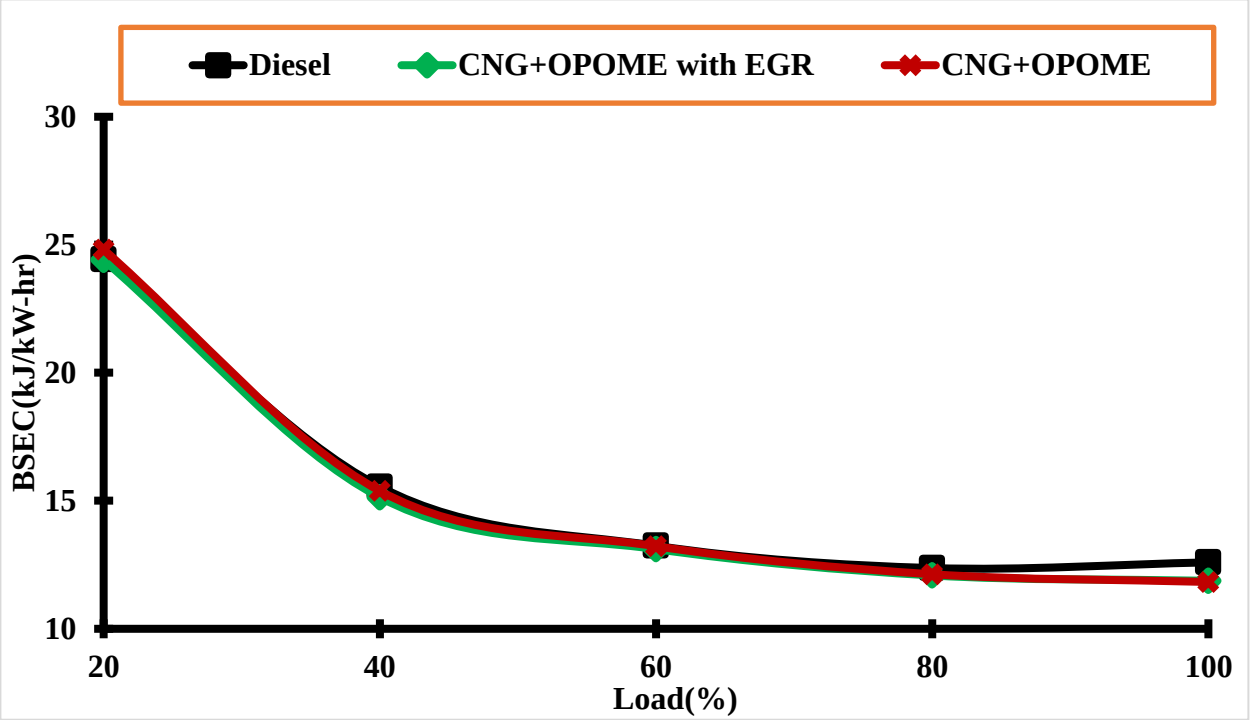

Figure 4.71: Variation in BSEC for OPOME as pilot fuel without and with the application of EGR.

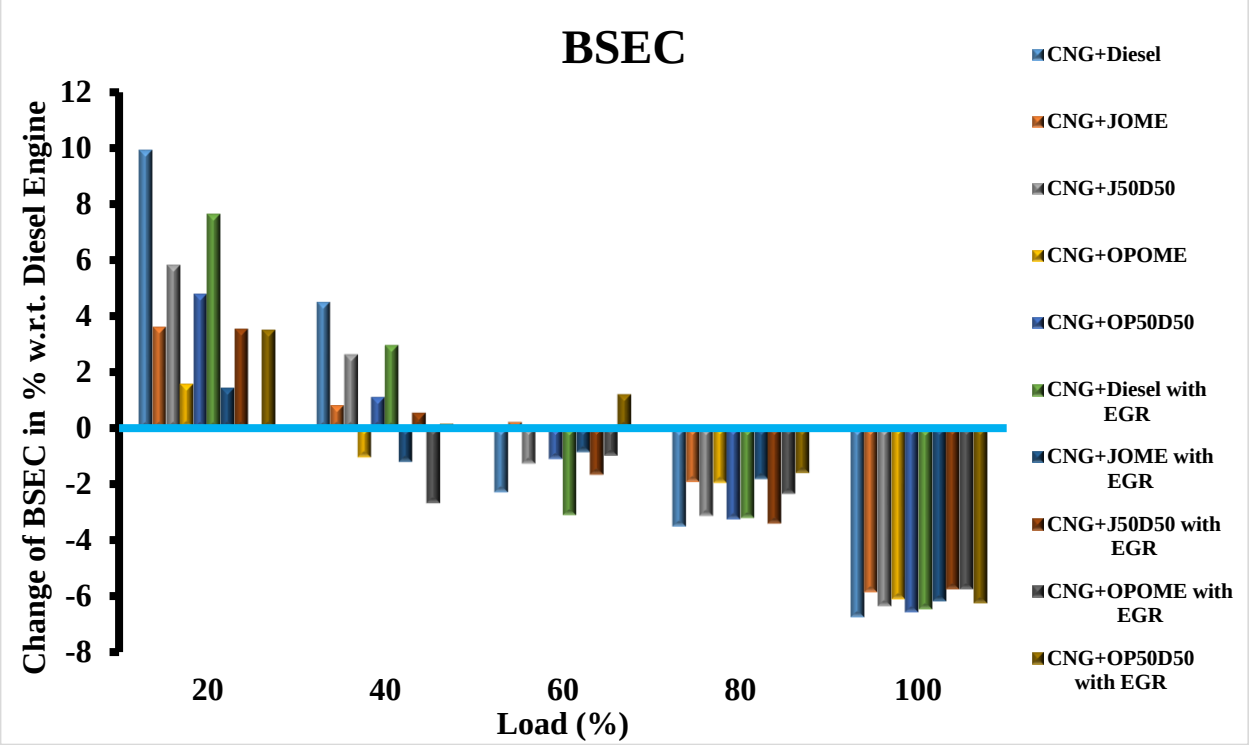

Figure 4.72: Percentage change in BSEC of dual fuel engine from baseline data at various loads

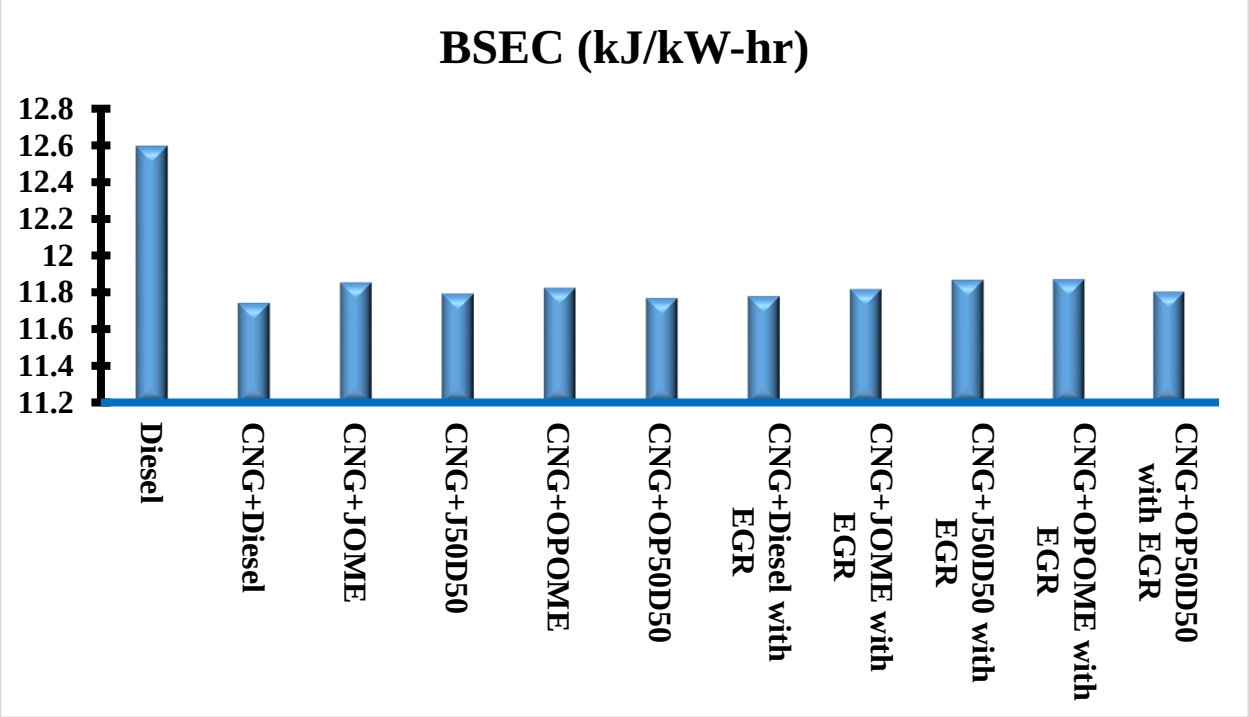

Figure 4.73: Highest BSEC of all operating modes

4.6.3 Exhaust gas temperature

The exhaust gas temperature (EGT) represents the type of combustion inside the combustion chamber. Longer ignition delay and uncontrolled combustion result in higher exhaust gas temperature. However, these two factors are not responsible for higher exhaust gas temperature of the engine (Tira, 2013). The higher compression ratio and higher calorific value also affect the exhaust gas temperature. The nature of burning in conventional diesel engine and dual fuel engine are different, so the exhaust gas temperature of this engine also different due to their nature. However, the important parameters which affect the exhaust gas temperature of dual fuel engine are combustion characteristics of the gaseous fuel.

The variation of exhaust gas temperature with load for dual fuel engine is shown in Figure 4.74. The exhaust gas temperature of the baseline data is notice higher compared to dual fuel engine at lower loading condition. This is due to poor gaseous fuel utilization in dual fuel engine at lower loading condition. However, improved gaseous fuel utilization with load increases the exhaust gas temperature of dual fuel engine at a faster rate. Hence at higher load, the exhaust gas temperature of dual fuel engine is found higher compared to a baseline data. The maximum exhaust gas temperature shown by a baseline data at full loading condition is 682°C which is lowest among all operating mode of dual fuel engine without application of EGR.

In dual fuel engine, due to incomplete combustion of diesel and CNG, CNG+diesel dual fuel mode shows lowest exhaust gas temperature at no load and 20% loading condition where CNG+OPOME dual fuel mode shows the highest. However, with increasing load, the rate of exhaust gas temperature for CNG+diesel dual fuel mode increases at a higher rate. Hence at higher load, the exhaust gas temperature of CNG + diesel engine has higher among all dual fuel

operating modes accept CNG+OP50D50 dual fuel mode. The maximum exhaust gas temperature of CNG + diesel, CNG + JOME, CNG + J50D50, CNG + OPOME and CNG + OP50D50 is found 704°C, 692°C, 698°C, 702°C, and 707°C respectively.

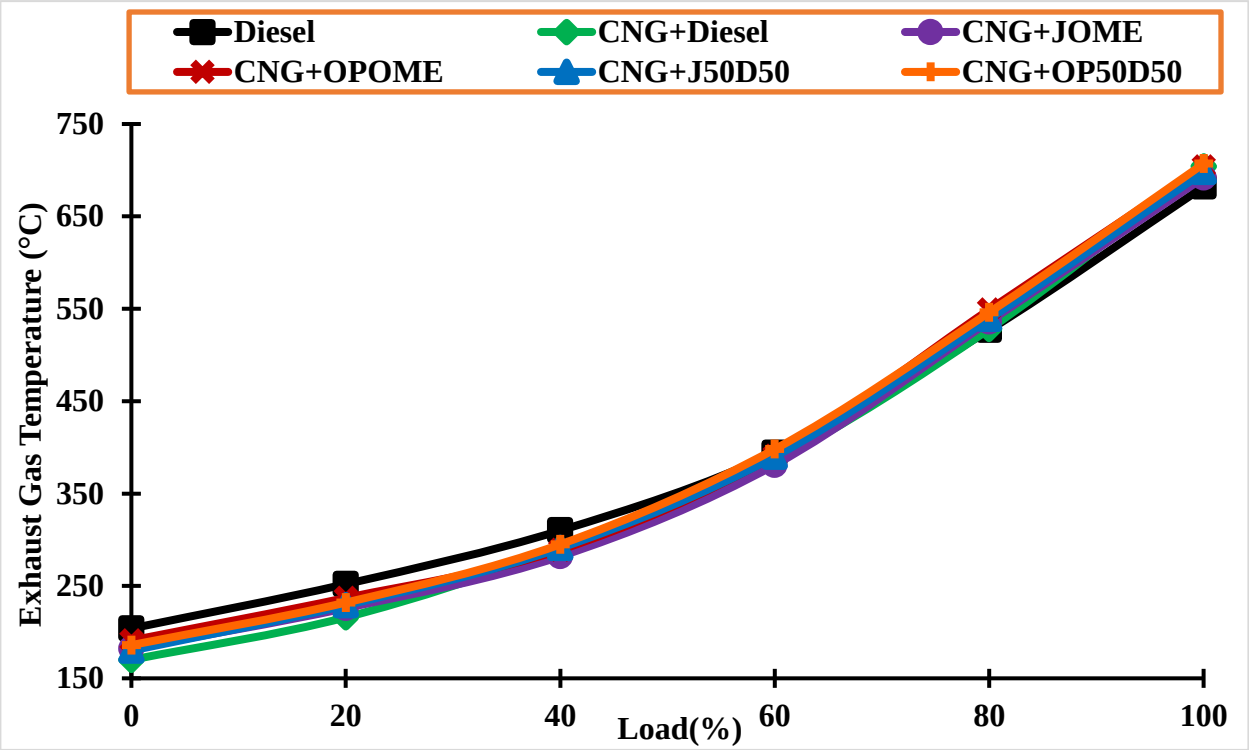

Figure 4.74: Variation in exhaust gas temperature of dual fuel engine without application of EGR.

The variation of exhaust gas temperature with load for dual fuel engine using EGR is shown in Figure 4.75. As discussed earlier, the application of EGR reduces the oxygen concentration inside the cylinder which increases the ignition delay of pilot fuel, however, the ignition delay of CNG is remained unaffected (Tomita et al., 2009). Which result in increasing exhaust gas temperature of dual fuel engine at low loading condition. At no load, the exhaust gas temperature of the baseline data is still found highest among all operating mode accept

CNG+OPOME dual fuel mode using EGR. At full load, the exhaust gas temperature of dual fuel mode using EGR is measured lower compared to a baseline data.

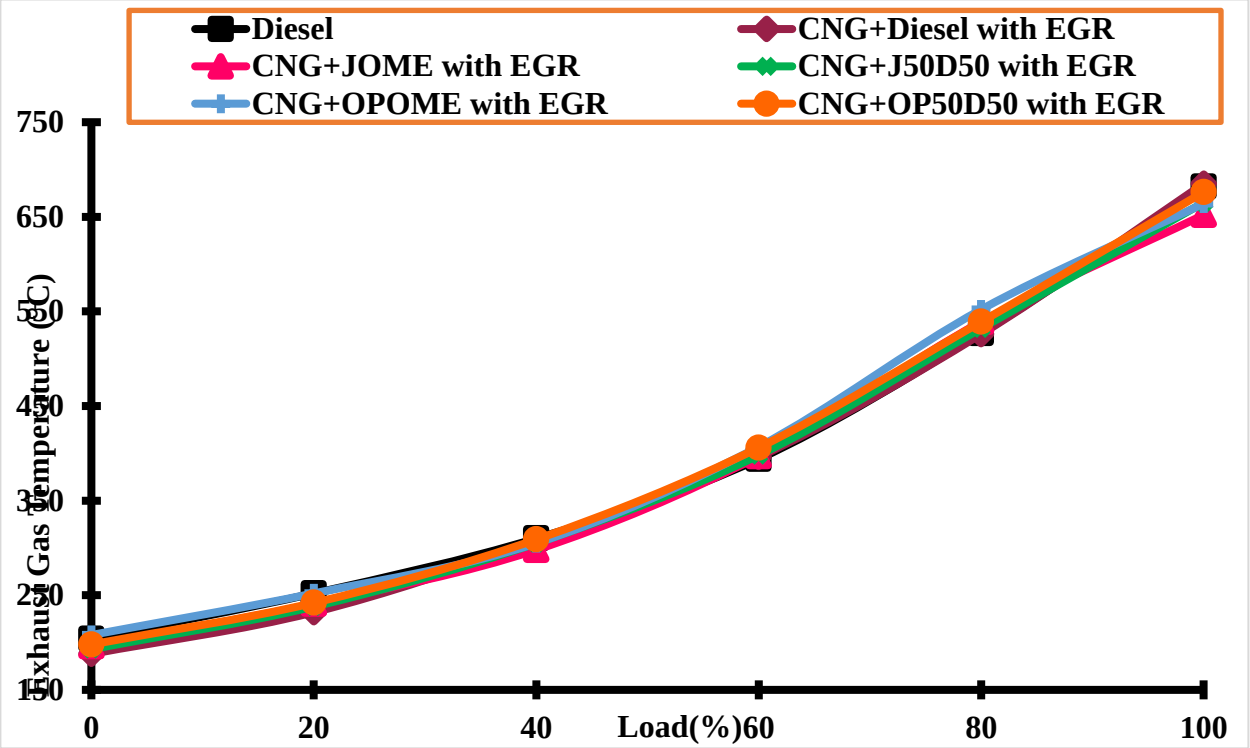

Figure 4.75: Variation in exhaust gas temperature of dual fuel engine using EGR.

The highest exhaust gas temperature of 685°C, 652°C, 665°C, 660°C and 676°C is observed for CNG + diesel, CNG + JOME, CNG + J50D50, CNG + OPOME and CNG + OP50D50 dual fuel modes respectively with the application of EGR at full load. The variation of exhaust gas temperature with load for dual fuel engine using JOME as pilot fuel without and with the application of EGR is shown in Figure 4.76 and the variation of exhaust gas temperature with load for dual fuel engine using OPOME as pilot fuel without and with the application of EGR is shown in Figure 4.77. Figure 4.78 shows the percentage change in exhaust gas temperature of all duel fuel operating modes with respect to a baseline data. Figure 4.79 shows the highest exhaust gas temperature of all operating modes.

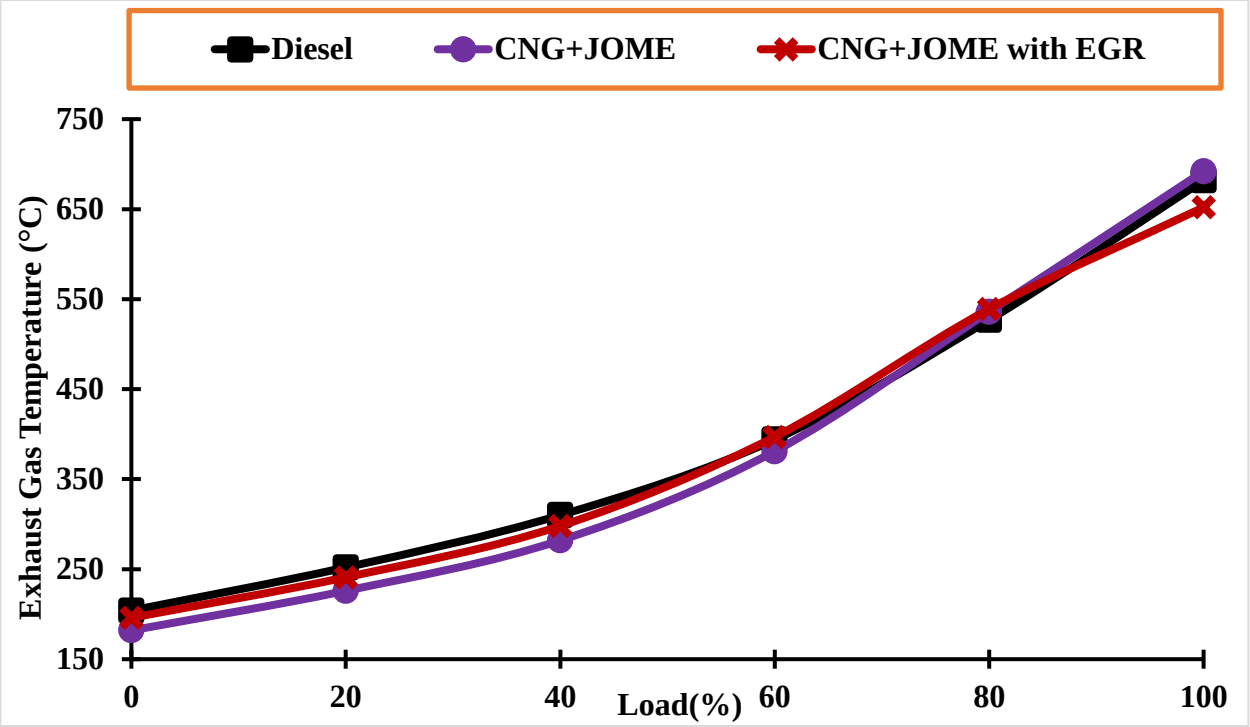

Figure 4.76: Variation in EGT for JOME as pilot fuel without and with the application of EGR.

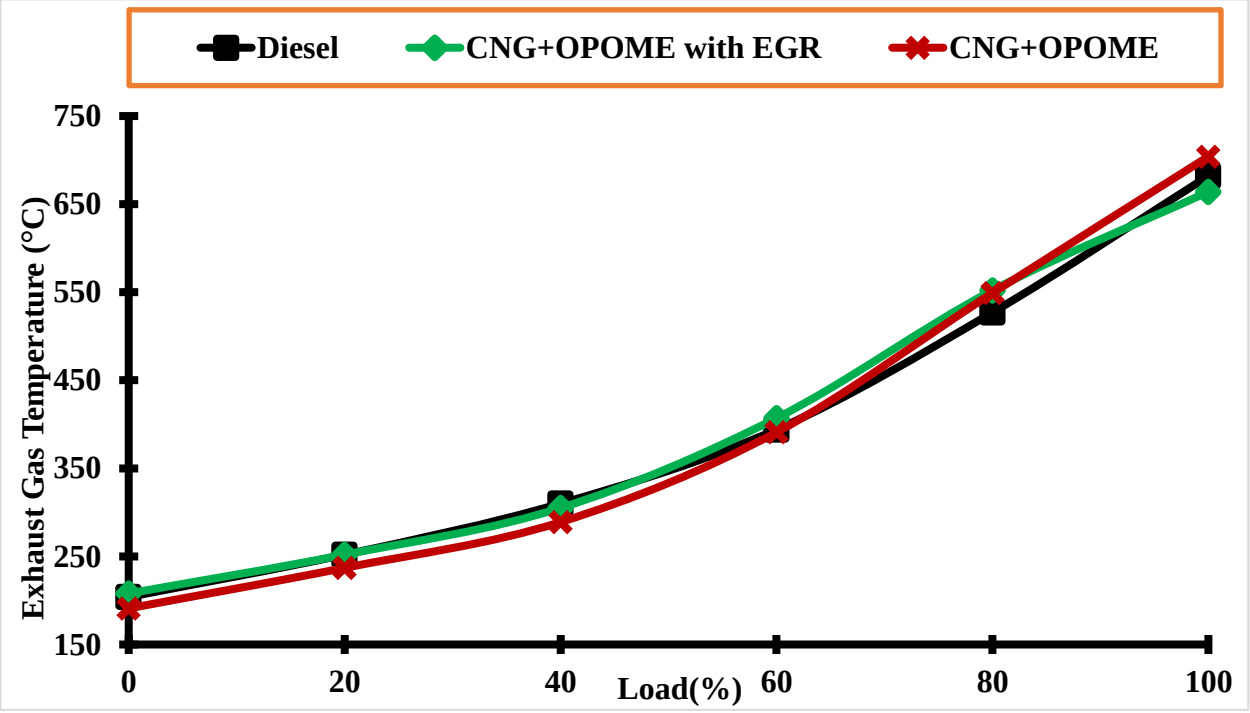

Figure 4.77: Variation in EGT for OPOME as pilot fuel without and with the application of EGR.

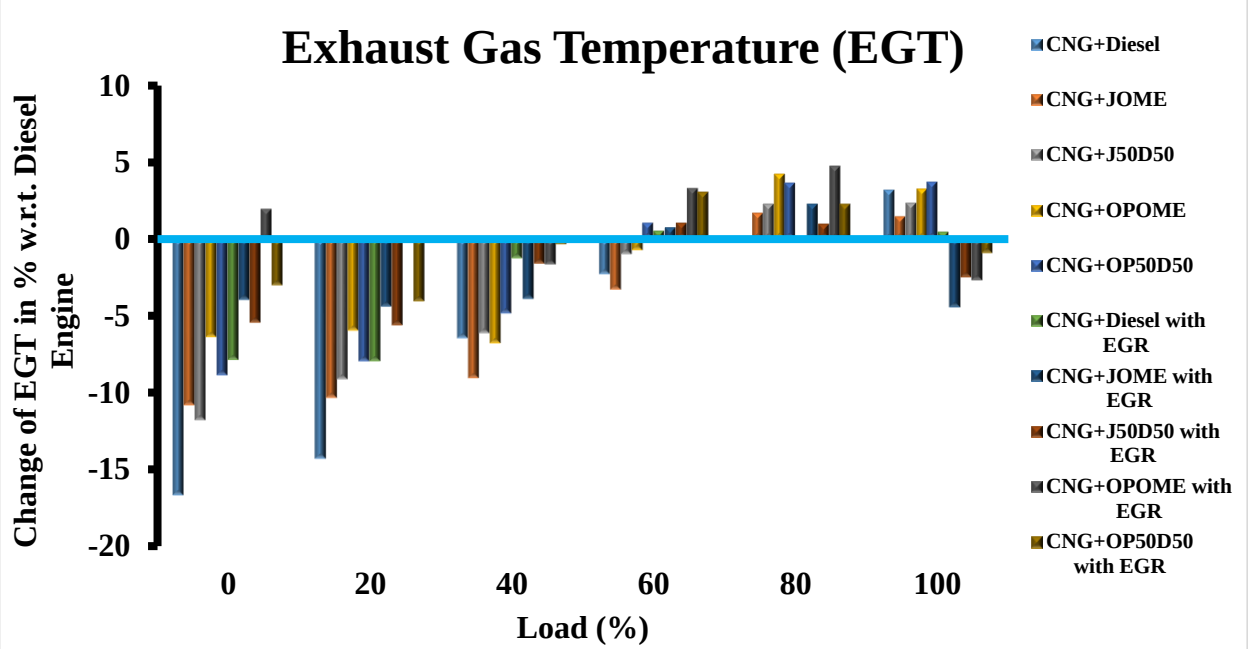

Figure 4.78: Percentage change in EGT of dual fuel engine from baseline data at various loads

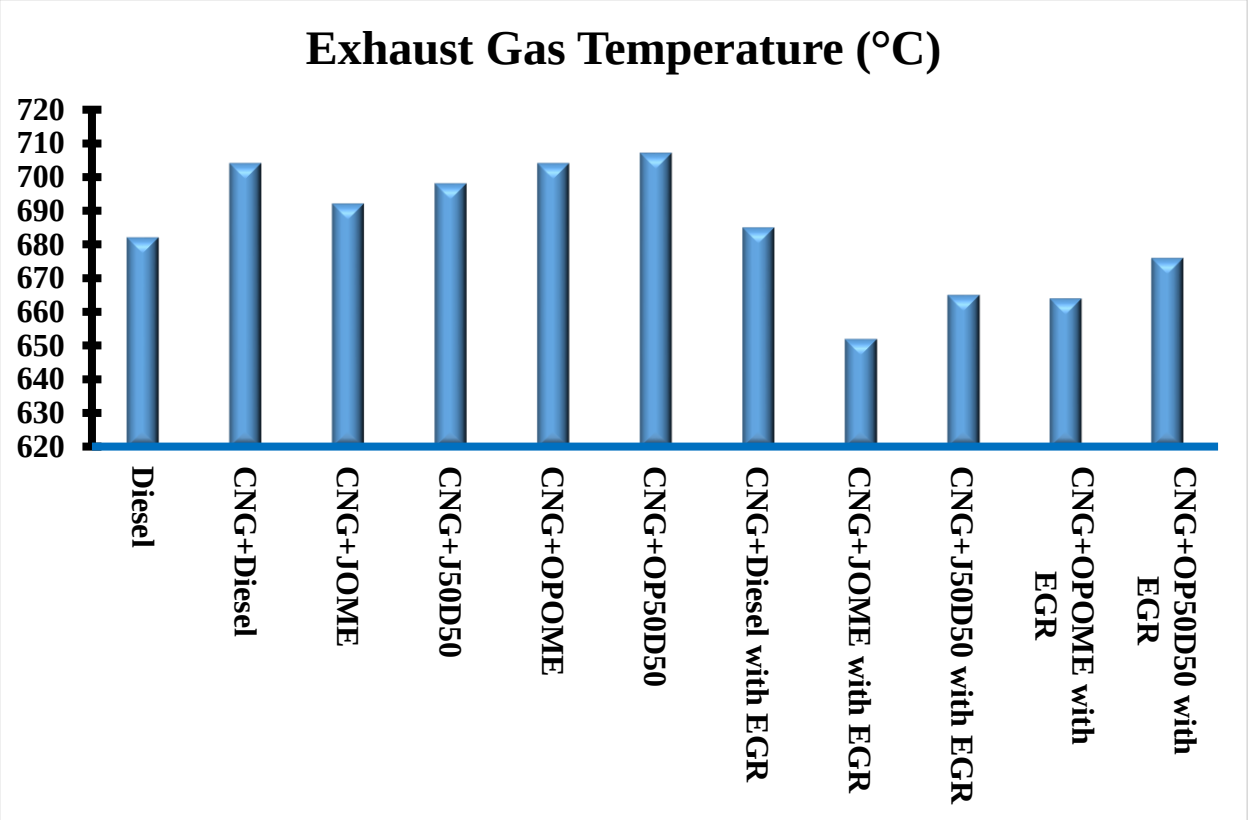

Figure 4.79: Peak EGT of all operating modes

4.7 Emissions Characteristics of Dual Fuel Engine

In this section emission characteristics of dual fuel engine (like; unburnt hydrocarbons, carbon monoxides, oxides of nitrogen, carbon dioxides, and smoke opacity) are measured and compared with the baseline data. The all fuel combination of dual fuel engine used in present work (i.e. CNG+diesel, CNG+JOME, CNG+J50D50, CNG+OPOME and CNG+OP50D50) without and with the application of EGR is explored in detail. The effect of the application of EGR to improve the emission characteristics of dual fuel engine for all loading condition is also analyzed.

4.7.1 Unburnt hydrocarbons

The level of unburnt hydrocarbons (UHC) shows the quantity of fuel which does not take part in combustion (Kumar and Kumar, 2016a). The main factors which affect the UHC emissions are; engine configuration, engine cylinder crevices, combustion temperature, fuel structure, residence time, oxygen availability etc. However, the mechanism of unburnt hydrocarbon formation inside the combustion chamber during combustion stroke is still at beginning and indefinable. The variation of unburnt hydrocarbons emissions with respect to load for dual fuel engine without application of EGR is shown in Figure 4.80.

It is observed that the unburnt hydrocarbon emissions of dual fuel engine has higher compared to the baseline data throughout the loading condition. The reason for that is poor gaseous fuel utilization in dual fuel engine (Krishnan et al., 2002). The UHC emissions in dual fuel engine increase in starting loading condition but reduced at higher load due to improved gaseous fuel combustion. However, at full load, the unburnt hydrocarbon emissions are reduced but it is still higher than a baseline data.

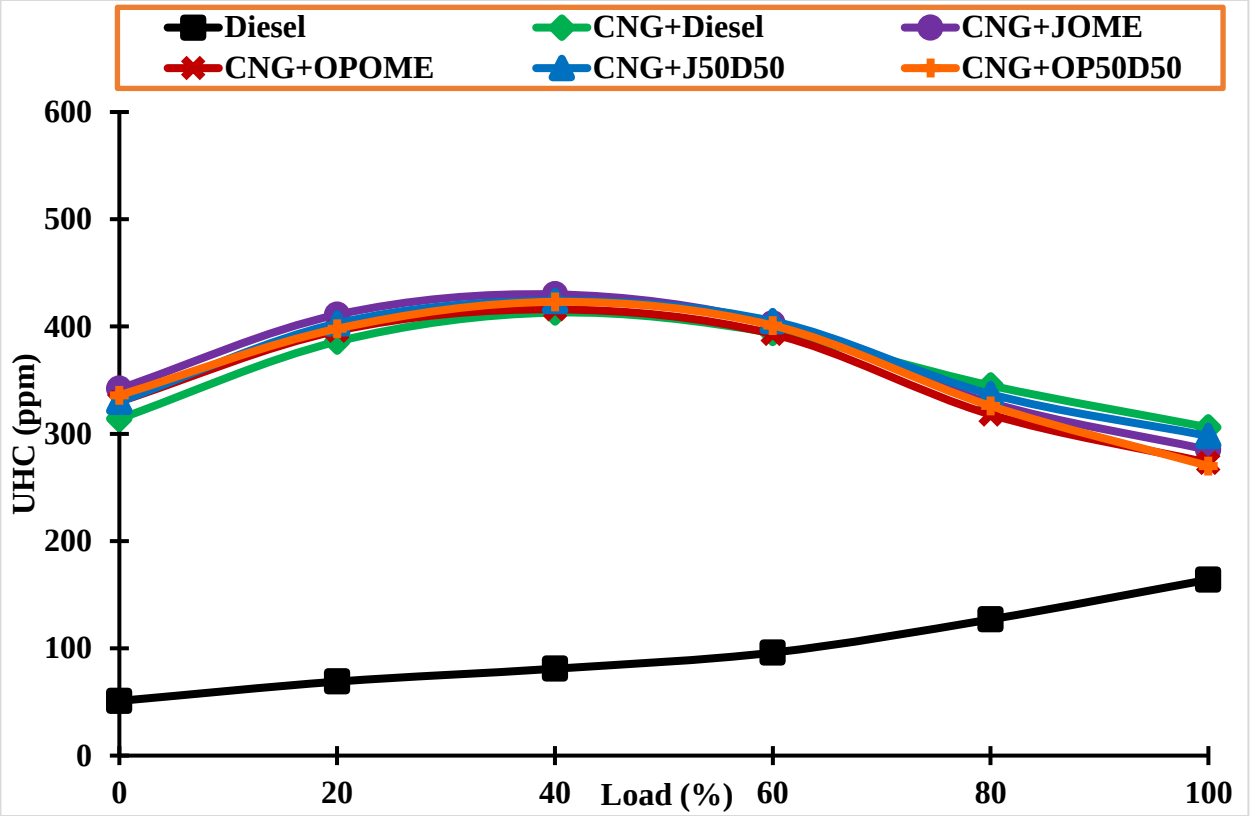

Figure 4.80: Variation in UHC emissions of dual fuel engine without application of EGR.

In dual fuel engine, CNG+diesel dual fuel mode emits lowest UHC emissions compared to other dual fuel modes at lower loading condition. However, at higher load, the UHC emissions of CNG+diesel dual fuel modes are notices higher compared to other dual fuel modes. The reason for that is oxygenation nature of other pilot fuel over petroleum diesel fuel, which increases the oxygen concentration inside the combustion chamber and results in lower UHC emissions. The CNG+OPOME dual fuel mode emits lowest UHC emissions among all dual fuel operating modes followed by CNG+OP50D50, CNG+JOME, CNG+J50D50 and CNG+diesel dual fuel mode at full loading condition. However, the difference is not significant because CNG dominates at higher load.

The application of EGR reduced the UHC emissions of dual fuel engine at lower load. This is because a portion of exhaust is reintroduced to the cylinder which reduces the oxygen availability in the combustion chamber, which enhances the gaseous fuel combustion at lower load (Srinivasan et al., 2007). Also, the UHC present in the recirculated exhaust gas gets a chance to re-burn in the followed cycle and results in a reduction of UHC emissions. The richer fuel-air mixture is supplied to the engine at higher load; the application of EGR further increases the fuel-air ratio of the mixture and become richer. The decrease oxygen concentration beyond a particular level reduced the combustion characteristics of the engine. Hence, at higher load, the application of EGR increases the UHC emissions of dual fuel engine. The variation of unburnt hydrocarbons emissions with respect to load for dual fuel engine using EGR is shown in Figure 4.81.

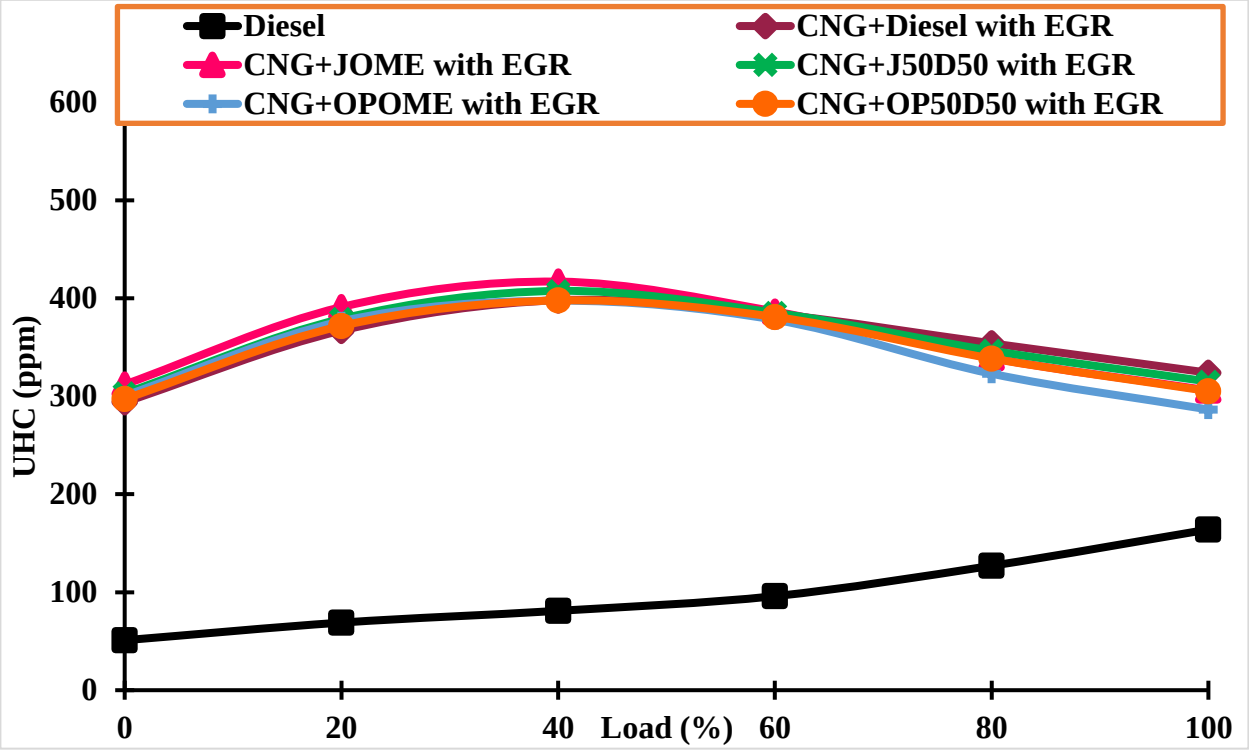

Figure 4.81: Variation in UHC emissions of dual fuel engine using EGR.

The variation of UHC emissions with load for dual fuel engine using JOME as pilot fuel without and with the application of EGR is shown in Figure 4.82 and the variation of UHC emissions with load for dual fuel engine using OPOME as pilot fuel without and with the application of EGR is shown in Figure 4.83. Figure 4.84 shows the percentage change in UHC emissions of all duel fuel operating modes with respect to a baseline data. Figure 4.85 shows the highest UHC emissions of all operating modes.

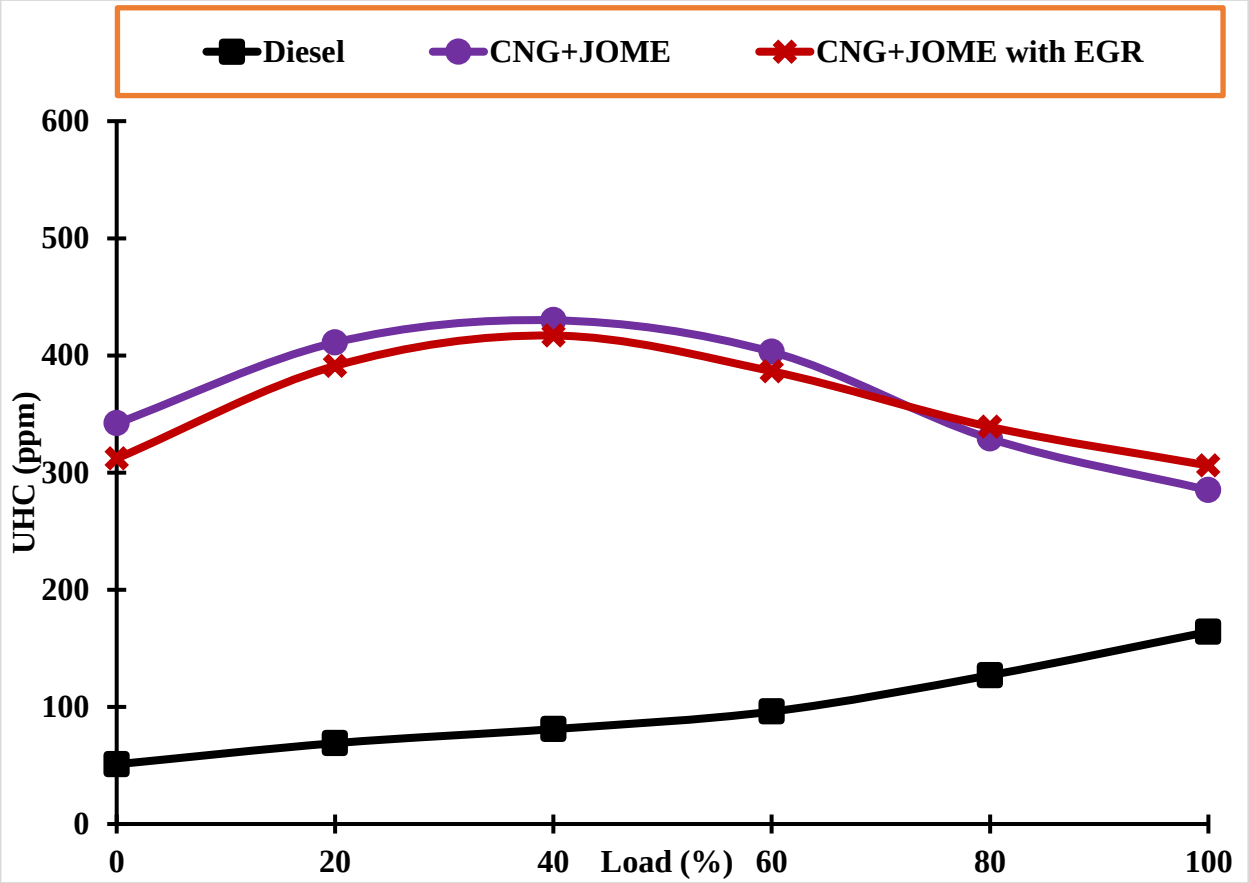

Figure 4.82: Variation in UHC emissions for JOME as pilot fuel without and with using EGR.

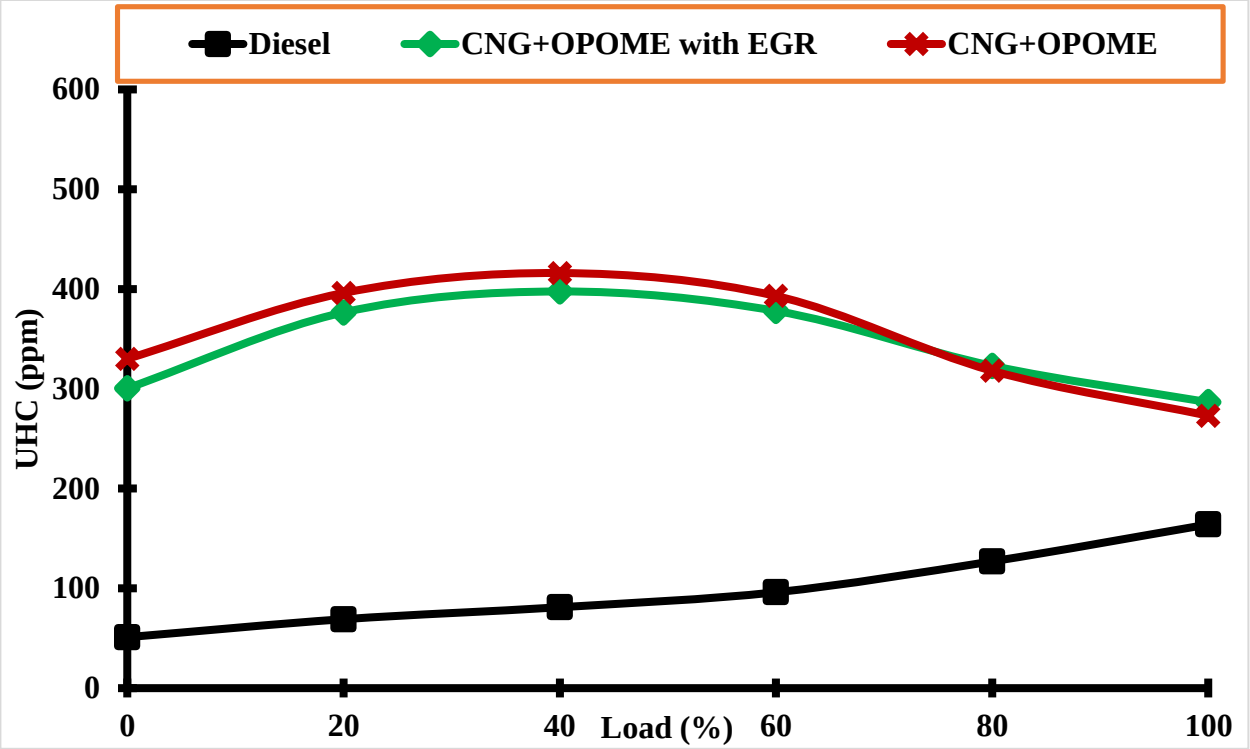

Figure 4.83: Variation in UHC emissions for OPOME as pilot fuel without and with using EGR.

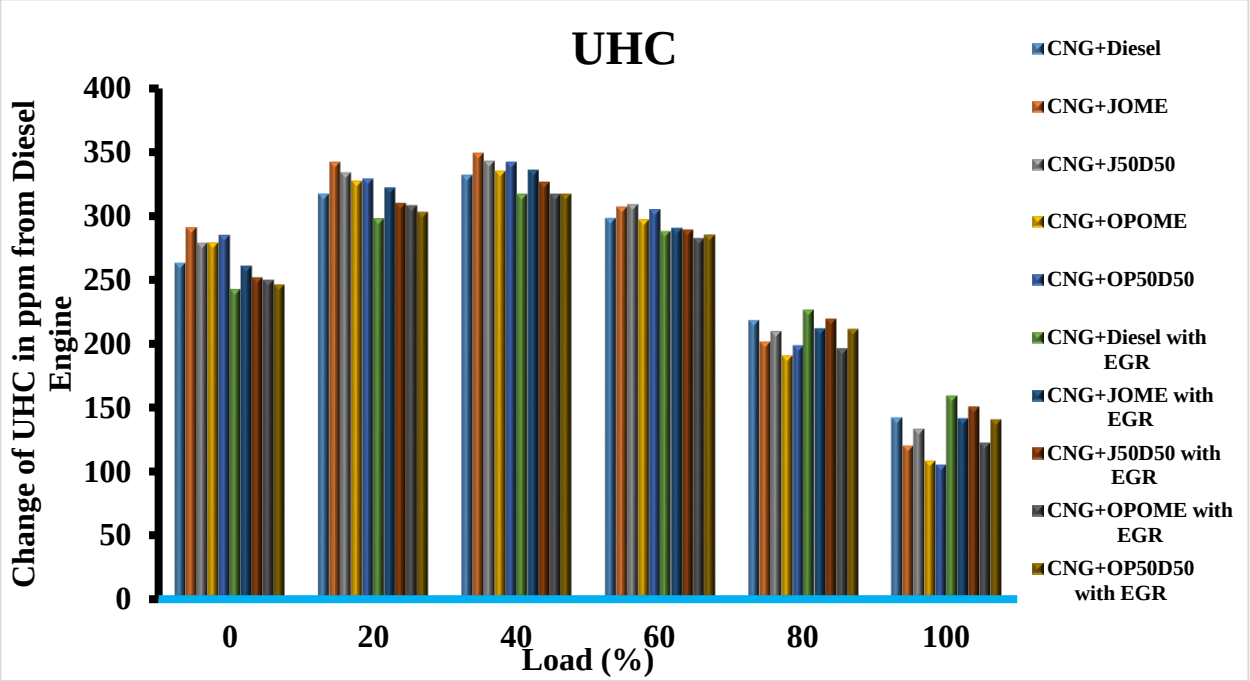

Figure 4.84: Variation in UHC emissions of Dual fuel engine from baseline data at various loads

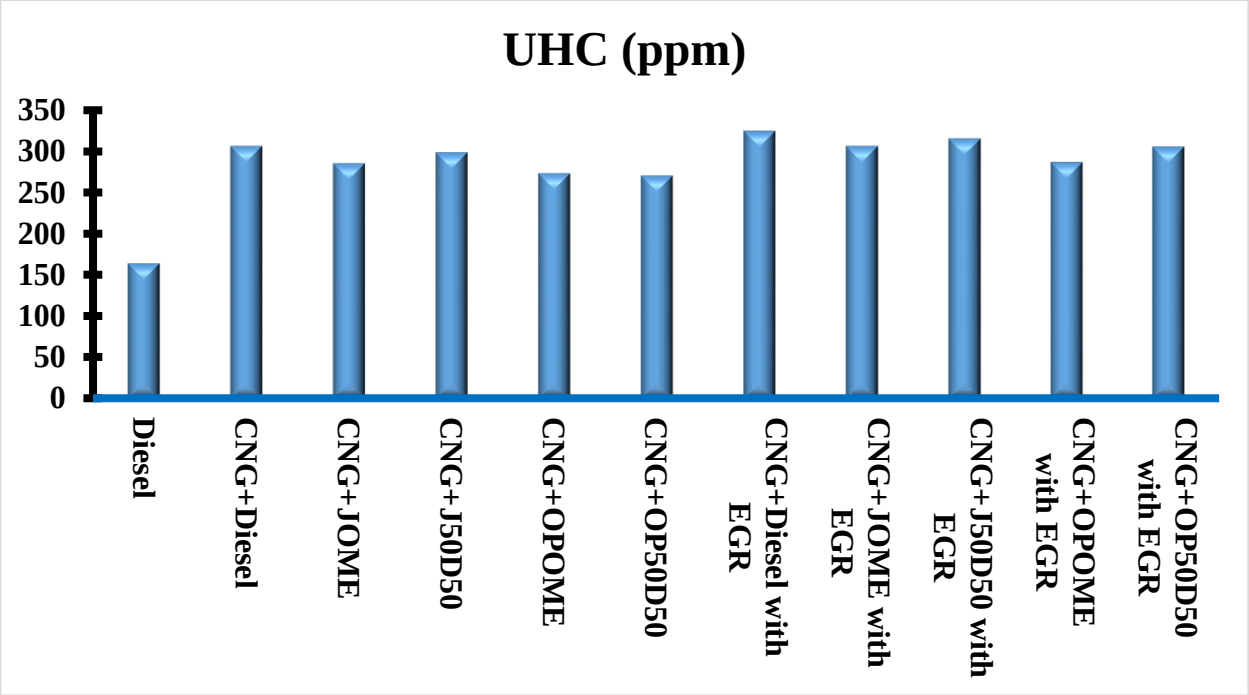

Figure 4.85: UHC emissions at full load of all operating modes

4.6.2 Carbon monoxides

The carbon monoxides (CO) in the exhaust of the engine shows the incomplete combustion of the fuel (Kumar and Kumar, 2016b). The formation of carbon monoxides is depended on the oxygen concentration inside the combustion chamber, that's why lower fuel air ratio results in higher CO emissions. However, the CO emissions are also depended on the start of injection timing, fuel injection pressure, atomization rate, combustion chamber design, engine load, speed, partially burned gaseous fuel and cylinder charge temperature. The CO is the major pollutant for internal combustion engine. However, the CO emissions problem is more complicated in CI engine as compared to SI engines.

The variation of carbon monoxides emissions with respect to load for dual fuel engine without application of EGR is shown in Figure 4.86. It is observed that the CO emission for dual

fuel engine has higher than the baseline data up to intermediate loading condition. This is due to poor gaseous fuel utilization at lower loading condition. At low loads, dual fuel engine is associated with slower combustion rates compared to a baseline data, which results in lower in-cylinder charge temperature and poor quality combustion. However, with improved gaseous fuel utilization and richer fuel-air mixture at higher load decrease the CO emission rate of dual fuel engine. Hence, at higher load, the CO emissions of dual fuel engine are much lower than a baseline data.

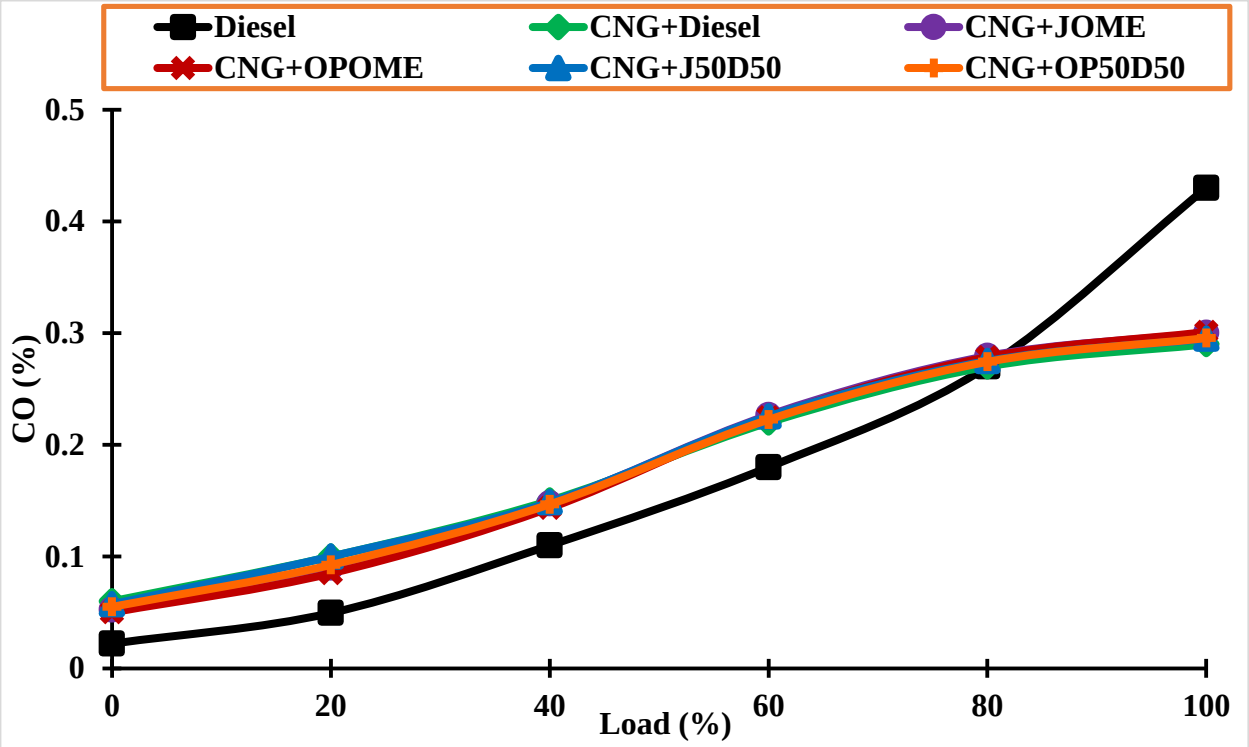

Figure 4.86: Variation in CO emissions of dual fuel engine without application of EGR.

In dual fuel engine, the gaseous fuel is more dominating over pilot fuel. Hence, the quality of pilot fuel shows the minor effect on CO emissions. However, its effect can be seen during measurement but it is not significant. The trend of CO emissions for dual fuel engine is

similar for all operating mode without application of EGR. However, at lower load, the incomplete combustion of diesel fuel in dual fuel engine result in higher CO emissions for CNG+diesel dual fuel mode compared to other dual fuel operating modes. However, at higher load, the lower calorific value of JOME, OPOME and their blend results in higher CO emissions compared to diesel as pilot fuel.

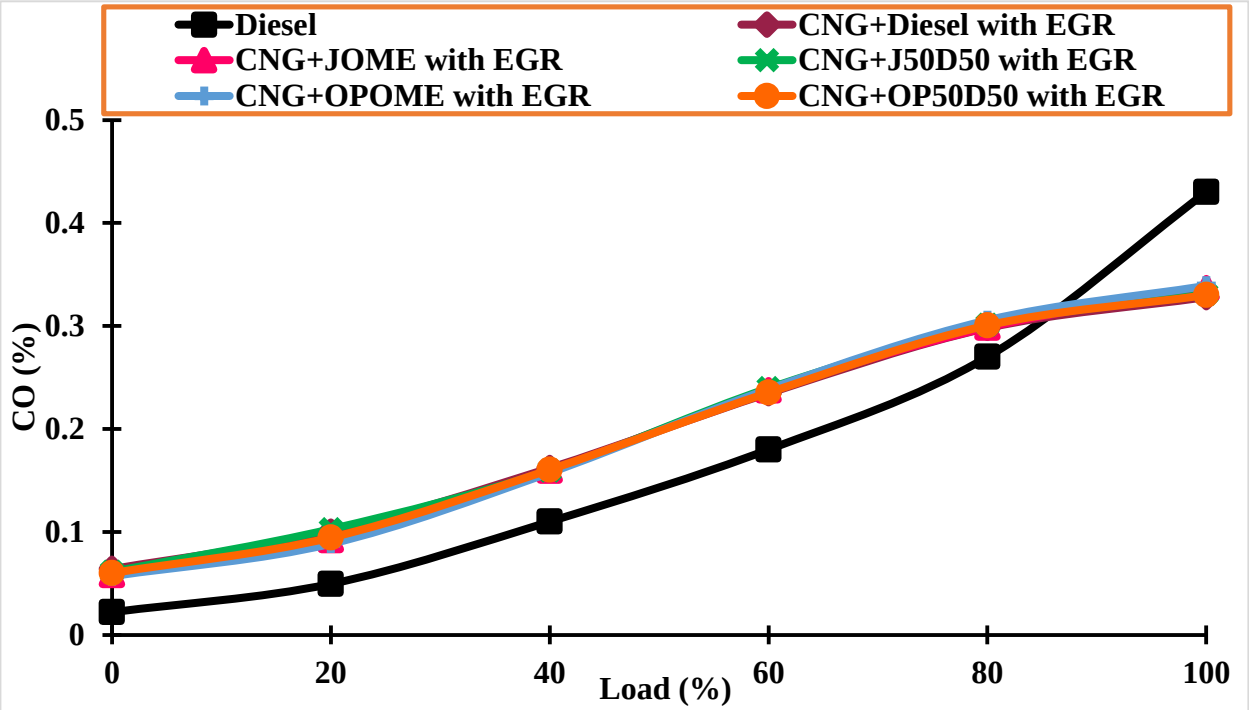

Figure 4.87: Variation in CO emissions of dual fuel engine with the application of EGR.

The application of EGR in dual fuel engine improves the CO emissions of the engine up to intermediate loading condition but still found higher than a baseline data. The variation of carbon monoxides emissions with respect to load for dual fuel engine with the application of EGR is shown in Figure 4.87. It is observed that the application of EGR decrease the CO emissions of dual fuel engine at lower load but increase the same at higher loading condition. The change can be seen from the data but it is very different to see the change in the Figure. At

full load, the CO emissions of dual fuel engine without and with the application of EGR are less than that of a baseline data.

The CO is not found the major air pollutant as compared to CO_2, NO_X, PM, SO_X, soot, smoke etc. The variation of CO emissions with load for dual fuel engine using JOME as pilot fuel without and with the application of EGR is shown in Figure 4.88 and the variation of CO emissions with load for dual fuel engine using OPOME as pilot fuel without and with the application of EGR is shown in Figure 4.89. Figure 4.90 represent the percentage change in CO emissions of all duel fuel operating modes with respect to a baseline data. Figure 4.91 shows the highest CO emissions of all operating modes.

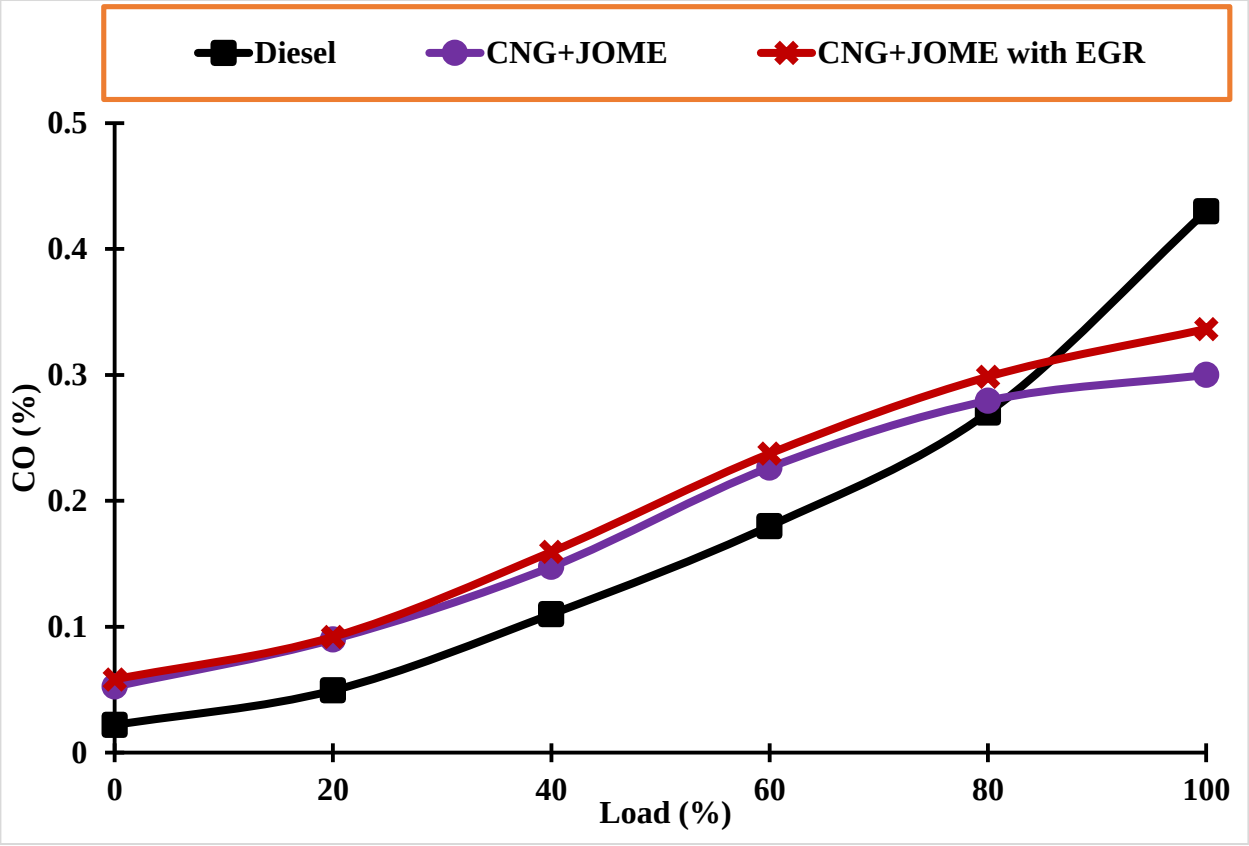

Figure 4.88: Variation in CO emissions for JOME as pilot fuel without and with using EGR.

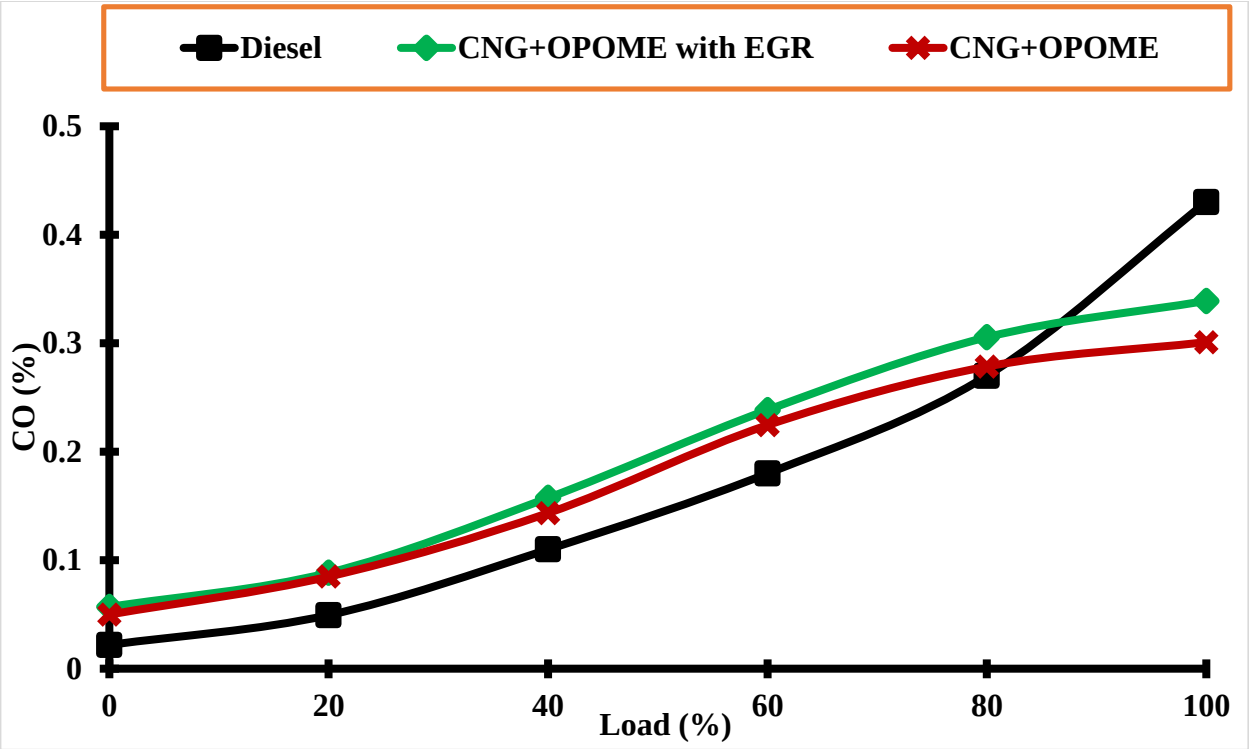

Figure 4.89: Variation in CO emissions for OPOME as pilot fuel without and with using EGR.

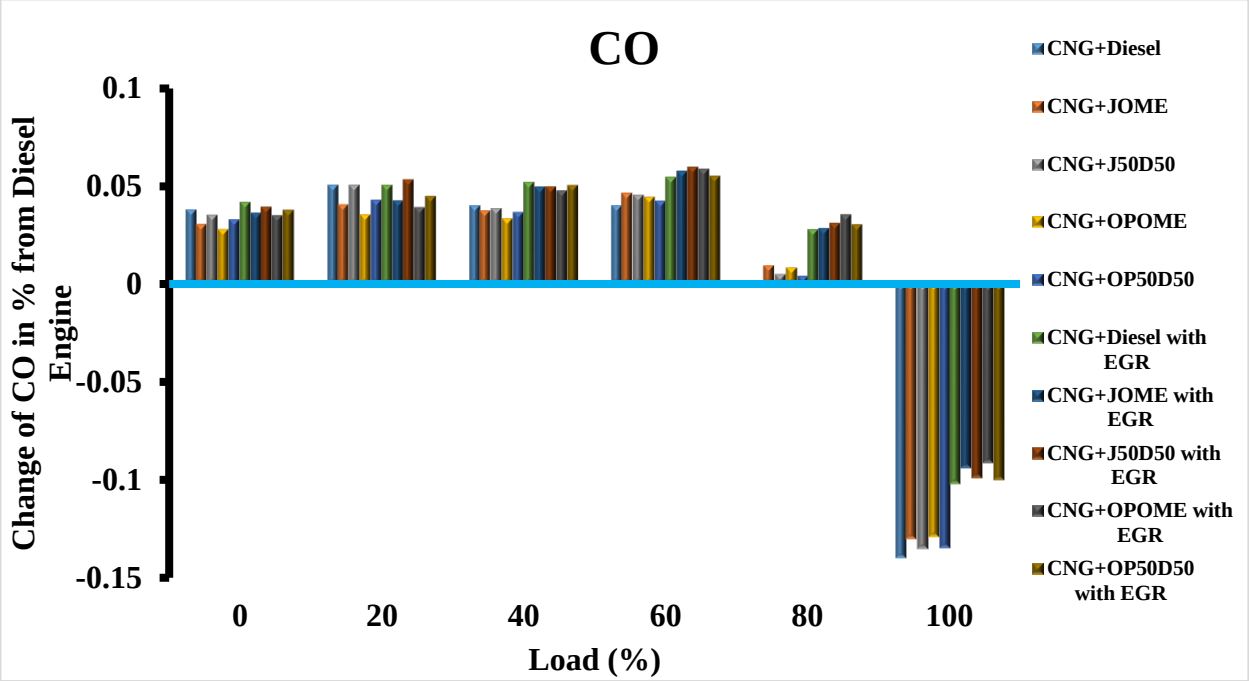

Figure 4.90: Variation in CO emissions of Dual fuel engine from baseline data at various loads

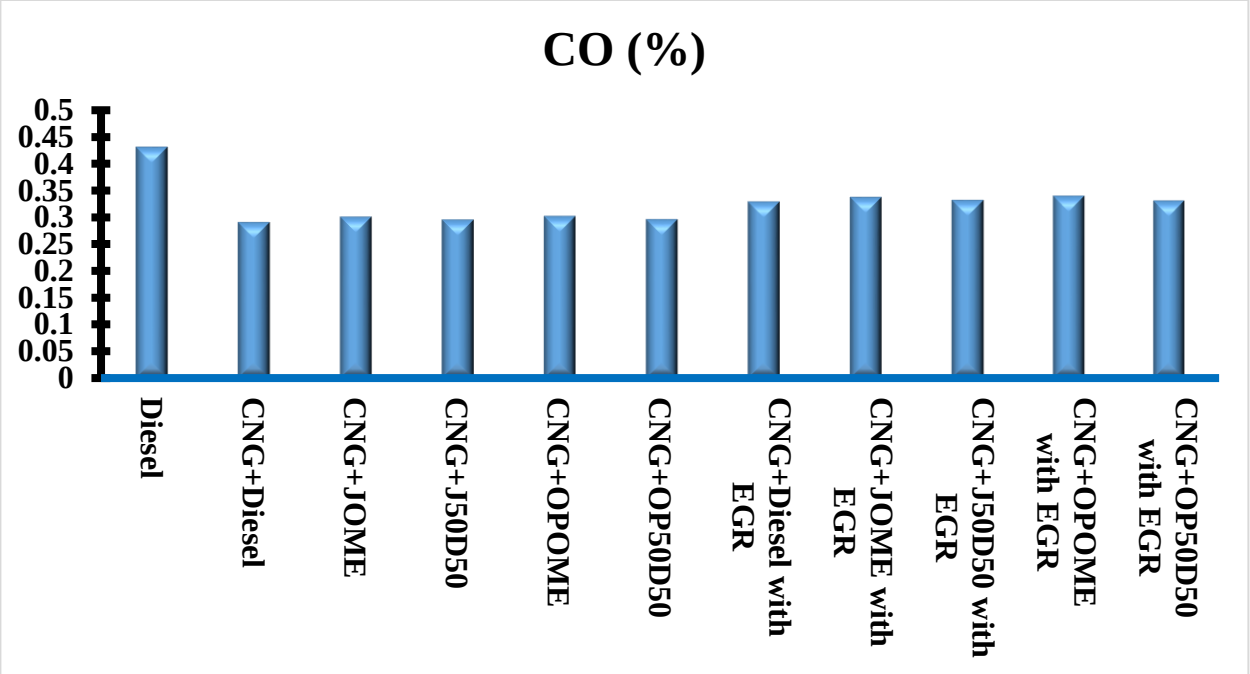

Figure 4.91: CO emissions at full load of all operating modes

4.7.3 Oxides of nitrogen

The oxides of nitrogen (NO_X) are the sum of NO_2 and NO. There are some other oxides of nitrogen also included sometimes, but they are minor in conventional diesel and dual fuel engines (Tira, 2013). The NO_X formation is dependent on the oxidation of atmospheric nitrogen. The most significant component, NO is described by the extended Zeldovich mechanism as discussed earlier, which is strongly affected by cylinder charge temperature. In dual fuel engine, part of the combustion process occurs in the lean, premixed regime. For normal diesel operation, most of the fuel is burned as a diffusion flame near stoichiometric equivalence ratio. Stoichiometric combustion produces higher NO_X due to higher combustion temperature. The variation of oxides of nitrogen emissions with respect to load for dual fuel engine without application of EGR is shown in Figure 4.92.

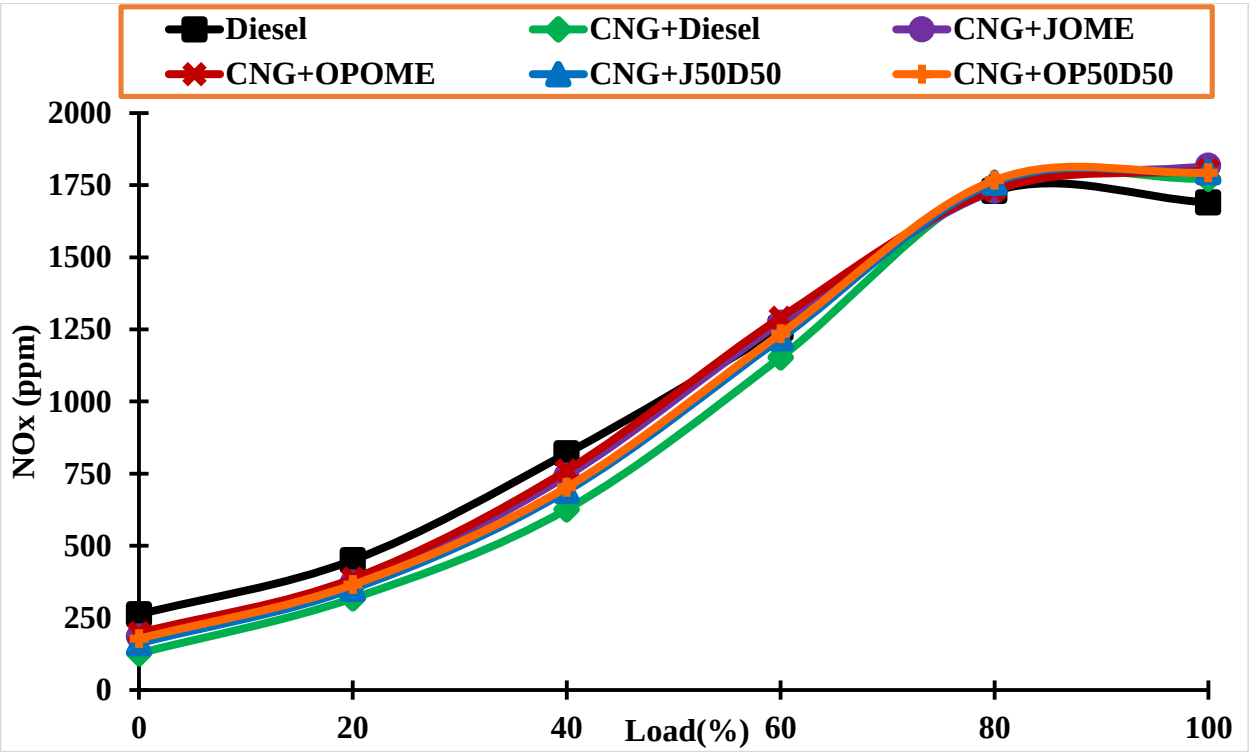

Figure 4.92: Variation in NO_X emissions of dual fuel engine without application of EGR.

It is observed that the baseline data shows higher NO_X emissions compared to dual fuel engine up to intermediate loading condition. The reason behind this is, incomplete combustion of CNG in dual fuel engine which reduces the in-cylinder combustion temperature of the engine. The leaner fuel-air mixture also reduces the combustion temperature as discussed earlier. However, at higher load, the improved CNG combustion, and stoichiometric fuel-air mixture increases the in-cylinder temperature of dual fuel engine which increases the NO_X emissions. Hence, at higher load, the NO_X emissions of dual fuel engine are found higher than a baseline data. However, the increment is not significant (Poonia et al., 1998).

In dual fuel engine, the quality of pilot fuel plays an important role in NO_X emissions. The lower cetane number and low autoignition temperature of OPOME and JOME improve the combustion characteristics of dual fuel engine at lower loading condition. It results in slightly

higher NO_X emissions for CNG+JOME and CNG+OPOME dual fuel modes compared to CNG+diesel dual fuel mode at lower loading condition. The NO_X emissions of CNG+J50D50 and CNG+OP50D50 dual fuel modes lie in between. As discussed earlier at higher load CNG is predominated over pilot fuel in dual fuel engine. The improved gaseous fuel combustion characteristics of dual fuel engine at higher load increase the in-cylinder temperature which results in higher NO_X emissions. The extra oxygen availability of JOME and OPOME further increases the NO_X emissions of CNG+JOME and CNG+OPOME dual fuel mode. Hence, at higher load, CNG+OPOME show the highest NO_X emissions among all operating modes.

The effect of the application of EGR on NO_X emissions with respect to load, for dual fuel engine is shown in Figure 4.93. It is known that application of EGR improves the combustion characteristics of dual fuel engine at low loading condition, which increase the in-cylinder temperature. However, due to reduced oxygen concentration inside the combustion chamber decrease the flame temperature. The overall effect of the application of EGR increases the in-cylinder temperature at lower loading condition. Hence, at lower load, slightly increase in NO_X emissions is noticed in dual fuel engine with the application of EGR. But it is still lower than a baseline data. The application of EGR shows magical advantages for reducing the NO_X emissions of dual fuel engine at higher loading condition. And it improves with increasing EGR quantity. However, the application of EGR at higher load reduces the performance of dual fuel engine. Hence the EGR for the present research is fixed at 15%, which is found an optimum condition after performing a number of tests. At higher load, the dual fuel engine using EGR emits low NO_X emissions compared to a baseline data.

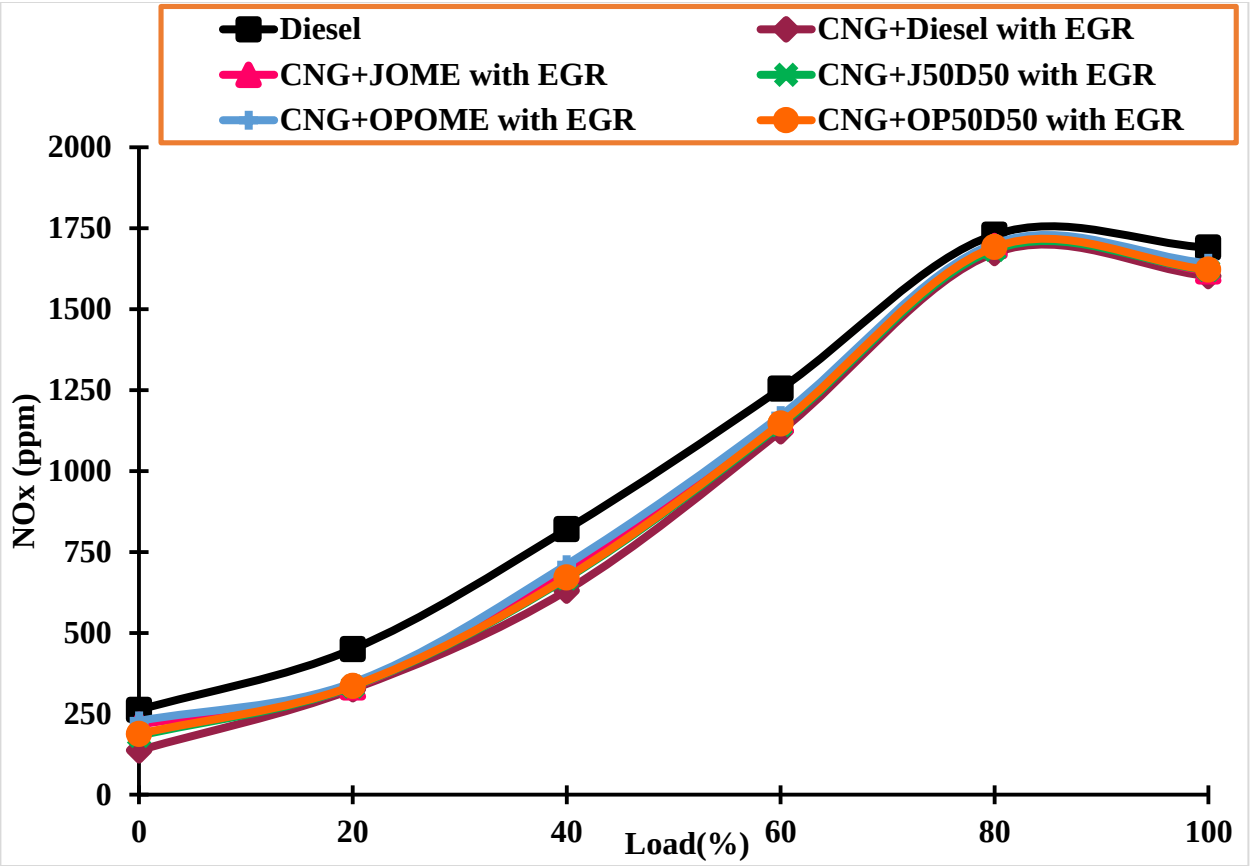

Figure 4.93: Variation in NO_X emissions of dual fuel engine using EGR.

The variation of NO_X emissions with load for dual fuel engine using JOME as pilot fuel without and with the application of EGR is shown in Figure 4.94 and the variation of NO_X emissions with load for dual fuel engine using OPOME as pilot fuel without and with the application of EGR is shown in Figure 4.95. Figure 4.96 shows the percentage change in NO_X emissions of all duel fuel operating modes with respect to a baseline data. Figure 4.97 shows the highest NO_X emissions of all operating modes.

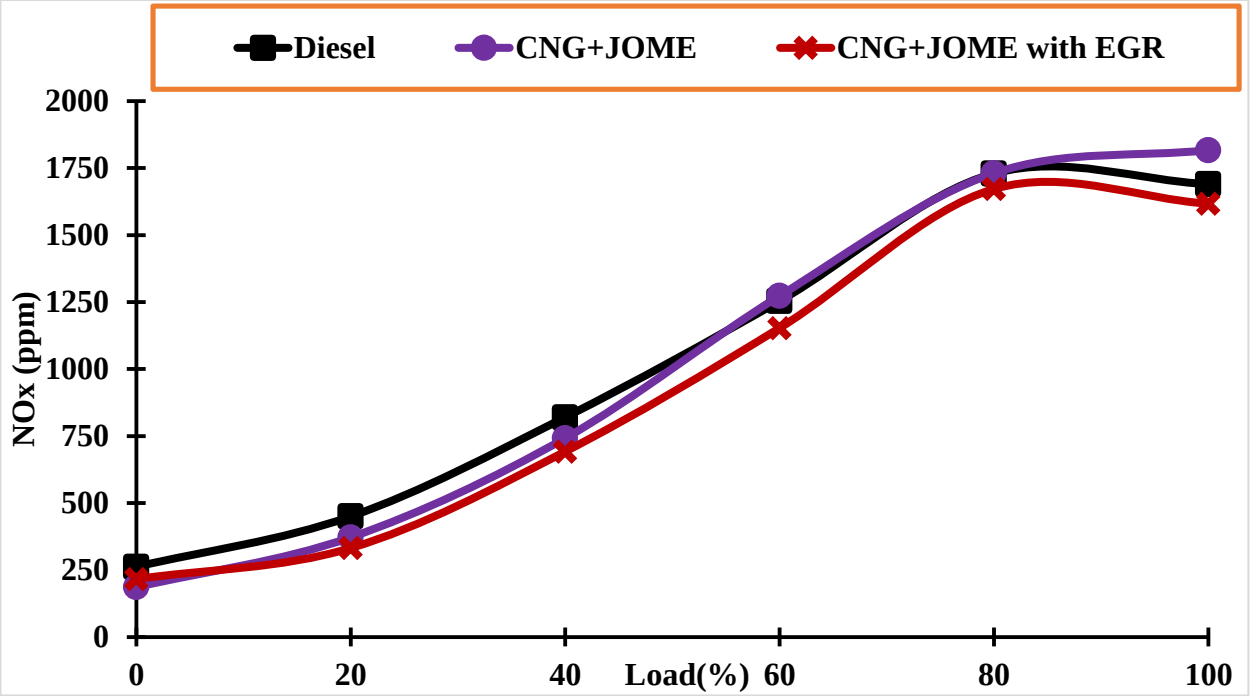

Figure 4.94: Variation in NO_X emissions for JOME as pilot fuel without and with EGR.

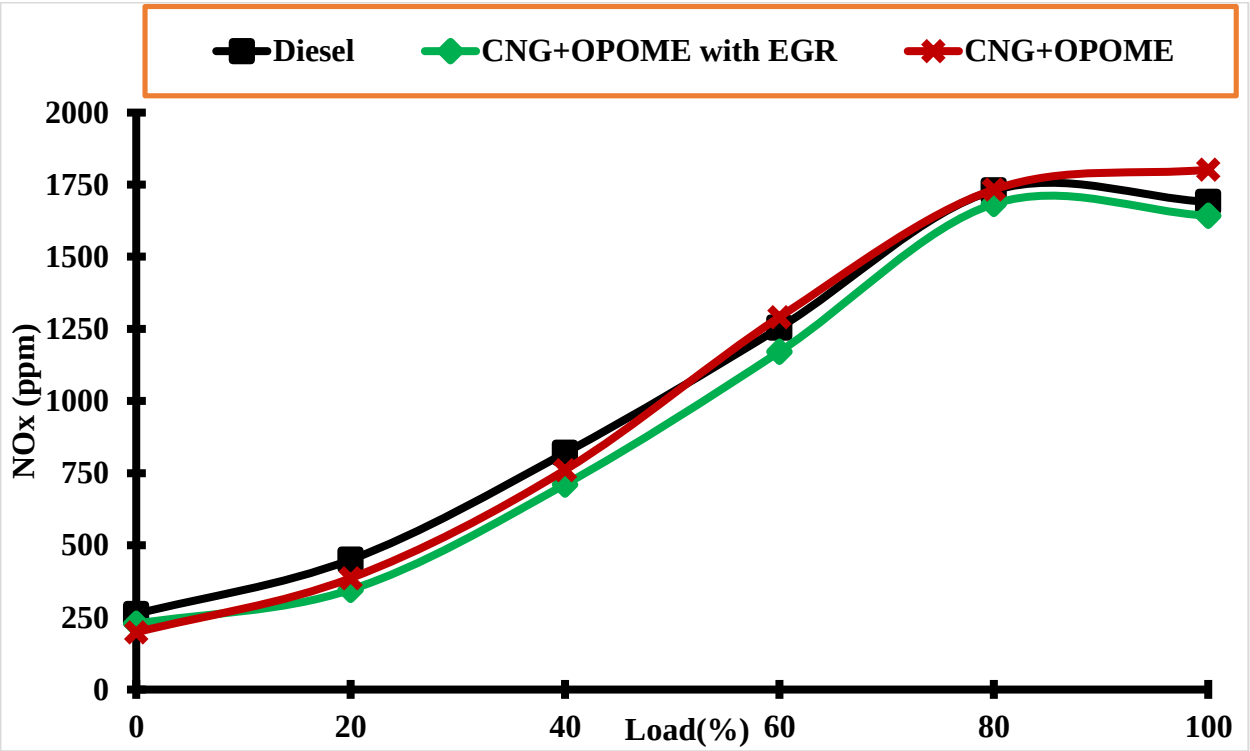

Figure 4.95: Variation in NO_X emissions for OPOME as pilot fuel without and with EGR.

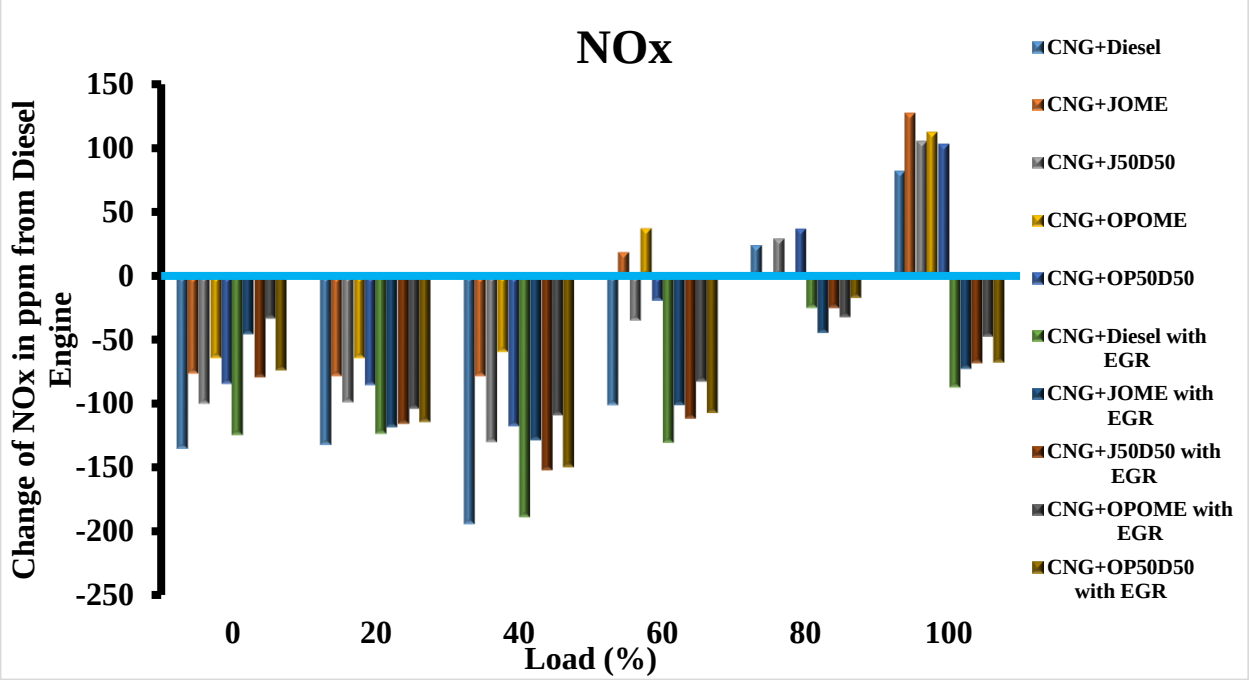

Figure 4.96: Variation in NO_X emissions of Dual fuel engine from baseline data at various loads

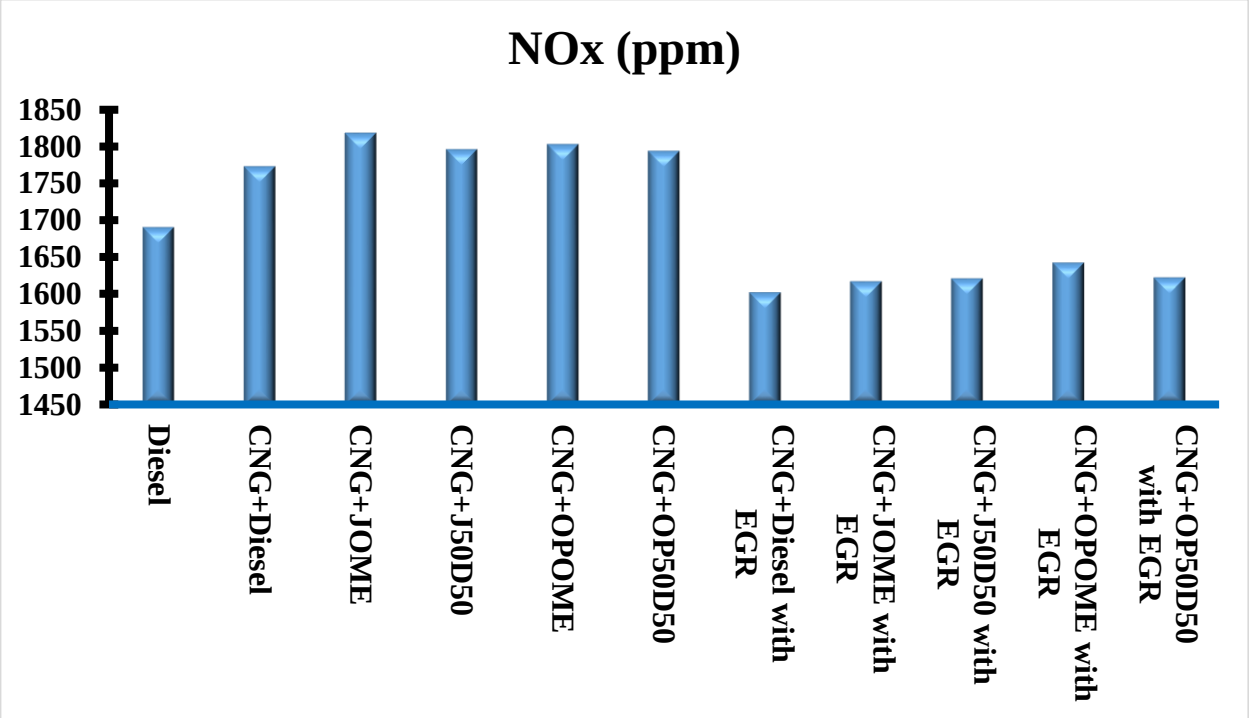

Figure 4.97: NO_X emissions at full load of all operating modes

4.7.4 Carbon dioxides

The carbon dioxide (CO_2) is one of the major emissions from any engine using hydrocarbon fuels (Pali et al., 2014). The CO_2 is the main component of greenhouse gasses which further causes serious health problems in living beings. It is also true that CO_2 composition in exhaust gasses shows the complete or incomplete combustion of fuel inside the combustion chamber. Hence, higher the CO_2 level in exhaust gasses shows complete combustion of hydrocarbon fuels. The variation of CO_2 emissions with respect to load for dual fuel engine without application of EGR is shown in Figure 4.98. It is observed that the dual fuel engine emits low CO_2 emissions compared to a baseline data for all loading conditions. The reason behind this is, lower carbon-hydrogen ratio of CNG compared to diesel fuel and the introduction of the leaner mixture in dual fuel engine.

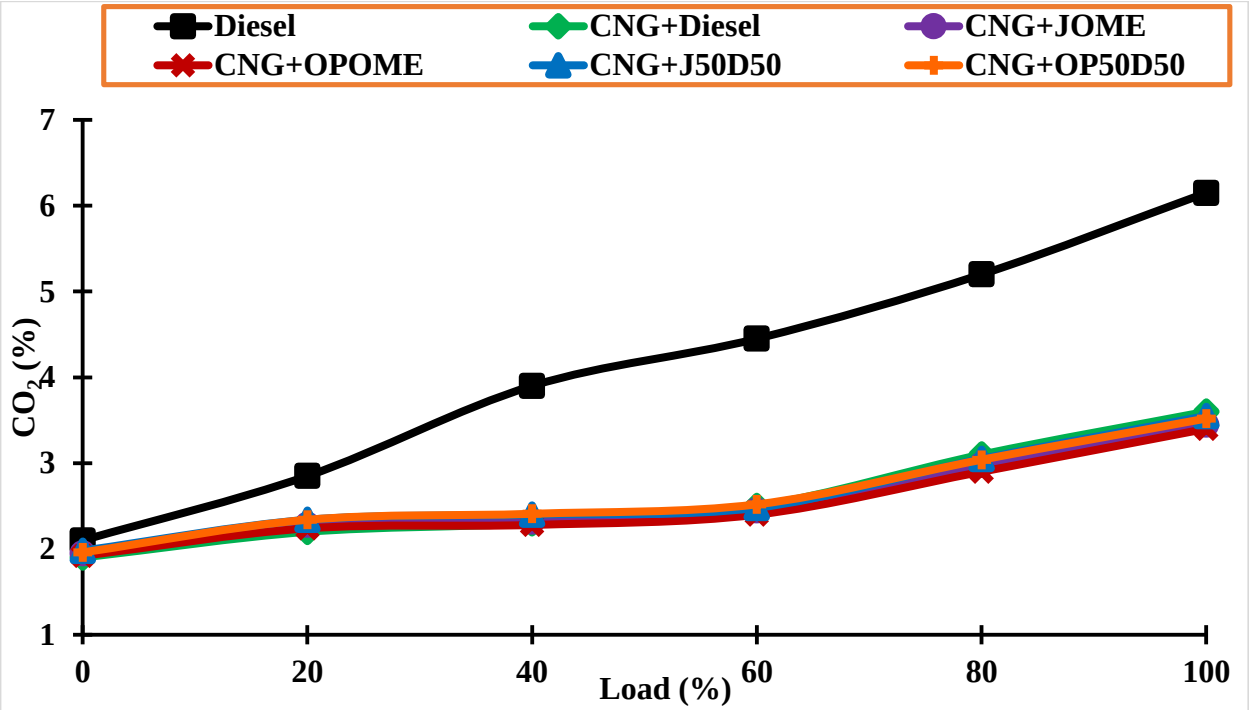

Figure 4.98: Variation in CO2 emission of dual fuel engine without application of EGR.

In dual fuel engine, as discussed earlier 80-90% energy is contributed by CNG hence the CO_2 emissions are totally depended on combustion of CNG. The effect of pilot fuel on CO_2 emissions is not significant. However, different pilot fuels show a change in CO_2 emissions but these changes are not significant. It is observed that use of biodiesel and its blend as pilot fuel reduce the CO_2 emissions by some extent as a consequence of higher viscosity, poor atomization, and incomplete combustion.

The variation of CO_2 emissions with respect to load for dual fuel engine with the application of EGR is shown in Figure 4.99.The application of EGR, recirculate some portion of unburnt hydrocarbons present in the exhaust gasses which result in slight increase in CO_2 emissions. However, the increase is not so high which can be seen in the graph. Hence, it can say that the application of EGR did not affect the CO_2 emissions of dual fuel engine.

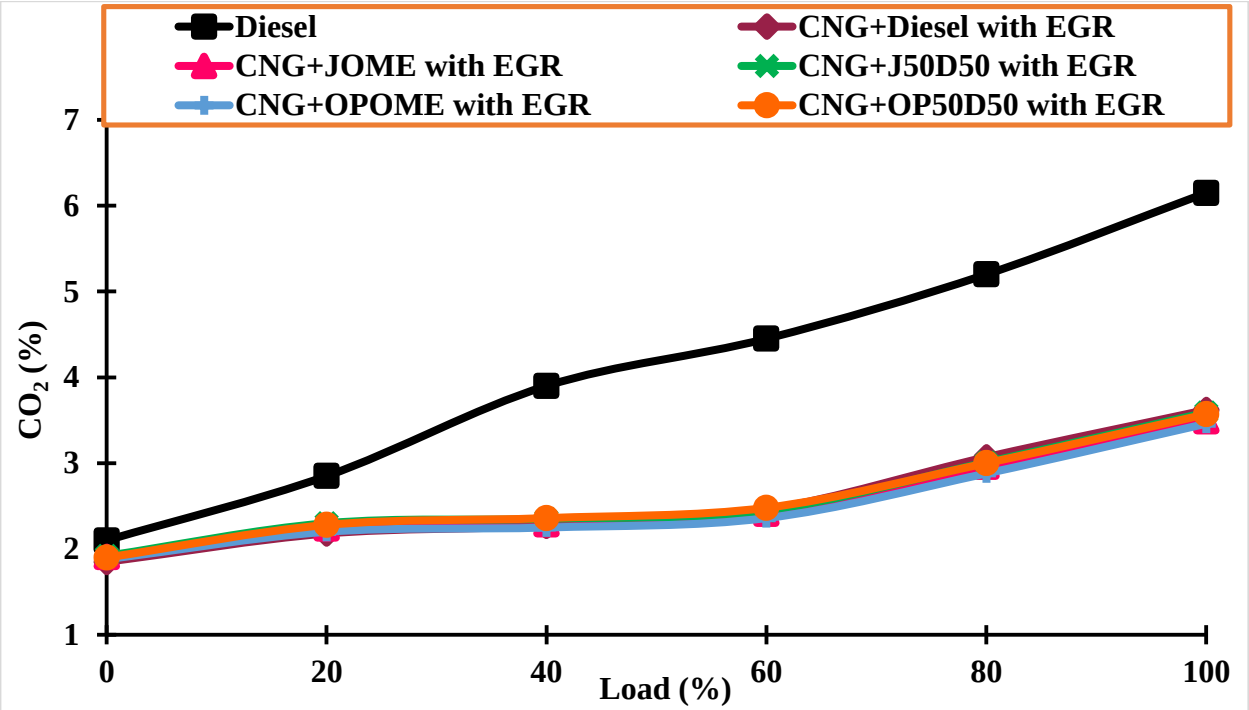

Figure 4.99: Variation in CO_2 emission of dual fuel engine using EGR.

The variation of CO emissions with load for dual fuel engine using JOME as pilot fuel without and with the application of EGR is shown in Figure 4.100 and the variation of CO_2 emissions with load for dual fuel engine using OPOME as pilot fuel without and with the application of EGR is shown in Figure 4.101. Figure 4.102 represent the percentage change in CO_2 emissions of all duel fuel operating modes with respect to a baseline data. Figure 4.103 shows the highest CO_2 emissions of all operating modes.

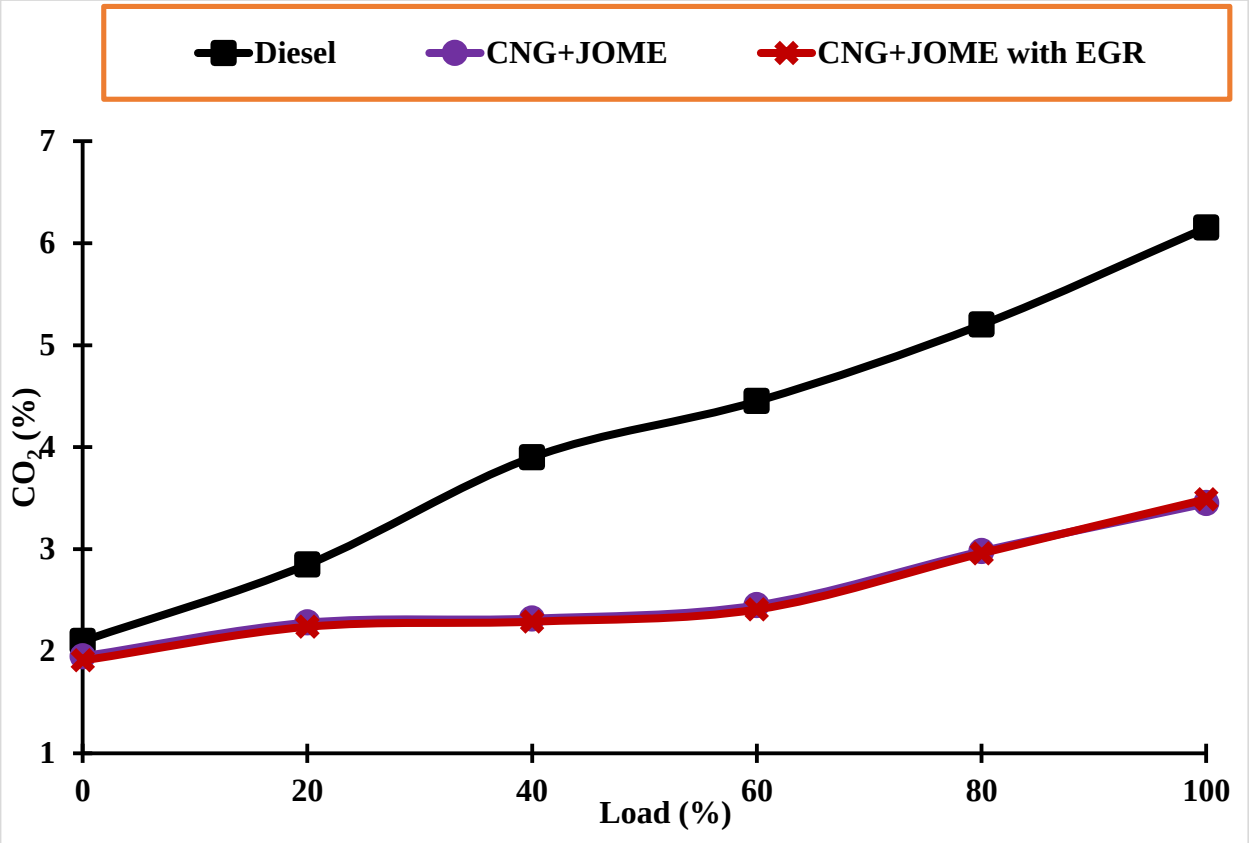

Figure 4.100: Variation in CO_2 emissions for JOME as pilot fuel without and with EGR.

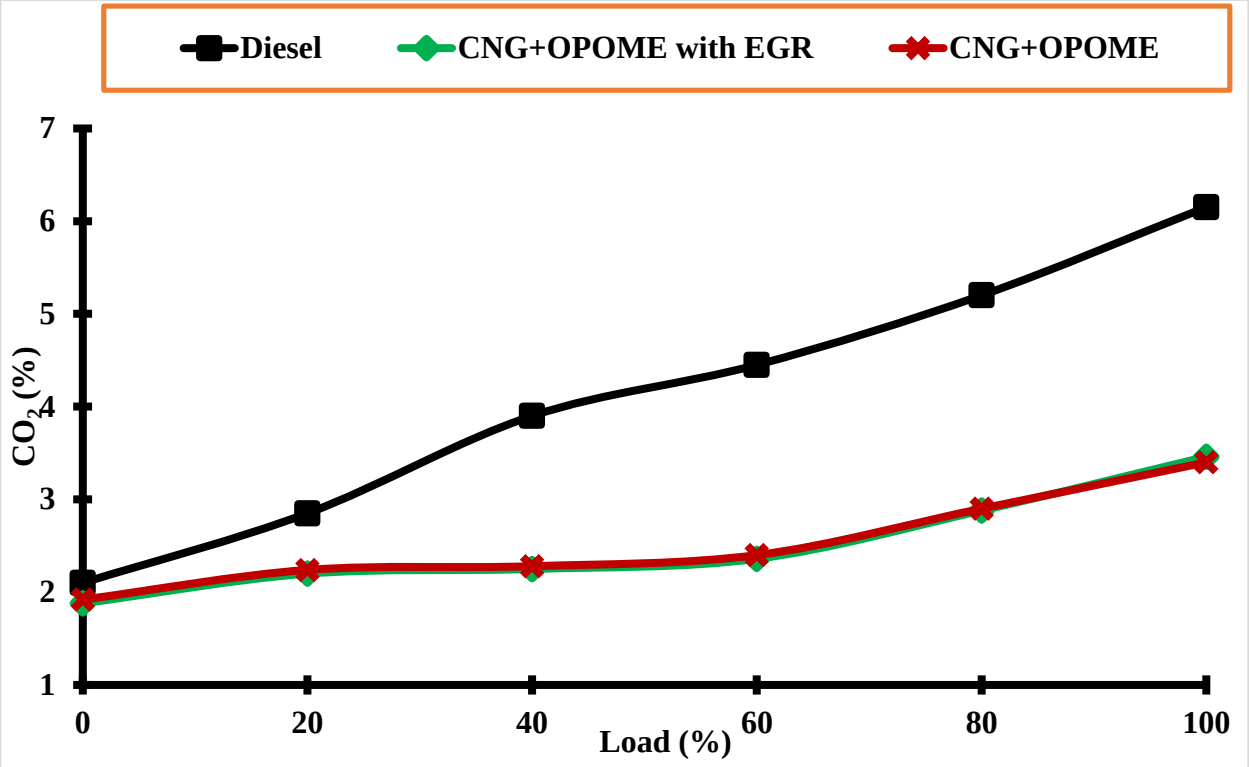

Figure 4.101: Variation in CO_2 emissions for OPOME as pilot fuel without and with EGR.

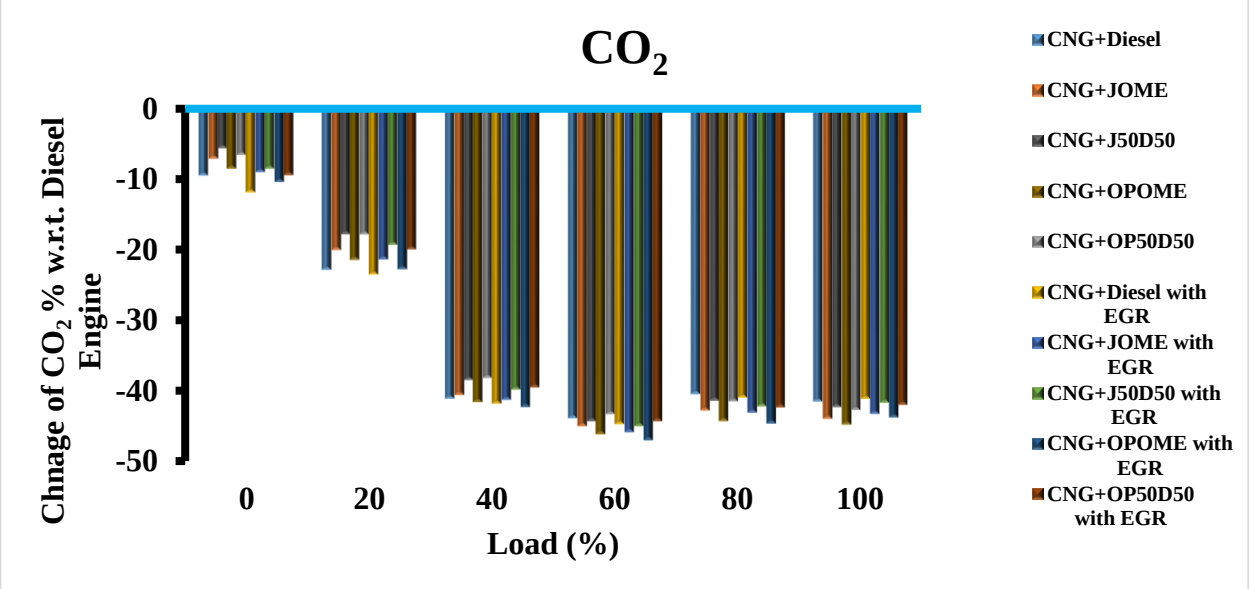

Figure 4.102: Percentage change in CO_2 emissions of Dual fuel engine w.r.t. baseline data at various loads

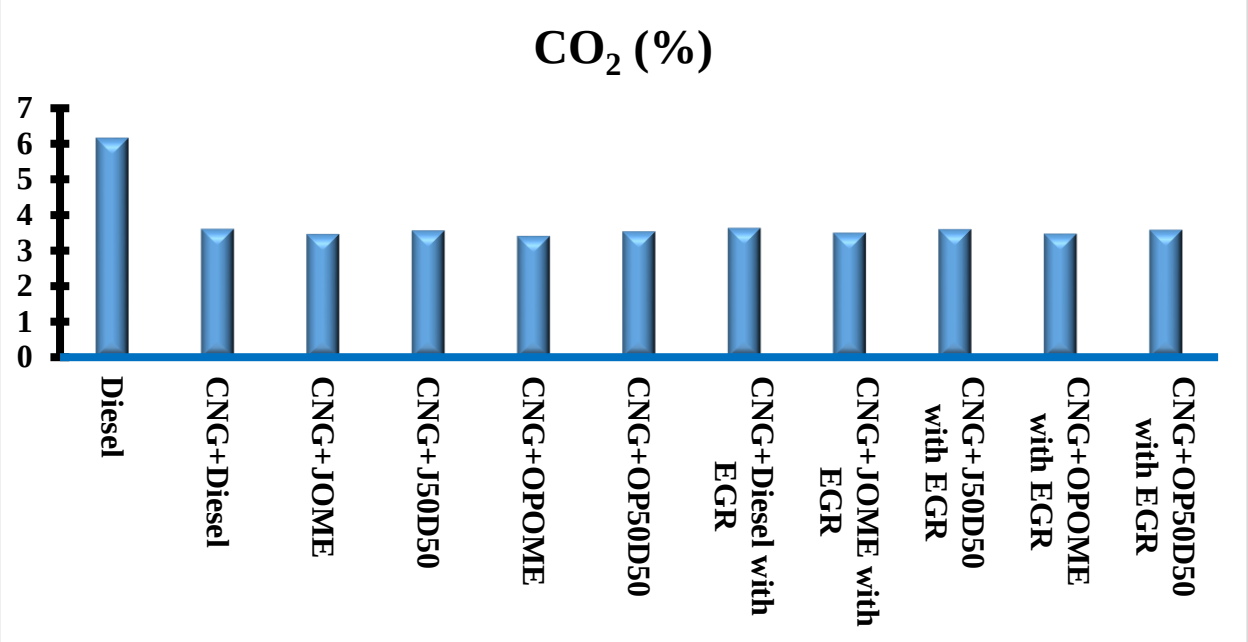

Figure 4.103: CO_2 emissions at full load of all operating modes

4.7.5 Smoke opacity

The particulate matter is essentially composed of soot, though some hydrocarbons, generally referred to as a soluble organic fraction (SOF) of the particulate emissions, are also adsorbed on the particle surface or simply emitted as liquid droplets (Pali et al., 2014; Tira, 2013). Among the particulate matter components, soot is recognized as the main substance which is responsible for the smoke opacity. Smoke opacity formation occurs at the extreme air deficiency. It increased as the air/fuel ratio decreases. Soot is produced by oxygen deficient thermal cracking of long-chain molecules.

The Figure 4.104 shows the variation of smoke opacity with load for dual fuel engine without application of EGR. The smoke opacity increases with increasing load for all modes of operations. However, for the baseline data, the rate of smoke emission is higher than that of dual fuel engine. The reason for this is decreasing oxygen availability with load and higher

carbon/hydrogen ratio of diesel. However, at low load, the smoke emissions are found higher in dual fuel engine compared to conventional diesel due to incomplete combustion of CNG. However, the improvement in combustion characteristics of CNG and less use of liquid fuel improves the smoke opacity of dual fuel engine at higher load. Hence, at high load, the smoke opacity of dual fuel engine is lower compared to conventional diesel. In dual fuel engine, the application of JOME, OPOME and their blends as pilot fuel increases the smoke opacity of dual fuel engine compare to CNG+diesel dual fuel mode for all loading condition.

The application of EGR in dual fuel engine increases the smoke opacity of dual fuel engine, especially at higher loading condition. The reason for this is incomplete combustion of gaseous fuel. However, the smoke opacity of dual fuel engine is still less than the baseline data at higher load. The white color smoke is noticed in dual fuel engine. The variation of smoke opacity with load for dual fuel engine with the application of EGR is shown in Figure 4.105.

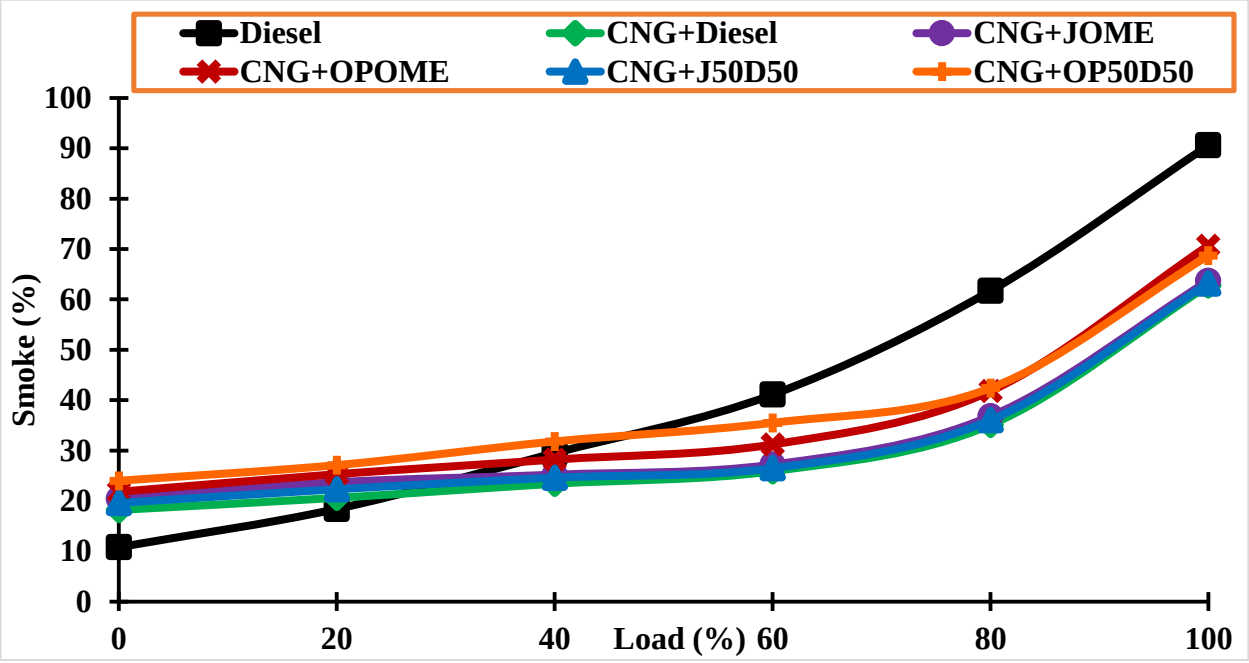

Figure 4.104: Variation in the smoke opacity of dual fuel engine without application of EGR.

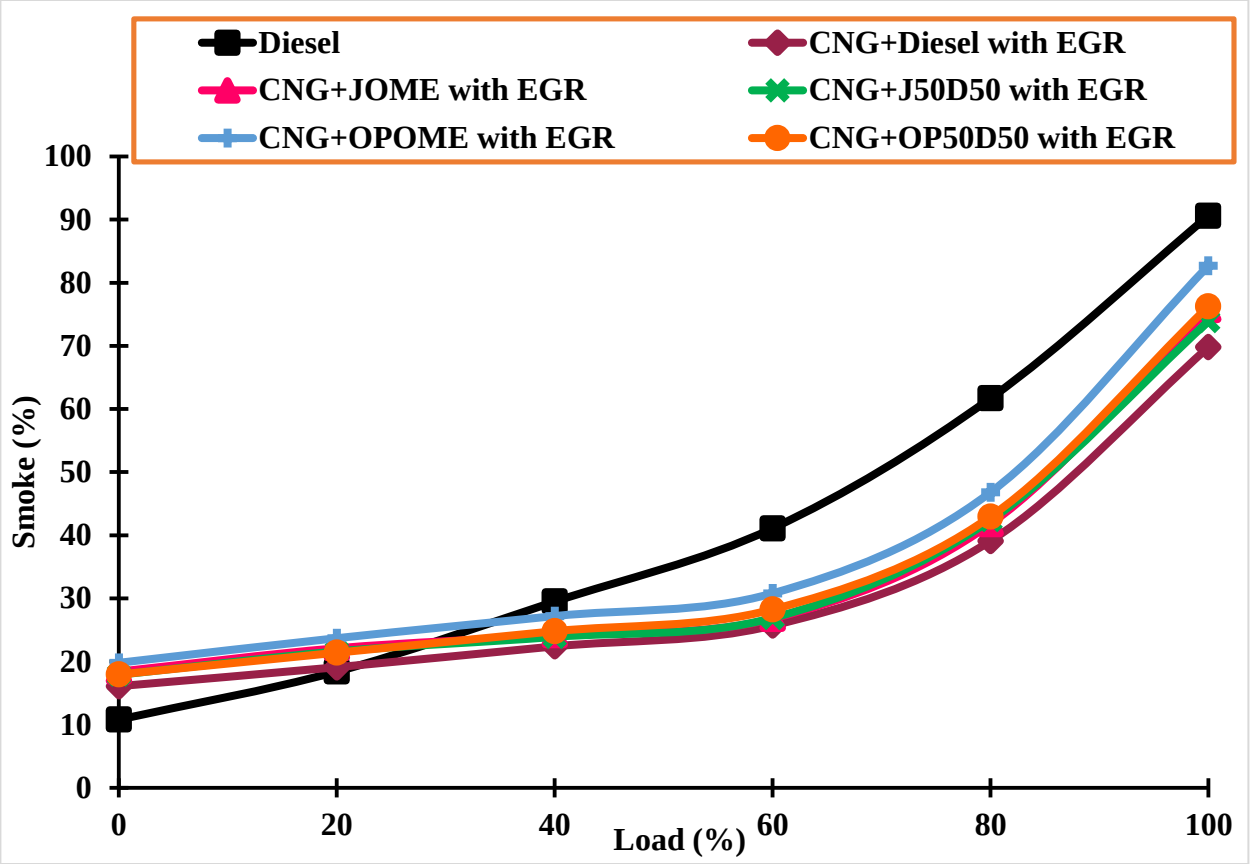

Figure 4.105: Variation in the smoke opacity of dual fuel engine with the application of EGR.

The variation of smoke opacity with load for dual fuel engine using JOME as pilot fuel without and with the application of EGR is shown in Figure 4.106 and the variation of smoke opacity with load for dual fuel engine using OPOME as pilot fuel without and with the application of EGR is shown in Figure 4.107. Figure 4.108 shows the percentage change in smoke opacity of all duel fuel operating modes with respect to a baseline data. Figure 4.109 shows the highest smoke opacity of all operating modes.

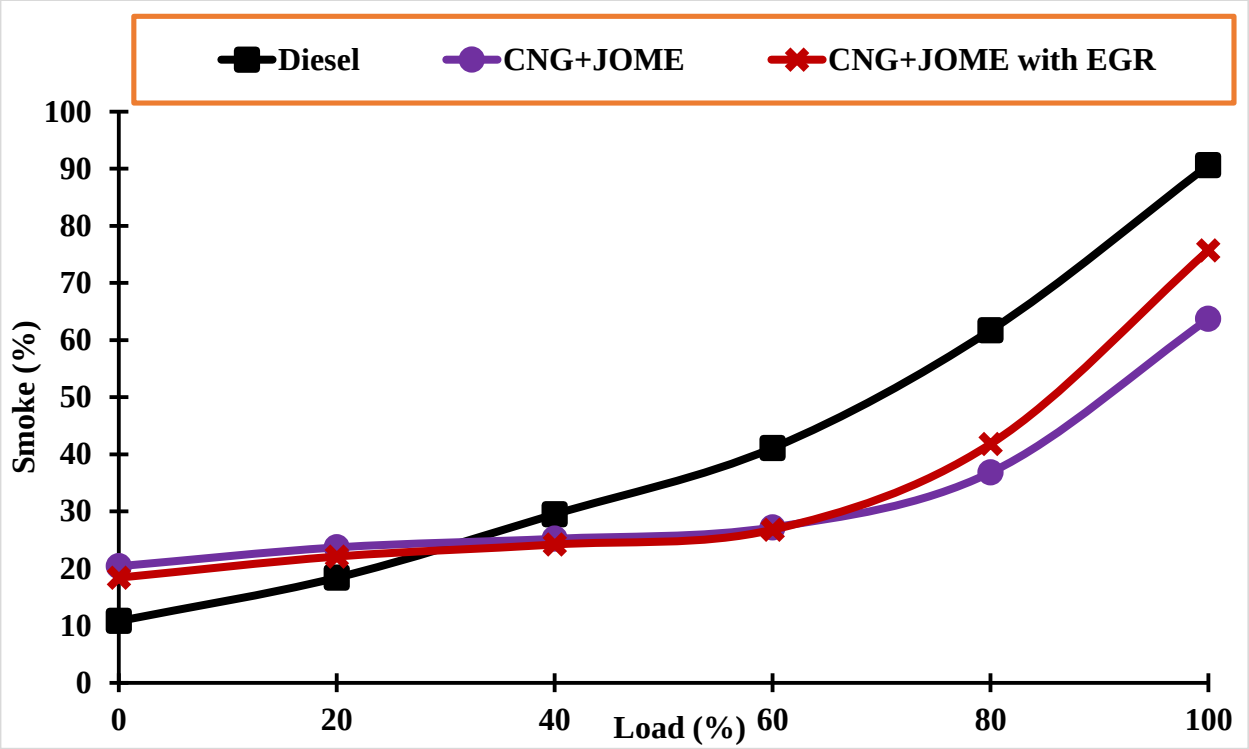

Figure 4.106: Variation in smoke opacity for JOME as pilot fuel without and with EGR.

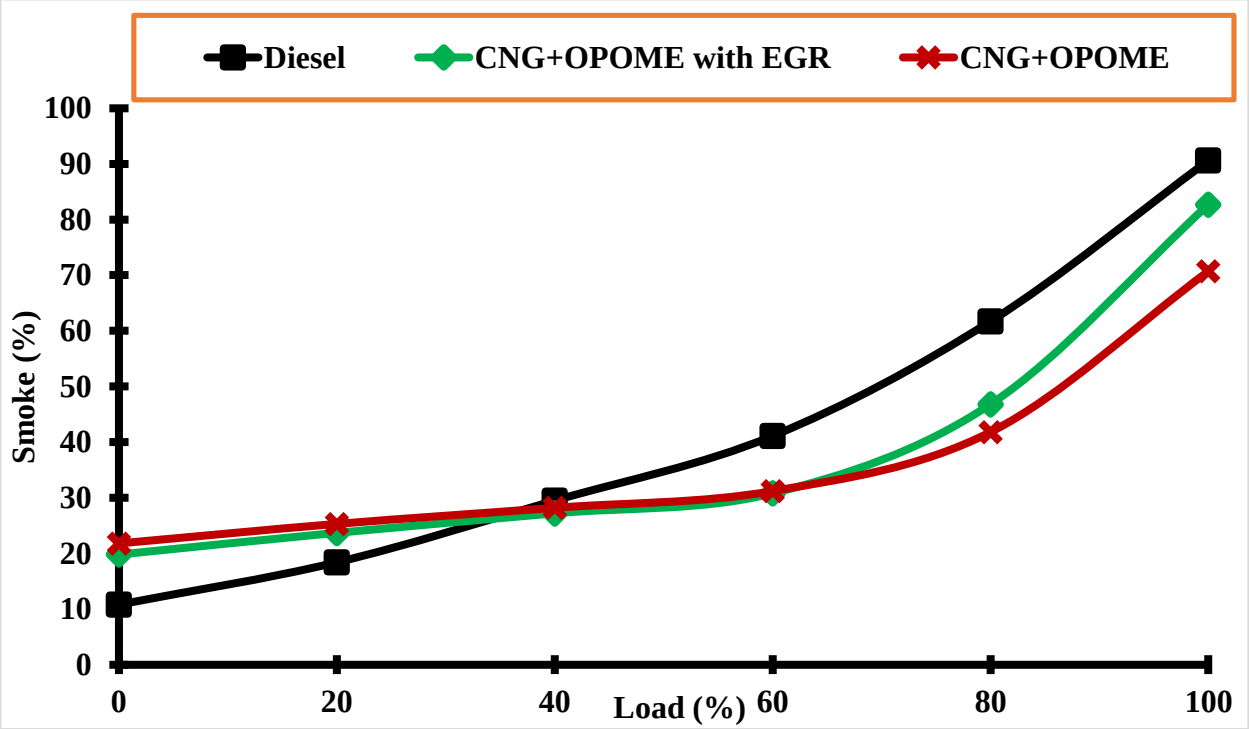

Figure 4.107: Variation in smoke opacity for OPOME as pilot fuel without and with EGR.

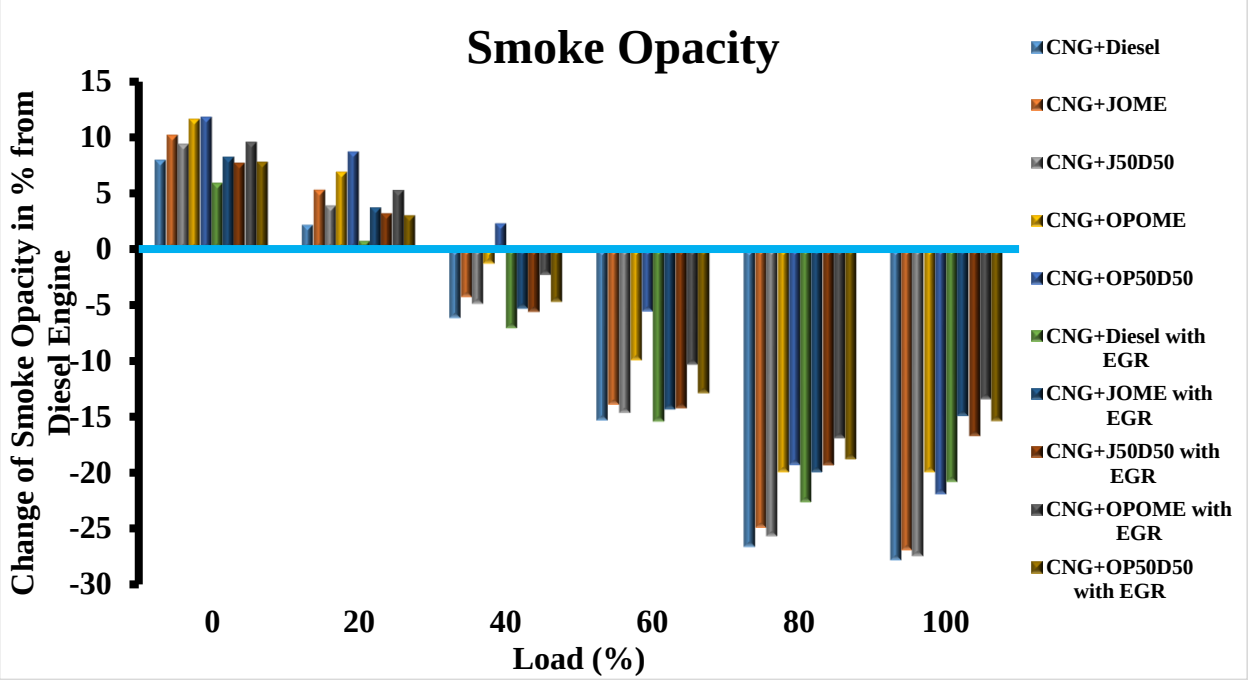

Figure 4.108: Variation in smoke opacity of Dual fuel engine from baseline data at various loads

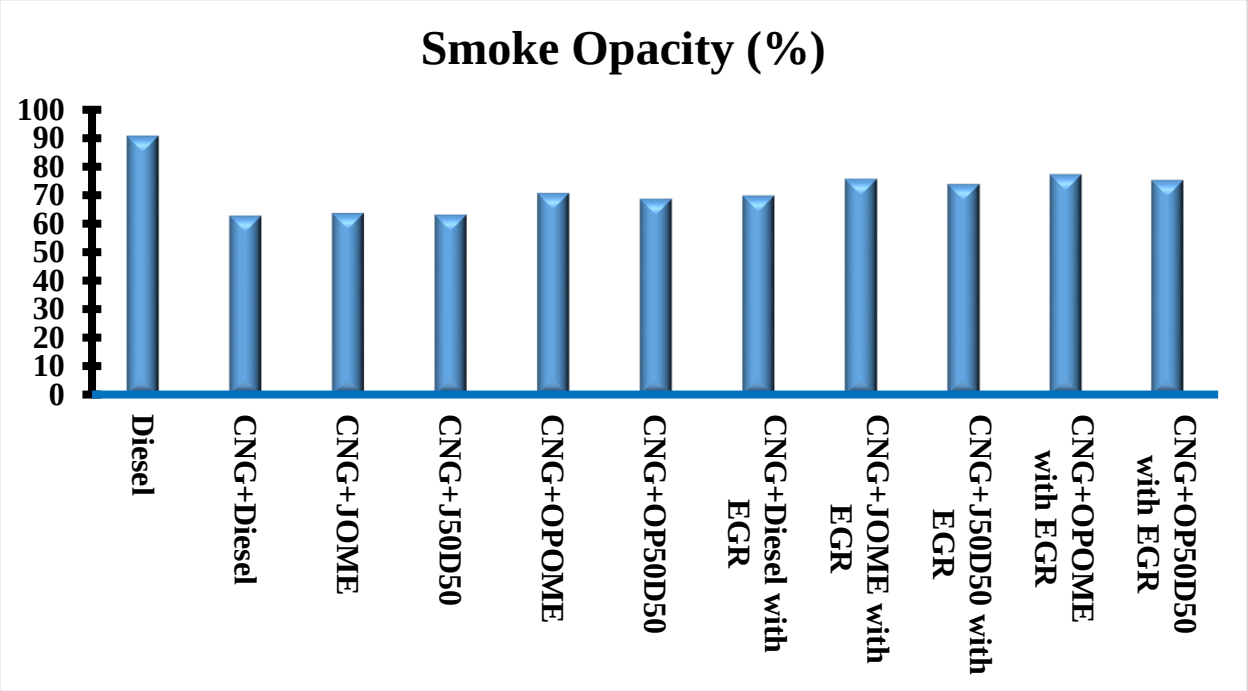

Figure 4.109: Smoke opacity at full load of all operating modes

CHAPTER 5

CONCLUSIONS AND FUTURE WORK

5.1 Conclusions

The objective of the present work is to explore the feasibility of using biodiesel and its blends as pilot fuel in dual fuel engine where CNG is a primary fuel. Along with that the effect of application of EGR in dual fuel engine is also explored.

It is found that the application of CNG in dual fuel engine is an attractive proposition. The NO_X, CO_2 and smoke emissions are reduced in dual fuel engine compared to a baseline data. However, dual fuel engine is associated with high CO and UHC emissions. It is observed that UHC emissions increased due to leaner gaseous fuel and air mixture, especially at lower load. The performance and emissions characteristics of dual fuel engine at lower and intermediate load are further improved by applying EGR. The present work also included the optimization of biodiesel production process, preparation of blends and evaluation of physicochemical properties of all pilot fuels. The ignition delay of all pilot fuels is also measured.

The main conclusions drawn from optimization of biodiesel production process, evaluation of physicochemical properties and ignition delay measurement are summarized as under:

1. The RSM is chosen as an optimization tool for optimizing the single stage transesterification and two stage transesterification processes. The maximum yield of

OPOME is obtained 97.2% in single stage transesterification, while the maximum yield for JOME is found 95.2% in two stage transesterification process.

2. The physicochemical properties, like kinematic viscosity, density, flash point, calorific value and cetane index are measured for diesel, JOME, OPOME and their blend. The most of the physicochemical properties are within prescribed limits of ASTM standard. OPOME has better physicochemical properties among all pilot fuel except calorific value.
3. The OPOME showed lowest ignition delay among all pilot fuels for all operating conditions followed by JOME and Diesel. The reason for this is high cetane number and low flash point, kinematic viscosity and density of OPOME.
4. The longer ignition delay of 1.5 °CA to 3°CA is observed in dual fuel engine compared to a baseline data. The longer ignition delay of pilot fuel is due to the presence of CNG with air in the combustion chamber.

The following conclusions are drawn by comparing the combustion, performance and emissions characteristics of dual fuel engine with baseline data

1. At higher load, the peak in-cylinder pressure of dual fuel engine is higher than baseline data, due to improved gaseous fuel utilization.
2. Dual fuel engine has peak BTE than baseline data. The peak BTE of 30.65% is found for dual fuel engine which is 2.07% higher than the baseline data.
3. The CO_2 emissions of dual fuel engine are lower compared to baseline data for all loading conditions.

4. The dual fuel engine has lower NO_X emissions as compared to baseline data up to 80% loading condition. However, at full load, the NO_X emissions of the dual fuel engine are slightly higher than the baseline data.
5. The CO and UHC emissions of dual fuel engine are higher than the baseline data, for all loading conditions. However, at higher load, CO emissions of dual fuel engine are found lower compared to a baseline data.
6. The smoke opacity of dual fuel engine is found lower compared to baseline data.

The effect of the use of different pilot fuel for CNG on the combustion, performance and emissions characteristics of dual fuel engine is studied. The following conclusions are drawn:

1. The OPOME and OP50D50 as pilot fuels show the highest in-cylinder pressure of 68.6 bar and 68.8 bar respectively followed by JOME and J50D50 as pilot fuel in dual fuel engine at lower load. The diesel as the pilot fuel shows the lowest in-cylinder pressure of 65.8 bar at lower load. However, at higher load, diesel as pilot fuel has highest in-cylinder pressure among all other fuel combination of dual fuel engine.
2. The use of biodiesel and its blend as pilot fuel improves the BTE of dual fuel engine compared to diesel as a pilot fuel for low and intermediate loads.
3. The CNG + diesel has highest BTE of 30.65% followed by CNG + OP50D50, CNG + J50D50, CNG + OPOME and CNG + JOME, which has highest BTE of 30.58%, 30.51%, 30.43% and 30.35% respectively at full load.
4. The CO, UHC and NO_X emissions are found lowest for CNG + OPOME and CNG + JOME as compared to CNG + diesel at lower and intermediate loads.

5. At higher load, slightly higher CO and NO_X emissions are noticed for CNG + JOME and CNG + OPOME as compared to CNG + diesel. However, the emissions of CNG + J50D50 and CNG + OP50D50 lie in between.
6. The use of biodiesel and its blend as a pilot fuel for CNG in dual fuel engine enhance the smoke opacity of the engine as compared to CNG + diesel dual fuel mode.

The application of EGR improves the performance of dual fuel engines. Some important conclusions drawn from the application of EGR are as follows:

1. The application of EGR in dual fuel engine increases the in-cylinder pressure at lower load, but it is still lower than baseline result. However, the application of EGR reduces the in-cylinder pressure at higher load.
2. The application of EGR improves the BTE of dual fuel engine at lower and intermediate loads. However, at higher load, the application of EGR has the adverse effect on BTE of the engine.
3. The CO and UHC emissions of dual fuel engine reduced at lower and intermediate loads with the application of EGR. However, application of EGR also has an adverse effect on CO and UHC emissions at higher load.
4. The use of EGR is an effective method for reducing NO_X emissions. The application of EGR in dual fuel engine reduces the NO_X emissions and improves the performance of the dual fuel engine.

It is concluded that the use of dual fuel combustion technique with different alternative fuels improves the combustion, performance and emissions characteristics of diesel dual fuel engine.

5.2 Future Work:

On the basis of experience gained during the present series of investigation, the following directions are indicated for further investigations and developments:

1. In the present work, CNG is used as primary fuel. There is a need to explore the use of other gaseous fuels such as H_2, LPG, biogas and producer gas as primary fuels.
2. Different biodiesel are used as pilot fuels in the present work. Future work can be done on other alternative liquid fuels derived either from coal or biomass.
3. It has been observed that the properties of the pilot fuel play a significant role on the performance and emissions characteristics in the dual fuel combustion mode. Further research in modifying the pilot fuel properties such as O_2, cetane number, density, bulk modulus, and H/C ratio by using different fuel additives will be very interesting. Moreover, it would be worthwhile to know the best pilot fuel characteristics for a specific gaseous fuel.
4. Hydrogen is a cleaner fuel but its combustion in dual fuel engine is a big challenge. To overcome this problem mixture of hydrogen and low-grade gaseous fuel can be used as primary fuel in dual fuel engine.

REFERENCES

- Abdelaal M.M. & Hegab A.H. Combustion and emission characteristics of a natural gas-fueled diesel engine with EGR, Energy Conversion and Management. 64 (2012), 301–12.
- Adomeit P., Becker M., Rohs H., Pischinger S., Greis A., Grunefeld G. Potential Soot and CO Reduction for HSDI Diesel Combustion Systems, SAE. (2006), 2006-01-1417.
- Agarwal A.K. Biofuels (Alcohols and Biodiesel) Applications as Fuels for Internal Combustion Engines, 33 (2007), 233–271.
- Agarwal D., Sinha S., Agarwal A.K. Experimental investigation of control of NO_X emissions in biodiesel-fueled compression ignition engine Renew, Energy. 31 (2006), 2356-69.
- Ahmed S., Hassan M.H., Kalam A., Rahman S.M.A., Abedin J., Shahir A. An experimental investigation of biodiesel production, characterization, engine performance, emission and noise of Brassica juncea methyl ester and its blends, Journal of Cleaner Production. 79 (2014).
- Alam M., Goto S., Sugiyama K., Kajiwara M., Mori M., Konno M., Motohashi M., Oyama K. Performance and Emissions of a DI Diesel Engine Operated with LPG and Ignition Improving Additives, SAE. (2001), 2001-013680.
- Alhassan Y., Kumar N., Bugaje I.M., Pali H.S., Kathkar P. Co-solvents Transesterification of Cotton Seed Oil into Biodiesel: Effects of reaction Conditions on Quality of Fatty Acids Methyl Esters, Energy Conversion and Management. 84 (2014), 640-48.

- Alkidas A.C. Combustion-chamber crevices: the major source of engine-out hydrocarbon emissions under fully warmed conditions, Progress in Energy and Combustion Science. 25 (1999), 253-73.
- Alla G.H.A., Soliman H.A., Badr O.A., Abd Rabbo M.F. Effects of diluents admissions and intake air temperature in exhaust gas recirculation on the emissions of an indirect injection dual fuel engine, Energy Convers Manage. 42 (2001), 1033-45.
- Alla G.H.A., Soliman H.A., Badr O.A., et al. Effect of injection timing on the performance of a dual fuel engine, Energy Convers. Manage. 43 (2) (2002), 269-77.
- Ashok B., Denis A.S., Kumar C.R. LPG diesel dual fuel engine – A critical review, Alexandria Engineering Journal (2015) 54, 105-126.
- Atabani A.E., Silitonga A.S., Ong H.C., et al. Non-Edible Vegetable Oils : A Critical Evaluation of Oil Extraction, Fatty Acid Compositions, Biodiesel Production, Characteristics, Engine Performance and Emissions Production, Renewable and Sustainable Energy Reviews. 18 (2013), 211-45.
- Atapour M., Kariminia H., Moslehabadi P.M. Optimization of Biodiesel Production by Alkali-Catalyzed Transesterification of used Frying Oil, Process Safety and Environmental Protection. 92 (2013), 179-85.
- Bagal N.L., Rutland C.J., Foster D.E., Narayanaswamy K., He Y. CO Emission Model for an Integrated Diesel Engine, Emissions, and Exhaust After treatment System Level Model, SAE. (2009), 2009-01-1511, 2, 1460-1472.
- Balasubramanian V., Sridhara K., Ganesan V. Performance Evaluation of a Small Agricultural Engine Operated on Dual Fuel (Diesel þ Natural Gas) System, SAE Technical Paper (1995), 951777.

- Balat M. & Balat H. Progress in Biodiesel Processing, Applied Energy. 87 (2010), 1815-35.
- Ban-Weiss G.A., Chen J.Y., Buchholz B.A., Dibble R.W. A numerical investigation into the anomalous slight NO_X increase when burning biodiesel; A new (old) theory, Fuel Processing Technology. 88 (2007), 659-67.
- Bari S., Yu C.W., Lim T.H. Effect of fuel injection timing with waste cooking oil as a fuel in a direct injection diesel engine, Proceedings of the Institution of Mechanical Engineers, Part D: Journal of Automobile Engineering. 218 (2004), 93–104.
- Boehman A.L., Song J., Alam M. Impact of Biodiesel Blending on Diesel Soot and the Regeneration of Particulate Filters, Energy & Fuels. 19 (2005), 1857-64.
- Bora B.J. & Saha U.K. Optimisation of injection timing and compression ratio of a raw biogas powered dual fuel diesel engine, Applied Thermal Engineering. 92 (2016), 111-21.
- Boretti A. Advances in hydrogen compression ignition internal combustion engines, International Journal of Hydrogen Energy. 36 (2011), 12601-06.
- Bose P.K. & Maji D. An experimental investigation on engine performance and emissions of a single cylinder diesel engine using hydrogen as inducted fuel and diesel as injected fuel with exhaust gas recirculation, International Journal of Hydrogen Energy. 34 (2009), 4847–54.
- BP Energy Outlook 2035 Country and regional insights - India, (2015) 2035.
- BP Statistical Review, W.E. June, BP Statistical Review of World Energy, (2015).
- Bueno A.V., Velasquez J.A., Milanez L.F. Internal Combustion Engine Indicating Measurements, Federal University of Ceara, UFC. 2012.

- Cacua K., Olmos-Villalba L., Herrera B., Gallego A. Effects of oxygen enriched air on the operation and performance of a diesel-biogas dual fuel engine, Biomass Bioenergy. 45 (2012), 159-67.
- Campbell M., Wyszynski L.P., Stone R. Combustion of LPG in a Spark Ignition Engine, SAE. (2004), 2004-01-0974.
- Carlucci A.P., de Risi A., Laforgia D., Naccarato F. Experimental investigation and combustion analysis of a direct injection dual-fuel diesel–natural gas engine, Energy. 33 (2008), 256-63.
- Chaniotis A. K. & Poulikakos D. Modeling and optimization of catalytic partial oxidation methane reforming for fuel cells, Journal of Power Sources. 142 (2005), 184-93.
- Chauhan B.S., Kumar N., Cho H.M. Performance and emission studies on an agriculture engine on neat Jatropha oil, Energy. 24 (2010).
- Chen C., Guo W., Ngo H.H., Lee D.J., Tung K.L., Jin P., Wang J., Wu Y. Challenges in biogas production from anaerobic membrane bioreactors, Renewable Energy. 98 (2016) 120-34.
- Chen Z. & Iwashina T. HC and CO Formation Factors in a PCI Engine, SAE. (2009), 2009-01-1889.
- Corbo P., Gambino M., Iannaccone S., Unich A. Comparison between Lean-Burn and Stoichiometric Technologies for CNG Heavy-Duty Engines, SAE. (1995), 950057.
- Crookes R.J., Korakianitis T., Namasivayam A.M. A systematic experimental assessment of the use of rapeseed methyl ester (RME) as a compression ignition engine fuel during conventional and dual–fuel operation, In: TechnischeAkademie Esslingen (TAE) 7th international colloquium fuels. 14-15 January 2009.

- Das L.M. Near-term introduction of hydrogen engines for automotive and agricultural application, Int J Hydrogen energy. 27 (2002), 479–87.
- De Almeida P. & Silva P.D. The peak of oil production-Timings and market recognition, Energy Policy. 37 (2009), 1267-76.
- Demirbas A. Importance of biodiesel as transportation fuel, Energy Policy. 35 (2007), 4661-70.
- Demirbas A. Progress and Recent Trends in Biodiesel Fuels, Energy Conversion and Management. 50 (2009), 14-34.
- Deshpande A., Anitescu G., Rice P. A., Tavlarides L.L. Supercritical Biodiesel Production and Power Cogeneration: Technical and Economic Feasibilities, Bioresource Technology. 101 (2010), 1834-43.
- Deublein D. & Steinhauser A. Biogas from Waste and Renewable Resources: an Introduction, Wiley-VCH, Weinheim. (2008), 10.
- Dhingra R., Overly J.G., Davis G.A., Das S., Hadley S., Tonn B. A Life-Cycle-Based Environmental Evaluation : Materials in New Generation Vehicles, SAE International. (2000).
- Edwin-Geo V., Nagarajan G., Nagalingam B. Studies on dual–fuel operation of rubber seed oil and its bio-diesel with hydrogen as the inducted fuel, Int J Hydrogen Energy. 33(21) (2008), 6357-67.
- Fernando S., Hall C., Jha S. NO_X Reduction from Biodiesel Fuels, Energy & Fuels. 20 (2005), 376-82.

- Gandure J., Ketlogetswe C., Temu A. Fuel Properties of Biodiesel Produced from Selected Plant Kernel Oils Indigenous to Botswana : A Comparative Analysis, Renewable Energy. 68 (2014), 414-20.
- Gatts T., Liu S., Liew C., Ralston B., Bell C., Li H. An experimental investigation of incomplete combustion of gaseous fuels of a heavy-duty diesel engine supplemented with hydrogen and natural gas, International Journal of Hydrogen Energy. 37 (2012), 7848-59.
- Gautam R., Kumar N., Pali H.S., Kumar P. Some experimental studies on use of methyl and ethyl esters as an Extender in small capacity diesel engine, Biofuels. (2016).
- Gautam R., Kumar N., Sharma P. Experimental Investigation on Use of Jatropha Oil Ethyl Easter and Diesel Blends in Small Capacity Diesel Engine, SAE International. (2013).
- Goldsworthy L. Combustion behaviour of a heavy duty common rail marine diesel engine fumigated with propane, Exp Thermal Fluid Sci. 42 (2012), 93-106.
- Gopal G., Srinivasa Rao P., Gopalakrishnan K.V., Murthy B.S. Use of hydrogen in dual-fuel engines, Int J Hydrogen Energy. 7 (1982), 267-72.
- Graboski M.S. & Mccormick R.L. Combustion of fat and vegetable oil derived fuels in diesel engines, Progr. Energy Combus. Sci. 24 (1998), 125–164.
- Gross C.W. & Kong S.C. Performance characteristics of a compression-ignition engine using direct-injection ammonia-DME mixtures, Fuel. 103 (2013), 1069–79.
- Gupta D.K., Sharma A., Pathak V., Kumar N. Synthesis of Linseed oil Biodiesel using a Non-Catalytic Supercritical Transesterification Process, SAE International Journal of Fuels and Lubricants. 7 (2014), 2014–01–1955.

- Heywood J. B. Internal Combustion Engine Fundamentals. New York : Tata McGrawHill, 1988.
- Hountalas D.T. & Papagiannakis R.G. Development of a simulation model for direct injection dual fuel dieseldnatural gas engines, SAE. (2000), 2000-01-0286.
- Huang J. & Crookes R.J. Assessment of simulated biogas as a fuel for the spark ignition engine, Fuel. 77 (1998), 1793-1801.
- Hussain J., Palaniradja K., Alagumurthi N., Manimaran R. Effect of Exhaust Gas Recirculation (EGR) on Performance and Emission characteristics of a Three Cylinder Direct Injection Compression Ignition Engine, Alexandria Engineering Journal. 51 (4) (2012). 241-47.
- International Energy Agency (IEA) Statistics - CO_2 Emissions from Fuel Combustion-Highlights (2011).
- International Energy Agency (IEA) Statistics-CO_2 Emissions from Fuel Combustion-Highlights. (2015)
- Ismael M.A., Heikal M.R., Bahroom M.B. Spray Characteristics and Wall Impingement of Diesel-CNG Dual Fuel Jet Using Schlieren Imaging Technique, International Journal of Materials, Mechanics and Manufacturing. (3) (2015).
- Jain S., Sharma M.P. Optimization of long-term storage stability of Jatropha curcas biodiesel using antioxidants by means of response surface methodology, Biomass and Bioenergy. 35 (2011) 4008-14.
- Johansson T.B., Williams R.H., Ishitani H., Edmonds J.A. Options for reducing CO_2 emissions from the energy supply sector, Energy Policy. 24 (1996), 985-1003.

- Johnson E. LPG: a secure, cleaner transport fuel? A policy recommendation for Europe, Energy Policy. 31 (2003), 1573-77.
- Kaewmai R., Kittikun A.H., Musikavong C. Greenhouse gas emissions of palm oil mills in Thailand, International Journal of Greenhouse Gas Control. 11 (2012), 141-51.
- Kannan D., Pachamuthu S., Nabi M.N., Hustad J.E., Lovas T. Theoretical and experimental investigation of diesel engine performance, combustion and emissions analysis fuelled with the blends of ethanol, diesel and jatropha methyl ester, Energy Convers Manage. 53 (2012), 322-31.
- Karavalakis G., Durbin T.D., Villela M., Miller J.W. Air pollutant emissions of light duty vehicles operating on various natural gas compositions, J Nat Gas Sci Eng. 4 (2012), 8-16.
- Karim G.A & Zhigang L. A predictive model for knock in dual fuel engines, SAE. (1992), 921550.
- Kitamura T., Ito T., Senda J., Fujimoto H. Mechanism of smokeless diesel combustion with oxygenated fuels based on the dependence of the equivalence Ratio and temperature on soot particle formation, Int J Engine Res. 3(4) (2002), 223-48.
- Korakianitis T., Namasivayam A.M., Crookes R.J. Diesel and rapeseed methyl ester (RME) pilot fuels for hydrogen and natural gas dual-fuel combustion in compression-ignition engines, Fuel. 90 (7) (2011), 2384-95.
- Korakianitis T., Namasivayam A.M., Crookes R.J. Hydrogen dual fuelling of compression ignition engines with emulsified biodiesel as pilot fuel, International Journal of Hydrogen Energy. 35 (2010), 13329-44.

- Krishnan S. R., Srinivasan K. K., Singh S., Bell S. R., Midkiff K. C., Gong W., Fiveland S. B., Willi M. Strategies for reduced NO_X emissions in pilot-ignited natural gas engines, J. Eng. Gas Turbines Power. 126(3) (2004), 665-71.
- Krishnan S.R., Srinivasan K.K., Raihan M.S. The effect of injection parameters and boost pressure on diesel-propane dual fuel low temperature combustion in a single-cylinder research engine, Fuel. 184 (2016), 490–502.
- Krishnan S.R., Srinivasan K.K., Singh S., Bell S.R., Midkiff K.C., Gong W., et al. Strategies for reduced NO_X emissions in pilot-ignited natural gas engines, Proceedings of the ASME-WA-ICEF Meeting, New Orleans USA. 39 (2002), 361–7.
- Kruyt B., Van Vuuren D.P., De Vries H.J.M., Groenenberg H. Indicators for energy security, Energy Policy. 37 (2009), 2166-81.
- Kumar N. Jatropha Curcus- A Sustainable Source for Production of biodiesel, Journal of Scientific and Industrial Research (JSIR). 64 (2005), 883-89.
- Kumar P. & Kumar N. Comparative study for of JOME and OPOME as pilot fuel, Energy Sources, Part A: Recovery, Utilization, and Environmental Effects. (2016c)
- Kumar P. & Kumar N. Effect of EGR on performance and emission characteristics of a dual fuel engine fuelled with CNG and JOME, Biofuels. (2016b). DOI: 10.1080/17597269.2016.1193838.
- Kumar P. & Kumar N. Experimental investigation of Jatropha oil methyl ester (JOME) as pilot fuel with CNG in a dual fuel engine, Biofuels. (2016a). DOI: 10.1080/17597269.2016.1163215.

- Labeckas G. & Slavinskas S. The effect of rapeseed oil methyl ester on direct injection diesel engine performance and exhaust emissions, Energy Convers Manage. 47 (2006), 1954-67.
- Ladommatos N, Abdelhalim S, Zhao H. The effects of exhaust gas recirculation on diesel combustion and emissions, Int J Engine Res. 1(1) (2000), 107–26.
- Lantz M., Svensson M., Bjornsson L., Borjesson P. The prospects for an expansion of biogas systems in Sweden—Incentives, barriers and potentials, Energy Policy. 35(2007), 1830-43.
- Lapuerta M., Armas O., Rodriguez-Fernandez J. Effect of biodiesel fuels on diesel engine emissions, Progress in Energy and Combustion Science. 34 (2008a), 198-223.
- Lata D. B. & Misra A. Analysis of ignition delay period of a dual fuel diesel engine with hydrogen and LPG as secondary fuels, International Journal of Hydrogen Energy. 36 (2011), 3746-56.
- Lee H. V., Yunus R., Juan J.C., Taufiq-Yap Y.H. Process Optimization Design for Jatropha-based Biodiesel Production using Response Surface Methodology, Fuel Processing Technology. 92 (2011), 2420–28.
- Li Y., Meng L., Nithyanandan K., Lee T.H., Lin Y., Chia-fon F., Liao L.S. Combustion, performance and emissions characteristics of a spark-ignition engine fueled with isopropanol-n-butanol-ethanol and gasoline blends, Fuel. 184 (2016), 864–72.
- Lin C.Y. & Fan C.L. Fuel Properties of Biodiesel Produced from Camellia Oleifera Abel Oil through Supercritical-Methanol Transesterification, Fuel. 90 (2011), 2240-44.

- Liu J., Yang F., Wang H., Ouyang M., Hao S. Effects of pilot fuel quantity on the emissions characteristics of a CNG/diesel dual fuel engine with optimized pilot injection timing, Applied Energy. 110 (2013), 201-06.
- Lounici M.S., Loubar K., Tarabet L., Balistrou M., Niculescu D., Tazerout M. Towards improvement of natural gas-diesel dual fuel mode: An experimental investigation on performance and exhaust emissions, Energy. (2014), 200-11.
- Lu X., Hou Y., Zu L., Huang Z. Experimental Study on the Auto-Ignition and Combustion Characteristics in the homogeneous Charge Compression Ignition (HCCI) Combustion Operation with Ethanol / n -heptane Blend Fuels by Port Injection, Fuel. 85 (2006), 2622-31.
- M.P. Poonia, A. Ramesh, R.R. Gaur. Experimental Investigation of the Factors Affecting the Performance of a LPG - Diesel Dual Fuel Engine, SAE Technical Paper. (1999).
- Manuale D.L., Mazzieri V.M., Torres G., Vera C.R., Yori J.C. Non-Catalytic Biodiesel Process with Adsorption-based Refining, Fuel. 90 (2011), 1188-96.
- Masi M. Experimental analysis on a spark ignition petrol engine fuelled with LPG (liquefied petroleum gas), Energy. 41 (2012), 252-60.
- Mathur H.B., Das L.M., Patro T.N. Hydrogen-fuelled diesel engine: performance improvement through charge dilution techniques, Int J Hydrogen Energy. 18 (1993), 421-31.
- McTaggart-Cowan G.P., Jones H.L., Rogak S.N., Bushe W.K., Hill P.G., Munshi S.R. The effects of high-pressure injection on a compression–ignition, direct injection of natural gas engine, ASME J Eng Gas Turb Power. 129(2) (2006), 579–88.

- Mendera K.Z., Spyra A., Smereka M. Mass Fraction Burned Analysis, Journal of KONES Internal Combustion Engines. 3-4 (2002), 193-201.
- Misra R.D. & Murthy M.S. Performance, emission and combustion evaluation of soapnut oil-diesel blends in a compression ignition engine, Fuel. 90 (7) (2011), 2514-18.
- Miyamoto N., Ogawa H., Arima T., Miyakawa K. Improvement of Diesel Combustion and Emissions with Various oxygenated Fuel Additives, SAE. (1996).
- Miyamoto N., Ogawa H., Shibuya M., Arai K., Esmilaire O. Influence of the Molecular Structure of Hydrocarbon Fuels on Diesel Exhaust Emissions, SAE. (1994).
- Mo M., Atabani A.E., Masjuki H.H., Kalam M.A., Masum B.M. A study on the effects of promising edible and non-edible biodiesel feedstocks on engine performance and emissions production : A comparative evaluation, 23 (2013) 391–404.
- Mohammadi A., Shiojib M., Nakaib Y., Ishikurab W., Tabo E.. Performance and combustion characteristics of a direct injection SI hydrogen engine, International Journal of Hydrogen Energy. 32 (2007), 296-304.
- Mohsin R., Majid Z.A., Shihnan A.H., Nasri N.S., Sharer Z. Effect of biodiesel blends on engine performance and exhaust emission for diesel dual fuel engine, Energy Conversion and Management. 88 (2014), 821-828.
- Mustafi N.N. & Raine R.R. A study of the emissions of a dual fuel engine operating with alternative gaseous fuels, SAE (2008), 2008-01-1394.
- Mustafi N.N., Raine R.R., Verhelst. Combustion and emissions characteristics of a dual fuel engine operated on alternative gaseous fuels, Fuel. 109 (2013), 669-78.

- Namasivayam A.M., Crookes R.J., Korakianitis T., Olsen J. Assessment of combustion in natural gas fuelled compression ignition engines with DME and RME pilot ignition, Proc I.Mech.E., Int J Engine Res. 10 (3) (2009), 165–74.
- Namasivayam A.M., Korakianitis T., Crookes R.J., Bob-Manuel K.D.H., Olsen J. Biodiesel, emulsified biodiesel and dimethyl ether as pilot fuels for natural gas fuelled engines, Applied Energy. 87 (2010), 769-78.
- Nigam P.S. & Singh A. Production of Liquid Biofuels from Renewable Resources, Progress in Energy and Combustion Science. 37 (2010).
- Nithyanandan K., Lin Y., Donahue R., Meng X., Zhang J., Lee C.F. Characterization of soot from diesel-CNG dual-fuel combustion in a CI engine, Fuel. 184 (2016), 145-52.
- Nithyanandan K., Zhang J., Li Y., Meng X., Donahue R., Lee C.F., Dou H. Diesel-like efficiency using CNG/diesel dual-fuel combustion, ASME J Energy Resour Technol. (2016).
- Olsen J., Crookes R.J., Bob-Manuel K.D.H. Experiments in dual fuelling a compression ignition engine by injecting di-methyl ether as a pilot fuel to ignite varying quantities of natural gas, SAE. (2007).
- Olsen J., Crookes R.J., Bob-Manuel K.D.H. Experiments in dual fuelling a compression ignition engine by injecting di-methyl ether as a pilot fuel to ignite varying quantities of natural gas, SAE. (2007), 2007-01-3624.
- Padhi S.K. Preparation and characterization from nonedible oils, Ph.D.thesis, NIT Rourkela. (2010).
- Pali H.S. & Kumar N. Combustion, performance and emissions of Shorea robusta methyl ester blends in a diesel engine, Biofuels. 7269 (2016), 1–10.

- Pali H.S., Kumar N. Some Experimental Studies on Combustion, Emission and Performance Characteristics of an Agricultural Diesel Engine Fueled with Blends of Kusum Oil Methyl Ester and Diesel, SAE International. (2014).
- Pali H.S., Kumar N., Mishra C. Some Experimental Studies on Combustion, Emission and Performance Characteristics of an Agricultural Diesel Engine Fueled with Blends of Kusum Oil Methyl Ester and Diesel, SAE International. (2014).
- Papagiannakis R.G. & Hountalas D.T. Combustion and exhaust emission characteristics of a dual fuel compression ignition engine operated with pilot diesel fuel and natural gas, Energy Convers Manage. 45 (18–19) (2004), 2971-87.
- Papagiannakis R.G. Study of air inlet preheating and EGR impacts for improving the operation of compression ignition engine running under dual fuel mode, Energy Conversion and Management. 68 (2013), 40-53.
- Papagiannakis R.G., Hountalas D.T., Rakopoulos C.D. Theoretical study of the effects of pilot fuel quantity and its injection timing on the performance and emissions of a dual fuel diesel engine, Energy Convers. Manage. 48 (11) (2007), 2951-61.
- Park C., Choi Y., Kim C., Oh S., Lim G., Moriyoshi Y. Performance and exhaust emission characteristics of a spark ignition engine using ethanol and ethanol reformed gas, Fuel. 89 (2010), 2118-25.
- Paul A., Panua R.S., Debroy D., Bose P.K. Effect of compressed natural gas dual fuel operation with diesel and Pongamia pinnata methyl ester (PPME) as pilot fuels on performance and emission characteristics of a CI (compression ignition) engine, Energy. 68 (2014), 495-509.

- Petroleum and Natural Gas Statistics, Ministry of petroleum & Natural as Economics and Statistcs Division, Delhi, Indian, (2014).
- Pirouzpanah V & Khoshbakhti S.R. Enhancement of the combustion process in dual-fuel engines at part loads using exhaust gas recirculation, Proc Inst Mech Eng Part D: J AutomobEng. 221 (2007), 877-88.
- Pirouzpanah V., Saray R.K., Sohrabi A., Niaei A. Comparison of thermal and radical effects of EGR gases on combustion process in dual fuel engines at part loads. Energy Conversion and Management. 48 (2007), 1909-18.
- Poonia M.P., Ramesh A., Gaur R.R. Effect of intake air temperature and pilot fuel quantity on the combustion characteristics of a LPG diesel dual fuel engine, SAE. (1998). 982455.
- Pradeep V. & Sharma R.P. Use of Hot EGR for NO_X control in a compression ignition engine fuelled with bio-diesel from Jatropha oil, Renewable Energy. 32 (2007), 1136-54.
- Prakash G., Ramesh A., Shaik A.B. An approach for estimation of ignition delay in a dual fuel engine, SAE. (1999), 1999–01-0232.
- Price P., Guo S., Hirschmann M. Performance of an evaporator for a LPG powered vehicle, Applied Thermal Engineering. 24 (2004), 1179-94.
- Rahmouni C., Tazerout M., Le Corre O. A Method to Determine Biogas Composition for Combustion Control, SAE. (2002), 2002-01-1708.
- Rakopoulos D.C., Rakopoulos C.D., Papagiannakis R.G., Kyritsis D.C. Combustion Heat Release Analysis of Ethanol or n-butanol Diesel Fuel Blends in Heavy-duty DI Diesel Engine, Fuel. 90 (2011), 1855-67.

- Raslavicius L., Kersys A., Mockus S., Kersiene N., Starevicius M. Liquefied petroleum gas (LPG) as a medium-term option in the transition to sustainable fuels and transport, Renew. Sustain. Energy Rev. 32 (2014), 513-25.
- Rathore V. & Madras G. Synthesis of Biodiesel from Edible and Non-Edible Oils in Supercritical Alcohols and Enzymatic Synthesis in Supercritical Carbon Dioxide, Fuel. 86 (2007), 2650-59.
- Rolf E. The influence of EGR on heat release rate and NO formation in a DI diesel engine, SAE Transactions Special publication. (2000), 2000-01-1807.
- Roubaud A. & Favrat D. Improving performances of a lean burn cogeneration biogas engine equipped with combustion prechambers, Fuel. 84 (2005), 2001-07.
- Roy M.M., Tomita E., Kawahara N., Harada Y., Sakane A. An experimental investigation on engine performance and emissions of a supercharged H_2 diesel dual-fuel engine, International Journal of Hydrogen Energy. 35 (2010), 844-53.
- Ryu K. Effects of pilot injection pressure on the combustion and emissions characteristics in a diesel engine using biodiesel-CNG dual fuel, Energy Conversion and Management. 76 (2013b) 506-16.
- Ryu K. Effects of pilot injection timing on the combustion and emissions characteristics in a diesel engine using biodiesel–CNG dual fuel, Appl. Energy. 111 (2013a), 721-30.
- Sahoo B.B., Sahoo N., Saha U.K. Effect of engine parameters and type of gaseous fuel on the performance of dual-fuel gas diesel engines-A critical review, Renewable and Sustainable Energy Reviews. 13 (2009), 1151-84.
- Sahoo P.K. & Das L.M. Process optimization for biodiesel production from Jatropha, Karanja and Polanga oils, Fuel. 88 (9) (2009), 1588-94.

- Saravanan N., Nagarajan G., Sanjay G., Dhanasekaran C., Kalaiselvan K.M. Combustion analysis on a DI diesel engine with hydrogen in dual fuel mode, Fuel. 87 (2008), 3591-99.

- Saravanan N., Nagarajan G., Sanjay G., Dhanasekaran C., Kalaiselvan K.M. Combustion analysis on a DI diesel engine with hydrogen in dual fuel mode, Fuel. 87 (2008), 3591-99.

- Selim M.Y.E. A study of some combustion characteristics of dual fuel engine using EGR. SAE. (2003), 2003-01-0766.
- Selim M.Y.E. Sensitivity of dual fuel engine combustion and knocking limits to gaseous fuel composition, Energy Conversion and Management. 45 (3) (2004), 411-25.
- Selim M.Y.E., Radwan M.S., Saleh H.E. Improving the performance of dual fuel engines running on natural gas/LPG by using pilot fuel derived from jojoba seeds, Renewable Energy. 33 (2008), 1173-85.
- Seung H.Y. & Chang S.L. Experimental investigation on the combustion and exhaust emission characteristics of biogas–biodiesel dual-fuel combustion in a CI engine, Fuel Process Technology. 92 (2011), 992–1000.
- Shahid E.M. & Jamal Y. A review of biodiesel as vehicular fuel, Renewable and Sustainable Energy Reviews. 12 (2008), 2484-94.
- Shahid E.M. & Jamal Y. Production of Biodiesel: A Technical Review, Renewable and Sustainable Energy Reviews. 15 (2011), 4732-45.
- Sharma Y.C., Singh B., Upadhyay S.N. Advancements in Development and Characterization of Biodiesel: A Review, Fuel. 87 (2008), 2355-73.

- Silitonga S., Atabani E., Mahlia T.M.I., Masjuki H.H., Badruddin I.A., Mekhilef S. A Review on Prospect of Jatropha Curcas for Biodiesel in Indonesia, Renewable and Sustainable Energy Reviews. 15 (2011), 3733-56.
- Singh S., Kong S.C., Reitz R.D., Krishnan S.R., Midkiff K.C. Modeling and experiments of dual-fuel engine combustion and emissions, SAE. (2004), 2004-01-0092.
- Sinha S., Agarwal A.K., Garg S. Biodiesel development from rice bran oil: Transesterification process optimization and fuel characterization, Energy Conversion and Management. 49 (2008), 1248-57.
- Soloiu V., Duggan M., Harp S., Vlcek B., Williams D. PFI (port fuel injection) of n-butanol and direct injection of biodiesel to attain LTC (low-temperature combustion) for low-emissions idling in a compression engine, Energy. 52 (2013), 143-154.
- Sombatwong P., Thaiyasuit P., Pianthong K. Effect of Pilot Fuel Quantity on the Performance and Emission of a Dual Producer Gas–Diesel Engine, Energy Procedia. (2013), 218-27.
- Song C., Hsu C.S., Moshida I. Introduction to chemistry of diesel fuels. In: Chemistry of Diesel Fuels, (Eds.), London: Taylor and Francis. (2000).
- Srinivasan K.K., Krishnan S.R., Qi Y., Midkiff K.C., Yang H. Analysis of diesel pilotignited natural gas low-temperature combustion with hot exhaust gas recirculation, Combust SciTechnol. 179(9) (2007), 1737–76.
- Stewart J., Clarke A., Chen R. An Experimental Study of the Dual-fuel Performance of A Small Compression Ignition Diesel Engine Operating with Three Gaseous Fuels, Proceedings of the Institution of Mechanical Engineers, Part D: Journal of Automobile Engineering. (2007), 943-56.

- Sun J., Caton J. A., Jacobs T. J. Oxides of nitrogen emissions from biodiesel- fuelled diesel engines, Progress in Energy and Combustion Science. 36 (2010), 677-695.
- Sun J., Caton J.A., Jacobs T.J. Oxides of nitrogen emissions from biodiesel fuelled diesel engines, Progress in Energy and Combustion Science. 36 (2010), 677-95.
- Tan K.T., Lee K.T., Mohamed A. R. Potential of Waste Palm Cooking Oil for Catalyst-Free Biodiesel Production, Energy. 36 (2011), 2085–88.
- Tan P.Q., Hu Z.Y., Lou D.M. Regulated and unregulated emissions from a light-duty diesel engine with different sulfur content fuels, Fuel. 88 (2009), 1086-91.
- Tate R.E., Watts K.C., Allen C.A.W., Wilkie K.I. The viscosities of three biodiesel fuels at temperatures up to 300°C, Fuel. 85 (2006), 1010-15.
- Teo C.L., Jamaluddin H., Zain N.A.M., Idris A. Biodiesel Production via Lipase Catalysed Transesterification of Microalgae Lipids from Tetraselmis sp., Renewable Energy. 68 (2014), 1-5.
- Tira H.S. Impact of alternative fuels and hydrogen enriched gaseous fuel on combustion and emissions in diesel engines, PhD Thesis. The University of Birmingham. (2013).
- Tomita E, Kawahara N, Piao Z, Fujita S, Hamamoto Y. Hydrogen combustion and exhaust emissions ignited with diesel oil in a dual fuel engine, SAE paper. (2001), 2001-01-3503.
- Tomita E., Harada Y., Kawahara N., Sakane A. Effect of EGR on combustion and exhaust emissions in supercharged dual-fuel natural gas engine ignited with diesel fuel, SAE. (2009), 2009-01-1832.

- Tsolakis A. & Megaritis A. Catalytic exhaust gas fuel reforming for diesel engines effects of water addition on hydrogen production and fuel conversion efficiency, International Journal of Hydrogen Energy. 29 (2004), 1409-19.
- Tsolakis A., Megaritis A., Wyszynski M.L. Application of Exhaust Gas Fuel Reforming in Compression Ignition Engines Fueled by Diesel and Biodiesel Fuel Mixtures, Energy & Fuels. 17 (2003), 1464-73.
- Tsolakis A., Megaritis A., Yap D., Abu-Jrai A. Combustion Characteristics and Exhaust Gas Emissions of a Diesel Engine Supplied with Reformed EGR, SAE. (2005b), 2005-01-2087.
- Ullah K., Kumar V., Dhingra S., Braccio G. Assessing the lignocellulosic biomass resources potential in developing countries : A critical review, Renewable and Sustainable Energy Reviews. 51 (2015), 682-98.
- Uma R., Kandpal T.C., Kishore V.V.N. Emission characteristics of an electricity generation system in diesel alone and dual fuel modes, Biomass Energy. (2004), 195-203.
- Uzun B.B., Kilic M., Ozbay N., Putun A.E., Putun E. Biodiesel Production from Waste Frying Oils: Optimization of Reaction Parameters and Determination of Fuel Properties, Energy. 44 (2012), 347–51.
- Van Gerpen J. Biodiesel Processing and Production, Fuel Processing Technology. 86 (2005), 1097–1107.
- Van Gerpen J., Shanks B., Pruszko R., Clements D., Knothe G. Biodiesel analytical methods. Golden, CO: National Renewable Energy Laboratory. (2004).
- Verhelst S. & Sierens R. Hydrogen engine-specific properties, International Journal of Hydrogen Energy. 26 (2001), 987-90.

- Vibhanshu V., Karnwal A., Kumar N. Performance, Emission and Combustion, Analysis of Diesel Engine Fueled with Blends of Mahua Oil Methyl Ester and Diesel, SAE International. (2014).
- Vijayabalan P. & Nagarajan G. Performance, Emission and Combustion of LPG Diesel Dual Fuel Engine using Glow Plug, JJMIE. 3 (2) (2009), 105-10.
- W. Mansor, W. Nurdiyana et al. Emissions and efficiency evaluations of a 6.8 liter diesel derivative dual fuel engine, Proceedings of The Canadian Society for Mechanical Engineering International Congress. 2014.
- Weaver C.S. & Turner S.H. Dual fuel natural gas/diesel engines: technology, performance, and emissions, SAE. (1994), 940548.
- White C.M., Steeper R.R., Lutz A.E. The hydrogen-fueled internal combustion engine: a technical review, International Journal of Hydrogen Energy. 31 (2006), 1292-1305.
- Wu X. & Leung D.Y.C. Optimization of Biodiesel Production from Camelina Oil using Orthogonal Experiment, Applied Energy. 88 (2011), 3615–24.
- Xinling L. & Zhen H. Emission reduction potential of using gas-to-liquid and dimethyl ether fuels on a turbocharged diesel engine, Science of The Total Environment. 407 (2009), 2234-44.
- Yadav V.S., Soni S.L., Sharma D. Performance and emission studies of direct injection C.I. engine in duel fuel mode (hydrogen-diesel) with EGR, international journal of hydrogen energy. 37 (2012), 3807-17.
- Yang B., Wang L., Ning L., Zeng K. Effects of pilot injection timing on the combustion noise and particle emissions of a diesel/natural gas dual-fuel engine at low load, Applied Thermal Engineering. 102 (2016), 822-28.

- Ying W., Li H., Jie Z., Longbao Z. Study of HCCI-DI Combustion and Emissions in a DME Engine, Fuel. 88 (2009), 2255-61.
- Yoon S.H. & Lee C.S. Experimental investigation on the combustion and exhaust emission characteristics of biogas–biodiesel dual fuel combustion in a CI engine, Fuel Process Technol. 92 (2011), 992–1000.
- Yoon S.H. & Lee C.S. Experimental investigation on the combustion and exhaust emission characteristics of biogas–biodiesel dual-fuel combustion in a CI engine, Fuel Process Technol. 92(5) (2011), 992-1000.
- Yuan X., Liu J., Zeng G., Shi J., Tong J., Huang G. Optimization of Conversion of Waste Rapeseed Oil with High FFA to Biodiesel using Response Surface Methodology, Renewable Energy. 33 (2008), 1678-84.
- Yucel Y. Optimization of Biocatalytic Biodiesel Production from Pomace Oil using Response Surface Methodology, Fuel Processing Technology. 99 (2012), 97–102.
- Yunus T.M., Atabani A.E., Anjum I., Badarudin A., Khayoon M.S., Triwahyono S. Recent scenario and technologies to utilize non-edible oils for biodiesel production, Renewable and Sustainable Energy Reviews. 37 (2014), 840-51.
- Zheng M., Reader G.T., Hawley J.G. Diesel engine exhaust gas recirculation—a review on advanced and novel concepts, Energy Conversion and Management. 45 (2004), 883-900.